

DISSERTATION

POTENTIATION OF BETA-LACTAM ANTIBIOTICS AGAINST  
*MYCOBACTERIUM TUBERCULOSIS* BY 2-AMINOIMIDAZOLES:  
INVESTIGATION INTO THE MECHANISM OF ACTION  
AND ITS RELEVANCE TO MYCOBACTERIAL BIOENERGETICS

Submitted by

Albert Byungyun Jeon

Department of Microbiology, Immunology, and Pathology

In partial fulfilment of the requirements

For the Degree of Doctor of Philosophy

Colorado State University

Fort Collins, Colorado

Summer 2017

Doctoral Committee:

Advisor: Randall Basaraba

Brad Borlee

Daniel Gustafson

Mary Jackson

Christian Melander

Andrés Obregón-Henao

Copyright by Albert Byungyun Jeon 2017

All Rights Reserved

## ABSTRACT

POTENTIATION OF BETA-LACTAM ANTIBIOTICS AGAINST  
*MYCOBACTERIUM TUBERCULOSIS* BY 2-AMINOIMIDAZOLES:  
INVESTIGATION INTO THE MECHANISM OF ACTION  
AND ITS RELEVANCE TO MYCOBACTERIAL BIOENERGETICS

Tuberculosis, caused by *Mycobacterium (M.) tuberculosis*, is a global health problem still causing morbidity and mortality due in part to the emergence of drug-resistance and the lack of new antimicrobial agents to treat the disease. While infection with drug-sensitive *M. tuberculosis* has cure rates between 90-95% with the conventional multidrug-regimen comprised of four different first-line anti-tuberculosis drugs, administered for a minimum of 6 months. In the event where premature termination of the treatment or poor patient compliance occurs, the disease may progress into latent tuberculosis, which holds the risk of reoccurring disease or even leads to development of drug-resistant strains that are refractory to first line anti-tuberculosis drugs. This persistence is a major hurdle in global tuberculosis control and warrants the development of a new class of anti-tuberculosis drugs or novel strategies to target persisting bacilli. However, the current anti-tuberculosis drug pipeline does not suggest an immediate solution required for the successful control of global tuberculosis epidemic. In sum, there is an urgent need for a new strategy to complement current tuberculosis chemotherapy.

2-aminoimidazoles and their derivatives have been shown to be effective inhibitors of bacterial biofilms. Not only does this class of small molecules inhibit the formation of or disperse biofilms, but they also exhibit a clinically relevant feature of potentially abrogating antibiotic resistance in important pathogenic bacteria. From the studies characterizing persistent *M. tuberculosis* bacilli after anti-tuberculosis therapy in animal models, it has been suggested that this subpopulation of bacilli share similarities with bacterial biofilms. Our group developed an *in vitro* culture system where *M. tuberculosis* can be cultured in biofilm-like surface-attached communities with host-derived macromolecules and

showed they express extensive drug-tolerance to one of the first-line anti-tuberculosis drug, isoniazid. Based on the previous effects of 2-aminoimidazoles on biofilms and drug-resistant bacteria, we hypothesized that 2-aminoimidazoles could reverse phenotypic drug-tolerance expressed by *M. tuberculosis* in our model and demonstrated that, indeed, derivatives of 2-aminoimidazoles effectively resensitized drug-tolerant bacilli to isoniazid. Additionally, a fortuitous but critical observation was made in which one of the potent 2-aminoimidazole derivatives potentiated the effect of  $\beta$ -lactam antibiotics against *M. tuberculosis*. As repurposing  $\beta$ -lactams in tuberculosis treatment regimen has potential therapeutic value, which are described throughout this dissertation.

In chapter 2, 2-aminoimidazole compounds are shown to be effective at potentiating multiple  $\beta$ -lactam antibiotics. Minimum inhibitory concentrations, as well as bactericidal concentrations, of  $\beta$ -lactams were dramatically reduced when combined with 2-aminoimidazoles. Through a transcriptional analysis of *M. tuberculosis* treated with 2B8, one of our lead 2-aminoimidazoles induced cell envelope related stress responses and suppressed mycolic acid biosynthesis. Thereafter, it was hypothesized that 2-aminoimidazoles disrupts one or more factors conferring *M. tuberculosis*  $\beta$ -lactam resistance, which we shown in chapter 3 is in large part due to a reduction in secretion of the enzyme  $\beta$ -lactamase and by increasing cell envelope permeability. 2B8 treated *M. tuberculosis* exhibited significantly lower  $\beta$ -lactamase activity in culture supernatant, which was due to a general protein secretion defect, and not from direct inhibition of  $\beta$ -lactamase enzyme activity by 2-aminoimidazole compounds. As expected from the transcriptional analysis, 2B8 induced alterations in cell envelope lipid composition highlighted by the accumulation of trehalose monomycolate, the reduction of trehalose dimycolate, as well as a decrease in mycolic acid biosynthesis. Additionally, increased sensitivity to the detergent SDS, increased permeability to multiple nucleic acid staining dyes, and increased bindings of peptidoglycan-targeting antibiotics were observed when with 2B8 treatment. Based on major findings from chapter 3, it was hypothesized that the underlying mechanisms of 2-aminoimidazoles are the disruption of proton motive force and the disturbance of mycobacterial bioenergetics. In chapter 4, the collapse of proton motive force with additional dose-dependent block of mycobacterial electron transport chain is highlighted. Through a

series of assays, we determined that 2B8 blocks the *M. tuberculosis* electron transport chain downstream of complex I and II, but upstream of complex IV. Taken together, these results collectively extend our current understanding of the various effects 2-aminoimidazole treatment has on *M. tuberculosis* susceptibility to  $\beta$ -lactam antibiotics through perturbation of mycobacterial bioenergetics which can provide a profound impact in improving current tuberculosis therapy. Furthermore, this study offers valuable information for the construction of the next generation of potent 2-aminoimidazoles to improve efficacy against *M. tuberculosis* as well as other compounds that may be developed as a new anti-TB drug targeting bioenergetics.

## ACKNOWLEDGEMENTS

I would like to express my sincere gratitude to my mentor, Dr. Randall Basaraba for taking an immature graduate student from a foreign country under his wings and developing me into a better scientist. I never regretted choosing him as my advisor throughout my whole training as he not only provided me with a proper guidance in my program, but also gave me unlimited faith and a great level of freedom with my research so I can fully enjoy the delight of independent scientific investigation. The experiences I amassed with him will undoubtedly contribute to future success in my scientific career. Besides his mentorship from academic perspective, he was always warm-hearted and caring for me and my wife and was a friend to whom we could lean on. For that matter, I would also like to thank Dr. Basaraba's wife, Dr. Susan Kraft for her kindness. They gave us a feeling that we were always welcomed like a family which is something we really missed being apart from our own.

I am also greatly thankful to my doctoral committee members; Dr. Brad Borlee for his encouragement and support, Dr. Daniel Gustafson for his unique perspectives as a clinical scientist, Dr. Mary Jackson for her scientific professionalism, critical discussion points and suggestions for experiments, and Dr. Christian Melander for his insights based on his chemical expertise, supporting my experiments with compounds while also having to make long trips from North Carolina to Fort Collins for our meetings, Dr. Andrés Obregón-Henao for enjoyable daily discussions, his input and guidance with this project that made this dissertation possible. Also, I thank Dr. Karen Dobos for serving as an alternative member in my preliminary examination committee.

I sincerely thank all previous and current members of Basaraba-Podell laboratory, especially Forrest Ackart and Alex Todd for their support in running the lab, Dr. Brendan Podell for his encouragements, and James DiLisio for keeping me light-hearted at all times. The experience I had in this lab was invaluable and will be a cornerstone for my career development.

Dr. Edward Hoover and Dr. Sue VandeWoude deserve a special acknowledgement for their efforts in securing valuable funding opportunities for veterinarians seeking biomedical research training. I

am really grateful that I was a recipient of the NIH T32 training grant which was made possible by them. I would also like to thank Connie Brewster for letting me share the office as well as wonderful memories past four years. I would also like to acknowledge Drs. Robert Abramovitch and Benjamin Johnson, Dr. Juan Belardinelli and Dr. Adam Chicco for their contribution in chapter 2, 3 and 4, respectively. I also thank Veronica Gruppo and Fábio Fontes for technical support.

Finally, I would like to extend my warmest gratitude to my family. My mother who always prayed for me and my father who was my role model as a scholar gave me unconditional love and will always claim a special place in my heart. Also, I thank my parents-in-laws and two families of my sisters-in-law for consistently giving me supports whenever I reached them. My friends in South Korea and friends who started the graduate program together also deserve many thanks.

## DEDICATION

*I dedicate this dissertation to my beautiful wife Narah who sacrificed her own dream to support mine  
while assuring me that she will always be the one who fully believes in my ability,  
our two little daughters Yuju and Evie, for coming into our lives as gifts from heaven,  
and our old friend Yangdol.*

## TABLE OF CONTENTS

ABSTRACT.....	ii
ACKNOWLEDGEMENTS.....	v
DEDICATION.....	vii
LIST OF TABLES.....	xiii
LIST OF FIGURES.....	xiv
CHAPTER ONE: Review of literature.....	1
1.1. Introduction: Tuberculosis and <i>Mycobacterium tuberculosis</i> .....	1
1.1.1. History of tuberculosis.....	1
1.1.2. Global burden of tuberculosis.....	2
1.1.3. The bacilli.....	3
1.1.4. The disease.....	4
1.1.5. Disease progression.....	4
1.2. Problems in controlling global tuberculosis epidemic.....	6
1.2.1. Vaccine.....	6
1.2.2. Diagnosis.....	7
1.2.3. Therapy.....	8
1.2.4. Research priorities.....	9
1.3. <i>M. tuberculosis</i> persistence that complicates TB therapy.....	10
1.3.1. Non-replicative persistence.....	10
1.3.2. Phenotypic drug-tolerance and genotypic drug-resistance.....	13
1.3.3. Intrinsic drug-resistance.....	15
1.4. Similarities between <i>M. tuberculosis</i> in granulomatous lesions and biofilms.....	15
1.4.1. Biofilms.....	15
1.4.2. Drug-tolerance and drug-resistance in biofilm-forming bacteria.....	17

1.4.3. Focus on extracellular <i>M. tuberculosis</i> within granulomatous lesion.....	19
1.4.4. <i>M. tuberculosis</i> <i>in vitro</i> drug-tolerance model using host derived factors.....	20
1.5. 2-AI based small molecules.....	21
1.5.1. Origin.....	21
1.5.2. 2-AI and other bacteria.....	23
1.5.3. Reversal of <i>M. tuberculosis</i> drug-tolerance by 2-AIs.....	24
1.6. $\beta$ -lactam antibiotics and tuberculosis.....	25
1.7. <i>M. tuberculosis</i> 's intrinsic resistance mechanisms against $\beta$ -lactams.....	29
1.7.1. Multidrug efflux pumps.....	30
1.7.2. Alterations in PBPs.....	30
1.7.3. Mycobacterial cell envelope.....	30
1.7.3.1. Overall structure of the mycobacterial cell envelope.....	31
1.7.3.2. Peptidoglycan.....	31
1.7.3.3. Arabinogalactan.....	32
1.7.3.4. Mycolic acids.....	34
1.7.3.5. Other cell wall glycolipids and phospholipids.....	35
1.7.3.6. Transcriptional regulation related to cell envelope stresses.....	38
1.7.4. $\beta$ -lactamases.....	41
1.7.4.1 <i>M. tuberculosis</i> $\beta$ -lactamase.....	41
1.7.4.2 Protein secretion machinery of <i>M. tuberculosis</i> .....	42
1.8. Mycobacterial metabolism and bioenergetics.....	44
1.8.1. Bacterial bioenergetics.....	45
1.8.2. PMF and the ETC.....	46
1.9. Overview of the dissertation.....	49
REFERENCES.....	52
CHAPTER TWO: 2-AI compounds potentiate $\beta$ -lactam activity against <i>M. tuberculosis</i> .....	87

2.1. Introduction.....	87
2.2. Materials and Methods.....	89
2.2.1. Bacterial strains, media and culture conditions.....	89
2.2.2. 2-AI compounds.....	89
2.2.3. Growth assays .....	89
2.2.4. Determination of minimum inhibitory concentration of $\beta$ -lactams against mycobacteria with or without 2-AI compounds .....	90
2.2.5. Evaluation of bactericidal activity of $\beta$ -lactams against <i>M. tuberculosis</i> .....	91
2.2.6. RNA isolation and next generation sequencing .....	91
2.2.7. Statistical analysis.....	93
2.3. Results.....	93
2.3.1. Normal growth of <i>M. tuberculosis</i> is affected by the presence of 2B8.....	93
2.3.2. 2B8 treated <i>M. tuberculosis</i> fails to grow in the presence of carbenicillin.....	94
2.3.3. 2-AI treatment reduces MIC of $\beta$ -lactams against mycobacteria.....	95
2.3.4. 2-AI improves bactericidal effect of $\beta$ -lactams.....	98
2.3.5. <i>M. tuberculosis</i> transcriptional responses to 2B8 .....	99
2.4. Discussion .....	104
REFERENCES .....	108
CHAPTER THREE: 2-AI compounds reduce $\beta$ -lactamase secretion and increase cell envelope permeability of <i>M. tuberculosis</i> .....	113
3.1. Introduction.....	113
3.2. Materials and Methods.....	114
3.2.1. Bacterial strains, media and culture conditions.....	114
3.2.2. Collection of <i>M. tuberculosis</i> culture filtrate proteins .....	114
3.2.3. $\beta$ -lactamase activity assay .....	115
3.2.4. Preparation and analysis of <i>M. tuberculosis</i> cell envelope lipids .....	115

3.2.5. SDS sensitivity assay .....	116
3.2.6. Dye accumulation assays .....	117
3.2.7. Evaluation of cell envelope permeability and cell membrane integrity using BOCILLIN®, BODIPY® FL vancomycin and propidium iodide .....	117
3.2.8. Statistical analysis .....	118
3.3. Results .....	118
3.3.1. 2-AI treated <i>M. tuberculosis</i> cultures have reduced $\beta$ -lactamase activity .....	118
3.3.2. 2-AI treatment alters <i>M. tuberculosis</i> cell envelope lipid composition .....	120
3.3.3. 2-AI treated <i>M. tuberculosis</i> becomes hypersensitive to SDS .....	124
3.3.4. 2-AI treatment increased <i>M. tuberculosis</i> permeability to nucleic acid staining dyes .....	125
3.3.5. 2-AI treatment acutely increases binding of penicillin V and vancomycin .....	129
3.4. Discussion .....	134
REFERENCES .....	141
CHAPTER FOUR: Collapse of PMF and ETC blockage in mycobacteria by 2-minoimidazoles .....	149
4.1. Introduction .....	149
4.2. Materials and methods .....	151
4.2.1. Bacterial strains, media, and culture conditions .....	151
4.2.2. Kinetic measurement of alamarBlue® reduction .....	151
4.2.3. Determination of $\Delta\psi$ by DiSC <sub>3</sub> (5) .....	152
4.2.4. Generation of inverted membrane vesicles .....	152
4.2.5. Determination of $\Delta\text{pH}$ with IMVs .....	153
4.2.6. Real-time measurement of oxygen consumption rate by high-resolution respirometry .....	153
4.2.7. Determination of 2-AI compounds MICs against mycobacteria with or without BSA .....	154
4.2.8. Quantification of intracellular ATP .....	154
4.2.9. ETC activity assay with IMVs .....	155
4.2.10. Determination of NADH/NAD <sup>+</sup> ratio .....	155

4.2.11. Determination of NADH oxidation by IMVs .....	156
4.2.12. Rescue of NADH oxidation block with clofazimine .....	157
4.2.13. $\beta$ -lactam potentiation assay with bioenergetics-affecting drugs .....	157
4.2.14. Statistical analysis .....	158
4.3. Results .....	158
4.3.1. 2B8 alters mycobacterial redox potential.....	158
4.3.2. 2B8 depolarizes mycobacterial membrane potential .....	159
4.3.4. 2B8 collapses $\Delta$ pH of <i>M. smegmatis</i> IMVs .....	160
4.3.5. 2B8 uncouples mycobacterial oxidative phosphorylation .....	161
4.3.6. 2B8 prevents CCCP from further increase of oxygen consumption.....	165
4.3.7. 2B8 depletes intracellular ATP levels in <i>M. tuberculosis</i> .....	166
4.3.8. 2B8 blocks ETC in <i>M. smegmatis</i> IMVs .....	168
4.3.9. 2B8 alters NADH/NAD <sup>+</sup> ratio in <i>M. tuberculosis</i> .....	169
4.3.10. 2B8 blocks NADH oxidation.....	171
4.3.11. NADH oxidation block by 2B8 can be rescued by CFZ.....	172
4.3.12. Bioenergetics-affecting drugs potentiate $\beta$ -lactams, but to a lesser extent than 2B8.....	174
4.4. Discussion .....	175
REFERENCES .....	180
CHAPTER FIVE: Concluding remarks and future directions .....	184
REFERENCES .....	189
LIST OF ABBREVIATIONS.....	193

## LIST OF TABLES

Table 1.1. List of WHO recommended antimicrobial agents for TB therapy.

Table 2.1. MIC of  $\beta$ -lactams against mycobacteria in combination with 2-AI compounds.

Table 3.1. MIC of vancomycin against 2B8 treated *M. tuberculosis* H37Rv.

Table 3.2. MIC of  $\beta$ -lactams against SDS treated *M. tuberculosis* H37Rv.

Table 4.1. MICs of 2-AI compounds against *M. smegmatis* and *M. tuberculosis* in the presence or the absence of BSA.

Table 4.2. Fold-reduction of  $\beta$ -lactam MICs against *M. tuberculosis* in combination with bioenergetics-targeting drugs.

Table 4.3. Comparison of low and high concentrations of 2B8 in assays conducted in this study.

Table 4.4. Summary of read-outs for all tested drugs.

## LIST OF FIGURES

Figure 1.1. Location of extracellular acid-fast bacilli in the acellular rim of the primary TB granuloma.

Figure 1.2. Structure of 2-AI compounds used in this study.

Figure 1.3. Reversal of isoniazid tolerance by 2-AI compounds.

Figure 1.4. Peptidoglycan biosynthesis pathway in bacteria.

Figure 1.5. Diagrammatic presentation of the mycobacterial cell wall.

Figure 1.6. Biosynthetic pathway of mycobacterial arabinogalactan.

Figure 1.7. Biosynthetic pathway of mycobacterial mycolic acids.

Figure 1.8. Structures of PDIM, PIM<sub>2</sub>, LM and LAM.

Figure 1.9. Proposed pathways for DAT, PAT, and SL-1 biosynthesis.

Figure 1.10. The regulatory network in response to cell wall stress involving SigE.

Figure 1.11. Simplified schematic diagram of *M. tuberculosis* electron transport chain and ATP synthase.

Figure 2.1. 2B8 inhibits growth of *M. tuberculosis*.

Figure 2.2. Inhibition of *M. tuberculosis* growth by 2B8 is removed by washing the culture.

Figure 2.3. 2B8 treated *M. tuberculosis* failed to thrive in the presence of carbenicillin.

Figure 2.4. 2B8 affects normal growth of *M. tuberculosis* H37Rv.

Figure 2.5. 2B8 potentiates mycobactericidal activity of  $\beta$ -lactams.

Figure 2.6. Transcriptional responses of *M. tuberculosis* to 2B8.

Figure 3.1.  $\beta$ -lactamase is not directly inhibited by 2-AI compounds.

Figure 3.2. Reduced  $\beta$ -lactamase activity in 2-AI treated *M. tuberculosis* CFP resulting from lower protein secretion.

Figure 3.3. 2-AI treatment alters cell envelope lipid composition of *M. tuberculosis*.

Figure 3.4. 2-AI treatment reduces MAMEs from extractable lipids in *M. tuberculosis*.

Figure 3.5. 2-AI treatment reduces free mycolic acids in *M. tuberculosis*.

Figure 3.6. 2-AI treatment increased *M. tuberculosis* sensitivity to SDS and permeability to nucleic acid staining dyes.

Figure 3.7. 2B8 treatment increased *M. tuberculosis* net accumulation of nucleic acid staining dyes.

Figure 3.8. 2B8 acutely increases binding of BODIPY® FL vancomycin and BOCILLIN® to *M. tuberculosis* while having no effect on cell membrane integrity.

Figure 3.9. 2-AI increased penicillin V and vancomycin binding to *M. tuberculosis*.

Figure 3.10. Unlabeled vancomycin competitively inhibits binding of BODIPY® FL vancomycin to *M. tuberculosis*.

Figure 4.1. 2B8 inhibits alamarblue® reduction by mycobacteria.

Figure 4.2. 2B8 depolarizes *M. smegmatis* membrane potential.

Figure 4.3. 2B8 collapses  $\Delta pH$  in mycobacterial IMVs.

Figure 4.4. Presence of BSA determines the outcome of 2B8 and CCCP-mediated changes in *M. smegmatis* respiration.

Figure 4.5. 2B8 increases *M. smegmatis* respiration at low concentration.

Figure 4.6. 2B8 increases *M. tuberculosis* respiration at low concentrations.

Figure 4.7. 2B8 prevents CCCP from increasing OCR further.

Figure 4.8. 2B8 reduces *M. tuberculosis* intracellular ATP levels.

Figure 4.9. 2B8 blocks ETC activity in mycobacterial IMVs.

Figure 4.10. 2B8 alters *M. tuberculosis* NADH/NAD<sup>+</sup> ratio.

Figure 4.11. 2B8 blocks NADH oxidation by mycobacterial IMVs.

Figure 4.12. CFZ partially rescues 2B8-induced blockage of NADH oxidation.

Figure 4.13. Diagram of 2B8's effect on mycobacterial membrane bioenergetics.

## CHAPTER ONE

### Review of literature

#### 1.1. Introduction: Tuberculosis and *Mycobacterium tuberculosis*

##### 1.1.1. History of tuberculosis

Tuberculosis (TB), caused by *Mycobacterium tuberculosis* (*M. tuberculosis*), is an ancient disease. There is evidence of the first *M. tuberculosis* infection in humans occurring approximately 9,000 years ago [1]. After the investigation into evolutionary origin of *M. tuberculosis* complex, investigators concluded that the common ancestor of *M. tuberculosis* complex was a human-specific bacterial pathogen. With the domestication of animals and expansion of agriculture, other members of the complex, such as *Mycobacterium bovis*, branched out and adapted to additional non-human hosts [2]. There is very little known about TB incidence before the 19<sup>th</sup> century, but the familiar clinical manifestations among people from different geographical regions resulted in a disease with different names like phthisis, consumption or the great white plague [3].

On March 24<sup>th</sup>, 1882, Robert Koch presented a finding that revolutionized the field of infectious disease where he revealed that he identified the causative agent of TB as a rod-shaped bacillus. Not only was the discovery significant in the sense that it shed light to etiological agent of the deadliest human disease at that time, but also it was Koch's experimental approach and techniques he employed that became a paradigm-shifting concept in the world of medical microbiology. Later came to be known as "Koch's Postulates", the set of criteria Koch used to identify the causative agent of TB gave the world a strategy to discover the etiology of other infectious diseases and also ways to treat or prevent them [4]. Eight years after his discovery, Koch claimed to have successfully treated TB with his new medicine made from extracts of the bacilli, tuberculin. Treatment with tuberculin was attempted in patients who flew from all over the world only to conclude later that the treatment was not therapeutically effective [5].

Unfortunately, following this initial treatment failure, there were no significant advances in controlling the spread of TB until the mid-20<sup>th</sup> century.

In the 1920s, the first vaccine for TB would be developed by Albert Calmette and Camille Guérin. This attenuated strain of *Mycobacterium bovis*, named BCG (bacilli Calmette-Guérin), however does not offer complete protection against the disease (more reviews on vaccines below) [6, 7].

Additionally, Selman Waksman developed the first antibiotics effective against the bacilli, streptomycin, in 1943 [7]. A series of antimicrobial agents were introduced after streptomycin in attempt to cure TB, but new drugs are still needed and being developed to treat the more recent resurgence in TB. Even after more than 130 years since the discovery of the etiological agent, controlling the spread of TB remains challenging due to the lack of an effective vaccine to prevent infections and new antimicrobial drugs that are effective against drug-susceptible and multidrug-resistant strains (MDR-TB) of *M. tuberculosis*.

## **1.2. Global burden of tuberculosis**

Although TB is an ancient disease as stated above, it is by no means a disease of the past. Despite the global incidence rate of TB reaching its peak at 2004 and slowly declining [8], global TB incidences in 2015 was estimated at 10.4 million which is about an 800,000 increase from prior year's 9.6 million according to the most recent TB report by WHO (2016). This indicates that the decline in incidence rate is not keeping pace with exponential global population growth.

The WHO implemented “End TB Strategy” in 2014 highlighting milestones to reach by 2020 including 20% reduction in TB incidence. The average decrease in TB incidence was 1.5% between 2014 and 2015 (average of 1.4% for prior ten years). There would need to be at least a 5% decrease per year to meet the goal set by End TB Strategy by 2020. Also, it should be noted that 60% of these cases were concentrated in countries including India, Indonesia, China, Nigeria, Pakistan, and South Africa [9]. While western Europe and North America experienced a dramatic fall of TB incidence during 20<sup>th</sup> century, under-developed countries did not benefit from the same trend [10]. This disparity is probably linked to socioeconomic factors such as high population density or malnutrition, as well as various TB

risk factors. For instance, co-infection cases of TB and human immunodeficiency virus (HIV) was over 50% in southern Africa [9] and diabetes co-morbidity was responsible for about 20% of TB cases in India in 2000 [11]. Worldwide, TB remains the number one cause of death humans from an infectious agent [9]. In the absence of the anti-TB drug treatment, 70% of the sputum smear-positive patients and 20% of culture-positive patients with pulmonary TB will die [12]. Advancement in TB treatment with anti-TB drugs prevented an estimated 39 million deaths between 2000 and 2015 in HIV-negative patients while overall deaths from TB continued to drop from 1.8 million in 2000 to 1.4 million in 2015. However, the global case fatality ratio in 2015 was 17% which still needs to be reduced to at least 10% by 2020 to meet the End TB Strategy milestone [9].

In sum, although significant progress has been made in decreasing incidence and death from TB, it remains a major public health problem due to the lack of sensitive and specific diagnostics, vaccines that prevent infection and new antimicrobial drugs that are effective as short-course therapy. Therefore the principal research challenge remains the development of new strategies to overcome these obstacles.

### **1.1.3. The bacilli**

*M. tuberculosis* is a non-spore forming, non-motile, aerobic, human pathogen in the genus Mycobacterium (the phylum Actinobacteria, the class Actinobacteria, the order Actinomycetales, the suborder Corynebacterineae, and the family Mycobacteriaceae). It is one of the 9 species that constitute the *Mycobacterium tuberculosis* complex. Microscopically, the organism is a rod-shaped bacillus, often forming a rope-like structures referred to as “cording”. It is unique in the sense that its cell wall resist decolorization process by acid-alcohol thus is neither classified as gram-positive or gram-negative, but as being acid-fast. Therefore, specialized staining techniques such as Ziehl-Neelsen or fluorescent staining using auramine are required for visualization microscopically [13].

Laboratory culture of *M. tuberculosis* can be accomplished by using egg-based media Lowenstein-Jensen or Middlebrook 7H10 or 7H11 agar, with liquid culture in 7H9 broth being preferable for larger cultures. Doubling time for *M. tuberculosis* is approximately 20 h, which is considerably slower

compared to other bacteria and represents a challenge for both *in vitro* and *in vivo* studies [14]. In research laboratories, the most commonly used strain is *M. tuberculosis* H37Rv. The strain H37 was isolated from a chronic patient, and underwent serial passages in laboratory settings. Depending on the media it was cultured in, the strain exhibited different virulence phenotypes and the more virulent strain was named H37Rv [15]. In 1998, the complete genome of H37Rv strain was sequenced, which significantly advanced our understanding of the organism [16]. Although it is considered a standard laboratory strain across the world, there have been reports about polymorphism occurring over time in different laboratories. So caution should be used when comparing research results conducted in different laboratories using *M. tuberculosis* H37Rv [17].

#### **1.1.4. The disease**

As an aerobic pathogen, *M. tuberculosis* predominantly infects the human lung, the site of primary infection when spread by aerosols. In pulmonary TB, various respiratory symptoms including cough and sputum production may be accompanied by non-specific systemic signs such as fever, weight loss, and night sweats [14, 18]. Unusual clinical manifestation like spontaneous pneumothorax, dyspnea or hemoptysis can also be present in some cases [19]. Primary extrapulmonary TB is less common and represents a particular challenge in the diagnosis and treatment of TB. Organs that may be affected by *M. tuberculosis* other than lung include but not limited to lymph nodes, pleura, kidney, bones, joints and also the central nervous system [20].

#### **1.1.5. Disease progression**

The spectrum of infection by *M. tuberculosis* in a patient can be roughly divided into latent TB infection (LTBI) and active TB. Patients with LTBI are asymptomatic and are in non-transmissible state while active TB patient can potentially transmit the disease. Some patients can have active TB without showing any clinical symptoms, hence subclinical TB [14]. TB can be contracted by inhalation of aerosols containing *M. tuberculosis* from a patient with active TB disease. Most healthy adults can

successfully clear *M. tuberculosis* or contain the infection but remain latently infected. It is estimated that a staggering 2 billion people globally have *M. tuberculosis* as have latent TB [21]. While the mechanism by which *M. tuberculosis* survives within the host without being eliminated or inducing clinical disease is not fully understood, our body of knowledge in TB immunopathology is constantly building.

Once *M. tuberculosis* enters the host, it is first recognized by the innate immune system via pattern recognition receptors on macrophages and dendritic cells, which may bind to *M. tuberculosis* cell envelope lipid components such as mannosylated lipoarabinomannan [22]. In the case of lung infection, alveolar macrophage or neutrophil engulfment of *M. tuberculosis* initiates a series of cell-mediated immune responses that are important in containing the infection. Other conventional bacteria are often eliminated by alveolar macrophages following phagolysosomal fusion and subsequent degradation, but *M. tuberculosis* is uniquely capable of blocking the fusion between phagosomes and lysosomes of infected macrophages [23-25]. The inability of macrophages to clear bacilli provides an intracellular niche that *M. tuberculosis* can use in the early stages of establishing infection to survive inside the host. This leads to persistence of bacilli inside the lung along with sustained immune cell recruitment that leads to a balance between survival of *M. tuberculosis* and bacterial killing by the host immune system. In most cases, these events will culminate in granuloma formation which is a cellular structure comprised mostly of infected and non-infected macrophages, lymphocytes, plasma cells and neutrophils admixed with lung epithelial and mesenchymal cells. This hallmark structure of mycobacterial disease serves to contain localized infection and prevent further spread of the disease within and between hosts[26]. Granuloma formation, from the host's standpoint, is a double-edged sword because while it prevents further dissemination of the bacilli, it also provides a shielded microenvironment where bacilli can survive and persist even following antimicrobial drug therapy. Poor diffusion of antibiotics into granulomas also contribute to the possible emergence of drug-resistance strains because bacilli can be exposed to sub-therapeutic concentrations of drug over the course of treatment [27].

Cell death within the granuloma results in a central accumulation of caseonecrotic material that may facilitate eroding of airway walls, and when combined with destruction of extracellular matrices, can

lead to cavity formation. *M. tuberculosis* infections that progress to cavitary disease can contribute to the proliferation of large numbers of bacilli that can be expelled through airways to infect other susceptible hosts [28].

## **1.2. Problems in controlling global tuberculosis epidemic**

### **1.2.1. Vaccine**

Currently, BCG is the only approved vaccine available to prevent or mitigate the severity of TB. However, there is a significant amount of variability in the level of protection among individuals and human populations. For example, the accepted practice is to vaccinate infants shortly after birth which can lessen the severity of childhood TB disease, but its protective capacity wanes off gradually when the person reaches adolescence and adulthood [29]. Moreover, several recent studies suggest that there are concerns regarding BCG's efficacy even in infants. South African's BCG coverage is almost 95%, while TB is most common cause of bacterial meningitis in young children even though more than 80% of children who had TB meningitis received BCG vaccination at birth [30-32]. Therefore, there are numerous vaccine candidates in the development pipeline to replace or boost BCG vaccination.

The optimal pre-exposure TB vaccines would prevent *M. tuberculosis* infection despite the variability of host susceptibility. It would be safe and effective when administered to newborns alone or in conjunction with BCG. The second group of candidates is classified as preventive post-exposure vaccines and administered to patients with LTBI to prevent progression to active TB. The last group of vaccine candidates under development is for therapeutic purposes and would be administered to patients recently infected or currently receiving treatment for LTBI or active TB disease as a strategy to shorten antimicrobial drug therapy [9].

One vaccine candidate of note is MTBVAC, which is the first live-attenuated *M. tuberculosis* to enter human clinical trial to date. The vaccine strain contains multiple genes encoding important immunodominant proteins that are missing in BCG. [33, 34]. The virulence of the strain is attenuated by

deletion of virulence genes *phoP* and *fadD26*. Because of the deletion of these genes, MTBVAC is not able to properly regulate transcription of the PhoP regulon and is defective in phthiocerol dimycocerosates (PDIM) biosynthesis and export. By virtue of *phoP* deletion, MTBVAC lacks diacyl trehalose (DAT), polyacyl trehalose (PAT) and PDIM. This represents an example of a strategy to limit *M. tuberculosis* virulence by inhibiting the expression of the cell envelope lipid structure, which contributes to the ability of bacilli to survive in the face of host defense mechanisms. The *M. tuberculosis* cell envelope will be discussed below in more details in regards to conferring antibiotic resistance.

### **1.2.2. Diagnosis**

The prompt and accurate diagnosis of *M. tuberculosis* infection is imperative to successful TB treatment. For detection of LTBI, the tuberculin skin test (TST) and interferon- $\gamma$  release assays (IGRA) are most often used. The TST involves intradermal injection of purified protein derivative, and the intradermal injection site is monitored for a subsequent delayed type hypersensitivity response in patients that are infected or recently exposed. Positive reaction can result from BCG vaccination or non-tuberculous mycobacterial infection which is the major limitation for this method [35]. On the other hand, IGRA is an *in vitro* blood test that quantifies the production of interferon- $\gamma$  from T cells upon stimulation by *M. tuberculosis* antigens 6kDa early secretory antigenic target and culture filtrate protein 10 [36]. These antigens are more specific to *M. tuberculosis* hence increased specificity. However, both assays are not ideal in that they do not predict progression of positive individuals to active TB disease. The remaining challenge is to develop a test with high predictive value so LTBI patients with higher risks for developing active TB could be accurately identified.

For active TB, X-rays, positron emission tomography-computed tomography, sputum smear microscopy, culture-based identification, and molecular tests are used [37]. Microscopic visualization of the organism on a sputum smear has been the most widely used first-line diagnostic assay especially for resource poor settings. However, recent advanced technologies such as XpertMTB/RIF molecular assay is being recommended by WHO as the test of choice for identifying patients with active TB disease [38, 39].

In addition to general diagnosis of the disease, detection of drug-resistance is also a critical diagnostic procedure that will help determine the appropriate TB therapy. Both traditional culture-based method and molecular-based methods are being used. For example, the aforementioned XpertMTB/RIF can also detect resistance to rifampicin, one of the first line anti-TB drugs [40] and GenoTypeMTBDR detects drug-resistance to both of the first line anti-TB drugs, isoniazid and rifampicin [41]. Another important research agenda in the development of improved TB diagnostics is an identification of novel TB-specific biomarkers, either host-specific or pathogen-specific. Combination of several biomarkers may be of value for distinguishing various stages of TB infection [42].

### 1.2.3. Therapy

Recommendation by WHO states that LTBI treatment consists of 6 to 9 months of isoniazid alone, 3 months of isoniazid and rifampicin, or 3 to 4 months of rifampicin alone [43]. In the case of active TB, for drug-sensitive pulmonary TB, patients are recommended for treatment with combination of isoniazid, rifampicin, pyrazinamide, and ethambutol for initial intensive phase and then the use of isoniazid and rifampicin for a subsequent continuation phase, which may last as long as 26 weeks. Modifications are made depending on the feasibility of directly observed therapy and HIV status [44]. For drug-resistant TB, fluoroquinolones, aminoglycosides, thioamides, and oxazolidinones are considered (Table 1.1) [14].

**Table 1.1. List of WHO recommended antimicrobial agents for TB therapy.** For drug-susceptible TB, initial 2 months of group 1 drugs treatment followed by 4 months of continuation phase with isoniazid and rifampicin are needed.  $\beta$ -lactams are categorized as group 5, recommended only for the MDR-TB.

	Description	Drugs
Group 1	First-line oral anti-TB drugs	Isoniazid, rifampicin, pyrazinamide, ethambutol
Group 2	Injectables	Streptomycin, kanamycin, amikacin, capreomycin
Group 3	Fluoroquinolones	Ciprofloxacin, ofloxacin, levofloxacin
Group 4	Oral second-line anti-TB drugs	Ethionamide, cycloserine, P-amino-salicylic acid
Group 5	Only considered for MDR-TB	Clofazimine, linezolid, amoxicillin/clavulanic acid

There has been limited progress in the development of new TB drugs. Bedaquiline (BDQ), which was approved by the United States FDA in 2012, was the first new anti-TB drug developed and approved in nearly 40 years [45]. In 2014, another new drug called delamanid was approved in Europe for treatment of drug-resistant *M. tuberculosis* [43]. However, it goes without saying that we are in need of more effective anti-TB drugs or novel treatment strategies to stop the ongoing spread of TB. The current TB drug pipeline includes a large library of candidates in various stages of development and testing, but the answer to how many of them will prove to be effective remains unknown.

Among the limitations of current TB drug therapy remains the high incidence of toxic side effects from a combination of multiple drugs, which contributes to poor patient compliance, and most importantly, the emergence of drug-tolerance and drug-resistance. Along with the development of new drugs, an innovative strategy to potentiate the activity and efficacy of existing antimicrobial drugs and drug combinations is a viable and promising option.

#### **1.2.4. Research priorities**

From basic microbial physiology to translational medicine, basic TB research plays an essential role in developing new treatment strategies. Not only is the *in vivo* pathogenesis and immunopathology in humans and animals still poorly understood, but a simple diagnostic that can rapidly and accurately detect both LTBI and active TB is urgently needed. A vaccine that is substantially more effective than BCG is also urgently needed. Lastly, identification of new molecular targets to weaken *M. tuberculosis* and overcome resistance to existing antimicrobial agents is needed. Moreover implementation of innovative strategies to circumvent limitations associated with current TB chemotherapy would potentially revolutionize the field of TB treatment. The rest of this literature review will be focused on the background of this particular project, which aims to describe a novel adjunctive strategy to treat TB. The backdrop includes targeting specifically bacilli that express non-replicative drug-tolerance when cultured as surface-attached communities of *M. tuberculosis* and reversal of drug tolerance by 2-aminoimidazole (2-AI) based small molecule compounds. Finally, we show how 2-AI can be used to increase the

susceptibility of *M. tuberculosis* to the  $\beta$ -lactam class of antimicrobial drugs, which are currently underutilized the treatment of TB.

### **1.3. *M. tuberculosis* persistence that complicates TB therapy**

#### **1.3.1. Non-replicative persistence**

Persistence, or persistent infection, by *M. tuberculosis*, stems from a subpopulation of bacilli that survive inside the host for a prolonged period of time. Historical evidence from autopsy of accidental death victims or from diseases other than TB, show the persistence of *M. tuberculosis* in individuals without clinical evidence or signs of active TB disease [46]. Persistent bacilli can survive even following aggressive antimicrobial therapy or immune pressure that create a harsh microenvironment [47]. Surviving bacilli may be genetically identical or similar to that of the original infection or be completely different suggesting re-exposure, all of which can reactivate and progress to active TB disease. However, recently developed molecular typing methods are able to provide some indication that links the initial infecting strain with the strain associated with reactivation disease [48, 49].

It is important to appreciate the host micro-environment in the development of non-replicative persistence (NRP) and *M. tuberculosis* drug-tolerance. In pulmonary granulomatous lesions, *M. tuberculosis* encounters diverse micro-environmental conditions to which it has to adapt, regardless whether bacilli are intracellular or extracellular. The microenvironment can be unfavorable or hostile to bacilli as it can be hypoxic, low in pH, limited nutrient availability, or exert sustained oxidative stress [50, 51]. This variation and diversity in micro-environmental conditions induce heterogeneous populations of *M. tuberculosis* that differ in response to antimicrobial drug treatment and favor the persistence of the population which is genetically susceptible but drug-tolerant [52, 53].

The mechanism *M. tuberculosis* uses to survive and persist host or antimicrobial drug treatment pressure remains an unanswered mystery that TB researchers have struggled with for a long time. *In vitro* and *in vivo* survival strategies used by other bacteria such as spore formation has not been associated with

*M. tuberculosis* [16, 54]. It is thought that *M. tuberculosis* persistence is closely related to non-replicative state of bacilli, although this criterion cannot be applied to all cases of persisting infections. When surgical removal of tubercle lesion became a viable treatment option with advancement in antibiotics to limit TB disease progression, it created opportunities for investigators to examine the metabolic state of bacilli within tubercle lesions [55]. A pioneering study in 1961 described that, from the comparison of total microscopic counts of bacilli and counts of viable bacilli, total counts did not increase over viable bacilli. This indicated that constant load of bacilli did not result from steady state equilibrium between replication and death, but from either very slowly or non-replicating bacilli [56]. Other evidence supporting the importance of non-replicative persistent bacilli is that the antimicrobial agents that target actively dividing cells have reduced efficacy on persisting population of bacilli [57].

Multiple *in vitro* and *in vivo* models have been developed and adapted to study NRP in *M. tuberculosis*. These models aim to recapitulate various conditions *M. tuberculosis* might encounter inside the host and serve as a trigger to switch into non-replicative state. Factors that researchers have investigated include but are not limited to availability of nutrients, changes in pH, presence of specific growth-limiting products, and limited oxygen concentration [53]. The most famous *in vitro* model was developed by Wayne and colleagues in which *M. tuberculosis* was cultured *in vitro* in air-tight culture tubes with specific headspace-to-culture ratio that resulted in a time-dependent gradual depletion of oxygen [58]. When the environment inside the tubes became hypoxic, bacilli adapted a non-replicative state that made the anti-TB agent isoniazid less effective. However, the *in vitro* culture model contributed to the discovery of new effective therapeutic options against non-replicative bacilli, for example metronidazole [59]. This nutrient starvation model was also used to study NRP in which *M. tuberculosis* cultured in minimal media exhibited a metabolic shunt and subsequent shutdown. Nutrient starvation has been shown to trigger bacilli to a non-replicative state, which expressed tolerance to isoniazid, rifampicin and metronidazole, but remained susceptible to pyrazinamide [60, 61]. These and other *in vitro* models of stress induced NRP demonstrate the value of these assays have for screening compounds that may target NRP. While changing *M. tuberculosis* culture conditions can be used to induce NRP, the level of

complexity can be increased by including host factors to further mimic the *in vivo* micro-environment in human and animal hosts.

Experimental animal models compensate for some of the limitations of *in vitro* models by providing host factors that accumulate at the site of infection which also contribute to the expression of NRP by bacilli. Like humans, there are numerous host and pathogen factors that determine the host response to infection and thus the *in vivo* micro-environment that harbor persistent bacilli. Certain strains of mice are inherently more resistant to TB than humans, while transgenic strains with an immunosuppressed phenotype are highly susceptible. Low-dose *M. tuberculosis* infection of wild type C57BL/6 mice progress to a plateau phase in bacterial lung load after one month of infection [62]. This stationary equilibrium is thought to be the expression of NRP induced by developing adaptive immune response of the host to infection. In addition to natural immunity, the stress of antimicrobial drug treatment can induce NRP in which suboptimal drug treatment is withdrawn prior to the complete eradication of bacilli, thus leaving a residual population of non-replicating bacilli [63, 64]. The persistent subpopulation of bacilli in this model was not culturable under standard *in vitro* culture conditions, but residual, viable bacilli were able to proliferate and induce reactivation disease following administration of an immunosuppressive agent [65]. Other useful animal models include guinea pigs which are more susceptible to TB than mice and they also provide pathologic advantages as they respond to infection with lung lesions that more closely resemble the naturally occurring infection in humans compared to mice [66].

Changes in transcriptional regulation in response to various external stimuli provide valuable information for studying bacterial adaptation to hostile environments. In the Wayne model described above, a metabolic switch to preferentially use fatty acids as a main carbon source via process termed the glyoxylate shunt was observed [67]. With methods such as microarray or next generation RNA sequencing, whole-genome profiling in bacilli exposed to these different stress conditions is possible. Using these techniques, critical response regulators that dictate the transcription of genes were identified when exposed to hypoxic stresses, such as DosS/DosR two component system regulator [68]. Also, by

virtue of targeted mutagenesis, mutant *M. tuberculosis* strains that lack functional genes linked to the expression of NRP have been identified. To name a few, knockout of *icl* which cannot undergo the glyoxylate shunt during hypoxia due to lack of isocitrate lyase enzyme [69], deletion of *pcaA* that encodes cyclopropane synthase [70], and absence of transcriptional regulator WhiB3 [71] all resulted in reduced persistence in mice. From these single-gene replacement studies, several metabolic pathways have been identified as being involved in NRP. These include metabolic pathways such as: 1) alternative carbon assimilation, 2) protein degradation pathways, 3) cell wall biosynthesis and export pathways, and 4) bioenergetics-related pathways leading to the ATP production [72-76].

### **1.3.2. Phenotypic drug-tolerance and genotypic drug-resistance**

The persistence phenotype is closely linked to bacilli that also tolerate antimicrobial treatment *in vitro* and *in vivo*. Despite being genetically identical, subpopulations of bacilli can differ in the expression of drug-tolerance, which can be reversed once stressors are removed. This tolerance is referred to as phenotypic drug-tolerance [77]. Besides, displaying the non-replicating phenotype, these bacilli can withstand or tolerate transient exposure to even high dose of antibiotics. A good example of the expression of drug-tolerance are bacteria that form and survive within biofilms [78]. The persistence of extracellular and intracellular bacilli within granulomatous or necrotizing lesions has been equated to biofilm formation and may explain the ability to tolerate prolonged antimicrobial therapy [79], a finding that led to inception of this project, and will be discussed in more details later.

In TB, even in the drug-susceptible cases, a complete eradication of TB requires a minimum of 6 month of extensive chemotherapy and is presumed necessary to effectively eradicate these persistent bacilli [80]. Wallis and colleagues attempted to describe the relationship between drug-tolerance, persistence and reactivation. They observed that *M. tuberculosis* isolates from drug-susceptible TB patients harboring persistent bacilli and at risk of developing reactivation disease, showed significantly increased *in vitro* drug-tolerance compared to isolates from active TB patients [81]. This study

demonstrates that in even drug-susceptible TB cases *M. tuberculosis* can become tolerant to anti-TB drugs, however all the factors that contribute to this phenotype *in vitro* and *in vivo* are unknown.

Drug-resistance, on the other hand, refers to the decreased sensitivity to antimicrobial drugs as the result of a mutation in genes involved in the drug binding, uptake or metabolism. The consequence of altered gene expression, such as mutations in drug targets, a loss of enzymes that activate drugs, and expression of efflux pumps can all manifest as drug-resistance. In the basic TB therapeutic regimens, five first line anti-TB drugs are used: isoniazid, rifampicin, ethambutol, pyrazinamide, and streptomycin. Resistance to isoniazid and rifampicin give rise to MDR-TB. Isoniazid was one of the first anti-TB drugs to be discovered and was introduced in 1952. Isoniazid functions as a pro-drug which requires enzymatic activation by catalase/oxidase KatG (encoded by *katG*). However, a recent study conducted with uninfected mice treated with isoniazid identified a novel metabolite 4-isonicotinoylnicotinamide, which is produced by *M. tuberculosis* via KatG [82]. This study suggests that isoniazid can also be activated by the host. Isoniazid inhibits biosynthesis of mycolic acid through acyl carrier protein reductase encoded by *inhA*. Both mutation in *katG* and *inhA* may confer resistance to isoniazid [83-86]. Rifampicin was introduced in 1972 and is used in combination with isoniazid as the basic multi-drug therapy for TB. It targets  $\beta$ -subunit of RNA polymerase and resistance can arise from mutation of gene that encodes *rpoB* [87]. Genotypic drug-resistance has been also revealed in other first and second line anti-TB drugs, as well as most recently developed BDQ [88]. BDQ is a diarylquinolone, which targets *M. tuberculosis* ATP synthase. Thus, mutation in *atpE* encoding for the F<sub>0</sub> subunit of the ATP synthase can confer resistance to BDQ [89]. Recently, it was shown that up regulation of efflux pump through mutation also induces antimicrobial drug-resistance [90].

In 2015, approximately 3.9% of new TB cases were considered multidrug-resistant. An estimated 21% of previously treated cases were confirmed MDR-TB as well. Problems with MDR-TB are only intensifying, as high TB burden countries showed accelerated increase MDR-TB cases compared to drug-susceptible cases (or slower decrease in countries with decreasing TB burden). Surveys have identified even more drug-resistant strains, including extensively drug-resistant (XDR-TB, MDR-TB with

resistance to at least one fluoroquinolone and a second line injectable agent), revealed that estimated 9.5% of MDR-TB was XDR-TB [9]. To make matters worse, *M. tuberculosis* resistant to all drugs available for TB therapy has been described recently as a totally drug-resistant case [91]. Taken together, the issue of emerging drug-resistance will remain a concern and will continue to demand new TB drug treatment strategies.

### **1.3.3. Intrinsic drug-resistance**

Yet another type of drug-resistance that can be exhibited by bacteria is intrinsic or inherent resistance. This type of resistance stems not from spontaneous genetic mutations but from the bacteria's natural structural or functional properties that allows them to resist activity of particular antimicrobial agents [92, 93]. Intrinsic drug-resistance can be expressed from the lack of target in the organism, inaccessibility of drug to its target site due to impermeability, highly efficient naturally occurring efflux pumps, and production of enzyme that inactivates the drug [94]. For example, both *Mycobacterium smegmatis* (*M. smegmatis*) and *M. tuberculosis* complex are naturally resistant to macrolides antibiotics owing to the presence of 23S rRNA methylase encoded by *erm* gene [95]. When the enzyme methylates the 23S rRNA, it leads to reduced affinity of the macrolide for the target [96, 97]. Intrinsic resistance of *M. tuberculosis* to antimicrobial agents will be discussed more in depth later in this chapter.

## **1.4. Similarities between *M. tuberculosis* in granulomatous lesions and biofilms**

### **1.4.1. Biofilms**

In some biofilm-forming bacteria, adhesion to abiotic or biotic surface is the earliest step in the formation of multicellular communities embedded in pathogen- or host-derived extracellular polymeric substances (EPS). This unique alternative form of bacterial life provides a survival advantage and the ability to persistence in harsh microenvironments [98, 99]. Not only the biofilm structure, but constant on-going intercellular communication within the community makes this form of existence significantly distinct from free-living planktonic mode of growth in bacteria.

The very first step in biofilm formation is adherence or attachment to biotic or abiotic surfaces. Attached bacteria can be released from the communities passively by hydrodynamic forces or voluntarily depending on changes in gene expression or in the environment [100-102]. The microbial attachment becomes irreversible with the aid of specialized organelles such as pili in *Escherichia coli* (*E. coli*) and other adhesion proteins that attach to eukaryotic extracellular matrix such as SagA in *Enterococcus* species [103, 104]. Firm attachment to the surfaces triggers subsequent transcriptional alterations in bacteria, leading to up-regulation of proteins that can produce EPS. EPS serve as structural scaffold, which promote cohesion between resident bacteria. EPS also augment the attachment as shown in *Pseudomonas aeruginosa* (*P. aeruginosa*) Psl, which facilitates bacterial adhesion to mucin and CdrA, which further stabilize the structure by binding to Psl [105, 106]. In general, EPS are comprised of sugars like polysaccharides, as well as proteins, lipids, and nucleic acids [107]. Typically serving as a physical diffusion barrier, EPS also serves as a mechanical barrier from hostile conditions. For example, EPS decelerate or block antimicrobial agents from reaching their target bacteria within biofilms. Alginate exopolysaccharide of *P. aeruginosa* is anionic EPS, which can bind to positively charged antibiotics like fluoroquinolones and sequester the drugs [108, 109]. They also accumulate signaling molecules to high enough concentrations that can also interfere with effective cell to cell communication [110]. These signaling molecules are produced by bacteria and accumulate to reach specific threshold levels, which can lead to the induction of gene expression related to various enzyme or EPS synthesis. This concentration-dependent physiological response to chemical signaling is referred to as quorum sensing in biofilms [111-113]. Once the environmental cues that initiate biofilm formation are removed, dispersal of the structure becomes an option. Also, increases in toxic byproducts of metabolism inside the biofilm can also trigger dispersion as well [114]. In *P. aeruginosa*, reduction of cyclic di-GMP plays important role in shifting from attached to the free-living planktonic lifestyle [115]. Also, EPS degrading enzymes and production of surfactants can detach bacteria from surfaces [116].

Biofilms cause problems in industrial settings contaminating water lines, pipelines and in medical devices like catheters and implants. They also create problems during infections of hosts because biofilms

are more refractory to antibiotic treatment compared to their planktonic counterparts [117-120]. Multiple strategies have been suggested to combat biofilms that resist antibiotics, including phage therapy and silver nanoparticles [121, 122]. Also, inhibition of attachment, the initial step of biofilm formation has also been explored. Compounds such as monomeric biphenyl mannosides as inhibitors of fimbriae encoded by *E. coli* FimH has led to successful prevention of biofilm formation [123]. Interfering with quorum-sensing system, as such as blocking two component system response regulators QseBC in *E. coli*, has also been shown to be a promising approach, since it does not exert selective pressure on bacteria therefore side-stepping emergence of drug-resistance [124]. In addition, enzymes that result in EPS destruction or chelating agents to eliminate critical metal cations from EPS are also potential options available [125, 126].

#### **1.4.2. Drug-tolerance and drug-resistance in biofilm-forming bacteria**

Arguably, the most clinically important feature of biofilms and biofilm-forming bacteria in infectious disease is drug-tolerance and drug-resistance [127]. First of all, as mentioned earlier, the EPS of biofilms form a physical permeability barrier to limit penetration of some antimicrobial agents, which can be degraded by enzymes within the biofilm matrix.

Another important factor contributing to drug-tolerance and drug-resistance is heterogeneity and slow growth leading to persistent phenotype of bacteria. Different areas of biofilm were stained using acridine orange, demonstrating diversity of bacterial populations in terms of metabolic heterogeneity [109]. Depending on the location of the bacteria and individual subpopulations within biofilms, chemical parameters such as pH, oxygen concentration, and nutrient availability vary dramatically which are driving force of bacterial phenotypic diversity [128]. Limiting oxygen concentration also affects the antimicrobial agents itself, shown by hampered action of aminoglycosides driven by low oxygen availability [129]. Nutrients are relatively more abundant near outer boundary of biofilms. Therefore, bacteria residing near the surface of the biofilms will have easier access to nutrients required for survival, proliferation and dispersion. On the other hand, bacteria located toward the center of the biofilms have

less access to nutrients, thus are less metabolically active. These organisms are more resistant to antibiotics, especially drugs in which the mode of actions targets cell division or molecular biosynthesis [130].

Biofilm-forming bacteria that express this type of phenotypic drug-tolerance display striking resemblance to non-replicating persistent subpopulation of *M. tuberculosis* *in vitro* and *in vivo*. Following antimicrobial drug treatment, the majority of bacteria are killed but subpopulations of bacteria survive, thus requiring prolonged drug treatment [131]. The treatment of active TB disease even from drug-sensitive *M. tuberculosis* necessitates prolonged treatment with a combination of antimicrobial drugs to eradicate persistent subpopulations of drug-tolerant bacilli [49]. Importantly, certain persistence genes have been described in biofilm-forming bacteria and multiple genes have also been implicated in the persistence of *M. tuberculosis* [132-134]. When antimicrobial treatments are removed, both persistent bacteria in biofilms and persistent *M. tuberculosis* retain the ability to resume normal growth and thus can lead to reactivation of the disease [135].

Most mycobacterial species will form a biofilm-like structure called a pellicle at the liquid-air interface *in vitro* when they are cultured without any detergent [136, 137]. Furthermore, when Kolter and colleagues attempted to survey any genetic elements that were required for biofilm formation in mycobacteria, they identified acetylated glycopeptidolipid being essential for attachment to abiotic surface in *M. smegmatis* [138]. Later on, a non-essential chaperone GroEL1 was identified to be important in the KasA interaction, which is the enzyme required for mycolic acid biosynthesis and its loss conferred a defect in the biofilm maturation stage in *M. smegmatis* [139]. These *in vitro* studies indicate that such surface-attached complex structures of mycobacterial species have characteristics of biofilm formation of initial attachment, maturation, and dispersal. Whether *M. tuberculosis* bacilli actually form biofilm *in vivo* upon infection is still debatable but similarities of non-replicating persistent *M. tuberculosis* and biofilm-forming bacteria suggest that *M. tuberculosis* may also adopt biofilm-like communities as a strategy to persist inside the host as extracellular multicellular structures. These similarities include phenotypic drug-tolerance, formation of surface-attached communities that follow

distinctive developmental stages that require specific genes, and also induction of formation that are triggered by external stress factors such as thiol reductive stress that elicit formation of *M. tuberculosis* biofilms [140, 141]. Therefore, prevention and dispersal strategies for biofilms represent another treatment strategy to specifically target persisting *M. tuberculosis*.

### **1.4.3. Focus on extracellular *M. tuberculosis* within granulomatous lesion**

When Canetti and colleagues conducted extensive histopathological examination of TB lesions from autopsies in 1955, they reported multiple cases of extracellular *M. tuberculosis* present in the host as clustered multicellular communities [142]. A study to determine the location of persisting *M. tuberculosis* *in vivo* within animal model lesions was conducted by Lenaerts and colleagues [143]. By examining guinea pig lung lesions from *M. tuberculosis* infection following anti-TB drug treatment, the group found that bacilli surviving were mostly situated extracellular, especially in an acellular rim of the primary granuloma lesions. Further follow up studies indicated that extracellular persistent bacilli were mixed within a milieu composed of host-derived cellular debris including extracellular DNAs (eDNA) (Figure 1.1) [79]. The multifaceted importance of eDNA derived from both host and pathogen in biofilm and host immunity has been shown previously in other bacterial species [144]. *Staphylococcus aureus* (*S. aureus*) secrete eDNA that promotes amyloid fiber formation which is crucial for its biofilm formation while eDNA in *P. aeruginosa* biofilm can present antimicrobial activity by cation chelation that induce destabilization of lipopolysaccharide [145, 146]. The prime example of host-derived eDNA contributing to host immunity is neutrophil extracellular traps where neutrophils secrete chromatin and other antimicrobial proteins to form structures that can entrap and confine bacteria [147]. However, perhaps the most important role of eDNA in host-pathogen interaction is associated with being a major component of the EPS in bacterial biofilms [148]. The presence of abundant host-derived eDNA associated with extracellular *M. tuberculosis* populations in necrotic lesions provided visual evidence that persistent *M. tuberculosis* *in vivo* shares common characteristics with biofilms from other bacteria which are also associated with host- or pathogen-derived eDNA. Stimulated by this observation, our group developed a

novel *in vitro* *M. tuberculosis* culture system that more closely mimics the *in vivo* microenvironment in animals and humans.

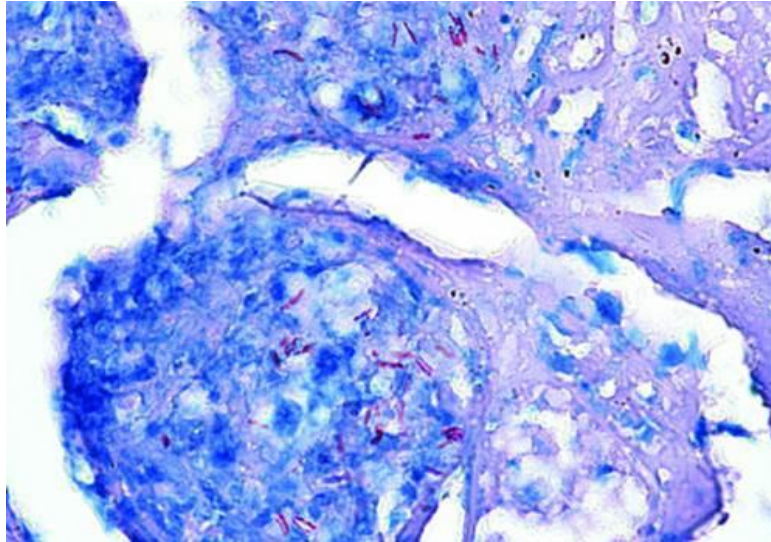


**Figure 1.1. Location of extracellular acid-fast bacilli in the acellular rim of the primary TB granuloma.** Primary lung lesion of an *M. tuberculosis*-infected guinea pig treated for 6 weeks with TMC207 (BDQ) is shown. Extracellular *M. tuberculosis* (red) bacilli are forming micro-communities associated within the acellular necrotic lesions.  $\times 400$ , acid fast staining. Adapted with permission from reference [143].

#### 1.4.4. *M. tuberculosis in vitro* drug-tolerance model using host derived factors

In mycobacteria including *M. tuberculosis*, many biofilms studies have focused on what is called a pellicle which forms at the liquid-air surface of the culture. Ojha and colleagues conducted studies using this culture model both in *M. smegmatis* and *M. tuberculosis*. Pellicles from both organisms contain rich levels of free mycolic acid and mutation in genes responsible for mycolic acid synthesis such as *kasB* resulted in defective biofilm formation [139, 149-151]. While this pellicle model represent a valuable model to differentiate between biofilm and planktonic *M. tuberculosis*, we reasoned that this model lacks a constituent of persistent bacilli within actual lesions, which is the host-derived macromolecules.

In an attempt to fill in this gap of current pellicle model, we developed a novel culture system in which we allowed *M. tuberculosis* to attach to either abiotic surfaces or a biotic surface in the form of

lysed human leukocytes [152]. We employed three modes of *M. tuberculosis* growth by removing or adding supplemental materials in RPMI mammalian cell culture media. First, to represent normal laboratory culture settings, the detergent tween 80 was added to establish non-aggregated, planktonic culture. Next, we removed tween 80 so *M. tuberculosis* bacilli can settle to the bottom of the culture material and attach to an abiotic surface. Lastly, in the media without any detergent, we provided lysed human leukocytes additionally for *M. tuberculosis* to attach to host derived macromolecules instead of abiotic surfaces. In this *in vitro* culture model, *M. tuberculosis* attached to abiotic or biotic surface expressed high level of drug-tolerance by tolerating up to ten-fold concentration of isoniazid MIC. Similar to biofilms in other bacteria, treatment of attached *M. tuberculosis* cultures with DNase I partially restored isoniazid susceptibility which points to the fact that eDNA is at least one of the important elements of attached micro-communities in the culture model. This *in vitro* drug-tolerance model provided us with a valuable tool that we could use to screen multiple anti-biofilm compounds to identify one that is effective against *M. tuberculosis*.

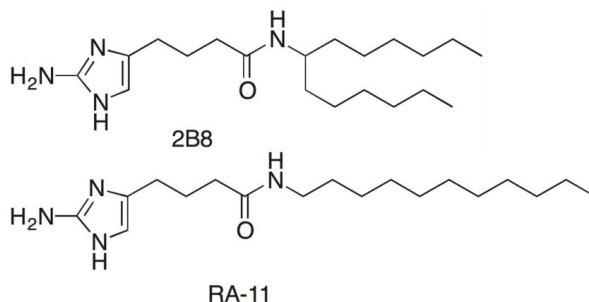
## **1.5. 2-AI based small molecules**

### **1.5.1. Origin**

Given the significance of biofilms in both industry and medical clinics, efforts have been made towards developing small molecules that can modulate the formation or dispersal of biofilms [135]. Our collaborator, Dr. Christian Melander, and his group focused on developing readily synthesizable small molecules from marine sponge species that are non-bactericidal, but have biofilm dispersing activity [153, 154]. Being a stationary life form, marine sponges need an antifouling mechanism to remove contaminating microorganism biofilms on their surfaces. Natural products from such marine sponges have provided this group with a scaffold from which to build a library of molecules having anti-biofilm properties [155-159]. One of the metabolites of interest was pyrrole-imidazoles. These are produced only by marine sponges as metabolites from Agelasidae, Dyctionellidae, Hymeniacionidae, and Axinellidae

species, reported to have anti-biofilm effects in bacteria such as *Phodospirillum salaxigens* and *Vibrio vulnificus* [160]. The structure that was common across all pyrrole-imidazoles was a 2-AI ring (Figure 1.2). Melander and colleagues were able to synthesize a library of potent anti-biofilm compounds that contain a crucial 2-AI structural moiety found in these pyrrole-imidazoles [161-166].

The nitroimidazoles, which has a similar imidazole ring structure, have shown anti-TB potential under hypoxic conditions [167]. For example, metronidazole (5-nitroimidazole) is being used to treat anaerobic bacterial infection and previously has been shown to have an effect to *M. tuberculosis* under hypoxic environments. However, metronidazole is not being used in current TB therapy because activity is limited against aerobic *M. tuberculosis* [59, 168, 169]. Further investigation into this compound has led to the identification of 4-nitroimidazo-oxine (PA-824), which has been shown to be effective against both aerobic and anaerobic populations of *M. tuberculosis* [170]. The important distinguishable features of PA-824 from metronidazole were: 1) nitro group location, 2) the presence of a lipophilic side chain, 3) the charged state of 2-position of nitroimidazole ring, and 4) being a monocyclic rather than bicyclic molecule [171]. The biological activity of nitroimidazoles and 2-AIs are likely different, considering the importance of the nitro group in nitroimidazoles for its activity. However, the previous work with nitroimidazoles show the importance of structure-activity relationships in this type of small molecule particularly against *M. tuberculosis* which will be discussed later in this dissertation concerning different types of 2-AI compounds that vary in efficacy and potency.



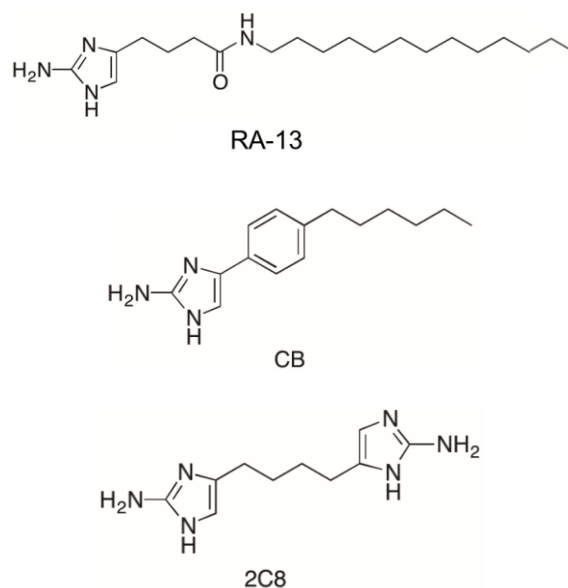


**Figure 1.2. Structures of 2-AI compounds used in this study.** The pKa for 2-AIs is 8.5 in general, and logD, a measure of lipophilicity at pH 7.4, is calculated as follows: 2B8 (2.76), RA11 (3.15), RA13 (4.04). RA13 has two additional carbon chains at the long-end of alkyl chain of RA11. Structures were initially published in reference [172].

### 1.5.2. 2-AI and other bacteria

Not only do 2-AI compounds have anti-biofilm properties, but they also had other biological activities that have potential clinical value. The class of compounds also reversed phenotypic drug-tolerance and genotypic drug-resistance in human pathogenic bacteria. With the emergence of drug-resistance across multiple clinically important bacterial pathogens, a variety of fields in medicine are impacted by the failure of antibiotic treatment to treat infections. In fact, WHO designated multi-drug-resistant bacteria as one of the top public health threats and CDC recently published a list of the top 18 drug-resistant bacterial pathogens that threaten global health [173, 174]. The benefit gained from the development of new antibiotics has been offset by the ongoing emergence of bacterial resistance. For instance, *Enterococcus faecium* and methicillin-resistant *S. aureus* (MRSA) both developed resistance against daptomycin less than a year after its introduction to the clinic [175].

One strategy that can be used to solve this problem would be the prolonged use of antibiotic cocktails. Current first line TB therapeutic regimens consist of a combination of isoniazid, rifampicin,

ethambutol, and pyrazinamide, used to treat drug-sensitive strains of *M. tuberculosis*. Another approach is combining a compound that may lack specific bactericidal effects but potentiate the activity of known antibiotics as an adjunctive therapy. The complementing compound, or adjuvant, aims to potentiate antimicrobial activity by blocking resistance mechanisms [176]. For example, enzymatic hydrolysis of  $\beta$ -lactams by  $\beta$ -lactamase can be blocked by the presence of the  $\beta$ -lactamase inhibitor clavulanic acid. Bacterial efflux pumps can also be targeted by efflux pump inhibitors to reduce the extrusion of antibiotics from inside the cells [177]. As an adjuvant, 2-AI compounds have been shown to suppress carbapenem resistance in *Klebsiella pneumoniae* (*K. pneumoniae*), oxacillin resistance in MRSA, and colistin resistance in *Acinetobacter baumannii* [165, 178-181]. A series of studies show promising responses and the potential value in using 2-AI compounds to function as novel adjuvants combined with conventional antibiotics as a strategy to overcome drug resistance.

### **1.5.3. Reversal of *M. tuberculosis* drug-tolerance by 2-AIs**

Because of the expression of drug tolerance by *M. tuberculosis* cultured as attached microbial communities *in vitro*, this model system has value in the screening of new drugs that specifically target persistent, non-replicating bacilli *in vivo*. Wang and colleague recently showed a small molecule called TCA1 successfully inhibited *M. tuberculosis* biofilm formation and exhibited bactericidal activity *in vitro* [182]. The mycobacterial biofilm model developed in our laboratory was instrumental in the discovery that 2-AI based small molecules not only inhibited and dispersed *M. tuberculosis* biofilms, but these compounds effectively reversed phenotypic tolerance to conventional anti-TB drugs isoniazid and rifampicin either alone or in combination. The Melander group screened an array of 2-AI compounds against *M. smegmatis* for anti-biofilm activity and selected 10 candidates based on the ability to reverse isoniazid drug tolerance in our *in vitro* model. *M. tuberculosis* grown in a variety of different culture conditions including planktonic, surface-attached untreated plastic wells, or surface-attached lysed human neutrophils, were treated with 2-AI compounds either alone or in combination with isoniazid. To surface-attached drug-tolerant *M. tuberculosis*, combination treatment restored isoniazid susceptibility as shown

by dose-dependent drop of minimum inhibitory concentration (MIC) (Figure 1.3) [172]. From this study, we further explored the feasibility of using 2-AI compounds as antimicrobial adjuvants to specifically target drug-tolerant and drug-resistant *M. tuberculosis*. The rationale was that this combination therapy had the potential to potentiate the activity of conventional anti-TB drugs against mixed populations of drug tolerant bacilli and thus represented a novel treatment strategy that could not only shorten treatment TB treatment intervals but also be effective against drug resistant strains of *M. tuberculosis*. This dissertation was built upon a serendipitous but keen observation that 2-AI compounds increased the effectiveness of the  $\beta$ -lactam class of antimicrobials drugs that are not clinically effective against *M. tuberculosis*. This approach has the potential to not only expand the number of available drugs to treat TB but represented a completely new strategy to treat drug resistant strains of *M. tuberculosis* as well.

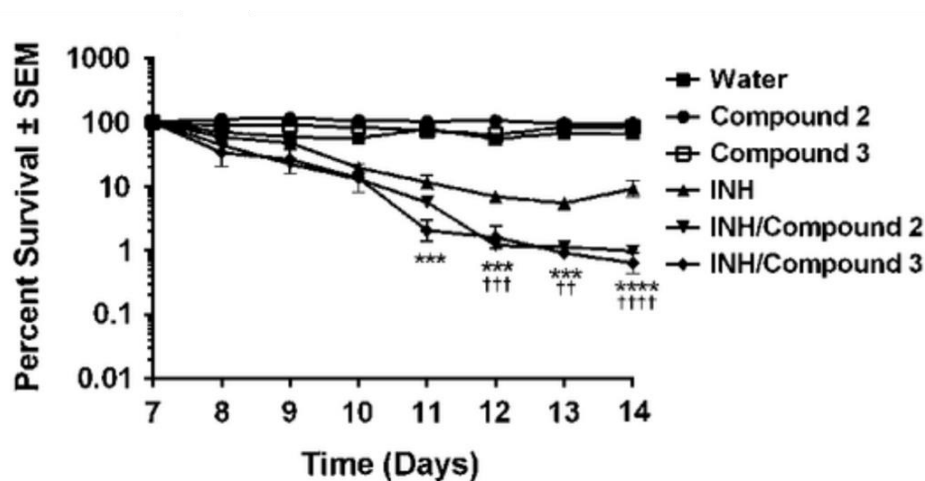


**Figure 1.3. Reversal of isoniazid tolerance by 2-AI compounds.** Combined treatment with 2-AI compounds potentiates the bactericidal activity of isoniazid (INH) against drug-tolerant *M. tuberculosis*. Adapted from reference [172] with permission.

### 1.6. $\beta$ -lactam antibiotics and tuberculosis

The concept of one organism antagonizing the growth of others has been a subject of microbiology research for decades. The practice of applying organic materials or chemicals toward

wound-healing process dates back to ancient times [183]. Discovery of the  $\beta$ -lactam class of antibiotics hold a special place in the history as they were the first antibiotics introduced and used to treat human infections [184].

The large family of  $\beta$ -lactams includes penicillins, cephalosporins, carbapenems, monobactams, and cephamycins [185]. Penicillin, the first  $\beta$ -lactam, was isolated from the saprophytic fungus *Penicillium notatum* by Alexander Flemming in 1928, although several other researchers had also encountered antagonistic activity of *Penicillium* mold against bacteria. The value of treating patients with penicillin was not immediately recognized and was not used as a clinical therapeutic agent until the 1940s [186]. The common  $\beta$ -lactam ring structure, which is conserved throughout the class of antibiotics was revealed in 1945 using X-ray crystallography. Resistance to penicillins due to the hydrolysis of the antibiotic by  $\beta$ -lactamase enzyme was first reported shortly thereafter [187]. Penicillins include natural penicillin and its derivatives like penicillin G and V, as well as methicillin, oxacillin and ampicillin [188]. Additionally, *Cephalosporium acremonium* producing broad spectrum antibiotic activity was isolated by Giuseppe Brotzu and the penicillin-like substance was named cephalosporin C, which later paved the way to semi-synthetic mass production of Cephalothin in 1962 [189]. Cephalosporins are further classified as first-, second-, third-, and fourth-generation cephalosporins.

Subsequently, other semi-synthetic cephalosporin related  $\beta$ -lactams like cephamycins were introduced. Cefoxitin is a well-known cephamycin derived from *Streptomyces lactamdurans*. Carbapenems are especially valuable clinically because of their relative resistance to hydrolysis by the  $\beta$ -lactamase enzyme. Imipenem, a famous carbapenem, derived from *Streptomyces cattleya* shows broad spectrum of activity against a wide range of bacteria. Lastly, monobactam antibiotics produced by *Chromobacterium violaceum* also shows good activity against gram-negative bacteria. Clavulanate, the first  $\beta$ -lactamase inhibitor, was discovered in 1976 and was recognized as a potential adjunctive therapy when used in combination with  $\beta$ -lactams. Semi-synthetic  $\beta$ -lactamase inhibitors sulbactam and tazobactam are also available for use today, and a novel  $\beta$ -lactamase inhibitor active against virtually all existing  $\beta$ -lactamase is currently being evaluated in human clinical trials [184, 186, 190-192].

After the introduction of  $\beta$ -lactams for clinical applications, there was an increase in confidence within the medical community infectious diseases could be eradicated with the help of vaccination and new antibiotics. In fact, United States Surgeon General William Stewart even erroneously quoted in 1960s that “it is time to close the book on infectious diseases” [193]. However, this quote proved to be premature considering that emergence of antibiotic resistance is still one of the most significant public health problems even today. In 1940, Edward Abraham and Ernst Chain found enzymatic activity in the culture supernatant of penicillin-resistant bacteria, but failed to recover the same protein in cultures from penicillin-sensitive bacteria, which was the first description of  $\beta$ -lactamase [194]. The Abraham group also demonstrated that emergence of resistance can be induced by selective pressures from antibiotics by showing that staphylococci cultures become resistant to antibiotics following repeated sub-culturing in the presence of antibiotics [195]. Multi-drug-resistant staphylococci emerged in 1947, and drug-resistance in Gram-negative organisms such as *E. coli* and *K. pneumonia* soon followed [196, 197]. Despite the obvious challenges posed by the ongoing emergence of antimicrobial drug resistance,  $\beta$ -lactam antibiotics are still drugs of choice to combat a wide variety of bacterial infections without severe side effects.

$\beta$ -lactams are bactericidal drugs [198]. Contrary to mammalian cells, the bacterial cell membrane is further surrounded by cell wall, which represents an excellent target for antimicrobial agents. The deepest layer of bacterial cell wall is the peptidoglycan layer. The peptidoglycan structure is crucial for maintenance of cell envelope integrity. It is formed by cross-linking of polysaccharide structures through oligopeptide links and is thicker in Gram-positive bacteria compared to Gram-negative bacteria [199]. In mycobacteria, the peptidoglycan layer is further protected by a specialized cell wall complex, which will be discussed in depth later.

The peptidoglycan layer of bacteria is formed by macromolecules made of sugars cross-linked by short polypeptides. In general, the biosynthesis of the peptidoglycan layer occurs in three stages that take place in three different locations within bacterial cell. First, phosphoenolpyruvate, a lactate residue is derived and attached to N-acetylglucosamine (NAG), which is further processed to generate N-acetylmuramic acid (NAM). On NAM, peptidyl linkages are formed with an enzymatic addition of amino acids

with its terminal amino acid residue being D-alanyl, D-alanine [200]. This nascent subunit, NAM-pentapeptide, is formed inside the cytoplasm. During the second stage at the cytoplasmic membrane, the NAM-pentapeptide precursor is conjugated with lipid, which acts as a transporter, forming a structure called lipid I. This is further complexed by the addition of NAG to make lipid II and translocates toward the bacterial cell membrane exterior. The cross-linked and translocated molecule with the adjacent peptidoglycan strand is initiated by the enzyme transpeptidase also referred to as penicillin-binding-protein (PBP). In this reaction, PBP also releases the terminal D-alanine residue by the activity of the enzyme carboxypeptidase (Figure 1.4) [201-203]. In the simplest terms,  $\beta$ -lactams act by inhibition of peptidoglycan biosynthesis of the bacterial cell wall by having an analogous structure to D-alanyl, D-alanine. The CO-N bond situated in the  $\beta$ -lactam ring of the drug molecule is in the same location as the CO-N bond in D-alanyl,D-alanine dipeptide. By having this structural similarity,  $\beta$ -lactams preferentially bind to PBPs and irreversibly blocks transpeptidase activity of the enzyme. Thus, the final transpeptidation process in peptidoglycan biosynthesis cannot be completed and cell wall integrity is impaired [204]. Some antimicrobial agents other than  $\beta$ -lactams also target bacterial cell wall biosynthesis. For example, cycloserine inhibits D-alanyl,D-alanine formation by alanine racemase and alanine ligase blockage while vancomycin binds to the terminal D-alanyl,D-alanine dipeptide and prevents further cross-linking [205, 206].

Current TB therapy does not routinely include the use of the  $\beta$ -lactam class of antibiotics owing to intrinsic resistance expressed by *M. tuberculosis* [208].  $\beta$ -lactams are arguably the most valuable class of antimicrobial agents introduced to date, with a long history of being effective against a wide variety of bacterial pathogens. As a whole  $\beta$ -lactams account for more than 50% of all commercially available antibiotics up to the early 2000s [209]. Increasing interest in repurposing this class of safe and effective drugs has emerged recently, with the potential impact on the treatment of TB being of particular interest [210, 211]. In early attempts, amoxicillin was combined with clavulanic acid to treat TB, and more recently Barry and colleague showed limited *in vitro* and *in vivo* efficacy of meropenem/clavulanate combination, which led to a clinical trial targeting drug-resistant *M. tuberculosis*. Additionally, an oral

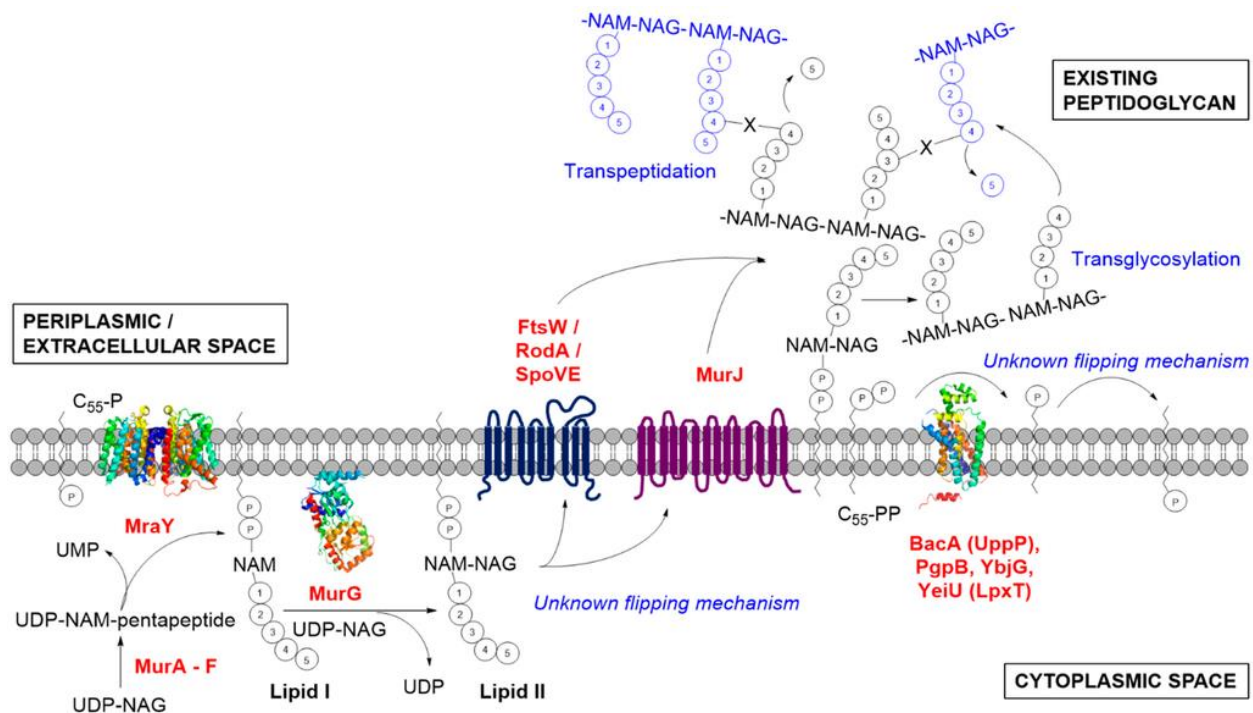


**Figure 1.4. Peptidoglycan biosynthesis pathway in bacteria.** Adapted from with permission from reference [207].

carbapenem, tebipenem has been shown to have a potent effect against *M. tuberculosis* when combined with clavulanate. Most recently, an orally bioavailable Faropenem showed inactivation of mycobacterial L, D-transpeptidases even in the absence of clavulanate and cephalosporin was combined with first-line anti-TB drugs as well as in triple combination with clavulanate [212-220].

### 1.7. *M. tuberculosis*'s intrinsic resistance mechanisms against $\beta$ -lactams

In general, intrinsic resistance of *M. tuberculosis* against many antimicrobial agents is attributed to its unique cell wall structure resulting in a low permeability diffusion barrier to these external agents [221]. Another common mechanism that affects efficacy of drugs, regardless of classes is the presence of efflux pumps [222]. Furthermore, *M. tuberculosis* has yet other characteristics that confer intrinsic resistance to  $\beta$ -lactams specifically in the form of expression of  $\beta$ -lactamase and altered affinity of PBPs to  $\beta$ -lactams [223-225].

### 1.7.1. Multidrug efflux pumps

*M. tuberculosis* possesses multiple efflux pumps used to exclude drugs from its interior. One of these, encoded by *Rv0194*, was shown to export  $\beta$ -lactams and deletion of the gene resulted in increased susceptibility to  $\beta$ -lactams [226, 227]. The question of how crucial the function of efflux pumps is in the context of  $\beta$ -lactam resistance still remains unknown as none of the adaptor proteins required for transportation of substrates have been identified as of yet.

### 1.7.2. Alterations in PBPs

Modification of PBPs, the target sites for  $\beta$ -lactams, would also allow bacteria to escape from the antibiotics' activity. There could be two distinct mechanisms where *M. tuberculosis* might achieve this goal. One is alteration in existing PBPs and the other is synthesis of entirely new PBPs [228, 229]. Point mutations in genes encoding PBPs can either alter the deacylation rate of PBPs allowing them to more rapidly restore its functionality after being bound to  $\beta$ -lactams or reduce affinity of PBPs to  $\beta$ -lactams [230]. In regards to creating a different repertoire of PBPs, it has been shown in *S. aureus* that it can produce alternative PBP2 with fully functional transpeptidase activity while exhibiting low affinity to  $\beta$ -lactams [231, 232]. However, currently there is no sound evidence that *M. tuberculosis* uses this strategy to express resistance against  $\beta$ -lactam antimicrobial drugs.

### 1.7.3. Mycobacterial cell envelope

Despite being conventionally classified as a Gram-positive bacterium, the *M. tuberculosis* cell wall structure exhibits far greater complexity compared to other Gram-positive bacteria. The unique and complex mycobacterial cell wall is among the two most critical features, along with the production of  $\beta$ -lactamase that confers  $\beta$ -lactam resistance to *M. tuberculosis*. The drug has to penetrate through the cell wall exhibiting unusually low permeable nature [233]. In fact, the diffusion of  $\beta$ -lactam antibiotics across the cell wall of mycobacteria has been shown to be limited compared to that of *E. coli* [224].

### 1.7.3.1. Overall structure of the mycobacterial cell envelope

From the broad perspective, the mycobacterial cell envelope in whole contains several layers (starting from the innermost structure): the cell membrane, a periplasmic space, a peptidoglycan layer and an arabinogalactan with covalently attached mycolic acids layer collectively referred to as the mycolyl-arabinogalactan-peptidoglycan (mAGP) complex (Figure 1.5) [234-236]. Densely populated lipids in the outer membrane disallow traditional Gram staining, but rather *M. tuberculosis* is positive when stained with acid-fast dyes [237]. The mycobacterial outer membrane composed of mycolic acids that comprise mAGP, form the inner leaflet of an asymmetrical bilayer with other extractable lipids such as trehalose dimycolate (TDM) and PDIM of the outer leaflet [238]. However, using cryo-electron tomography techniques on *M. smegmatis*, the structure has been revised such that the outer membrane is a symmetrical lipid bilayer. Data suggests that the outermost layer of the mycobacterial cell envelope as consisting of a symmetrical bilayer lipid membrane with extractable lipids present in both the inner and outer leaflets [239]. This outer membrane containing mixture of mycolic acids, the extractable lipids including PDIM, sulfolipids (SL-1), and glycolipids like lipomannan and lipoarabinomannan forms a boundary to the extracellular space or capsular polysaccharides. This hydrophobic outer membrane represents the major permeability barrier to hydrophilic molecules as arabinogalactan underneath it is a hydrophilic layer [240-242].

### 1.7.3.2. Peptidoglycan

The peptidoglycan layer is located exterior to the plasma membrane and possesses cross-linked NAG and NAM pentapeptides and the initial step forming these long polymers is catalyzed by enzymes of the Mur family [244-246]. *M. tuberculosis* possesses a type A1 $\gamma$  peptidoglycan layer where pentapeptide sequences linking glycan chains are L-alanine-D-glutamate-meso-diaminopimelic acid-D-alanine-D-alanine [246-248]. During the cross-linking process, the side chain of meso-diaminopimelic acid (position 3) from the nascent glycan chain is linked to either the same position 3 or D-alanine at

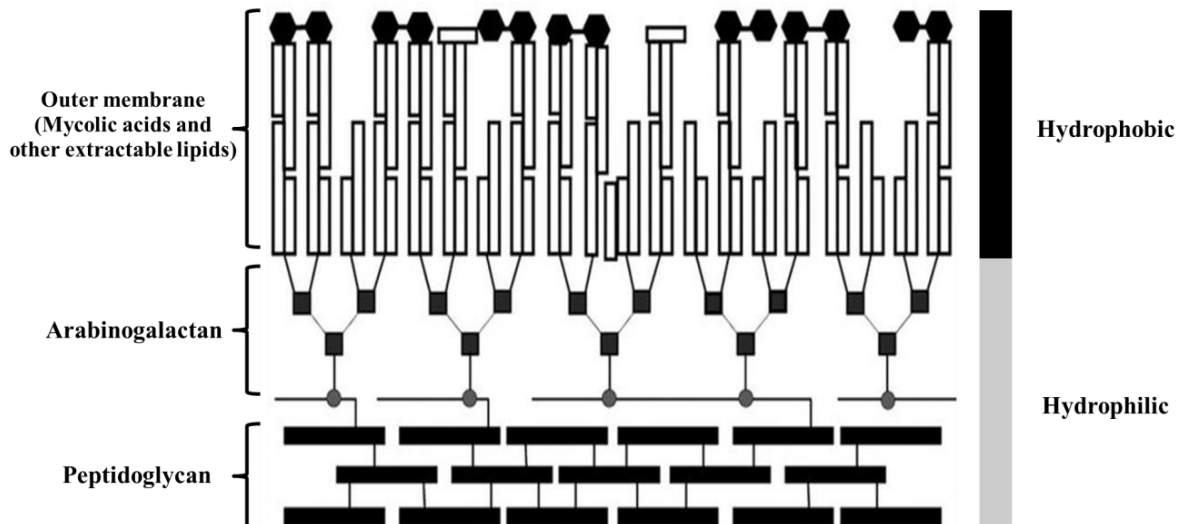


**Figure 1.5. Diagrammatic presentation of the mycobacterial cell wall.** The inner cell membrane lies beneath the peptidoglycan layer. The outer membrane of the cell wall is over-simplified and does not include all components of the lipid bilayer. Three major layers depicted here are sometimes referred to as mycolylarabinogalactan-peptidoglycan (mAGP) complex. The grayscale bar on the right indicates the permeability barrier in outer membrane due to its hydrophobicity. This figure was adapted with permission from reference [243].

position 4. When position 3 of the nascent glycan chain is linked to position 4 of the existing glycan chain, it is referred to as 4-3 cross-linkage. In mycobacteria, the PBPs PonA1, PonA2, LdtA and LdtB introduce incoming subunits to the pre-existing peptidoglycan layer [249]. In *Mycobacterium abscessus* and *M. tuberculosis*, the other form of 3-3 cross-linking predominates occupying up to 80% of the peptidoglycan chains [250, 251]. This type of cross-linking is promoted by actions of D,D-carboxypeptidase and L,D-transpeptidase and this difference across mycobacterium species or under different growth conditions may play a role in  $\beta$ -lactam susceptibility due to the fact that only carbapenems are effective in blocking this type of cross-linking [252-254].

### 1.7.3.3. Arabinogalactan

Arabinogalactan is covalently attached to the N-acetyl-glucosamine residues in the peptidoglycan layer through a phosphodiester bond with rhamnose as a linker unit. Arabinan chains are attached to the galactan domain at three different positions and branched toward the exterior of the cell where it is

covalently attached in turn with mycolic acids [246, 255]. Biosynthesis of arabinogalactan involves a multiple stepwise process. In brief, it starts with the linker unit formation by GlcNAc transferase WecA encoded by *Rv1302*, catalyzing transfer of GlcNAc to decaprenyl phosphate. To this precursor molecule, rhamnose is added by WbbL and additional galactan residues are added by GifT1 and GifT2. Before the addition of arabinosyl residues are added to the chain, it is thought to be flipped across the cell membrane through an unknown mechanism [256, 257]. At the extracellular space, concerted actions from arabinosyltransferases add arabinosyl residues and ends with the addition of terminal arabinofuranosyl residues (Figure 1.6) [258-260].

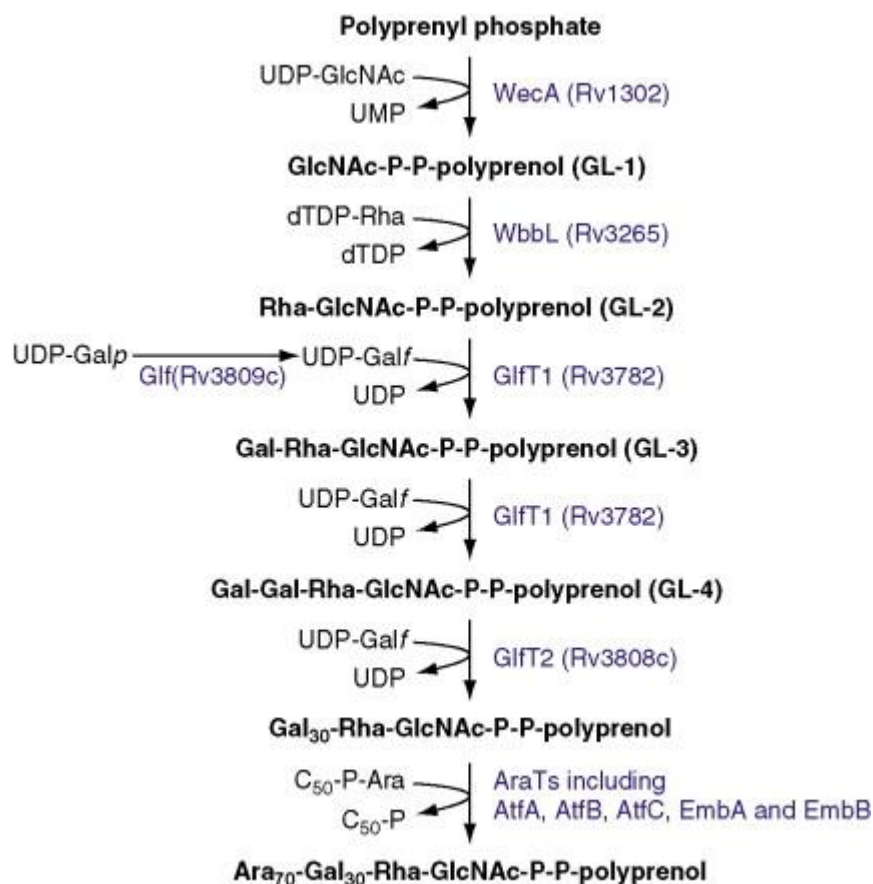


**Figure 1.6. Biosynthetic pathway of mycobacterial arabinogalactan.** Adapted with permission from reference [260].

#### 1.7.3.4. Mycolic acids

Mycolic acids are unusually long-branched (C<sub>60</sub> to C<sub>90</sub>) fatty acids. The length of the carbon chain in mycolic acids is considerably longer than that of fatty acid found in typical inner cell membranes of other bacteria [261]. Mycolic acids confer the majority of the hydrophobicity to the mycobacterial outer membrane. For instance, when comparing the cephalosporin concentrations at the exterior of cell wall to that of the periplasmic region, it was 500 to 5,000-fold higher which is considerably concentrated as compared to that of conventional Gram-negative bacteria [262]. Furthermore, the unique pattern of unsaturation that occurs in *M. tuberculosis* mycolic acids also gives rise to decreased fluidity which further contributes to the crucial role of mycolic acids in establishing a permeability barrier [242].

Mycolic acids in *M. tuberculosis* are sub-divided into  $\alpha$ -, keto-, and methoxy-mycolic acids according to functional groups attached. It should also be noted that mycolic acids can be found in three distinct forms: 1) bound to arabinogalactan forming mAGP complex, 2) as part of extractable lipids like trehalose monomycolate (TMM) and TDM, and 3) in a form of free mycolic acids which are an important component of *M. tuberculosis* biofilms [263]. The biosynthesis of mycobacterial mycolic acids begins with the formation of fatty acids through eukaryotic-like fatty acid synthase I (FAS I). Mycobacteria possess a single gene encoding FAS I (*fas*, *Rv2524c*) and this enzyme produces long chain acyl-CoA. The unique feature of acyl-CoA produced by mycobacterial FAS I is that they are distributed in bimodal fashion, where C<sub>16</sub>-C<sub>18</sub> acyl-CoA is shuttled into FAS II system directly and C<sub>24</sub>-C<sub>26</sub> acyl-CoA is incorporated into mycolic acid biosynthesis later after carboxylation as an  $\alpha$ -branch. The malonyl-CoA is also produced by carboxylation of acetyl-CoA through the enzymatic action of acyl-CoA carboxylases. *M. tuberculosis* has multiple genes encoding  $\alpha$ -subunits (*accA1* to *accA3*), carboxyltransferase domain (*accD1* to *accD6*), and  $\epsilon$ -subunit (*accE*). Then it is transferred to acyl carrier proteins (ACP) by malonyl-CoA:ACP transacylase (FabD, *Rv2243*) to produce malonyl-ACP. Condensation of acyl-CoA and malonyl-ACP is catalyzed by  $\beta$ -ketoacyl-ACP synthase III (FabH, *Rv0533c*) occurs through a series of enzymatic reactions by MabA, HadAB, HadBC, and InhA, the acyl-ACP is produced. Further elongation

by KasA and KasB yields  $\beta$ -ketoacyl-ACP again to re-enter the FAS II system and the elongation terminates when acyl-ACP obtains sufficient chain length required for further modification by multiple enzymes such as PcaA, MmaA1, MmaA2, MmaA3, MmaA4. The FadD32 (*Rv3801c*) finally activates the meromycolate before the condensation step with  $C_{24}$ - $C_{26}$   $\alpha$ -branch [264-266]. The polyketide synthase 13 (Pks13) is responsible for the condensation reaction between the two activated fatty acid, an  $\alpha$ -branch  $C_{24}$ - $C_{26}$  carboxyacyl-CoA and a  $C_{50}$ - $C_{60}$  meromycolate. This step gives rise to mycolic  $\beta$ -ketoester, which is reduced in turn by CmrA (*Rv2508*). Transfer of the final product to arabinogalactan or other mycolic acids-bearing structures is governed by Antigen 85 complex (Figure 1.7) [264, 267-269]. Mycolic acids also appear in TMMs and TDMs as extractable lipids in the outer membrane. For TMM and TDM, mycolic acids are esterified with trehalose of which biosynthesis of both occur inside the cytoplasm and, by the inner membrane transporter MmpL3, TMM which is then translocated to the periplasm where subsequent formation of TDM occurs through mycolyltransferases of Antigen 85 complex [267, 268, 270-272].

#### **1.7.3.5. Other cell wall glycolipids and phospholipids**

The phospholipids including phosphatidyl inositol mannosides (PIMs), lipomannan (LM), and lipoarabinomannan (LAM) are important constituents of the inner cell membrane, but has been recently shown to be exposed at the outer surface of the cell as well [273]. They can be generated from precursor phosphatidyl myo-inositol. Again, biosynthesis of these molecules starts inside the cytoplasm. The mid-product of PIMs, AcPIM<sub>4</sub> is flipped to the extracellular space then can be glycosylated to further produce LM and LAM [274]. In *M. tuberculosis*, arabinan in LAM is additionally attached with mannose residues to yield mannose-capped LAM (ManLAM) [275]. There is yet another prominent glycolipid structure called PDIMs which are long-chained phthiocerol esterified by polymethyl-branched fatty acids (Figure 1.8). PDIMs can be found in the outer membrane which indicates their possible role in permeability barrier [276].

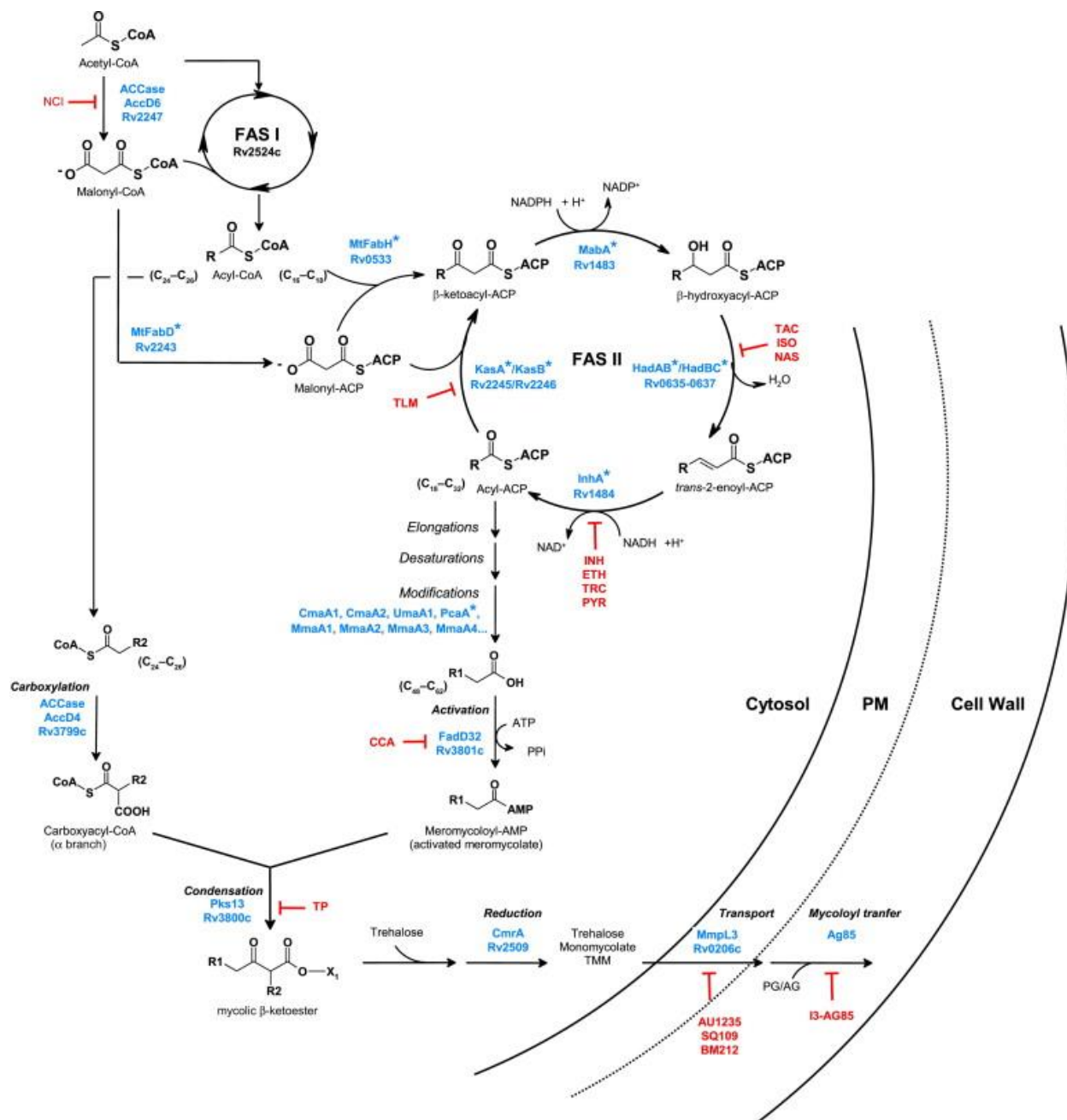


**Figure 1.7. Biosynthetic pathway of mycobacterial mycolic acids.** Compounds in red indicate inhibitory effects and proteins in blue indicate enzymatic facilitation of the process. Adapted with permission from reference [266].

Other extractable lipids in the outer membrane of *M. tuberculosis* include DAT, PAT, and SL-1.

SL-1 is the most commonly encountered sulfolipid in *M. tuberculosis* (Figure 1.8). Its synthesis is

initiated by sulfation of trehalose to form trehalose-2-sulfate by sulfotransferase Sft0 (*Rv0295c*) [277].

The acyltransferase PapA2 esterifies trehalose-2-sulfate to produce a monoacylated intermediate SL<sub>659</sub>. Then the polyketide synthase Pks2 generates methyl-branched phthioceranoyl chains, which are transferred to SL<sub>659</sub> by PapA1 to produce SL<sub>1278</sub>. Chp1 completes the process by additional acylations to finally produce SL-1 at the cytoplasm. The membrane transporter MmpL8 is thought to be responsible for the translocation of SL-1 and another transmembrane protein called Sap is thought to be important for this process as well (Figure 1.9) [278]. The biosyntheses of DAT and PAT are processed in a similar manner with that of SL-1. The acyltransferase PapA3 transfers a palmitoyl group to the glucosyl residues of trehalose to generate trehalose 2-palmitate. Then Pks3 and Pks4 synthesize mycolipenoyl groups using the starter unit provided by FadD21, which is transferred by PapA3 again to trehalose 2-palmitate for production of DAT. DAT is then translocated across the inner membrane by MmpL10 and further elaborations occur by Chp2 at the periplasmic surface of the inner membrane (Figure 1.9) [279, 280].

Taken together, along with the extensive mycolic acids layer which forms the core of outer membrane of *M. tuberculosis*, multiple lipid containing structural molecules contribute to formation of a formidable hydrophobic barrier that impedes the penetration by antimicrobial agents.

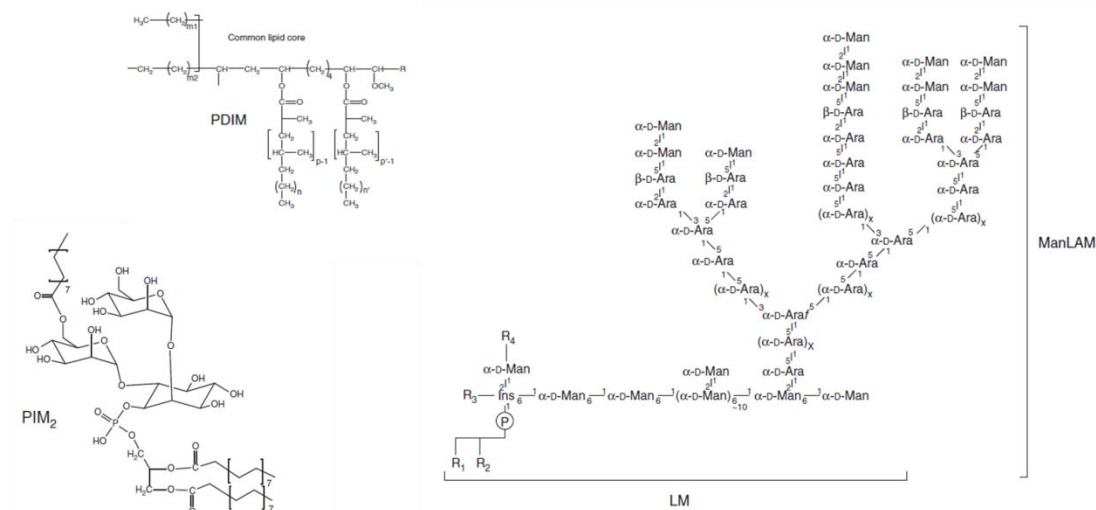


**Figure 1.8. Structures of PDIM, PIM<sub>2</sub>, LM and LAM.** Adapted with permission from reference [281].

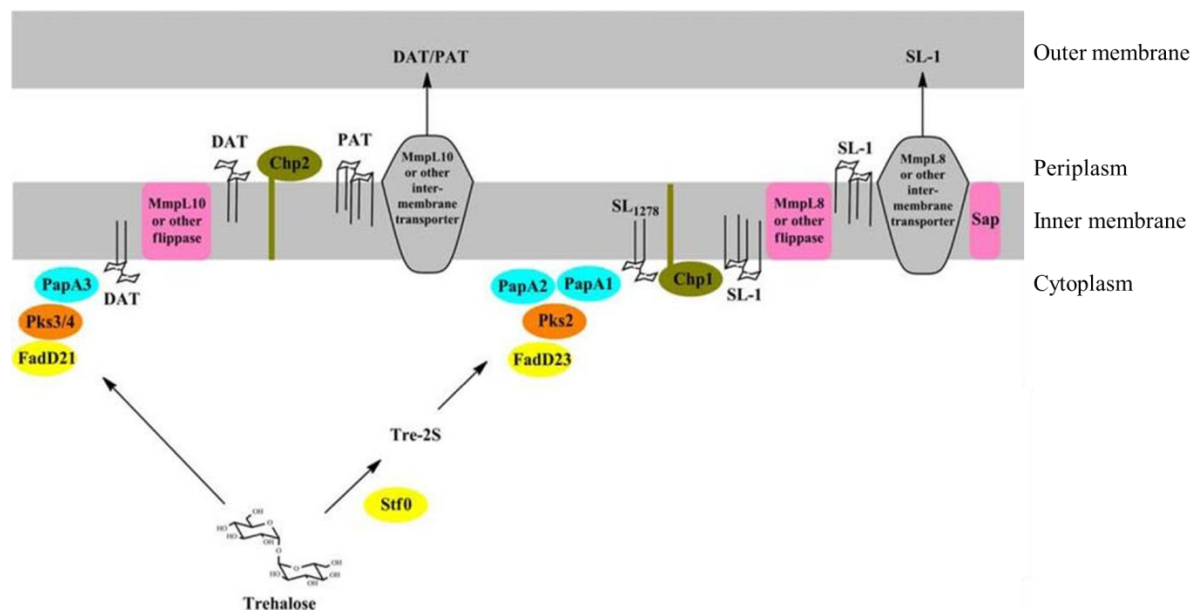


**Figure 1.9. Proposed pathways for DAT, PAT, and SL-1 biosynthesis.** The precursor DAT is synthesized at the cytoplasm and exported to periplasmic space where it is finally converted to PAT whereas SL-1 biosynthesis is completed at the cytoplasm. Adapted with permission from reference (license link: <https://creativecommons.org/licenses/by/4.0/>) [280].

### 1.7.3.6. Transcriptional regulation related to cell envelope stresses

*M. tuberculosis* is confronted by numerous micro-environmental stresses upon establishment of infection inside the host. One of them is surface-related stress. As reviewed in this chapter, an impermeable barrier formed by the complex mycobacterial cell wall plays a crucial role in protecting bacilli against the effects of harsh microenvironments. For example, *M. tuberculosis* can be exposed to alveolar surfactant, antimicrobial peptides, lysosomal enzymes inside the host, and antibiotics that causes damage to cell envelope structures [282-285]. Thus, *M. tuberculosis* has developed sophisticated mechanisms of sensing and responding to dangers exerted upon the cell wall. An example is the employment of transcriptional regulators to rapidly respond to environmental stress, which induces the expression of tightly regulated functional proteins.

There are approximately 190 transcriptional regulators in the *M. tuberculosis* genome [16]. Besides unconfirmed putative transcriptional regulators, there are 13  $\sigma$  factors, 11 two-component regulatory systems, 5 orphan response regulators, and 11 protein kinases [286]. Through extensive

research, environmental cues that trigger some of these transcriptional regulators have been elucidated. For instance, response to heat shock is regulated by transcriptional control via three different  $\sigma$  factors: SigB, SigE, and SigH [287-289]. In the bacterial RNA polymerase, sigma factor is one of the subunits which aids in promoter region recognition [290]. Each  $\sigma$  factor in *M. tuberculosis* has its own specificity in terms of response switch to promote transcription of different set of genes. Mutants lacking in *sigE* gene exhibited increased sensitivity to detergent, and therefore SigE was implicated in sensing surface-related stress. The organism lacking SigE was also hypersensitive to the proton ionophore carbonyl cyanide chlorophenylhydrazone (CCCP) and did not survive in macrophages. The SigE belongs to the group of extracytoplasmic-function (ECF) sigma factors which are responsive to environmental changes [291]. Subsequent research revealed that SigE was required for transcriptional induction of 23 genes in response to SDS exposure, further supporting its role in responding to cell wall stresses [288, 292]. A putative PspA protein encoded by *Rv2744c* is an example of a gene induced by cell wall stress. In *E. coli*, membrane-attacking agents and defective protein secretion trigger upregulation of this gene. It is also important to note that PspA protein protects *E. coli* from CCCP by maintenance of normal electron transport [293-295]. Interestingly, some genes induced by SigE by cell wall stress encode proteins involved in fatty acid degradation *fadE23* and *fadE24*, along with genes involved in mycolic acid biosynthesis, metabolizing and detoxifying fatty acids, thus suggesting a probable role of SigE in maintaining proper cell wall integrity as well as detoxification of the cell [296]. Transcription of *tatA*, encoding for a protein that constitute the Twin-arginine protein transport (Tat) system, is also under control of SigE. The gene encoding another component of the Tat system TatB (*tatB*) is also located downstream of *sigE* alongside with a SigE specific putative anti-sigma factor encoding *rseA* [290]. Expression of SigE (and SigB) is also closely related to two-component system regulator MprAB and polyphosphate kinase 1, which is highly conserved in many bacterial species to serve as a prerequisite for MprAB-SigE signaling cascade by phosphorylating MprA (Figure 1.10). It has been also shown to have an important role in biofilm formation by *P. aeruginosa* [297]. Two-component systems are comprised of histidine kinases that sense specific environmental cues and the cognate response regulators. MptAB

induces both *sigE* and *sigB* upon cell wall stresses. Deletion of *mprAB* resulted in down regulation of SigE regulon [298, 299].

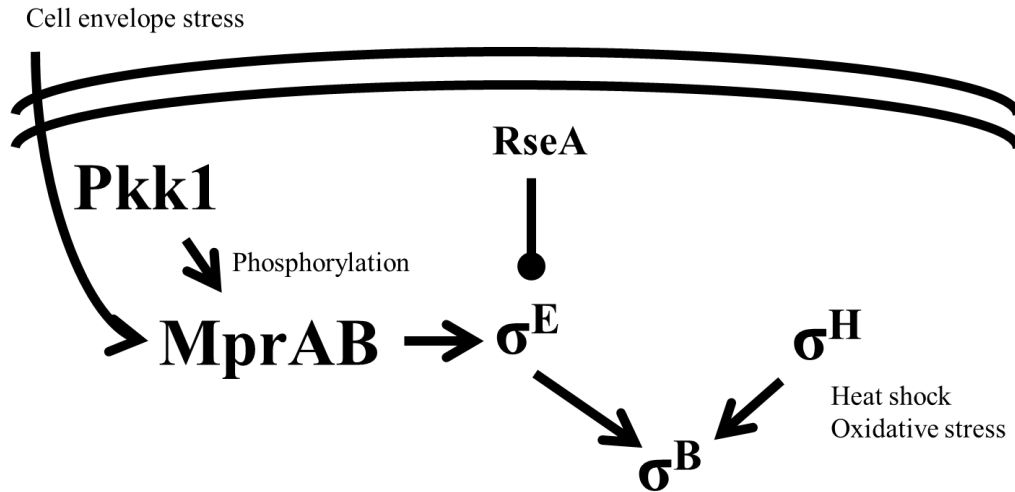


**Figure 1.10. The regulatory network in response to cell wall stress involving SigE.** Adapted from reference [290] with permission.

SigB is a major housekeeping sigma factor along with SigA. Transcription of *sigB* is entirely controlled by SigE in an unstressed environment, but can be influenced by other  $\sigma$  factors such as SigH and SigL depending on the type of stresses. The *sigB* mutant is also hypersensitive to SDS and its regulon encodes proteins involved in cell wall biosynthesis processes, lipid metabolisms, and detoxifications [300].

The importance of the sigma factor network in dealing with cell wall associated stress was further confirmed by studying *M. tuberculosis*'s response to cell envelope-attacking agent thioridazine (TRZ), a phenothiazine anti-psychotic drug which is being considered for treatment of drug-resistant *M. tuberculosis* [301]. In the work done by the Kaushal group, TRZ induced differential expression of genes encoding efflux pumps, oxido-reductases as well as proteins involved in fatty acid metabolism. TRZ treatment results in significant expression of SigB regulon genes and subsequent cell wall damage. Moreover, the mutant of SigE was hypersensitive to TRZ [302]. They also identified yet another sigma

factor, SigH, to be important as a key cell wall stress response regulator. This sigma factor was previously well known for its role as a response regulator to heat shock and oxidative stress [303]. Exposure to SDS and TRZ induced expression of MT2816 (*Rv2745c*). The protein encoded by this gene was involved in responding to heat shock, detoxification, lipid metabolism, and cell wall biosynthesis processes. For induction of this regulator protein transcription, SigH, but not SigE, was required [304].

#### **1.7.4. $\beta$ -lactamases**

##### **1.7.4.1 *M. tuberculosis* $\beta$ -lactamase**

In addition to a hardy cell wall that prevents diffusion of antibiotics, production of  $\beta$ -lactamase by *M. tuberculosis* largely contributes to its intrinsic  $\beta$ -lactam resistance. The presence of an enzyme that can degrade  $\beta$ -lactams has been a problem for other pathogenic bacteria as well, thus  $\beta$ -lactamase inhibitors were indispensable in the history of  $\beta$ -lactams usage [305]. In all pathogenic mycobacterial species, the presence of  $\beta$ -lactamase has been reported [306]. Coupled with the permeability barrier of mycobacterial cell wall,  $\beta$ -lactamase enzyme activity presents a major  $\beta$ -lactam resistance mechanism. As discussed above,  $\beta$ -lactamase is translocated through the Tat pathway and is encoded by the *blaC* in *M. tuberculosis* [307]. *M. tuberculosis*  $\beta$ -lactamase is a class A  $\beta$ -lactamase that possesses broad spectrum activity. This class of  $\beta$ -lactamases has a flexible substrate-binding site, which contributes to the highly promiscuous characteristic of the enzyme [308]. In terms of enzyme activity, mycobacterial  $\beta$ -lactamase does not exhibit significantly higher level of activity compared to  $\beta$ -lactamase secreted by other pathogenic bacteria. Nonetheless, with the low diffusion rate of drugs through the mycobacterial cell wall, *M. tuberculosis*  $\beta$ -lactamase is highly efficient in degrading target substrates [240]. Especially, compared to other  $\beta$ -lactamases, *M. tuberculosis*  $\beta$ -lactamase shows an impressive level of activity against the carbapenem class of  $\beta$ -lactams whereas most other  $\beta$ -lactamases are ineffective [309, 310]. Previously, it was thought that *M. tuberculosis*  $\beta$ -lactamase was constitutively expressed. However, recent findings by Sala and colleagues show that the transcriptional repressor BlaI binds to the recognition sites in the *blaC*

gene when there is no  $\beta$ -lactam pressure. In the presence of  $\beta$ -lactams, BlaI escapes the binding site and frees *blaC* from transcriptional suppression [311]. Purified BlaC protein has been shown to be effectively inhibited by all three available  $\beta$ -lactamase inhibitor clavulanic acid, sulbactam, and tazobactam. Of those, clavulanic acid was the most promising as the effect was irreversible by allowing secondary conformational changes in  $\beta$ -lactamase that leads to occupied active sites by reactive intermediates. Inhibition by sulbactam and tazobactam were reversible [310].

In sum, potentiation of  $\beta$ -lactams against *M. tuberculosis* seems plausible through disrupting one or more resistance mechanism and it could provide a valuable therapeutic option against not only drug-susceptible but also drug-resistant *M. tuberculosis* strains.

#### **1.7.4.2 Protein secretion machinery of *M. tuberculosis***

The dual-edged sword is the lipid rich hydrophobic cell wall of *M. tuberculosis* which protects the cell but also can be an obstacle for secretory products to be exported. Just like other bacteria, mycobacteria have a general secretion pathway (Sec system) [312-314]. The system is composed of protein targeting units, a motor protein, and a membrane channel (translocase) [315]. The Sec translocase has SecY, SecE, and SecG that are integral membrane proteins. SecA is an ATPase that provides the driving force for protein translocation, which allows secretion of unfolded proteins across the cell membrane. The excreted proteins have a signal sequences at their N-terminus which is recognized by SecA ATPase [316]. Translocation of protein through this system requires energy provided by the proton motive force (PMF). One interesting feature of mycobacterial proteins exported through this system is that they contain an unique aspartate-proline motif at the N-terminus near signal sequence [317]. Also, mycobacteria has another homologue of SecA, SecA2, of which the role is still unclear [318].

Another well-established system is Tat system [319]. This system involves receptor protein and a protein conduction channel formed by TatA and TatC, or TatA, TatB, and TatC. Energy generated by PMF is also required for this system. A major difference between Sec and Tat systems is that, unlike Sec, the Tat system is able to transfer folded proteins. Substrates of the Tat system have N-terminal signal

sequences that are similar to the Sec system signal sequences, however contain two conserved arginines followed by two uncharged amino acid residues that are necessary for proper protein translocation [320-323]. In *M. tuberculosis*, small subsets of proteins such as phospholipase C enzymes are predicted to be exported through the Tat system [324]. These proteins were identified using a  $\beta$ -lactamase reporter system described by Braunstein and colleagues.  $\beta$ -lactamase enzymes target  $\beta$ -lactam antibiotics binding in the peptidoglycan layer outside the cell membrane, thus the enzyme has to be translocated beyond the cell membrane to be effective. In their study, they truncated the signal sequence of  $\beta$ -lactamase, which were then fused with proteins with unknown export pathways. If the exported chimera shared the same secretory mechanism as  $\beta$ -lactamase, the mutant would therefore exhibit  $\beta$ -lactam resistance. By characterizing the translocation of the reporter protein, they showed that mycobacterial  $\beta$ -lactamase translocation is Tat system specific where both twin-arginine motif and a functional Tat system were required [325, 326]. More recently, Cole and colleagues showed non-coding RNA encoded by PhoP dependent *Mcr7* regulated *tatC* transcription and impacted Tat system. In this study, they illustrated the secretion defect of  $\beta$ -lactamase in the *M. tuberculosis phoP* mutant [327].

Alternative protein secretion systems exist in mycobacteria. Immunodominant proteins like early secreted antigen target 6 kDa (ESAT-6) and culture filtrate protein 10 kDa (CFP-10) lack Sec system signal sequences [36]. The first evidence of a specific machinery responsible for the secretion of these proteins were suggested by Stanley and colleagues where deletion of genes in the vicinity of *esxB*A operon (includes genes that encode ESAT-6 and CFP-10) resulted in defective secretion of both ESAT-6 and CFP-10 [328]. The location of these individual genes was termed RD1 and the related functional secretory system was named ESX-1. Later, further characterization of the ESX-1 system was established, revealing a requirement for ATPases (*Rv3868*, *Rv3870*, and *Rv3871*) and other genes such as *Rv3870*, *Rv3871*, *Rv3614c*, and *Rv3615c* [329]. The process of protein secretion by ESX-1 also requires energy generated through PMF.

## 1.8. Mycobacterial metabolism and bioenergetics

*M. tuberculosis* is an extremely flexible organism in terms of metabolic capacity with the ability to utilize various carbon sources as a source of energy for survival and replication. This flexibility provides the bacteria with unique ability to adapt to different *in vitro* and *in vivo* microenvironments that vary in nutrient availability. Metabolism and bioenergetics of mycobacteria is still an area that is under-researched and many questions relating to the role metabolism and nutrient availability play in pathogenicity, persistence, and drug susceptibility remain unanswered. In addition, there is an increasing interest in identifying specific metabolic and bioenergetics pathways that may serve as molecular targets in the development of new anti-TB drugs.

When grown *in vitro*, *M. tuberculosis* can use various carbohydrates as carbon sources to feed subsequent glycolytic pathways though it can also catabolize fatty acids through  $\beta$ -oxidation [330]. When glycerol is present in laboratory media like 7H9, it is a preferred carbon source for *M. tuberculosis* over other sugars. Catabolism of glycerol is initiated by phosphorylation to yield glycerol-3-phosphate by glycerol kinase. This intermediate product is oxidized to dihydroxyacetone phosphate by glycerol-3-phosphate dehydrogenase to the TCA cycle. In contrast with other bacteria,  $\alpha$ -ketoglutarate is initially converted to succinyl semialdehyde then oxidized to succinate which is a distinguishing feature of the *M. tuberculosis* TCA cycle [331]. When 1 M of glycerol is completely oxidized, it produces 7 M of NADH or FADH<sub>2</sub>. These molecules are important because they are used as endogenous reduced electron carriers in the *M. tuberculosis* electron transport chain (ETC) [332].

Evidence from animal model studies suggests *M. tuberculosis* changes its preference for carbon source from glycerol to fatty acids (or host lipids) *in vivo* [333-336]. Catabolism of fatty acids in this case is supported by the glyoxylate shunt, which enables conservation of carbons [69]. In this pathway, the isocitrate lyase converts isocitrate to succinate and glyoxylate and the importance is reiterated by the requirement of host lipid cholesterol for *M. tuberculosis* persistence inside lungs of mice [337].

### 1.8.1. Bacterial bioenergetics

Being an obligate aerobic bacterium, metabolism of *M. tuberculosis* is directly linked to oxygen consumption through respiration and membrane bioenergetics of the bacteria. The term bioenergetics is used to describe functional electron transporting complexes located in cell membrane generating energy in the form of ATP via ion gradient across membranes [338]. Maintenance of ATP and homeostasis of multiple parameters of bioenergetics are crucial for bacterial longevity and survival [339]. For that reason, bacterial bioenergetics is becoming an increasingly important area of research and in new drug discovery. In particular, the most recent anti-TB drug approved by the FDA, BDQ, targets mycobacterial bioenergetics [340-344]. Aside from inhibiting  $F_1F_0$ -ATP synthase which is the acting target of BDQ, other unique components of mycobacterial bioenergetics such as NADH dehydrogenase II (NDH-2) can also be an attractive target to explore [345].

In the field of membrane bioenergetics, pioneering research was conducted by Peter Mitchell in the 1960s when he first proposed the chemiosmotic theory [346-348]. Simply put, chemiosmosis is the movement of ions across the cell membrane following their electrochemical gradient. For example, the concentration of  $H^+$  ions (protons) is higher at the exterior of the cell membrane. By an electrochemical gradient force, protons diffusion through ATP synthase located in the cell membrane is coupled to ATP generation [349]. This electrochemical gradient is generated by multiple proton pumps (complexes) that send protons to the exterior of the cell membrane to achieve the differential concentration gradient. Complexes are fueled by multiple source of energy such as NADH and FADH generated as a byproduct of catabolism of molecules like glucose and lipids. This phenomenon is central to cells that are utilizing oxygen during respiration [350]. Electrons are also passed through complexes by carrier molecules until being accepted by the terminal electron acceptor oxygen to form water which completes the ETC [351].

Respiration of the cell is coupled with phosphorylation of ADP to generate ATP (oxidative phosphorylation). In other words, consumption of oxygen occurs only when ADP is phosphorylated to generate ATP, which is powered by the proton gradient across the cell membrane. However, uncoupling

agents such as CCCP facilitates consumption of oxygen in the absence of ADP phosphorylation thereby “uncoupling” the oxidative phosphorylation. Generally, uncouplers act by collapsing the proton gradient that exists across the cell membrane [352].

### 1.8.2. PMF and the ETC

PMF is the energy generated by the proton gradient. As electrons flow through the ETC, protons are pumped to the exterior of the cell membrane [338, 353]. ATP generation driven by PMF is a critical prerequisite for the majority of cellular processes that require energy in the form of ATP [340, 354-357]. Additionally, some classes of protein such as resistance-nodulation-division (RND) family proteins can use this proton gradient directly without consuming ATP to drive their cellular functions [270, 358]. The PMF is a sum of electrical potential energy ( $\Delta\psi$ ) and chemical potential energy created by the transmembrane proton gradient ( $\Delta\text{pH}$ ). Therefore, any perturbation on one of these components can compromise PMF required for various biological processes [359-361]. Normal mycobacterial growth is perturbed by agents that disrupt the PMF such as CCCP, demonstrating importance of PMF in proper metabolism of the bacteria. Especially in anaerobic condition, non-replicative *M. tuberculosis* still generates significant PMF both by  $\Delta\psi$  and  $\Delta\text{pH}$ . This is disrupted abruptly by TRZ which blocks NDH-2 suggesting the importance of NADH as an electron carrier that fuels the ETC to establish proton gradient [362]. How *M. tuberculosis* generates PMF under a low oxygen environment remains to be elucidated. One possible explanation is related to nitric oxide catabolism, which can provide nitrate as a potential electron acceptor [363, 364]. Indeed, the *M. tuberculosis* genome has sets of genes encoding for proteins involved in nitrate/nitrite exchange [16].

Oxidative phosphorylation in mycobacteria is facilitated through actions of proton pumps, non-proton pumping enzyme complexes, electron carriers between complexes, and ATP synthase (Figure 1.11) [365, 366]. The first complex of the chain is membrane-bound NADH dehydrogenase that relays electrons from NADH to menaquinone of which two sets of genes that encode proteins in *M. tuberculosis* have been identified. The conventional NADH dehydrogenase I (NDH-1) is encoded by the *M.*

*tuberculosis* operon ranging from *Rv3145* to *Rv3158*. This enzyme utilizes flavin mononucleotide (FMN) to transfer electrons from NADH to menaquinone. During this process, four protons are pumped out to the exterior of the cell membrane to generate PMF [367]. Unlike classical NDH-1, NDH-2 is a non-proton pumping NADH dehydrogenase encoded by *ndh* and *ndhA* genes in *M. tuberculosis* [368]. The enzyme complex is a membrane protein that is widely conserved in bacteria [369]. *M. tuberculosis* carries a couple of genes encoding for this enzyme, *ndh* and *ndhA*. Proteins encoded by these genes share homology in the NADH binding region, so both are functionally active in transferring electrons to menaquinone species [370]. *M. smegmatis* relies more on NDH-2 for oxidation of NADH more so than *M. tuberculosis*, and is therefore essential in *M. smegmatis*. The usage of NDH-1 compared to NDH-2 in *M. smegmatis* is only about 5% [371]. This phenomenon is less drastic but still true in *M. tuberculosis* also. In *M. tuberculosis*, NDH-1 activity is 25-50% lower than that of NDH-2 and NDH-1 inhibitors are less effective in *M. tuberculosis* compared to other bacteria [368]. Therefore, researchers have questioned the necessity of NDH-2 in *M. tuberculosis* in the presence of NDH-1. One possibility is that, being a non-proton pumping complex, NDH-2 is not affected by a high electrochemical gradient which could decelerate the rate of the enzyme reactions [372]. During aerobic respiration, oxidation of NADH or succinate allows the electron transfer to menaquinone. The conventional ETC's complex II is represented by succinate dehydrogenase which is a vital link between the ETC and the TCA cycle [373]. Succinate dehydrogenase oxidizes succinate to fumarate and also transfers electrons to oxidized menaquinone. In most mycobacteria, there are two separate proteins, Sdh1 and Sdh2, that carry out this function and this redundancy may represent metabolic flexibility during hypoxia [374]. The mycobacterial ETC can shuttle electrons directly from menaquinol to a cytochrome *bd*-type menaquinol oxidase or the cytochrome *c* pathway [76]. Compared to the eukaryotic mitochondrial ubiquinone/ubiquinol complex, menaquinone in *M. tuberculosis* has a better capability to transfer electrons under oxygen-limited conditions [375, 376]. The cytochrome *bd*-type oxidase is a preferred pathway in oxygen limiting condition whereas the cytochrome *c* pathway (menaquinol-cytochrome *c* oxidoreductase *bc<sub>1</sub>* complex combined with *aa<sub>3</sub>*-type cytochrome *c* oxidase) is the main pathway used by bacteria respiring under aerobic conditions [377].

Finally,  $F_1F_0$ -ATP synthase generates ATP by proton influx dictated by the proton gradient formed by concerted efforts of the ETC described so far. The synthesis of ATP is facilitated under conditions such as high proton gradient and low intracellular ATP levels. In *M. tuberculosis* the *atp* operon (*Rv1304* to *Rv1311*) encoding for ATP synthase is essential for growth [378-380]. The final electron acceptor at this stage is oxygen, while under low oxygen conditions, other alternative electron acceptors like nitrate and fumarate are available [381, 382]. It is suggested that functional ATP synthase activity may be a critical requirement for NADH oxidation by allowing translocated protons to re-enter the cytoplasm [378]. For example, the *M. smegmatis* cell membrane has been shown to be extremely impermeable to protons. This would indicate that proton translocation into the cytoplasm would only be possible through ATP synthase [383].

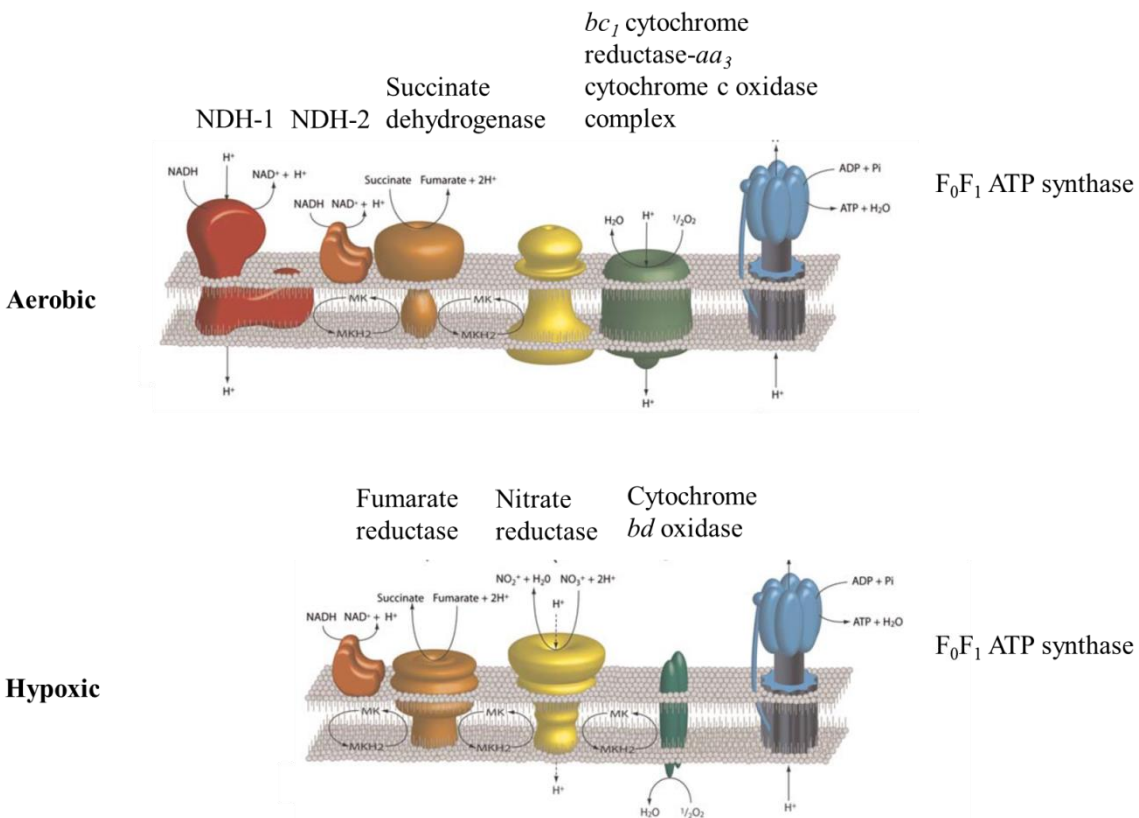


**Figure 1.11. Simplified schematic diagram of *M. tuberculosis* ETC and ATP synthase.** Top panel represents utilized complexes during aerobic condition and lower panel represents hypothetical scenario under oxygen-limited conditions. Adapted with permission from reference [366].

There are important classes of drugs developed recently that target *M. tuberculosis* bioenergetics. First, diarylquinolines (represented by BDQ) target F<sub>0</sub>F<sub>1</sub>-ATP synthase. A resistant mutant study revealed the specific molecular target to be an oligomeric c ring situated in the enzyme complex encoded by *atpE* [384]. The second class of drugs includes phenothiazine analogs. The target of this class of drugs is NADH dehydrogenase [368, 385, 386]. A well-studied phenothiazine as anti-TB drug is TRZ. TRZ targets NDH-2 of *M. tuberculosis* and also has been shown to have a cell envelope permeabilizing effect as well [387]. When tested in a mouse *M. tuberculosis* infection model, phenothiazine analogs were effective in reducing bacterial loads in the lungs [368]. Recently in *M. smegmatis*, two novel compounds scopafungin and gramicidin S have been identified as inhibitors of NDH-2 [388]. Lastly, a class of imidazopyridine amide (IPA) compounds has been identified as a potent blocker of ETC through targeting cytochrome *bc<sub>1</sub>* complex and showed suppressive effects on *M. tuberculosis* growth both *in vitro* and *in vivo* [389]. These studies further illustrate that specifically targeting the ETC of *M. tuberculosis* with new drug candidates shows promise in the ongoing search for the next generation of anti-TB drugs.

## 1.9. Overview of the dissertation

The potential clinical use of  $\beta$ -lactams in TB therapy using a novel strategy to circumvent intrinsic resistance mechanism of *M. tuberculosis* would represent a significant improvement over current anti-TB therapy. 2-AI compounds have demonstrated potential to be used as an adjunctive therapy by reversing  $\beta$ -lactams resistance in other bacteria such as MRSA. Additionally, our data showing that *M. tuberculosis* drug-tolerance in non-replicative culture could be reversed by 2-AI compounds, further underpin the potential value of these small molecules along with antimicrobial drug combinations targeting *M. tuberculosis*. Thus, our previous data with 2-AI compounds raised three critical questions. First, can 2-AI compounds be combined with various  $\beta$ -lactams to potentiate their antibacterial activity against *M. tuberculosis*? Second, what intrinsic defense mechanisms of *M. tuberculosis* against  $\beta$ -lactams

do 2-AI compounds disrupt? Lastly, how do 2-AI compounds achieve that goal? To answer these questions we developed three hypotheses and associated specific aims.

Hypothesis 1 and specific aim 1: We hypothesized that intrinsic  $\beta$ -lactam resistance of *M. tuberculosis* can be reversed by combination with 2-AI compounds. To address this question, we compared the MIC of multiple  $\beta$ -lactams against *M. tuberculosis* as drug alone or in combination with selected 2-AI compounds. Additionally, we assessed bactericidal activity of  $\beta$ -lactams against *M. tuberculosis* in the presence of 2-AI compounds. In Chapter 2, our initial observation of  $\beta$ -lactam potentiation by 2-AI and results of supporting experiments are presented.

Hypothesis 2 and specific aim 2: We hypothesized that 2-AI compounds could have a disruptive effect on mycobacterial cell envelope based on the observed membrane-permeabilizing or cell wall structure alteration induced by these compounds in other bacteria [390, 391]. Chapter 3 summarizes our findings as well as another important factors that contributes to intrinsic  $\beta$ -lactam resistance, that being  $\beta$ -lactamase activity in the presence of 2-AI compounds. We showed that 2-AI compound treatment alters major cell envelope lipid structure composition in *M. tuberculosis* and lead to significant permeability changes. Additionally, we show that 2-AI compounds do not directly inhibit  $\beta$ -lactamase enzyme, but hamper the overall  $\beta$ -lactamase activity by inducing defective protein secretion. Thus, we will have assessed two of the most critical mechanisms that contribute to the expression of intrinsic  $\beta$ -lactam resistance of *M. tuberculosis* and whether 2-AI compounds affect those parameters or not.

Hypothesis 3 and specific aim 3: Based on our findings in aims 1 and 2, we hypothesized that 2-AI compounds affect one or more components of *M. tuberculosis* bioenergetics. More specifically, we investigated whether 2-AI compounds compromise mycobacterial capacity to generate PMF either by dissipation of membrane potential or collapse in  $\Delta\text{pH}$ . In chapter 4, we summarize a series of experiments to test the impact 2-AI compounds have on *M. tuberculosis* bioenergetics. The overall goal of this section is to demonstrate that 2-AI compounds affect read-outs related to bioenergetic homeostasis such as redox potential, oxygen consumption, PMF, and ETC function.

Chapter 5 will be devoted to discuss overall conclusions and our current understanding of how 2-AI based small molecules may function as an adjunctive therapy in combination with antimicrobial drugs. Also, we will discuss the significance of these findings in the context of using 2-AI based small molecules in the development of a novel treatment to treat human TB patients.

## REFERENCES

1. Hershkovitz I, Donoghue HD, Minnikin DE, Besra GS, Lee OY, Gernaey AM, et al. Detection and molecular characterization of 9,000-year-old *Mycobacterium tuberculosis* from a Neolithic settlement in the Eastern Mediterranean. *PLoS One*. 2008;3(10):e3426. doi: 10.1371/journal.pone.0003426. PubMed PMID: 18923677; PubMed Central PMCID: PMCPMC2565837.
2. Wirth T, Hildebrand F, Allix-Beguec C, Wolbeling F, Kubica T, Kremer K, et al. Origin, spread and demography of the *Mycobacterium tuberculosis* complex. *PLoS Pathog*. 2008;4(9):e1000160. doi: 10.1371/journal.ppat.1000160. PubMed PMID: 18802459; PubMed Central PMCID: PMCPMC2528947.
3. Daniel TM. The early history of tuberculosis in central East Africa: insights from the clinical records of the first twenty years of Mengo Hospital and review of relevant literature. *Int J Tuberc Lung Dis*. 1998;2(10):784-90. PubMed PMID: 9783522.
4. Gradmann C. Robert Koch and the white death: from tuberculosis to tuberculin. *Microbes Infect*. 2006;8(1):294-301. doi: 10.1016/j.micinf.2005.06.004. PubMed PMID: 16126424.
5. Goetz T. *The remedy : Robert Koch, Arthur Conan Doyle, and the quest to cure tuberculosis*. New York, New York: Gotham Books; 2014. xx, 298 pages p.
6. Barnes DS. Historical perspectives on the etiology of tuberculosis. *Microbes Infect*. 2000;2(4):431-40. PubMed PMID: 10817646.
7. Woodruff HB. Selman A. Waksman, winner of the 1952 Nobel Prize for physiology or medicine. *Appl Environ Microbiol*. 2014;80(1):2-8. doi: 10.1128/AEM.01143-13. PubMed PMID: 24162573; PubMed Central PMCID: PMCPMC3911012.
8. Dye C, Williams BG. The population dynamics and control of tuberculosis. *Science*. 2010;328(5980):856-61. doi: 10.1126/science.1185449. PubMed PMID: 20466923.
9. WHO. *Global Tuberculosis Report 2016*. 2016.
10. Lienhardt C, Glaziou P, Uplekar M, Lonnroth K, Getahun H, Raviglione M. Global tuberculosis control: lessons learnt and future prospects. *Nat Rev Microbiol*. 2012;10(6):407-16. doi: 10.1038/nrmicro2797. PubMed PMID: 22580364.
11. Gajalakshmi V, Peto R, Kanaka TS, Jha P. Smoking and mortality from tuberculosis and other diseases in India: retrospective study of 43000 adult male deaths and 35000 controls. *Lancet*. 2003;362(9383):507-15. doi: 10.1016/S0140-6736(03)14109-8. PubMed PMID: 12932381.
12. Tiemersma EW, van der Werf MJ, Borgdorff MW, Williams BG, Nagelkerke NJ. Natural history of tuberculosis: duration and fatality of untreated pulmonary tuberculosis in HIV negative patients: a systematic review. *PLoS One*. 2011;6(4):e17601. doi: 10.1371/journal.pone.0017601. PubMed PMID: 21483732; PubMed Central PMCID: PMCPMC3070694.
13. McMurray DN. *Mycobacteria and Nocardia*. In: Baron S, editor. *Medical Microbiology*. 4th ed. Galveston (TX)1996.

14. Pai M, Behr MA, Dowdy D, Dheda K, Divangahi M, Boehme CC, et al. Tuberculosis. *Nat Rev Dis Primers*. 2016;2:16076. doi: 10.1038/nrdp.2016.76. PubMed PMID: 27784885.
15. Camus JC, Pryor MJ, Medigue C, Cole ST. Re-annotation of the genome sequence of *Mycobacterium tuberculosis* H37Rv. *Microbiology*. 2002;148(Pt 10):2967-73. doi: 10.1099/00221287-148-10-2967. PubMed PMID: 12368430.
16. Cole ST, Brosch R, Parkhill J, Garnier T, Churcher C, Harris D, et al. Deciphering the biology of *Mycobacterium tuberculosis* from the complete genome sequence. *Nature*. 1998;393(6685):537-44. doi: 10.1038/31159. PubMed PMID: 9634230.
17. Ioerger TR, Feng Y, Ganesula K, Chen X, Dobos KM, Fortune S, et al. Variation among genome sequences of H37Rv strains of *Mycobacterium tuberculosis* from multiple laboratories. *J Bacteriol*. 2010;192(14):3645-53. doi: 10.1128/JB.00166-10. PubMed PMID: 20472797; PubMed Central PMCID: PMC2897344.
18. Lawn SD, Zumla AI. Tuberculosis. *Lancet*. 2011;378(9785):57-72. doi: 10.1016/S0140-6736(10)62173-3. PubMed PMID: 21420161.
19. Huseby JS, Hudson LD. Miliary tuberculosis and adult respiratory distress syndrome. *Ann Intern Med*. 1976;85(5):609-11. PubMed PMID: 984612.
20. Hopewell P, Jasmar R. Overview of Clinical Tuberculosis. In: Cole ST, Eisenach KD, McMurray DN, Jacobs WR, Jr., editors. *Tuberculosis and the Tubercle Bacillus*. Washington D.C.: ASM Press; 2005.
21. Dye C, Scheele S, Dolin P, Pathania V, Raviglione MC. Consensus statement. Global burden of tuberculosis: estimated incidence, prevalence, and mortality by country. WHO Global Surveillance and Monitoring Project. *JAMA*. 1999;282(7):677-86. PubMed PMID: 10517722.
22. Kang PB, Azad AK, Torrelles JB, Kaufman TM, Beharka A, Tibesar E, et al. The human macrophage mannose receptor directs *Mycobacterium tuberculosis* lipoarabinomannan-mediated phagosome biogenesis. *J Exp Med*. 2005;202(7):987-99. doi: 10.1084/jem.20051239. PubMed PMID: 16203868; PubMed Central PMCID: PMC2213176.
23. Ting LM, Kim AC, Cattamanchi A, Ernst JD. *Mycobacterium tuberculosis* inhibits IFN-gamma transcriptional responses without inhibiting activation of STAT1. *J Immunol*. 1999;163(7):3898-906. PubMed PMID: 10490990.
24. Koul A, Herget T, Klebl B, Ullrich A. Interplay between mycobacteria and host signalling pathways. *Nat Rev Microbiol*. 2004;2(3):189-202. doi: 10.1038/nrmicro840. PubMed PMID: 15083155.
25. Goren MB, D'Arcy Hart P, Young MR, Armstrong JA. Prevention of phagosome-lysosome fusion in cultured macrophages by sulfatides of *Mycobacterium tuberculosis*. *Proc Natl Acad Sci U S A*. 1976;73(7):2510-4. PubMed PMID: 821057; PubMed Central PMCID: PMC430628.
26. Saunders BM, Britton WJ. Life and death in the granuloma: immunopathology of tuberculosis. *Immunol Cell Biol*. 2007;85(2):103-11. doi: 10.1038/sj.icb.7100027. PubMed PMID: 17213830.

27. Dartois V. *The path of anti-tuberculosis drugs: from blood to lesions to mycobacterial cells.* *Nat Rev Microbiol.* 2014;12(3):159-67. doi: 10.1038/nrmicro3200. PubMed PMID: 24487820; PubMed Central PMCID: PMC4341982.
28. Kaplan G, Post FA, Moreira AL, Wainwright H, Kreiswirth BN, Tanverdi M, et al. *Mycobacterium tuberculosis growth at the cavity surface: a microenvironment with failed immunity.* *Infect Immun.* 2003;71(12):7099-108. PubMed PMID: 14638800; PubMed Central PMCID: PMC308931.
29. Kaufmann SH, Weiner J, von Reyn CF. *Novel approaches to tuberculosis vaccine development.* *Int J Infect Dis.* 2016. doi: 10.1016/j.ijid.2016.10.018. PubMed PMID: 27816661.
30. Kaufmann SH, Cotton MF, Eisele B, Gengenbacher M, Grode L, Hesselning AC, et al. *The BCG replacement vaccine VPM1002: from drawing board to clinical trial.* *Expert Rev Vaccines.* 2014;13(5):619-30. doi: 10.1586/14760584.2014.905746. PubMed PMID: 24702486.
31. Donald PR, van Zyl LE, de Villiers J. *BCG vaccination status of children with tuberculous meningitis and the use of unsupervised isoniazid prophylaxis.* *S Afr Med J.* 1995;85(3):167-70. PubMed PMID: 7777968.
32. Wolzak NK, Cooke ML, Orth H, van Toorn R. *The changing profile of pediatric meningitis at a referral centre in Cape Town, South Africa.* *J Trop Pediatr.* 2012;58(6):491-5. doi: 10.1093/tropej/fms031. PubMed PMID: 22791086.
33. Arbues A, Aguilo JI, Gonzalo-Asensio J, Marinova D, Uranga S, Puentes E, et al. *Construction, characterization and preclinical evaluation of MTBVAC, the first live-attenuated M. tuberculosis-based vaccine to enter clinical trials.* *Vaccine.* 2013;31(42):4867-73. doi: 10.1016/j.vaccine.2013.07.051. PubMed PMID: 23965219.
34. Aguilo N, Uranga S, Marinova D, Monzon M, Badiola J, Martin C. *MTBVAC vaccine is safe, immunogenic and confers protective efficacy against Mycobacterium tuberculosis in newborn mice.* *Tuberculosis (Edinb).* 2016;96:71-4. doi: 10.1016/j.tube.2015.10.010. PubMed PMID: 26786657; PubMed Central PMCID: PMC4727503.
35. Farhat M, Greenaway C, Pai M, Menzies D. *False-positive tuberculin skin tests: what is the absolute effect of BCG and non-tuberculous mycobacteria?* *Int J Tuberc Lung Dis.* 2006;10(11):1192-204. PubMed PMID: 17131776.
36. Sorensen AL, Nagai S, Houen G, Andersen P, Andersen AB. *Purification and characterization of a low-molecular-mass T-cell antigen secreted by Mycobacterium tuberculosis.* *Infect Immun.* 1995;63(5):1710-7. PubMed PMID: 7729876; PubMed Central PMCID: PMC173214.
37. Gazi MA, Islam MR, Kibria MG, Mahmud Z. *General and advanced diagnostic tools to detect Mycobacterium tuberculosis and their drug susceptibility: a review.* *Eur J Clin Microbiol Infect Dis.* 2015;34(5):851-61. doi: 10.1007/s10096-014-2306-5. PubMed PMID: 25560709.
38. Naidoo P, Dunbar R, Lombard C, du Toit E, Caldwell J, Detjen A, et al. *Comparing Tuberculosis Diagnostic Yield in Smear/Culture and Xpert(R) MTB/RIF-Based Algorithms Using a Non-Randomised Stepped-Wedge Design.* *PLoS One.* 2016;11(3):e0150487. doi: 10.1371/journal.pone.0150487. PubMed PMID: 26930400; PubMed Central PMCID: PMC4773132.

39. Detjen AK, DiNardo AR, Leyden J, Steingart KR, Menzies D, Schiller I, et al. Xpert MTB/RIF assay for the diagnosis of pulmonary tuberculosis in children: a systematic review and meta-analysis. *Lancet Respir Med*. 2015;3(6):451-61. doi: 10.1016/S2213-2600(15)00095-8. PubMed PMID: 25812968; PubMed Central PMCID: PMC4756280.
40. Trajman A, Durovni B, Saraceni V, Menezes A, Cordeiro-Santos M, Cobelens F, et al. Impact on Patients' Treatment Outcomes of XpertMTB/RIF Implementation for the Diagnosis of Tuberculosis: Follow-Up of a Stepped-Wedge Randomized Clinical Trial. *PLoS One*. 2015;10(4):e0123252. doi: 10.1371/journal.pone.0123252. PubMed PMID: 25915745; PubMed Central PMCID: PMC4411054.
41. Cavusoglu C, Turhan A, Akinci P, Soyler I. Evaluation of the Genotype MTBDR assay for rapid detection of rifampin and isoniazid resistance in *Mycobacterium tuberculosis* isolates. *J Clin Microbiol*. 2006;44(7):2338-42. doi: 10.1128/JCM.00425-06. PubMed PMID: 16825346; PubMed Central PMCID: PMC1489470.
42. Wallis RS, Wang C, Doherty TM, Onyebujoh P, Vahedi M, Laang H, et al. Biomarkers for tuberculosis disease activity, cure, and relapse. *Lancet Infect Dis*. 2010;10(2):68-9. doi: 10.1016/S1473-3099(10)70003-7. PubMed PMID: 20113972.
43. Zumla A, Chakaya J, Centis R, D'Ambrosio L, Mwaba P, Bates M, et al. Tuberculosis treatment and management--an update on treatment regimens, trials, new drugs, and adjunct therapies. *Lancet Respir Med*. 2015;3(3):220-34. doi: 10.1016/S2213-2600(15)00063-6. PubMed PMID: 25773212.
44. Nahid P, Dorman SE, Alipanah N, Barry PM, Brozek JL, Cattamanchi A, et al. Official American Thoracic Society/Centers for Disease Control and Prevention/Infectious Diseases Society of America Clinical Practice Guidelines: Treatment of Drug-Susceptible Tuberculosis. *Clin Infect Dis*. 2016;63(7):e147-95. doi: 10.1093/cid/ciw376. PubMed PMID: 27516382.
45. Cox E, Laessig K. FDA approval of bedaquiline--the benefit-risk balance for drug-resistant tuberculosis. *N Engl J Med*. 2014;371(8):689-91. doi: 10.1056/NEJMp1314385. PubMed PMID: 25140952.
46. Feldman WH, Baggenstoss AH. The residual infectivity of the primary complex of tuberculosis. *Am J Pathol*. 1938;14(4):473-90. PubMed PMID: 19970404; PubMed Central PMCID: PMC1964987.
47. Zhang Y, Yew WW, Barer MR. Targeting persists for tuberculosis control. *Antimicrob Agents Chemother*. 2012;56(5):2223-30. doi: 10.1128/AAC.06288-11. PubMed PMID: 22391538; PubMed Central PMCID: PMC3346619.
48. Lillebaek T, Dirksen A, Baess I, Strunge B, Thomsen VO, Andersen AB. Molecular evidence of endogenous reactivation of *Mycobacterium tuberculosis* after 33 years of latent infection. *J Infect Dis*. 2002;185(3):401-4. doi: 10.1086/338342. PubMed PMID: 11807725.
49. Stewart GR, Robertson BD, Young DB. Tuberculosis: a problem with persistence. *Nat Rev Microbiol*. 2003;1(2):97-105. doi: 10.1038/nrmicro749. PubMed PMID: 15035039.
50. Gengenbacher M, Kaufmann SH. *Mycobacterium tuberculosis*: success through dormancy. *FEMS Microbiol Rev*. 2012;36(3):514-32. doi: 10.1111/j.1574-6976.2012.00331.x. PubMed PMID: 22320122; PubMed Central PMCID: PMC3319523.

51. Ehlers S, Schaible UE. *The granuloma in tuberculosis: dynamics of a host-pathogen collusion.* *Front Immunol.* 2012;3:411. doi: 10.3389/fimmu.2012.00411. PubMed PMID: 23308075; PubMed Central PMCID: PMC3538277.
52. Bacon J, Alderwick LJ, Allnut JA, Gabasova E, Watson R, Hatch KA, et al. *Non-replicating Mycobacterium tuberculosis elicits a reduced infectivity profile with corresponding modifications to the cell wall and extracellular matrix.* *PLoS One.* 2014;9(2):e87329. doi: 10.1371/journal.pone.0087329. PubMed PMID: 24516549; PubMed Central PMCID: PMC3916317.
53. Gomez JE, McKinney JD. *M. tuberculosis persistence, latency, and drug tolerance.* *Tuberculosis (Edinb).* 2004;84(1-2):29-44. PubMed PMID: 14670344.
54. Paredes-Sabja D, Cofre-Araneda G, Brito-Silva C, Pizarro-Guajardo M, Sarker MR. *Clostridium difficile spore-macrophage interactions: spore survival.* *PLoS One.* 2012;7(8):e43635. doi: 10.1371/journal.pone.0043635. PubMed PMID: 22952726; PubMed Central PMCID: PMC3428350.
55. Meyer JA. *Tuberculosis, the Adirondacks, and coming of age for thoracic surgery.* *Ann Thorac Surg.* 1991;52(4):881-5. PubMed PMID: 1929650.
56. Rees RJ, Hart PD. *Analysis of the host-parasite equilibrium in chronic murine tuberculosis by total and viable bacillary counts.* *Br J Exp Pathol.* 1961;42:83-8. PubMed PMID: 13740304; PubMed Central PMCID: PMC2083177.
57. Evangelopoulos D, da Fonseca JD, Waddell SJ. *Understanding anti-tuberculosis drug efficacy: rethinking bacterial populations and how we model them.* *Int J Infect Dis.* 2015;32:76-80. doi: 10.1016/j.ijid.2014.11.028. PubMed PMID: 25809760.
58. Wayne LG, Hayes LG. *An in vitro model for sequential study of shutdown of Mycobacterium tuberculosis through two stages of nonreplicating persistence.* *Infect Immun.* 1996;64(6):2062-9. PubMed PMID: 8675308; PubMed Central PMCID: PMC174037.
59. Wayne LG, Sramek HA. *Metronidazole is bactericidal to dormant cells of Mycobacterium tuberculosis.* *Antimicrob Agents Chemother.* 1994;38(9):2054-8. PubMed PMID: 7811018; PubMed Central PMCID: PMC284683.
60. Betts JC, Lukey PT, Robb LC, McAdam RA, Duncan K. *Evaluation of a nutrient starvation model of Mycobacterium tuberculosis persistence by gene and protein expression profiling.* *Mol Microbiol.* 2002;43(3):717-31. PubMed PMID: 11929527.
61. Cho SH, Warit S, Wan B, Hwang CH, Pauli GF, Franzblau SG. *Low-oxygen-recovery assay for high-throughput screening of compounds against nonreplicating Mycobacterium tuberculosis.* *Antimicrob Agents Chemother.* 2007;51(4):1380-5. doi: 10.1128/AAC.00055-06. PubMed PMID: 17210775; PubMed Central PMCID: PMC1855511.
62. Rhoades ER, Frank AA, Orme IM. *Progression of chronic pulmonary tuberculosis in mice aerogenically infected with virulent Mycobacterium tuberculosis.* *Tuber Lung Dis.* 1997;78(1):57-66. PubMed PMID: 9666963.

63. Loring WE, Vandiviere HM. The treated pulmonary lesion and its tubercle bacillus. I. Pathology and pathogenesis. *Am J Med Sci.* 1956;232(1):20-9. PubMed PMID: 13326886.
64. Vandiviere HM, Loring WE, Melvin I, Willis S. The treated pulmonary lesion and its tubercle bacillus. II. The death and resurrection. *Am J Med Sci.* 1956;232(1):30-7; passim. PubMed PMID: 13326887.
65. McCune RM, Feldmann FM, Lambert HP, McDermott W. Microbial persistence. I. The capacity of tubercle bacilli to survive sterilization in mouse tissues. *J Exp Med.* 1966;123(3):445-68. PubMed PMID: 4957010; PubMed Central PMCID: PMCPMC2138153.
66. Basaraba RJ. Experimental tuberculosis: the role of comparative pathology in the discovery of improved tuberculosis treatment strategies. *Tuberculosis (Edinb).* 2008;88 Suppl 1:S35-47. doi: 10.1016/S1472-9792(08)70035-0. PubMed PMID: 18762152.
67. Wayne LG, Lin KY. Glyoxylate metabolism and adaptation of *Mycobacterium tuberculosis* to survival under anaerobic conditions. *Infect Immun.* 1982;37(3):1042-9. PubMed PMID: 6813266; PubMed Central PMCID: PMCPMC347645.
68. Sherman DR, Voskuil M, Schnappinger D, Liao R, Harrell MI, Schoolnik GK. Regulation of the *Mycobacterium tuberculosis* hypoxic response gene encoding alpha-crystallin. *Proc Natl Acad Sci U S A.* 2001;98(13):7534-9. doi: 10.1073/pnas.121172498. PubMed PMID: 11416222; PubMed Central PMCID: PMCPMC34703.
69. McKinney JD, Honer zu Bentrup K, Munoz-Elias EJ, Miczak A, Chen B, Chan WT, et al. Persistence of *Mycobacterium tuberculosis* in macrophages and mice requires the glyoxylate shunt enzyme isocitrate lyase. *Nature.* 2000;406(6797):735-8. doi: 10.1038/35021074. PubMed PMID: 10963599.
70. Glickman MS, Cox JS, Jacobs WR, Jr. A novel mycolic acid cyclopropane synthetase is required for cording, persistence, and virulence of *Mycobacterium tuberculosis*. *Mol Cell.* 2000;5(4):717-27. PubMed PMID: 10882107.
71. Steyn AJ, Collins DM, Hondalus MK, Jacobs WR, Jr., Kawakami RP, Bloom BR. *Mycobacterium tuberculosis* WhiB3 interacts with RpoV to affect host survival but is dispensable for in vivo growth. *Proc Natl Acad Sci U S A.* 2002;99(5):3147-52. doi: 10.1073/pnas.052705399. PubMed PMID: 11880648; PubMed Central PMCID: PMCPMC122487.
72. Keren I, Minami S, Rubin E, Lewis K. Characterization and transcriptome analysis of *Mycobacterium tuberculosis* persisters. *MBio.* 2011;2(3):e00100-11. doi: 10.1128/mBio.00100-11. PubMed PMID: 21673191; PubMed Central PMCID: PMCPMC3119538.
73. Voskuil MI, Visconti KC, Schoolnik GK. *Mycobacterium tuberculosis* gene expression during adaptation to stationary phase and low-oxygen dormancy. *Tuberculosis (Edinb).* 2004;84(3-4):218-27. doi: 10.1016/j.tube.2004.02.003. PubMed PMID: 15207491.
74. Black PA, Warren RM, Louw GE, van Helden PD, Victor TC, Kana BD. Energy metabolism and drug efflux in *Mycobacterium tuberculosis*. *Antimicrob Agents Chemother.* 2014;58(5):2491-503. doi: 10.1128/AAC.02293-13. PubMed PMID: 24614376; PubMed Central PMCID: PMCPMC3993223.

75. Watanabe S, Zimmermann M, Goodwin MB, Sauer U, Barry CE, 3rd, Boshoff HI. Fumarate reductase activity maintains an energized membrane in anaerobic *Mycobacterium tuberculosis*. *PLoS Pathog.* 2011;7(10):e1002287. doi: 10.1371/journal.ppat.1002287. PubMed PMID: 21998585; PubMed Central PMCID: PMC3188519.
76. Boshoff HI, Barry CE, 3rd. Tuberculosis - metabolism and respiration in the absence of growth. *Nat Rev Microbiol.* 2005;3(1):70-80. doi: 10.1038/nrmicro1065. PubMed PMID: 15608701.
77. Brauner A, Fridman O, Gefen O, Balaban NQ. Distinguishing between resistance, tolerance and persistence to antibiotic treatment. *Nat Rev Microbiol.* 2016;14(5):320-30. doi: 10.1038/nrmicro.2016.34. PubMed PMID: 27080241.
78. Olsen I. Biofilm-specific antibiotic tolerance and resistance. *Eur J Clin Microbiol Infect Dis.* 2015;34(5):877-86. doi: 10.1007/s10096-015-2323-z. PubMed PMID: 25630538.
79. Hoff DR, Ryan GJ, Driver ER, Ssemakulu CC, De Groot MA, Basaraba RJ, et al. Location of intra- and extracellular *M. tuberculosis* populations in lungs of mice and guinea pigs during disease progression and after drug treatment. *PLoS One.* 2011;6(3):e17550. doi: 10.1371/journal.pone.0017550. PubMed PMID: 21445321; PubMed Central PMCID: PMC3061964.
80. Mitchison D, Davies G. The chemotherapy of tuberculosis: past, present and future. *Int J Tuberc Lung Dis.* 2012;16(6):724-32. doi: 10.5588/ijtld.12.0083. PubMed PMID: 22613684; PubMed Central PMCID: PMC3736084.
81. Wallis RS, Patil S, Cheon SH, Edmonds K, Phillips M, Perkins MD, et al. Drug tolerance in *Mycobacterium tuberculosis*. *Antimicrob Agents Chemother.* 1999;43(11):2600-6. PubMed PMID: 10543735; PubMed Central PMCID: PMC389531.
82. Mahapatra S, Woolhiser LK, Lenaerts AJ, Johnson JL, Eisenach KD, Joloba ML, et al. A novel metabolite of antituberculosis therapy demonstrates host activation of isoniazid and formation of the isoniazid-NAD<sup>+</sup> adduct. *Antimicrob Agents Chemother.* 2012;56(1):28-35. doi: 10.1128/AAC.05486-11. PubMed PMID: 22037847; PubMed Central PMCID: PMC3256082.
83. Zhang Y, Heym B, Allen B, Young D, Cole S. The catalase-peroxidase gene and isoniazid resistance of *Mycobacterium tuberculosis*. *Nature.* 1992;358(6387):591-3. doi: 10.1038/358591a0. PubMed PMID: 1501713.
84. Rawat R, Whitty A, Tonge PJ. The isoniazid-NAD adduct is a slow, tight-binding inhibitor of InhA, the *Mycobacterium tuberculosis* enoyl reductase: adduct affinity and drug resistance. *Proc Natl Acad Sci U S A.* 2003;100(24):13881-6. doi: 10.1073/pnas.2235848100. PubMed PMID: 14623976; PubMed Central PMCID: PMC283515.
85. Hazbon MH, Brimacombe M, Bobadilla del Valle M, Cavatore M, Guerrero MI, Varma-Basil M, et al. Population genetics study of isoniazid resistance mutations and evolution of multidrug-resistant *Mycobacterium tuberculosis*. *Antimicrob Agents Chemother.* 2006;50(8):2640-9. doi: 10.1128/AAC.00112-06. PubMed PMID: 16870753; PubMed Central PMCID: PMC1538650.
86. Ramaswamy SV, Reich R, Dou SJ, Jasperse L, Pan X, Wanger A, et al. Single nucleotide polymorphisms in genes associated with isoniazid resistance in *Mycobacterium tuberculosis*. *Antimicrob*

- Agents Chemother.* 2003;47(4):1241-50. PubMed PMID: 12654653; PubMed Central PMCID: PMCPMC152487.
87. Telenti A, Imboden P, Marchesi F, Lowrie D, Cole S, Colston MJ, et al. Detection of rifampicin-resistance mutations in *Mycobacterium tuberculosis*. *Lancet.* 1993;341(8846):647-50. PubMed PMID: 8095569.
88. Palomino JC, Martin A. Drug Resistance Mechanisms in *Mycobacterium tuberculosis*. *Antibiotics (Basel).* 2014;3(3):317-40. doi: 10.3390/antibiotics3030317. PubMed PMID: 27025748; PubMed Central PMCID: PMCPMC4790366.
89. Andries K, Verhasselt P, Guillemont J, Gohlmann HW, Neefs JM, Winkler H, et al. A diarylquinoline drug active on the ATP synthase of *Mycobacterium tuberculosis*. *Science.* 2005;307(5707):223-7. doi: 10.1126/science.1106753. PubMed PMID: 15591164.
90. Andries K, Villellas C, Coeck N, Thys K, Gevers T, Vranckx L, et al. Acquired resistance of *Mycobacterium tuberculosis* to bedaquiline. *PLoS One.* 2014;9(7):e102135. doi: 10.1371/journal.pone.0102135. PubMed PMID: 25010492; PubMed Central PMCID: PMCPMC4092087.
91. Migliori GB, Centis R, D'Ambrosio L, Spanevello A, Borroni E, Cirillo DM, et al. Totally drug-resistant and extremely drug-resistant tuberculosis: the same disease? *Clin Infect Dis.* 2012;54(9):1379-80. doi: 10.1093/cid/cis128. PubMed PMID: 22492321.
92. Leclercq R, Courvalin P. Intrinsic and unusual resistance to macrolide, lincosamide, and streptogramin antibiotics in bacteria. *Antimicrob Agents Chemother.* 1991;35(7):1273-6. PubMed PMID: 1929281; PubMed Central PMCID: PMCPMC245157.
93. Olaitan AO, Morand S, Rolain JM. Mechanisms of polymyxin resistance: acquired and intrinsic resistance in bacteria. *Front Microbiol.* 2014;5:643. doi: 10.3389/fmicb.2014.00643. PubMed PMID: 25505462; PubMed Central PMCID: PMCPMC4244539.
94. Berger-Bachi B. Resistance mechanisms of gram-positive bacteria. *Int J Med Microbiol.* 2002;292(1):27-35. doi: 10.1078/1438-4221-00185. PubMed PMID: 12139425.
95. Roberts MC, Sutcliffe J, Courvalin P, Jensen LB, Rood J, Seppala H. Nomenclature for macrolide and macrolide-lincosamide-streptogramin B resistance determinants. *Antimicrob Agents Chemother.* 1999;43(12):2823-30. PubMed PMID: 10582867; PubMed Central PMCID: PMCPMC89572.
96. Nash KA. Intrinsic macrolide resistance in *Mycobacterium smegmatis* is conferred by a novel *erm* gene, *erm(38)*. *Antimicrob Agents Chemother.* 2003;47(10):3053-60. PubMed PMID: 14506008; PubMed Central PMCID: PMCPMC201133.
97. Andini N, Nash KA. Intrinsic macrolide resistance of the *Mycobacterium tuberculosis* complex is inducible. *Antimicrob Agents Chemother.* 2006;50(7):2560-2. doi: 10.1128/AAC.00264-06. PubMed PMID: 16801446; PubMed Central PMCID: PMCPMC1489773.

98. Borges A, Saavedra MJ, Simoes M. The activity of ferulic and gallic acids in biofilm prevention and control of pathogenic bacteria. *Biofouling*. 2012;28(7):755-67. doi: 10.1080/08927014.2012.706751. PubMed PMID: 22823343.
99. Flemming HC, Wingender J, Szewzyk U, Steinberg P, Rice SA, Kjelleberg S. Biofilms: an emergent form of bacterial life. *Nat Rev Microbiol*. 2016;14(9):563-75. doi: 10.1038/nrmicro.2016.94. PubMed PMID: 27510863.
100. Dunne WM, Jr. Bacterial adhesion: seen any good biofilms lately? *Clin Microbiol Rev*. 2002;15(2):155-66. PubMed PMID: 11932228; PubMed Central PMCID: PMC118072.
101. Anderson GG, O'Toole GA. Innate and induced resistance mechanisms of bacterial biofilms. *Curr Top Microbiol Immunol*. 2008;322:85-105. PubMed PMID: 18453273.
102. Fux CA, Costerton JW, Stewart PS, Stoodley P. Survival strategies of infectious biofilms. *Trends Microbiol*. 2005;13(1):34-40. doi: 10.1016/j.tim.2004.11.010. PubMed PMID: 15639630.
103. Beloin C, Roux A, Ghigo JM. *Escherichia coli* biofilms. *Curr Top Microbiol Immunol*. 2008;322:249-89. PubMed PMID: 18453280; PubMed Central PMCID: PMC12864707.
104. Mohamed JA, Teng F, Nallapareddy SR, Murray BE. Pleiotropic effects of 2 *Enterococcus faecalis* *sagA*-like genes, *salA* and *salB*, which encode proteins that are antigenic during human infection, on biofilm formation and binding to collagen type I and fibronectin. *J Infect Dis*. 2006;193(2):231-40. doi: 10.1086/498871. PubMed PMID: 16362887.
105. Ma L, Jackson KD, Landry RM, Parsek MR, Wozniak DJ. Analysis of *Pseudomonas aeruginosa* conditional *psl* variants reveals roles for the *psl* polysaccharide in adhesion and maintaining biofilm structure postattachment. *J Bacteriol*. 2006;188(23):8213-21. doi: 10.1128/JB.01202-06. PubMed PMID: 16980452; PubMed Central PMCID: PMC1698210.
106. Borlee BR, Goldman AD, Murakami K, Samudrala R, Wozniak DJ, Parsek MR. *Pseudomonas aeruginosa* uses a cyclic-di-GMP-regulated adhesin to reinforce the biofilm extracellular matrix. *Mol Microbiol*. 2010;75(4):827-42. doi: 10.1111/j.1365-2958.2009.06991.x. PubMed PMID: 20088866; PubMed Central PMCID: PMC2847200.
107. Kostakioti M, Hadjifrangiskou M, Hultgren SJ. Bacterial biofilms: development, dispersal, and therapeutic strategies in the dawn of the postantibiotic era. *Cold Spring Harb Perspect Med*. 2013;3(4):a010306. doi: 10.1101/cshperspect.a010306. PubMed PMID: 23545571; PubMed Central PMCID: PMC3683961.
108. Yu Q, Griffin EF, Moreau-Marquis S, Schwartzman JD, Stanton BA, O'Toole GA. In vitro evaluation of tobramycin and aztreonam versus *Pseudomonas aeruginosa* biofilms on cystic fibrosis-derived human airway epithelial cells. *J Antimicrob Chemother*. 2012;67(11):2673-81. doi: 10.1093/jac/dks296. PubMed PMID: 22843834; PubMed Central PMCID: PMC3468082.
109. Mah TF, O'Toole GA. Mechanisms of biofilm resistance to antimicrobial agents. *Trends Microbiol*. 2001;9(1):34-9. PubMed PMID: 11166241.

110. Favre-Bonte S, Kohler T, Van Delden C. Biofilm formation by *Pseudomonas aeruginosa*: role of the C4-HSL cell-to-cell signal and inhibition by azithromycin. *J Antimicrob Chemother.* 2003;52(4):598-604. doi: 10.1093/jac/dkg397. PubMed PMID: 12951348.
111. Hastings JW, Greenberg EP. Quorum sensing: the explanation of a curious phenomenon reveals a common characteristic of bacteria. *J Bacteriol.* 1999;181(9):2667-8. PubMed PMID: 10217751; PubMed Central PMCID: PMCPMC93702.
112. Geier H, Mostowy S, Cangelosi GA, Behr MA, Ford TE. Autoinducer-2 triggers the oxidative stress response in *Mycobacterium avium*, leading to biofilm formation. *Appl Environ Microbiol.* 2008;74(6):1798-804. doi: 10.1128/AEM.02066-07. PubMed PMID: 18245256; PubMed Central PMCID: PMCPMC2268301.
113. Dandekar AA, Greenberg EP. Microbiology: Plan B for quorum sensing. *Nat Chem Biol.* 2013;9(5):292-3. doi: 10.1038/nchembio.1233. PubMed PMID: 23594781.
114. Karatan E, Watnick P. Signals, regulatory networks, and materials that build and break bacterial biofilms. *Microbiol Mol Biol Rev.* 2009;73(2):310-47. doi: 10.1128/MMBR.00041-08. PubMed PMID: 19487730; PubMed Central PMCID: PMCPMC2698413.
115. Marcondes S, Cardoso MH, Morganti RP, Thomazzi SM, Lilla S, Murad F, et al. Cyclic GMP-independent mechanisms contribute to the inhibition of platelet adhesion by nitric oxide donor: a role for alpha-actinin nitration. *Proc Natl Acad Sci U S A.* 2006;103(9):3434-9. doi: 10.1073/pnas.0509397103. PubMed PMID: 16492779; PubMed Central PMCID: PMCPMC1413892.
116. Boyd A, Chakrabarty AM. Role of alginate lyase in cell detachment of *Pseudomonas aeruginosa*. *Appl Environ Microbiol.* 1994;60(7):2355-9. PubMed PMID: 8074516; PubMed Central PMCID: PMCPMC201655.
117. Hall-Stoodley L, Stoodley P. Developmental regulation of microbial biofilms. *Curr Opin Biotechnol.* 2002;13(3):228-33. PubMed PMID: 12180097.
118. Kaplan JB. Biofilm dispersal: mechanisms, clinical implications, and potential therapeutic uses. *J Dent Res.* 2010;89(3):205-18. doi: 10.1177/0022034509359403. PubMed PMID: 20139339; PubMed Central PMCID: PMCPMC3318030.
119. Hoiby N, Bjarnsholt T, Givskov M, Molin S, Ciofu O. Antibiotic resistance of bacterial biofilms. *Int J Antimicrob Agents.* 2010;35(4):322-32. doi: 10.1016/j.ijantimicag.2009.12.011. PubMed PMID: 20149602.
120. Hoiby N, Ciofu O, Bjarnsholt T. *Pseudomonas aeruginosa* biofilms in cystic fibrosis. *Future Microbiol.* 2010;5(11):1663-74. doi: 10.2217/fmb.10.125. PubMed PMID: 21133688.
121. Chen X, Schluesener HJ. Nanosilver: a nanoparticle in medical application. *Toxicol Lett.* 2008;176(1):1-12. doi: 10.1016/j.toxlet.2007.10.004. PubMed PMID: 18022772.
122. Sutherland IW, Hughes KA, Skillman LC, Tait K. The interaction of phage and biofilms. *FEMS Microbiol Lett.* 2004;232(1):1-6. PubMed PMID: 15061140.

123. Han Z, Pinkner JS, Ford B, Obermann R, Nolan W, Wildman SA, et al. Structure-based drug design and optimization of mannoside bacterial FimH antagonists. *J Med Chem.* 2010;53(12):4779-92. doi: 10.1021/jm100438s. PubMed PMID: 20507142; PubMed Central PMCID: PMCPMC2894565.
124. Rasko DA, Moreira CG, Li de R, Reading NC, Ritchie JM, Waldor MK, et al. Targeting QseC signaling and virulence for antibiotic development. *Science.* 2008;321(5892):1078-80. doi: 10.1126/science.1160354. PubMed PMID: 18719281; PubMed Central PMCID: PMCPMC2605406.
125. Guiton PS, Hung CS, Kline KA, Roth R, Kau AL, Hayes E, et al. Contribution of autolysin and Sortase a during *Enterococcus faecalis* DNA-dependent biofilm development. *Infect Immun.* 2009;77(9):3626-38. doi: 10.1128/IAI.00219-09. PubMed PMID: 19528211; PubMed Central PMCID: PMCPMC2738007.
126. Bahna P, Dvorak T, Hanna H, Yasko AW, Hachem R, Raad I. Orthopaedic metal devices coated with a novel antiseptic dye for the prevention of bacterial infections. *Int J Antimicrob Agents.* 2007;29(5):593-6. doi: 10.1016/j.ijantimicag.2006.12.013. PubMed PMID: 17317111.
127. Flemming K, Klingenberg C, Cavanagh JP, Sletteng M, Stensen W, Svendsen JS, et al. High in vitro antimicrobial activity of synthetic antimicrobial peptidomimetics against staphylococcal biofilms. *J Antimicrob Chemother.* 2009;63(1):136-45. doi: 10.1093/jac/dkn464. PubMed PMID: 19010828.
128. Borriello G, Werner E, Roe F, Kim AM, Ehrlich GD, Stewart PS. Oxygen limitation contributes to antibiotic tolerance of *Pseudomonas aeruginosa* in biofilms. *Antimicrob Agents Chemother.* 2004;48(7):2659-64. doi: 10.1128/AAC.48.7.2659-2664.2004. PubMed PMID: 15215123; PubMed Central PMCID: PMCPMC434183.
129. Wimpenny J, Manz W, Szewzyk U. Heterogeneity in biofilms. *FEMS Microbiol Rev.* 2000;24(5):661-71. PubMed PMID: 11077157.
130. Costerton JW, Stewart PS, Greenberg EP. Bacterial biofilms: a common cause of persistent infections. *Science.* 1999;284(5418):1318-22. PubMed PMID: 10334980.
131. Hogan D, Kolter R. Why are bacteria refractory to antimicrobials? *Curr Opin Microbiol.* 2002;5(5):472-7. PubMed PMID: 12354553.
132. Beenken KE, Dunman PM, McAleese F, Macapagal D, Murphy E, Projan SJ, et al. Global gene expression in *Staphylococcus aureus* biofilms. *J Bacteriol.* 2004;186(14):4665-84. doi: 10.1128/JB.186.14.4665-4684.2004. PubMed PMID: 15231800; PubMed Central PMCID: PMCPMC438561.
133. Ruisheng A, Grewal PS. *purL* gene expression affects biofilm formation and symbiotic persistence of *Photobacterium aerophilum* in the nematode *Heterorhabditis bacteriophora*. *Microbiology.* 2011;157(Pt 9):2595-603. doi: 10.1099/mic.0.048959-0. PubMed PMID: 21700665.
134. Keren I, Shah D, Spoering A, Kaldalu N, Lewis K. Specialized persister cells and the mechanism of multidrug tolerance in *Escherichia coli*. *J Bacteriol.* 2004;186(24):8172-80. doi: 10.1128/JB.186.24.8172-8180.2004. PubMed PMID: 15576765; PubMed Central PMCID: PMCPMC532439.

135. Richards JJ, Melander C. Controlling bacterial biofilms. *Chembiochem*. 2009;10(14):2287-94. doi: 10.1002/cbic.200900317. PubMed PMID: 19681090.
136. Hall-Stoodley L, Lappin-Scott H. Biofilm formation by the rapidly growing mycobacterial species *Mycobacterium fortuitum*. *FEMS Microbiol Lett*. 1998;168(1):77-84. PubMed PMID: 9812366.
137. Carter G, Wu M, Drummond DC, Bermudez LE. Characterization of biofilm formation by clinical isolates of *Mycobacterium avium*. *J Med Microbiol*. 2003;52(Pt 9):747-52. doi: 10.1099/jmm.0.05224-0. PubMed PMID: 12909649.
138. Recht J, Kolter R. Glycopeptidolipid acetylation affects sliding motility and biofilm formation in *Mycobacterium smegmatis*. *J Bacteriol*. 2001;183(19):5718-24. doi: 10.1128/JB.183.19.5718-5724.2001. PubMed PMID: 11544235; PubMed Central PMCID: PMCPMC95464.
139. Ojha A, Anand M, Bhatt A, Kremer L, Jacobs WR, Jr., Hatfull GF. GroEL1: a dedicated chaperone involved in mycolic acid biosynthesis during biofilm formation in mycobacteria. *Cell*. 2005;123(5):861-73. doi: 10.1016/j.cell.2005.09.012. PubMed PMID: 16325580.
140. Molloy S. Biofilms: biofilm microanatomy. *Nat Rev Microbiol*. 2013;11(5):300. doi: 10.1038/nrmicro3024. PubMed PMID: 23588247.
141. Trivedi A, Mavi PS, Bhatt D, Kumar A. Thiol reductive stress induces cellulose-anchored biofilm formation in *Mycobacterium tuberculosis*. *Nat Commun*. 2016;7:11392. doi: 10.1038/ncomms11392. PubMed PMID: 27109928; PubMed Central PMCID: PMCPMC4848537.
142. G C. *The tubercle bacillus in the pulmonary lesion of man; histobacteriology and its bearing on the therapy of pulmonary tuberculosis*. New York: Springer Publishing Company; 1955 1955.
143. Lenaerts AJ, Hoff D, Aly S, Ehlers S, Andries K, Cantarero L, et al. Location of persisting mycobacteria in a Guinea pig model of tuberculosis revealed by r207910. *Antimicrob Agents Chemother*. 2007;51(9):3338-45. doi: 10.1128/AAC.00276-07. PubMed PMID: 17517834; PubMed Central PMCID: PMCPMC2043239.
144. Vorkapic D, Pressler K, Schild S. Multifaceted roles of extracellular DNA in bacterial physiology. *Curr Genet*. 2016;62(1):71-9. doi: 10.1007/s00294-015-0514-x. PubMed PMID: 26328805; PubMed Central PMCID: PMCPMC4723616.
145. Schwartz K, Ganesan M, Payne DE, Solomon MJ, Boles BR. Extracellular DNA facilitates the formation of functional amyloids in *Staphylococcus aureus* biofilms. *Mol Microbiol*. 2016;99(1):123-34. doi: 10.1111/mmi.13219. PubMed PMID: 26365835; PubMed Central PMCID: PMCPMC4715698.
146. Mulcahy H, Charron-Mazenod L, Lewenza S. Extracellular DNA chelates cations and induces antibiotic resistance in *Pseudomonas aeruginosa* biofilms. *PLoS Pathog*. 2008;4(11):e1000213. doi: 10.1371/journal.ppat.1000213. PubMed PMID: 19023416; PubMed Central PMCID: PMCPMC2581603.
147. Kaplan MJ, Radic M. Neutrophil extracellular traps: double-edged swords of innate immunity. *J Immunol*. 2012;189(6):2689-95. doi: 10.4049/jimmunol.1201719. PubMed PMID: 22956760; PubMed Central PMCID: PMCPMC3439169.

148. Das T, Sehar S, Manefield M. The roles of extracellular DNA in the structural integrity of extracellular polymeric substance and bacterial biofilm development. *Environ Microbiol Rep*. 2013;5(6):778-86. doi: 10.1111/1758-2229.12085. PubMed PMID: 24249286.
149. Ojha A, Hatfull GF. The role of iron in *Mycobacterium smegmatis* biofilm formation: the exochelin siderophore is essential in limiting iron conditions for biofilm formation but not for planktonic growth. *Mol Microbiol*. 2007;66(2):468-83. doi: 10.1111/j.1365-2958.2007.05935.x. PubMed PMID: 17854402; PubMed Central PMCID: PMCPMC2170428.
150. Ojha AK, Baughn AD, Sambandan D, Hsu T, Trivelli X, Guerardel Y, et al. Growth of *Mycobacterium tuberculosis* biofilms containing free mycolic acids and harbouring drug-tolerant bacteria. *Mol Microbiol*. 2008;69(1):164-74. doi: 10.1111/j.1365-2958.2008.06274.x. PubMed PMID: 18466296; PubMed Central PMCID: PMCPMC2615189.
151. Islam MS, Richards JP, Ojha AK. Targeting drug tolerance in mycobacteria: a perspective from mycobacterial biofilms. *Expert Rev Anti Infect Ther*. 2012;10(9):1055-66. doi: 10.1586/eri.12.88. PubMed PMID: 23106280; PubMed Central PMCID: PMCPMC3562728.
152. Ackart DF, Hascall-Dove L, Caceres SM, Kirk NM, Podell BK, Melander C, et al. Expression of antimicrobial drug tolerance by attached communities of *Mycobacterium tuberculosis*. *Pathog Dis*. 2014;70(3):359-69. doi: 10.1111/2049-632X.12144. PubMed PMID: 24478060; PubMed Central PMCID: PMCPMC4361083.
153. Stowe SD, Richards JJ, Tucker AT, Thompson R, Melander C, Cavanagh J. Anti-biofilm compounds derived from marine sponges. *Mar Drugs*. 2011;9(10):2010-35. doi: 10.3390/md9102010. PubMed PMID: 22073007; PubMed Central PMCID: PMCPMC3210616.
154. Peng L, DeSousa J, Su Z, Novak BM, Nevzorov AA, Garland ER, et al. Inhibition of *Acinetobacter baumannii* biofilm formation on a methacrylate polymer containing a 2-aminoimidazole subunit. *Chem Commun (Camb)*. 2011;47(17):4896-8. doi: 10.1039/c1cc10691k. PubMed PMID: 21442111.
155. Sipkema D, Franssen MC, Osinga R, Tramper J, Wijffels RH. Marine sponges as pharmacy. *Mar Biotechnol (NY)*. 2005;7(3):142-62. doi: 10.1007/s10126-004-0405-5. PubMed PMID: 15776313.
156. Fusetani N. Antifouling marine natural products. *Nat Prod Rep*. 2011;28(2):400-10. doi: 10.1039/c0np00034e. PubMed PMID: 21082120.
157. Huggins WM, Minrovic BM, Corey BW, Jacobs AC, Melander RJ, Sommer RD, et al. 1,2,4-Triazolidine-3-thiones as Narrow Spectrum Antibiotics against Multidrug-Resistant *Acinetobacter baumannii*. *ACS Med Chem Lett*. 2017;8(1):27-31. doi: 10.1021/acsmedchemlett.6b00296. PubMed PMID: 28105270; PubMed Central PMCID: PMCPMC5238477.
158. Corey BW, Thompson MG, Hittle LE, Jacobs AC, Asafo-Adjei EA, Huggins WM, et al. 1,2,4-Triazolidine-3-thiones Have Specific Activity against *Acinetobacter baumannii* among Common Nosocomial Pathogens. *ACS Infect Dis*. 2017;3(1):62-71. doi: 10.1021/acsinfecdis.6b00133. PubMed PMID: 27764938.
159. Koswatta PB, Lovely CJ. Structure and synthesis of 2-aminoimidazole alkaloids from *Leucetta* and *Clathrina* sponges. *Nat Prod Rep*. 2011;28(3):511-28. doi: 10.1039/c0np00001a. PubMed PMID: 20981389.

160. Huigens RW, 3rd, Ma L, Gambino C, Moeller PD, Basso A, Cavanagh J, et al. Control of bacterial biofilms with marine alkaloid derivatives. *Mol Biosyst.* 2008;4(6):614-21. doi: 10.1039/b719989a. PubMed PMID: 18493660.
161. Rogers SA, Bero JD, Melander C. Chemical synthesis and biological screening of 2-aminoimidazole-based bacterial and fungal antibiofilm agents. *Chembiochem.* 2010;11(3):396-410. doi: 10.1002/cbic.200900617. PubMed PMID: 20049758.
162. Rogers SA, Melander C. Construction and screening of a 2-aminoimidazole library identifies a small molecule capable of inhibiting and dispersing bacterial biofilms across order, class, and phylum. *Angew Chem Int Ed Engl.* 2008;47(28):5229-31. doi: 10.1002/anie.200800862. PubMed PMID: 18528836.
163. Stowe SD, Tucker AT, Thompson R, Piper A, Richards JJ, Rogers SA, et al. Evaluation of the toxicity of 2-aminoimidazole antibiofilm agents using both cellular and model organism systems. *Drug Chem Toxicol.* 2012;35(3):310-5. doi: 10.3109/01480545.2011.614620. PubMed PMID: 22292413; PubMed Central PMCID: PMC3434693.
164. Richards JJ, Ballard TE, Melander C. Inhibition and dispersion of *Pseudomonas aeruginosa* biofilms with reverse amide 2-aminoimidazole oroidin analogues. *Org Biomol Chem.* 2008;6(8):1356-63. doi: 10.1039/b719082d. PubMed PMID: 18385842.
165. Su Z, Peng L, Worthington RJ, Melander C. Evaluation of 4,5-disubstituted-2-aminoimidazole-triazole conjugates for antibiofilm/antibiotic resensitization activity against MRSA and *Acinetobacter baumannii*. *ChemMedChem.* 2011;6(12):2243-51. doi: 10.1002/cmdc.201100316. PubMed PMID: 21928438.
166. Richards JJ, Reed CS, Melander C. Effects of N-pyrrole substitution on the anti-biofilm activities of oroidin derivatives against *Acinetobacter baumannii*. *Bioorg Med Chem Lett.* 2008;18(15):4325-7. doi: 10.1016/j.bmcl.2008.06.089. PubMed PMID: 18625555.
167. Mukherjee T, Boshoff H. Nitroimidazoles for the treatment of TB: past, present and future. *Future Med Chem.* 2011;3(11):1427-54. doi: 10.4155/fmc.11.90. PubMed PMID: 21879846; PubMed Central PMCID: PMC3225966.
168. Ashtekar DR, Costa-Perira R, Nagrajan K, Vishvanathan N, Bhatt AD, Rittel W. In vitro and in vivo activities of the nitroimidazole CGI 17341 against *Mycobacterium tuberculosis*. *Antimicrob Agents Chemother.* 1993;37(2):183-6. PubMed PMID: 8452346; PubMed Central PMCID: PMC187635.
169. Dick T, Lee BH, Murugasu-Oei B. Oxygen depletion induced dormancy in *Mycobacterium smegmatis*. *FEMS Microbiol Lett.* 1998;163(2):159-64. PubMed PMID: 9673018.
170. Lenaerts AJ, Gruppo V, Marietta KS, Johnson CM, Driscoll DK, Tompkins NM, et al. Preclinical testing of the nitroimidazopyran PA-824 for activity against *Mycobacterium tuberculosis* in a series of in vitro and in vivo models. *Antimicrob Agents Chemother.* 2005;49(6):2294-301. doi: 10.1128/AAC.49.6.2294-2301.2005. PubMed PMID: 15917524; PubMed Central PMCID: PMC1140539.
171. Kim P, Zhang L, Manjunatha UH, Singh R, Patel S, Jiricek J, et al. Structure-activity relationships of antitubercular nitroimidazoles. 1. Structural features associated with aerobic and anaerobic activities of

- 4- and 5-nitroimidazoles. *J Med Chem.* 2009;52(5):1317-28. doi: 10.1021/jm801246z. PubMed PMID: 19209889; PubMed Central PMCID: PMCPMC2765526.
172. Ackart DF, Lindsey EA, Podell BK, Melander RJ, Basaraba RJ, Melander C. Reversal of *Mycobacterium tuberculosis* phenotypic drug resistance by 2-aminoimidazole-based small molecules. *Pathog Dis.* 2014;70(3):370-8. doi: 10.1111/2049-632X.12143. PubMed PMID: 24478046; PubMed Central PMCID: PMCPMC4367863.
173. Bassetti M, Righi E. New antibiotics and antimicrobial combination therapy for the treatment of gram-negative bacterial infections. *Curr Opin Crit Care.* 2015;21(5):402-11. doi: 10.1097/MCC.0000000000000235. PubMed PMID: 26263298.
174. Prevention CfDca. *Antibiotic Resistance Threats in the United States, 2013.* U.S. Department of Health and Human Services, 2013.
175. Humphries RM, Pollett S, Sakoulas G. A current perspective on daptomycin for the clinical microbiologist. *Clin Microbiol Rev.* 2013;26(4):759-80. doi: 10.1128/CMR.00030-13. PubMed PMID: 24092854; PubMed Central PMCID: PMCPMC3811228.
176. Worthington RJ, Melander C. Combination approaches to combat multidrug-resistant bacteria. *Trends Biotechnol.* 2013;31(3):177-84. doi: 10.1016/j.tibtech.2012.12.006. PubMed PMID: 23333434; PubMed Central PMCID: PMCPMC3594660.
177. Handzlik J, Matys A, Kiec-Kononowicz K. Recent Advances in Multi-Drug Resistance (MDR) Efflux Pump Inhibitors of Gram-Positive Bacteria *S. aureus*. *Antibiotics (Basel).* 2013;2(1):28-45. doi: 10.3390/antibiotics2010028. PubMed PMID: 27029290; PubMed Central PMCID: PMCPMC4790296.
178. Harris TL, Worthington RJ, Melander C. Potent small-molecule suppression of oxacillin resistance in methicillin-resistant *Staphylococcus aureus*. *Angew Chem Int Ed Engl.* 2012;51(45):11254-7. doi: 10.1002/anie.201206911. PubMed PMID: 23047322; PubMed Central PMCID: PMCPMC3829614.
179. Worthington RJ, Bunders CA, Reed CS, Melander C. Small molecule suppression of carbapenem resistance in NDM-1 producing *Klebsiella pneumoniae*. *ACS Med Chem Lett.* 2012;3(5):357-61. doi: 10.1021/ml200290p. PubMed PMID: 22844552; PubMed Central PMCID: PMCPMC3405495.
180. Su Z, Yeagley AA, Su R, Peng L, Melander C. Structural studies on 4,5-disubstituted 2-aminoimidazole-based biofilm modulators that suppress bacterial resistance to beta-lactams. *ChemMedChem.* 2012;7(11):2030-9. doi: 10.1002/cmdc.201200350. PubMed PMID: 23011973.
181. Rogers SA, Huigens RW, 3rd, Cavanagh J, Melander C. Synergistic effects between conventional antibiotics and 2-aminoimidazole-derived antibiofilm agents. *Antimicrob Agents Chemother.* 2010;54(5):2112-8. doi: 10.1128/AAC.01418-09. PubMed PMID: 20211901; PubMed Central PMCID: PMCPMC2863642.
182. Wang F, Sambandan D, Halder R, Wang J, Batt SM, Weinrick B, et al. Identification of a small molecule with activity against drug-resistant and persistent tuberculosis. *Proc Natl Acad Sci U S A.* 2013;110(27):E2510-7. doi: 10.1073/pnas.1309171110. PubMed PMID: 23776209; PubMed Central PMCID: PMCPMC3703973.

183. Mohr KI. *History of Antibiotics Research. Curr Top Microbiol Immunol.* 2016;398:237-72. doi: 10.1007/82\_2016\_499. PubMed PMID: 27738915.
184. Abraham OA, Rosa VM, Antonio SM, Claudia G, Del Rosario MM. *Review of Antibiotic and Non-Antibiotic Properties of Beta-lactam Molecules. Antiinflamm Antiallergy Agents Med Chem.* 2016;15(1):3-14. PubMed PMID: 27185396.
185. Kong KF, Schneper L, Mathee K. *Beta-lactam antibiotics: from antibiosis to resistance and bacteriology. APMIS.* 2010;118(1):1-36. doi: 10.1111/j.1600-0463.2009.02563.x. PubMed PMID: 20041868; PubMed Central PMCID: PMCPMC2894812.
186. Livermore DM, Woodford N. *The beta-lactamase threat in Enterobacteriaceae, Pseudomonas and Acinetobacter. Trends Microbiol.* 2006;14(9):413-20. doi: 10.1016/j.tim.2006.07.008. PubMed PMID: 16876996.
187. Bellamy WD, Klimek JW. *Some Properties of Penicillin-resistant Staphylococci. J Bacteriol.* 1948;55(2):153-60. PubMed PMID: 16561443; PubMed Central PMCID: PMCPMC518424.
188. Chan K, Mack D, El-Mugamar H. *Empirical use of beta-lactam-beta-lactamase inhibitors. Infect Dis (Lond).* 2016;48(9):703-4. doi: 10.3109/23744235.2016.1169552. PubMed PMID: 27207186.
189. Abraham EP, Newton GG. *New penicillins, cephalosporin C, and penicillinase. Endeavour.* 1961;20:92-100. PubMed PMID: 13858999.
190. Brown AG, Butterworth D, Cole M, Hanscomb G, Hood JD, Reading C, et al. *Naturally-occurring beta-lactamase inhibitors with antibacterial activity. J Antibiot (Tokyo).* 1976;29(6):668-9. PubMed PMID: 950324.
191. Lee NL, Yuen KY, Kumana CR. *Beta-lactam antibiotic and beta-lactamase inhibitor combinations. JAMA.* 2001;285(4):386-8. PubMed PMID: 11242403.
192. Stachyra T, Pechereau MC, Bruneau JM, Claudon M, Frere JM, Miossec C, et al. *Mechanistic studies of the inactivation of TEM-1 and P99 by NXL104, a novel non-beta-lactam beta-lactamase inhibitor. Antimicrob Agents Chemother.* 2010;54(12):5132-8. doi: 10.1128/AAC.00568-10. PubMed PMID: 20921316; PubMed Central PMCID: PMCPMC2981269.
193. Spellberg B, Taylor-Blake B. *On the exoneration of Dr. William H. Stewart: debunking an urban legend. Infect Dis Poverty.* 2013;2(1):3. doi: 10.1186/2049-9957-2-3. PubMed PMID: 23849720; PubMed Central PMCID: PMCPMC3707092.
194. Abraham EP, Chain E. *An enzyme from bacteria able to destroy penicillin. 1940. Rev Infect Dis.* 1988;10(4):677-8. PubMed PMID: 3055168.
195. Abraham EP, Chain E, Fletcher CM, Florey HW, Gardner AD, Heatley NG, et al. *Further observations on penicillin. 1941. Eur J Clin Pharmacol.* 1992;42(1):3-9. PubMed PMID: 1541313.
196. Finland M. *Changing ecology of bacterial infections as related to antibacterial therapy. J Infect Dis.* 1970;122(5):419-31. PubMed PMID: 5476392.

- 197.Barber M. Staphylococcal infection due to penicillin-resistant strains. *Br Med J.* 1947;2(4534):863-5. *PubMed PMID:* 20272443; *PubMed Central PMCID:* PMCPMC2056216.
- 198.Rolinson GN, Macdonald AC, Wilson DA. Bactericidal action of beta-lactam antibiotics on *Escherichia coli* with particular reference to ampicillin and amoxycillin. *J Antimicrob Chemother.* 1977;3(6):541-53. *PubMed PMID:* 340439.
- 199.Young KD. Microbiology: The bacterial cell wall takes centre stage. *Nature.* 2016;537(7622):622-4. *doi:* 10.1038/537622a. *PubMed PMID:* 27680934.
- 200.Park JT, Johnson MJ. Accumulation of labile phosphate in *Staphylococcus aureus* grown in the presence of penicillin. *J Biol Chem.* 1949;179(2):585-92. *PubMed PMID:* 18149992.
- 201.Ruiz N. Lipid Flippases for Bacterial Peptidoglycan Biosynthesis. *Lipid Insights.* 2015;8(Suppl 1):21-31. *doi:* 10.4137/LPI.S31783. *PubMed PMID:* 26792999; *PubMed Central PMCID:* PMCPMC4714577.
- 202.Gautam A, Vyas R, Tewari R. Peptidoglycan biosynthesis machinery: a rich source of drug targets. *Crit Rev Biotechnol.* 2011;31(4):295-336. *doi:* 10.3109/07388551.2010.525498. *PubMed PMID:* 21091161.
- 203.Moraes GL, Gomes GC, Monteiro de Sousa PR, Alves CN, Govender T, Kruger HG, et al. Structural and functional features of enzymes of *Mycobacterium tuberculosis* peptidoglycan biosynthesis as targets for drug development. *Tuberculosis (Edinb).* 2015;95(2):95-111. *doi:* 10.1016/j.tube.2015.01.006. *PubMed PMID:* 25701501; *PubMed Central PMCID:* PMCPMC4659487.
- 204.Fisher JF, Meroueh SO, Mobashery S. Bacterial resistance to beta-lactam antibiotics: compelling opportunism, compelling opportunity. *Chem Rev.* 2005;105(2):395-424. *doi:* 10.1021/cr030102i. *PubMed PMID:* 15700950.
- 205.Zygmunt WA. Antagonism of D-Cycloserine Inhibition of Mycobacterial Growth by D-Alanine. *J Bacteriol.* 1963;85:1217-20. *PubMed PMID:* 14047211; *PubMed Central PMCID:* PMCPMC278322.
- 206.Nieto M, Perkins HR. Modifications of the acyl-D-alanyl-D-alanine terminus affecting complex-formation with vancomycin. *Biochem J.* 1971;123(5):789-803. *PubMed PMID:* 5124386; *PubMed Central PMCID:* PMCPMC1177079.
- 207.Teo AC, Roper DI. Core Steps of Membrane-Bound Peptidoglycan Biosynthesis: Recent Advances, Insight and Opportunities. *Antibiotics (Basel).* 2015;4(4):495-520. *doi:* 10.3390/antibiotics4040495. *PubMed PMID:* 27025638; *PubMed Central PMCID:* PMCPMC4790310.
- 208.Diacon AH, van der Merwe L, Barnard M, von Groote-Bidlingmaier F, Lange C, Garcia-Basteiro AL, et al. beta-Lactams against Tuberculosis--New Trick for an Old Dog? *N Engl J Med.* 2016;375(4):393-4. *doi:* 10.1056/NEJMc1513236. *PubMed PMID:* 27433841.
- 209.Elander RP. Industrial production of beta-lactam antibiotics. *Appl Microbiol Biotechnol.* 2003;61(5-6):385-92. *doi:* 10.1007/s00253-003-1274-y. *PubMed PMID:* 12679848.

210. Gonzalo X, Drobniewski F. Is there a place for beta-lactams in the treatment of multidrug-resistant/extensively drug-resistant tuberculosis? Synergy between meropenem and amoxicillin/clavulanate. *J Antimicrob Chemother.* 2013;68(2):366-9. doi: 10.1093/jac/dks395. PubMed PMID: 23070734.
211. Kurz SG, Bonomo RA. Reappraising the use of beta-lactams to treat tuberculosis. *Expert Rev Anti Infect Ther.* 2012;10(9):999-1006. doi: 10.1586/eri.12.96. PubMed PMID: 23106275; PubMed Central PMCID: PMC3728824.
212. Chambers HF, Kocagoz T, Sipit T, Turner J, Hopewell PC. Activity of amoxicillin/clavulanate in patients with tuberculosis. *Clin Infect Dis.* 1998;26(4):874-7. PubMed PMID: 9564467.
213. Donald PR, Sirgel FA, Venter A, Parkin DP, Van de Wal BW, Barendse A, et al. Early bactericidal activity of amoxicillin in combination with clavulanic acid in patients with sputum smear-positive pulmonary tuberculosis. *Scand J Infect Dis.* 2001;33(6):466-9. PubMed PMID: 11450868.
214. Payen MC, De Wit S, Martin C, Sergysels R, Muylle I, Van Laethem Y, et al. Clinical use of the meropenem-clavulanate combination for extensively drug-resistant tuberculosis. *Int J Tuberc Lung Dis.* 2012;16(4):558-60. doi: 10.5588/ijtld.11.0414. PubMed PMID: 22325421.
215. Hugonnet JE, Tremblay LW, Boshoff HI, Barry CE, 3rd, Blanchard JS. Meropenem-clavulanate is effective against extensively drug-resistant *Mycobacterium tuberculosis*. *Science.* 2009;323(5918):1215-8. doi: 10.1126/science.1167498. PubMed PMID: 19251630; PubMed Central PMCID: PMC2679150.
216. Ramon-Garcia S, Gonzalez Del Rio R, Villarejo AS, Sweet GD, Cunningham F, Barros D, et al. Repurposing clinically approved cephalosporins for tuberculosis therapy. *Sci Rep.* 2016;6:34293. doi: 10.1038/srep34293. PubMed PMID: 27678056; PubMed Central PMCID: PMC5039641.
217. Hazra S, Xu H, Blanchard JS. Tebipenem, a new carbapenem antibiotic, is a slow substrate that inhibits the beta-lactamase from *Mycobacterium tuberculosis*. *Biochemistry.* 2014;53(22):3671-8. doi: 10.1021/bi500339j. PubMed PMID: 24846409; PubMed Central PMCID: PMC4053071.
218. Bianchet MA, Pan YH, Basta LAB, Saavedra H, Lloyd EP, Kumar P, et al. Structural insight into the inactivation of *Mycobacterium tuberculosis* non-classical transpeptidase LdtMt2 by biapenem and tebipenem. *BMC Biochem.* 2017;18(1):8. doi: 10.1186/s12858-017-0082-4. PubMed PMID: 28545389.
219. Maitra A, Bates S, Kolvekar T, Devarajan PV, Guzman JD, Bhakta S. Repurposing-a ray of hope in tackling extensively drug resistance in tuberculosis. *Int J Infect Dis.* 2015;32:50-5. doi: 10.1016/j.ijid.2014.12.031. PubMed PMID: 25809756.
220. Dhar N, Dubee V, Ballell L, Cuinet G, Hugonnet JE, Signorino-Gelo F, et al. Rapid cytolysis of *Mycobacterium tuberculosis* by faropenem, an orally bioavailable beta-lactam antibiotic. *Antimicrob Agents Chemother.* 2015;59(2):1308-19. doi: 10.1128/AAC.03461-14. PubMed PMID: 25421469; PubMed Central PMCID: PMC4335862.
221. Almeida Da Silva PE, Palomino JC. Molecular basis and mechanisms of drug resistance in *Mycobacterium tuberculosis*: classical and new drugs. *J Antimicrob Chemother.* 2011;66(7):1417-30. doi: 10.1093/jac/dkr173. PubMed PMID: 21558086.

222. De Rossi E, Ainsa JA, Riccardi G. Role of mycobacterial efflux transporters in drug resistance: an unresolved question. *FEMS Microbiol Rev.* 2006;30(1):36-52. doi: 10.1111/j.1574-6976.2005.00002.x. PubMed PMID: 16438679.
223. Kasik JE. The Nature of Mycobacterial Penicillinase. *Am Rev Respir Dis.* 1965;91:117-9. doi: 10.1164/arrd.1965.91.1.117. PubMed PMID: 14259993.
224. Chambers HF, Moreau D, Yajko D, Miick C, Wagner C, Hackbarth C, et al. Can penicillins and other beta-lactam antibiotics be used to treat tuberculosis? *Antimicrob Agents Chemother.* 1995;39(12):2620-4. PubMed PMID: 8592990; PubMed Central PMCID: PMCPMC163000.
225. Mukherjee T, Basu D, Mahapatra S, Goffin C, van Beeumen J, Basu J. Biochemical characterization of the 49 kDa penicillin-binding protein of *Mycobacterium smegmatis*. *Biochem J.* 1996;320 ( Pt 1):197-200. PubMed PMID: 8947487; PubMed Central PMCID: PMCPMC1217917.
226. Danilchanka O, Mailaender C, Niederweis M. Identification of a novel multidrug efflux pump of *Mycobacterium tuberculosis*. *Antimicrob Agents Chemother.* 2008;52(7):2503-11. doi: 10.1128/AAC.00298-08. PubMed PMID: 18458127; PubMed Central PMCID: PMCPMC2443884.
227. Lun S, Miranda D, Kubler A, Guo H, Maiga MC, Winglee K, et al. Synthetic lethality reveals mechanisms of *Mycobacterium tuberculosis* resistance to beta-lactams. *MBio.* 2014;5(5):e01767-14. doi: 10.1128/mBio.01767-14. PubMed PMID: 25227469; PubMed Central PMCID: PMCPMC4172077.
228. Wivagg CN, Wellington S, Gomez JE, Hung DT. Loss of a Class A Penicillin-Binding Protein Alters beta-Lactam Susceptibilities in *Mycobacterium tuberculosis*. *ACS Infect Dis.* 2016;2(2):104-10. doi: 10.1021/acsinfecdis.5b00119. PubMed PMID: 27624961.
229. Wivagg CN, Bhattacharyya RP, Hung DT. Mechanisms of beta-lactam killing and resistance in the context of *Mycobacterium tuberculosis*. *J Antibiot (Tokyo).* 2014;67(9):645-54. doi: 10.1038/ja.2014.94. PubMed PMID: 25052484.
230. Zapun A, Contreras-Martel C, Vernet T. Penicillin-binding proteins and beta-lactam resistance. *FEMS Microbiol Rev.* 2008;32(2):361-85. doi: 10.1111/j.1574-6976.2007.00095.x. PubMed PMID: 18248419.
231. Pinho MG, de Lencastre H, Tomasz A. An acquired and a native penicillin-binding protein cooperate in building the cell wall of drug-resistant staphylococci. *Proc Natl Acad Sci U S A.* 2001;98(19):10886-91. doi: 10.1073/pnas.191260798. PubMed PMID: 11517340; PubMed Central PMCID: PMCPMC58569.
232. Mukhopadhyay S, Chakrabarti P. Altered permeability and beta-lactam resistance in a mutant of *Mycobacterium smegmatis*. *Antimicrob Agents Chemother.* 1997;41(8):1721-4. PubMed PMID: 9257748; PubMed Central PMCID: PMCPMC163992.
233. Nikaido H, Jarlier V. Permeability of the mycobacterial cell wall. *Res Microbiol.* 1991;142(4):437-43. PubMed PMID: 1871430.
234. Brennan PJ. Structure, function, and biogenesis of the cell wall of *Mycobacterium tuberculosis*. *Tuberculosis (Edinb).* 2003;83(1-3):91-7. PubMed PMID: 12758196.

235. Chatterjee D. *The mycobacterial cell wall: structure, biosynthesis and sites of drug action*. *Curr Opin Chem Biol*. 1997;1(4):579-88. PubMed PMID: 9667898.
236. Grzegorzewicz AE, de Sousa-d'Auria C, McNeil MR, Huc-Claustre E, Jones V, Petit C, et al. *Assembling of the Mycobacterium tuberculosis Cell Wall Core*. *J Biol Chem*. 2016;291(36):18867-79. doi: 10.1074/jbc.M116.739227. PubMed PMID: 27417139; PubMed Central PMCID: PMC5009262.
237. Hett EC, Rubin EJ. *Bacterial growth and cell division: a mycobacterial perspective*. *Microbiol Mol Biol Rev*. 2008;72(1):126-56, table of contents. doi: 10.1128/MMBR.00028-07. PubMed PMID: 18322037; PubMed Central PMCID: PMC2268284.
238. Liu J, Rosenberg EY, Nikaido H. *Fluidity of the lipid domain of cell wall from Mycobacterium chelonae*. *Proc Natl Acad Sci U S A*. 1995;92(24):11254-8. PubMed PMID: 7479975; PubMed Central PMCID: PMC40610.
239. Hoffmann C, Leis A, Niederweis M, Plitzko JM, Engelhardt H. *Disclosure of the mycobacterial outer membrane: cryo-electron tomography and vitreous sections reveal the lipid bilayer structure*. *Proc Natl Acad Sci U S A*. 2008;105(10):3963-7. doi: 10.1073/pnas.0709530105. PubMed PMID: 18316738; PubMed Central PMCID: PMC2268800.
240. Jarlier V, Gutmann L, Nikaido H. *Interplay of cell wall barrier and beta-lactamase activity determines high resistance to beta-lactam antibiotics in Mycobacterium chelonae*. *Antimicrob Agents Chemother*. 1991;35(9):1937-9. PubMed PMID: 1952873; PubMed Central PMCID: PMC245299.
241. Jarlier V, Nikaido H. *Mycobacterial cell wall: structure and role in natural resistance to antibiotics*. *FEMS Microbiol Lett*. 1994;123(1-2):11-8. PubMed PMID: 7988876.
242. Liu J, Barry CE, 3rd, Besra GS, Nikaido H. *Mycolic acid structure determines the fluidity of the mycobacterial cell wall*. *J Biol Chem*. 1996;271(47):29545-51. PubMed PMID: 8939881.
243. Tahlan K, Wilson R, Kastrinsky DB, Arora K, Nair V, Fischer E, et al. *SQ109 targets MmpL3, a membrane transporter of trehalose monomycolate involved in mycolic acid donation to the cell wall core of Mycobacterium tuberculosis*. *Antimicrob Agents Chemother*. 2012;56(4):1797-809. doi: 10.1128/AAC.05708-11. PubMed PMID: 22252828; PubMed Central PMCID: PMC3318387.
244. De Smet KA, Kempell KE, Gallagher A, Duncan K, Young DB. *Alteration of a single amino acid residue reverses fosfomycin resistance of recombinant MurA from Mycobacterium tuberculosis*. *Microbiology*. 1999;145 ( Pt 11):3177-84. doi: 10.1099/00221287-145-11-3177. PubMed PMID: 10589726.
245. Yang Y, Severin A, Chopra R, Krishnamurthy G, Singh G, Hu W, et al. *3,5-dioxypyrazolidines, novel inhibitors of UDP-N-acetylenolpyruvylglucosamine reductase (MurB) with activity against gram-positive bacteria*. *Antimicrob Agents Chemother*. 2006;50(2):556-64. doi: 10.1128/AAC.50.2.556-564.2006. PubMed PMID: 16436710; PubMed Central PMCID: PMC1366903.
246. Crick DC, Mahapatra S, Brennan PJ. *Biosynthesis of the arabinogalactan-peptidoglycan complex of Mycobacterium tuberculosis*. *Glycobiology*. 2001;11(9):107R-18R. PubMed PMID: 11555614.

247. Pavelka MS, Jr., Mahapatra S, Crick DC. *Genetics of Peptidoglycan Biosynthesis*. *Microbiol Spectr*. 2014;2(4):MGM2-0034-2013. doi: 10.1128/microbiolspec.MGM2-0034-2013. PubMed PMID: 26104213.
248. Mahapatra S, Scherman H, Brennan PJ, Crick DC. N Glycolylation of the nucleotide precursors of peptidoglycan biosynthesis of *Mycobacterium* spp. is altered by drug treatment. *J Bacteriol*. 2005;187(7):2341-7. doi: 10.1128/JB.187.7.2341-2347.2005. PubMed PMID: 15774877; PubMed Central PMCID: PMC1065221.
249. Kieser KJ, Baranowski C, Chao MC, Long JE, Sasseti CM, Waldor MK, et al. Peptidoglycan synthesis in *Mycobacterium tuberculosis* is organized into networks with varying drug susceptibility. *Proc Natl Acad Sci U S A*. 2015;112(42):13087-92. doi: 10.1073/pnas.1514135112. PubMed PMID: 26438867; PubMed Central PMCID: PMC1065221.
250. Goffin C, Ghuysen JM. Multimodular penicillin-binding proteins: an enigmatic family of orthologs and paralogs. *Microbiol Mol Biol Rev*. 1998;62(4):1079-93. PubMed PMID: 9841666; PubMed Central PMCID: PMC98940.
251. Lavollay M, Arthur M, Fourgeaud M, Dubost L, Marie A, Veziris N, et al. The peptidoglycan of stationary-phase *Mycobacterium tuberculosis* predominantly contains cross-links generated by L,D-transpeptidation. *J Bacteriol*. 2008;190(12):4360-6. doi: 10.1128/JB.00239-08. PubMed PMID: 18408028; PubMed Central PMCID: PMC2446752.
252. Mainardi JL, Legrand R, Arthur M, Schoot B, van Heijenoort J, Gutmann L. Novel mechanism of beta-lactam resistance due to bypass of DD-transpeptidation in *Enterococcus faecium*. *J Biol Chem*. 2000;275(22):16490-6. doi: 10.1074/jbc.M909877199. PubMed PMID: 10748168.
253. Mainardi JL, Hugonnet JE, Rusconi F, Fourgeaud M, Dubost L, Mouton RP, et al. Unexpected inhibition of peptidoglycan LD-transpeptidase from *Enterococcus faecium* by the beta-lactam imipenem. *J Biol Chem*. 2007;282(42):30414-22. doi: 10.1074/jbc.M704286200. PubMed PMID: 17646161.
254. Kieser KJ, Rubin EJ. How sisters grow apart: mycobacterial growth and division. *Nat Rev Microbiol*. 2014;12(8):550-62. doi: 10.1038/nrmicro3299. PubMed PMID: 24998739.
255. McNeil M, Wallner SJ, Hunter SW, Brennan PJ. Demonstration that the galactosyl and arabinosyl residues in the cell-wall arabinogalactan of *Mycobacterium leprae* and *Mycobacterium tuberculosis* are furanoid. *Carbohydr Res*. 1987;166(2):299-308. PubMed PMID: 3119212.
256. Jankute M, Grover S, Rana AK, Besra GS. Arabinogalactan and lipoarabinomannan biosynthesis: structure, biogenesis and their potential as drug targets. *Future Microbiol*. 2012;7(1):129-47. doi: 10.2217/fmb.11.123. PubMed PMID: 22191451.
257. Besra GS, Brennan PJ. The mycobacterial cell wall: biosynthesis of arabinogalactan and lipoarabinomannan. *Biochem Soc Trans*. 1997;25(3):845-50. PubMed PMID: 9388559.
258. Birch HL, Alderwick LJ, Bhatt A, Rittmann D, Krumbach K, Singh A, et al. Biosynthesis of mycobacterial arabinogalactan: identification of a novel alpha(1-->3) arabinofuranosyltransferase. *Mol Microbiol*. 2008;69(5):1191-206. doi: 10.1111/j.1365-2958.2008.06354.x. PubMed PMID: 18627460; PubMed Central PMCID: PMC2610374.

259. Alderwick LJ, Birch HL, Mishra AK, Eggeling L, Besra GS. Structure, function and biosynthesis of the *Mycobacterium tuberculosis* cell wall: arabinogalactan and lipoarabinomannan assembly with a view to discovering new drug targets. *Biochem Soc Trans.* 2007;35(Pt 5):1325-8. doi: 10.1042/BST0351325. PubMed PMID: 17956343.
260. Kaur D, Guerin ME, Skovierova H, Brennan PJ, Jackson M. Chapter 2: Biogenesis of the cell wall and other glycoconjugates of *Mycobacterium tuberculosis*. *Adv Appl Microbiol.* 2009;69:23-78. doi: 10.1016/S0065-2164(09)69002-X. PubMed PMID: 19729090; PubMed Central PMCID: PMC3066434.
261. Asselineau J, Lederer E. Structure of the mycolic acids of *Mycobacteria*. *Nature.* 1950;166(4227):782-3. PubMed PMID: 14780245.
262. Jarlier V, Nikaido H. Permeability barrier to hydrophilic solutes in *Mycobacterium chelonae*. *J Bacteriol.* 1990;172(3):1418-23. PubMed PMID: 2307653; PubMed Central PMCID: PMC208614.
263. Verschoor JA, Baird MS, Grooten J. Towards understanding the functional diversity of cell wall mycolic acids of *Mycobacterium tuberculosis*. *Prog Lipid Res.* 2012;51(4):325-39. doi: 10.1016/j.plipres.2012.05.002. PubMed PMID: 22659327.
264. Bhatt A, Molle V, Besra GS, Jacobs WR, Jr., Kremer L. The *Mycobacterium tuberculosis* FAS-II condensing enzymes: their role in mycolic acid biosynthesis, acid-fastness, pathogenesis and in future drug development. *Mol Microbiol.* 2007;64(6):1442-54. doi: 10.1111/j.1365-2958.2007.05761.x. PubMed PMID: 17555433.
265. Quadri LE. Biosynthesis of mycobacterial lipids by polyketide synthases and beyond. *Crit Rev Biochem Mol Biol.* 2014;49(3):179-211. doi: 10.3109/10409238.2014.896859. PubMed PMID: 24625105.
266. Marrakchi H, Laneelle MA, Daffe M. Mycolic acids: structures, biosynthesis, and beyond. *Chem Biol.* 2014;21(1):67-85. doi: 10.1016/j.chembiol.2013.11.011. PubMed PMID: 24374164.
267. Varela C, Rittmann D, Singh A, Krumbach K, Bhatt K, Eggeling L, et al. MmpL genes are associated with mycolic acid metabolism in mycobacteria and corynebacteria. *Chem Biol.* 2012;19(4):498-506. doi: 10.1016/j.chembiol.2012.03.006. PubMed PMID: 22520756; PubMed Central PMCID: PMC3370651.
268. Grzegorzewicz AE, Pham H, Gundi VA, Scherman MS, North EJ, Hess T, et al. Inhibition of mycolic acid transport across the *Mycobacterium tuberculosis* plasma membrane. *Nat Chem Biol.* 2012;8(4):334-41. doi: 10.1038/nchembio.794. PubMed PMID: 22344175; PubMed Central PMCID: PMC3307863.
269. Gavalda S, Bardou F, Laval F, Bon C, Malaga W, Chalut C, et al. The polyketide synthase Pks13 catalyzes a novel mechanism of lipid transfer in mycobacteria. *Chem Biol.* 2014;21(12):1660-9. doi: 10.1016/j.chembiol.2014.10.011. PubMed PMID: 25467124.
270. Degiacomi G, Benjak A, Madacki J, Boldrin F, Provvedi R, Palu G, et al. Essentiality of mmpL3 and impact of its silencing on *Mycobacterium tuberculosis* gene expression. *Sci Rep.* 2017;7:43495. doi: 10.1038/srep43495. PubMed PMID: 28240248; PubMed Central PMCID: PMC5327466.

271. Favrot L, Grzegorzewicz AE, Lajiness DH, Marvin RK, Boucau J, Isailovic D, et al. Mechanism of inhibition of *Mycobacterium tuberculosis* antigen 85 by ebselen. *Nat Commun.* 2013;4:2748. doi: 10.1038/ncomms3748. PubMed PMID: 24193546; PubMed Central PMCID: PMC4049535.
272. Warriar T, Tropis M, Werngren J, Diehl A, Gengenbacher M, Schlegel B, et al. Antigen 85C inhibition restricts *Mycobacterium tuberculosis* growth through disruption of cord factor biosynthesis. *Antimicrob Agents Chemother.* 2012;56(4):1735-43. doi: 10.1128/AAC.05742-11. PubMed PMID: 22290959; PubMed Central PMCID: PMC3318338.
273. Pitarque S, Larrouy-Maumus G, Payre B, Jackson M, Puzo G, Nigou J. The immunomodulatory lipoglycans, lipoarabinomannan and lipomannan, are exposed at the mycobacterial cell surface. *Tuberculosis (Edinb).* 2008;88(6):560-5. doi: 10.1016/j.tube.2008.04.002. PubMed PMID: 18539533; PubMed Central PMCID: PMC2613510.
274. Kaur D, McNeil MR, Khoo KH, Chatterjee D, Crick DC, Jackson M, et al. New insights into the biosynthesis of mycobacterial lipomannan arising from deletion of a conserved gene. *J Biol Chem.* 2007;282(37):27133-40. doi: 10.1074/jbc.M703389200. PubMed PMID: 17606615.
275. Kaur D, Obregon-Henao A, Pham H, Chatterjee D, Brennan PJ, Jackson M. Lipoarabinomannan of *Mycobacterium*: mannose capping by a multifunctional terminal mannosyltransferase. *Proc Natl Acad Sci U S A.* 2008;105(46):17973-7. doi: 10.1073/pnas.0807761105. PubMed PMID: 19004785; PubMed Central PMCID: PMC2584715.
276. Camacho LR, Constant P, Raynaud C, Laneelle MA, Triccas JA, Gicquel B, et al. Analysis of the phthiocerol dimycocerosate locus of *Mycobacterium tuberculosis*. Evidence that this lipid is involved in the cell wall permeability barrier. *J Biol Chem.* 2001;276(23):19845-54. doi: 10.1074/jbc.M100662200. PubMed PMID: 11279114.
277. Mougous JD, Petzold CJ, Senaratne RH, Lee DH, Akey DL, Lin FL, et al. Identification, function and structure of the mycobacterial sulfotransferase that initiates sulfolipid-1 biosynthesis. *Nat Struct Mol Biol.* 2004;11(8):721-9. doi: 10.1038/nsmb802. PubMed PMID: 15258569.
278. Seeliger JC, Holsclaw CM, Schelle MW, Botyanszki Z, Gilmore SA, Tully SE, et al. Elucidation and chemical modulation of sulfolipid-1 biosynthesis in *Mycobacterium tuberculosis*. *J Biol Chem.* 2012;287(11):7990-8000. doi: 10.1074/jbc.M111.315473. PubMed PMID: 22194604; PubMed Central PMCID: PMC3318749.
279. Daffe M, Lacave C, Laneelle MA, Gillois M, Laneelle G. Polyphthienoyl trehalose, glycolipids specific for virulent strains of the tubercle bacillus. *Eur J Biochem.* 1988;172(3):579-84. PubMed PMID: 3127210.
280. Belardinelli JM, Larrouy-Maumus G, Jones V, Sorio de Carvalho LP, McNeil MR, Jackson M. Biosynthesis and translocation of unsulfated acyltrehaloses in *Mycobacterium tuberculosis*. *J Biol Chem.* 2014;289(40):27952-65. doi: 10.1074/jbc.M114.581199. PubMed PMID: 25124040; PubMed Central PMCID: PMC4183827.
281. Jackson M. The mycobacterial cell envelope-lipids. *Cold Spring Harb Perspect Med.* 2014;4(10). doi: 10.1101/cshperspect.a021105. PubMed PMID: 25104772; PubMed Central PMCID: PMC4200213.

282. Manganelli R. *Sigma Factors: Key Molecules in Mycobacterium tuberculosis Physiology and Virulence*. *Microbiol Spectr*. 2014;2(1):MGM2-0007-2013. doi: 10.1128/microbiolspec.MGM2-0007-2013. PubMed PMID: 26082107.
283. Koo IC, Ohol YM, Wu P, Morisaki JH, Cox JS, Brown EJ. Role for lysosomal enzyme beta-hexosaminidase in the control of mycobacteria infection. *Proc Natl Acad Sci U S A*. 2008;105(2):710-5. doi: 10.1073/pnas.0708110105. PubMed PMID: 18180457; PubMed Central PMCID: PMC2206601.
284. Alonso S, Pethe K, Russell DG, Purdy GE. Lysosomal killing of *Mycobacterium* mediated by ubiquitin-derived peptides is enhanced by autophagy. *Proc Natl Acad Sci U S A*. 2007;104(14):6031-6. doi: 10.1073/pnas.0700036104. PubMed PMID: 17389386; PubMed Central PMCID: PMC21851611.
285. Purdy GE, Russell DG. Lysosomal ubiquitin and the demise of *Mycobacterium tuberculosis*. *Cell Microbiol*. 2007;9(12):2768-74. doi: 10.1111/j.1462-5822.2007.01039.x. PubMed PMID: 17714517.
286. Av-Gay Y, Jamil S, Drews SJ. Expression and characterization of the *Mycobacterium tuberculosis* serine/threonine protein kinase PknB. *Infect Immun*. 1999;67(11):5676-82. PubMed PMID: 10531215; PubMed Central PMCID: PMC96941.
287. Manganelli R, Dubnau E, Tyagi S, Kramer FR, Smith I. Differential expression of 10 sigma factor genes in *Mycobacterium tuberculosis*. *Mol Microbiol*. 1999;31(2):715-24. PubMed PMID: 10027986.
288. Manganelli R, Voskuil MI, Schoolnik GK, Smith I. The *Mycobacterium tuberculosis* ECF sigma factor sigmaE: role in global gene expression and survival in macrophages. *Mol Microbiol*. 2001;41(2):423-37. PubMed PMID: 11489128.
289. Manganelli R, Voskuil MI, Schoolnik GK, Dubnau E, Gomez M, Smith I. Role of the extracytoplasmic-function sigma factor sigma(H) in *Mycobacterium tuberculosis* global gene expression. *Mol Microbiol*. 2002;45(2):365-74. PubMed PMID: 12123450.
290. Rodrigue S, Provvedi R, Jacques PE, Gaudreau L, Manganelli R. The sigma factors of *Mycobacterium tuberculosis*. *FEMS Microbiol Rev*. 2006;30(6):926-41. doi: 10.1111/j.1574-6976.2006.00040.x. PubMed PMID: 17064287.
291. Missiakas D, Raina S. The extracytoplasmic function sigma factors: role and regulation. *Mol Microbiol*. 1998;28(6):1059-66. PubMed PMID: 9680198.
292. Manganelli R, Provvedi R, Rodrigue S, Beaucher J, Gaudreau L, Smith I. Sigma factors and global gene regulation in *Mycobacterium tuberculosis*. *J Bacteriol*. 2004;186(4):895-902. PubMed PMID: 14761983; PubMed Central PMCID: PMC2344228.
293. Rhodius VA, Suh WC, Nonaka G, West J, Gross CA. Conserved and variable functions of the sigmaE stress response in related genomes. *PLoS Biol*. 2006;4(1):e2. doi: 10.1371/journal.pbio.0040002. PubMed PMID: 16336047; PubMed Central PMCID: PMC1312014.
294. Ando M, Yoshimatsu T, Ko C, Converse PJ, Bishai WR. Deletion of *Mycobacterium tuberculosis* sigma factor E results in delayed time to death with bacterial persistence in the lungs of aerosol-infected

- mice. *Infect Immun.* 2003;71(12):7170-2. PubMed PMID: 14638810; PubMed Central PMCID: PMCPMC308924.
295. Dona V, Rodrigue S, Dainese E, Palu G, Gaudreau L, Manganelli R, et al. Evidence of complex transcriptional, translational, and posttranslational regulation of the extracytoplasmic function sigma factor sigmaE in *Mycobacterium tuberculosis*. *J Bacteriol.* 2008;190(17):5963-71. doi: 10.1128/JB.00622-08. PubMed PMID: 18606740; PubMed Central PMCID: PMCPMC2519537.
296. Wilson M, DeRisi J, Kristensen HH, Imboden P, Rane S, Brown PO, et al. Exploring drug-induced alterations in gene expression in *Mycobacterium tuberculosis* by microarray hybridization. *Proc Natl Acad Sci U S A.* 1999;96(22):12833-8. PubMed PMID: 10536008; PubMed Central PMCID: PMCPMC23119.
297. Sureka K, Dey S, Datta P, Singh AK, Dasgupta A, Rodrigue S, et al. Polyphosphate kinase is involved in stress-induced mprAB-sigE-rel signalling in mycobacteria. *Mol Microbiol.* 2007;65(2):261-76. doi: 10.1111/j.1365-2958.2007.05814.x. PubMed PMID: 17630969.
298. Pang X, Vu P, Byrd TF, Ghanny S, Soteropoulos P, Mukamolova GV, et al. Evidence for complex interactions of stress-associated regulons in an mprAB deletion mutant of *Mycobacterium tuberculosis*. *Microbiology.* 2007;153(Pt 4):1229-42. doi: 10.1099/mic.0.29281-0. PubMed PMID: 17379732.
299. He H, Hovey R, Kane J, Singh V, Zahrt TC. MprAB is a stress-responsive two-component system that directly regulates expression of sigma factors SigB and SigE in *Mycobacterium tuberculosis*. *J Bacteriol.* 2006;188(6):2134-43. doi: 10.1128/JB.188.6.2134-2143.2006. PubMed PMID: 16513743; PubMed Central PMCID: PMCPMC1428128.
300. Fontan PA, Voskuil MI, Gomez M, Tan D, Pardini M, Manganelli R, et al. The *Mycobacterium tuberculosis* sigma factor sigmaB is required for full response to cell envelope stress and hypoxia in vitro, but it is dispensable for in vivo growth. *J Bacteriol.* 2009;191(18):5628-33. doi: 10.1128/JB.00510-09. PubMed PMID: 19592585; PubMed Central PMCID: PMCPMC2737972.
301. Amaral L, Martins M, Viveiros M, Molnar J, Kristiansen JE. Promising therapy of XDR-TB/MDR-TB with thioridazine an inhibitor of bacterial efflux pumps. *Curr Drug Targets.* 2008;9(9):816-9. PubMed PMID: 18781927.
302. Dutta NK, Mehra S, Kaushal D. A *Mycobacterium tuberculosis* sigma factor network responds to cell-envelope damage by the promising anti-mycobacterial thioridazine. *PLoS One.* 2010;5(4):e10069. doi: 10.1371/journal.pone.0010069. PubMed PMID: 20386700; PubMed Central PMCID: PMCPMC2851646.
303. Fernandes ND, Wu QL, Kong D, Puyang X, Garg S, Husson RN. A mycobacterial extracytoplasmic sigma factor involved in survival following heat shock and oxidative stress. *J Bacteriol.* 1999;181(14):4266-74. PubMed PMID: 10400584; PubMed Central PMCID: PMCPMC93928.
304. Mehra S, Dutta NK, Mollenkopf HJ, Kaushal D. *Mycobacterium tuberculosis* MT2816 encodes a key stress-response regulator. *J Infect Dis.* 2010;202(6):943-53. doi: 10.1086/654820. PubMed PMID: 20701538; PubMed Central PMCID: PMCPMC3052882.

305. Drawz SM, Bonomo RA. Three decades of beta-lactamase inhibitors. *Clin Microbiol Rev.* 2010;23(1):160-201. doi: 10.1128/CMR.00037-09. PubMed PMID: 20065329; PubMed Central PMCID: PMC2806661.
306. Kasik JE, Monick M, Schwarz B. beta-Lactamase activity in slow-growing nonpigmented mycobacteria and their sensitivity to certain beta-lactam antibiotics. *Tubercle.* 1980;61(4):213-9. PubMed PMID: 6792754.
307. Voladri RK, Lakey DL, Hennigan SH, Menzies BE, Edwards KM, Kernodle DS. Recombinant expression and characterization of the major beta-lactamase of *Mycobacterium tuberculosis*. *Antimicrob Agents Chemother.* 1998;42(6):1375-81. PubMed PMID: 9624479; PubMed Central PMCID: PMC105607.
308. Wang F, Cassidy C, Sacchettini JC. Crystal structure and activity studies of the *Mycobacterium tuberculosis* beta-lactamase reveal its critical role in resistance to beta-lactam antibiotics. *Antimicrob Agents Chemother.* 2006;50(8):2762-71. doi: 10.1128/AAC.00320-06. PubMed PMID: 16870770; PubMed Central PMCID: PMC1538687.
309. Tremblay LW, Fan F, Blanchard JS. Biochemical and structural characterization of *Mycobacterium tuberculosis* beta-lactamase with the carbapenems ertapenem and doripenem. *Biochemistry.* 2010;49(17):3766-73. doi: 10.1021/bi100232q. PubMed PMID: 20353175; PubMed Central PMCID: PMC2860635.
310. Hugonnet JE, Blanchard JS. Irreversible inhibition of the *Mycobacterium tuberculosis* beta-lactamase by clavulanate. *Biochemistry.* 2007;46(43):11998-2004. doi: 10.1021/bi701506h. PubMed PMID: 17915954; PubMed Central PMCID: PMC2593862.
311. Sala C, Haouz A, Saul FA, Miras I, Rosenkrands I, Alzari PM, et al. Genome-wide regulon and crystal structure of *BlaI* (*Rv1846c*) from *Mycobacterium tuberculosis*. *Mol Microbiol.* 2009;71(5):1102-16. doi: 10.1111/j.1365-2958.2008.06583.x. PubMed PMID: 19154333.
312. Wickner W, Driessen AJ, Hartl FU. The enzymology of protein translocation across the *Escherichia coli* plasma membrane. *Annu Rev Biochem.* 1991;60:101-24. doi: 10.1146/annurev.bi.60.070191.000533. PubMed PMID: 1831965.
313. Driessen AJ, Manting EH, van der Does C. The structural basis of protein targeting and translocation in bacteria. *Nat Struct Biol.* 2001;8(6):492-8. doi: 10.1038/88549. PubMed PMID: 11373615.
314. Osborne AR, Rapoport TA, van den Berg B. Protein translocation by the *Sec61/SecY* channel. *Annu Rev Cell Dev Biol.* 2005;21:529-50. doi: 10.1146/annurev.cellbio.21.012704.133214. PubMed PMID: 16212506.
315. Natale P, Bruser T, Driessen AJ. *Sec-* and *Tat-*mediated protein secretion across the bacterial cytoplasmic membrane--distinct translocases and mechanisms. *Biochim Biophys Acta.* 2008;1778(9):1735-56. doi: 10.1016/j.bbamem.2007.07.015. PubMed PMID: 17935691.
316. Scott JR, Barnett TC. Surface proteins of gram-positive bacteria and how they get there. *Annu Rev Microbiol.* 2006;60:397-423. doi: 10.1146/annurev.micro.60.080805.142256. PubMed PMID: 16753030.

317. Wiker HG, Wilson MA, Schoolnik GK. Extracytoplasmic proteins of *Mycobacterium tuberculosis* - mature secreted proteins often start with aspartic acid and proline. *Microbiology*. 2000;146 ( Pt 7):1525-33. doi: 10.1099/00221287-146-7-1525. PubMed PMID: 10878117.
318. Rigel NW, Braunstein M. A new twist on an old pathway--accessory Sec [corrected] systems. *Mol Microbiol*. 2008;69(2):291-302. doi: 10.1111/j.1365-2958.2008.06294.x. PubMed PMID: 18544071; PubMed Central PMCID: PMCPMC2597500.
319. Berks BC, Palmer T, Sargent F. Protein targeting by the bacterial twin-arginine translocation (Tat) pathway. *Curr Opin Microbiol*. 2005;8(2):174-81. doi: 10.1016/j.mib.2005.02.010. PubMed PMID: 15802249.
320. Robinson C, Bolhuis A. Tat-dependent protein targeting in prokaryotes and chloroplasts. *Biochim Biophys Acta*. 2004;1694(1-3):135-47. doi: 10.1016/j.bbamcr.2004.03.010. PubMed PMID: 15546663.
321. Chaddock AM, Mant A, Karnachov I, Brink S, Herrmann RG, Klosgen RB, et al. A new type of signal peptide: central role of a twin-arginine motif in transfer signals for the delta pH-dependent thylakoidal protein translocase. *EMBO J*. 1995;14(12):2715-22. PubMed PMID: 7796800; PubMed Central PMCID: PMCPMC398390.
322. Berks BC. A common export pathway for proteins binding complex redox cofactors? *Mol Microbiol*. 1996;22(3):393-404. PubMed PMID: 8939424.
323. Halbig D, Wiegert T, Blaudeck N, Freudl R, Sprenger GA. The efficient export of NADP-containing glucose-fructose oxidoreductase to the periplasm of *Zymomonas mobilis* depends both on an intact twin-arginine motif in the signal peptide and on the generation of a structural export signal induced by cofactor binding. *Eur J Biochem*. 1999;263(2):543-51. PubMed PMID: 10406965.
324. Champion PA, Cox JS. Protein secretion systems in *Mycobacteria*. *Cell Microbiol*. 2007;9(6):1376-84. doi: 10.1111/j.1462-5822.2007.00943.x. PubMed PMID: 17466013.
325. McCann JR, McDonough JA, Pavelka MS, Braunstein M. Beta-lactamase can function as a reporter of bacterial protein export during *Mycobacterium tuberculosis* infection of host cells. *Microbiology*. 2007;153(Pt 10):3350-9. doi: 10.1099/mic.0.2007/008516-0. PubMed PMID: 17906134; PubMed Central PMCID: PMCPMC2635098.
326. McDonough JA, McCann JR, Tekippe EM, Silverman JS, Rigel NW, Braunstein M. Identification of functional Tat signal sequences in *Mycobacterium tuberculosis* proteins. *J Bacteriol*. 2008;190(19):6428-38. doi: 10.1128/JB.00749-08. PubMed PMID: 18658266; PubMed Central PMCID: PMCPMC2566002.
327. Solans L, Gonzalo-Asensio J, Sala C, Benjak A, Uplekar S, Rougemont J, et al. The PhoP-dependent ncRNA Mcr7 modulates the TAT secretion system in *Mycobacterium tuberculosis*. *PLoS Pathog*. 2014;10(5):e1004183. doi: 10.1371/journal.ppat.1004183. PubMed PMID: 24874799; PubMed Central PMCID: PMCPMC4038636.
328. Stanley SA, Raghavan S, Hwang WW, Cox JS. Acute infection and macrophage subversion by *Mycobacterium tuberculosis* require a specialized secretion system. *Proc Natl Acad Sci U S A*. 2003;100(22):13001-6. doi: 10.1073/pnas.2235593100. PubMed PMID: 14557536; PubMed Central PMCID: PMCPMC240734.

329. MacGurn JA, Raghavan S, Stanley SA, Cox JS. A non-RD1 gene cluster is required for Snm secretion in *Mycobacterium tuberculosis*. *Mol Microbiol*. 2005;57(6):1653-63. doi: 10.1111/j.1365-2958.2005.04800.x. PubMed PMID: 16135231.
330. Ramakrishnan T, Murthy PS, Gopinathan KP. Intermediary metabolism of mycobacteria. *Bacteriol Rev*. 1972;36(1):65-108. PubMed PMID: 4553808; PubMed Central PMCID: PMCPMC378425.
331. Tian J, Bryk R, Itoh M, Suematsu M, Nathan C. Variant tricarboxylic acid cycle in *Mycobacterium tuberculosis*: identification of alpha-ketoglutarate decarboxylase. *Proc Natl Acad Sci U S A*. 2005;102(30):10670-5. doi: 10.1073/pnas.0501605102. PubMed PMID: 16027371; PubMed Central PMCID: PMCPMC1180764.
332. Prasada Reddy TL, Suryanarayana Murthy P, Venkitasubramanian TA. Respiratory chains of *Mycobacterium smegmatis*. *Indian J Biochem Biophys*. 1975;12(3):255-9. PubMed PMID: 1221028.
333. Schnappinger D, Ehrt S, Voskuil MI, Liu Y, Mangan JA, Monahan IM, et al. Transcriptional Adaptation of *Mycobacterium tuberculosis* within Macrophages: Insights into the Phagosomal Environment. *J Exp Med*. 2003;198(5):693-704. doi: 10.1084/jem.20030846. PubMed PMID: 12953091; PubMed Central PMCID: PMCPMC2194186.
334. Eoh H, Rhee KY. Methylcitrate cycle defines the bactericidal essentiality of isocitrate lyase for survival of *Mycobacterium tuberculosis* on fatty acids. *Proc Natl Acad Sci U S A*. 2014;111(13):4976-81. doi: 10.1073/pnas.1400390111. PubMed PMID: 24639517; PubMed Central PMCID: PMCPMC3977286.
335. Pandey AK, Sassetti CM. Mycobacterial persistence requires the utilization of host cholesterol. *Proc Natl Acad Sci U S A*. 2008;105(11):4376-80. doi: 10.1073/pnas.0711159105. PubMed PMID: 18334639; PubMed Central PMCID: PMCPMC2393810.
336. Munoz-Elias EJ, Upton AM, Cherian J, McKinney JD. Role of the methylcitrate cycle in *Mycobacterium tuberculosis* metabolism, intracellular growth, and virulence. *Mol Microbiol*. 2006;60(5):1109-22. doi: 10.1111/j.1365-2958.2006.05155.x. PubMed PMID: 16689789.
337. Gatfield J, Pieters J. Essential role for cholesterol in entry of mycobacteria into macrophages. *Science*. 2000;288(5471):1647-50. PubMed PMID: 10834844.
338. Kracke F, Vassilev I, Kromer JO. Microbial electron transport and energy conservation - the foundation for optimizing bioelectrochemical systems. *Front Microbiol*. 2015;6:575. doi: 10.3389/fmicb.2015.00575. PubMed PMID: 26124754; PubMed Central PMCID: PMCPMC4463002.
339. Lane N, Martin WF. The origin of membrane bioenergetics. *Cell*. 2012;151(7):1406-16. doi: 10.1016/j.cell.2012.11.050. PubMed PMID: 23260134.
340. Cook GM, Greening C, Hards K, Berney M. Energetics of pathogenic bacteria and opportunities for drug development. *Adv Microb Physiol*. 2014;65:1-62. doi: 10.1016/bs.ampbs.2014.08.001. PubMed PMID: 25476763.

- 341.Hards K, Robson JR, Berney M, Shaw L, Bald D, Koul A, et al. Bactericidal mode of action of bedaquiline. *J Antimicrob Chemother.* 2015;70(7):2028-37. doi: 10.1093/jac/dkv054. PubMed PMID: 25754998.
- 342.Lakshmanan M, Xavier AS. Bedaquiline - The first ATP synthase inhibitor against multi drug resistant tuberculosis. *J Young Pharm.* 2013;5(4):112-5. doi: 10.1016/j.jyp.2013.12.002. PubMed PMID: 24563587; PubMed Central PMCID: PMC3930122.
- 343.Farha MA, Verschoor CP, Bowdish D, Brown ED. Collapsing the proton motive force to identify synergistic combinations against *Staphylococcus aureus*. *Chem Biol.* 2013;20(9):1168-78. doi: 10.1016/j.chembiol.2013.07.006. PubMed PMID: 23972939.
- 344.Lu P, Haagsma AC, Pham H, Maaskant JJ, Mol S, Lill H, et al. Pyrazinoic acid decreases the proton motive force, respiratory ATP synthesis activity, and cellular ATP levels. *Antimicrob Agents Chemother.* 2011;55(11):5354-7. doi: 10.1128/AAC.00507-11. PubMed PMID: 21876062; PubMed Central PMCID: PMC3195041.
- 345.Lamprecht DA, Finin PM, Rahman MA, Cumming BM, Russell SL, Jonnala SR, et al. Turning the respiratory flexibility of *Mycobacterium tuberculosis* against itself. *Nat Commun.* 2016;7:12393. doi: 10.1038/ncomms12393. PubMed PMID: 27506290; PubMed Central PMCID: PMC4987515.
- 346.Mitchell P. Chemiosmotic coupling in oxidative and photosynthetic phosphorylation. *Biol Rev Camb Philos Soc.* 1966;41(3):445-502. PubMed PMID: 5329743.
- 347.Mitchell P, Moyle J. Chemiosmotic hypothesis of oxidative phosphorylation. *Nature.* 1967;213(5072):137-9. PubMed PMID: 4291593.
- 348.Mitchell P. A chemiosmotic molecular mechanism for proton-translocating adenosine triphosphatases. *FEBS Lett.* 1974;43(2):189-94. PubMed PMID: 4277328.
- 349.Mitchell P, Koppenol WH. Chemiosmotic ATPase mechanisms. *Ann N Y Acad Sci.* 1982;402:584-601. PubMed PMID: 6188405.
- 350.Haddock BA, Jones CW. Bacterial respiration. *Bacteriol Rev.* 1977;41(1):47-99. PubMed PMID: 140652; PubMed Central PMCID: PMC413996.
- 351.Mitchell P. Coupling of phosphorylation to electron and hydrogen transfer by a chemi-osmotic type of mechanism. *Nature.* 1961;191:144-8. PubMed PMID: 13771349.
- 352.Kadenbach B. Intrinsic and extrinsic uncoupling of oxidative phosphorylation. *Biochim Biophys Acta.* 2003;1604(2):77-94. PubMed PMID: 12765765.
- 353.Rao M, Streur TL, Aldwell FE, Cook GM. Intracellular pH regulation by *Mycobacterium smegmatis* and *Mycobacterium bovis* BCG. *Microbiology.* 2001;147(Pt 4):1017-24. doi: 10.1099/00221287-147-4-1017. PubMed PMID: 11283297.
- 354.Maloney PC, Kashket ER, Wilson TH. A protonmotive force drives ATP synthesis in bacteria. *Proc Natl Acad Sci U S A.* 1974;71(10):3896-900. PubMed PMID: 4279406; PubMed Central PMCID: PMC434292.

355. Chakraborti PK, Bhatt K, Banerjee SK, Misra P. Role of an ABC importer in mycobacterial drug resistance. *Biosci Rep.* 1999;19(4):293-300. PubMed PMID: 10589994.
356. Zhang Y, Wade MM, Scorpio A, Zhang H, Sun Z. Mode of action of pyrazinamide: disruption of *Mycobacterium tuberculosis* membrane transport and energetics by pyrazinoic acid. *J Antimicrob Chemother.* 2003;52(5):790-5. doi: 10.1093/jac/dkg446. PubMed PMID: 14563891.
357. Chung HJ, Montville TJ, Chikindas ML. Nisin depletes ATP and proton motive force in mycobacteria. *Lett Appl Microbiol.* 2000;31(6):416-20. PubMed PMID: 11123548.
358. Nikaido H, Takatsuka Y. Mechanisms of RND multidrug efflux pumps. *Biochim Biophys Acta.* 2009;1794(5):769-81. doi: 10.1016/j.bbapap.2008.10.004. PubMed PMID: 19026770; PubMed Central PMCID: PMC2696896.
359. Russell JB, Houlihan AJ. Ionophore resistance of ruminal bacteria and its potential impact on human health. *Fems Microbiology Reviews.* 2003;27(1):65-74. doi: 10.1016/S0168-6445(03)00019-6. PubMed PMID: WOS:000182646500004.
360. Terada H. Uncouplers of Oxidative-Phosphorylation. *Environ Health Persp.* 1990;87:213-8. doi: Doi 10.2307/3431027. PubMed PMID: WOS:A1990DW47600030.
361. Li W, Upadhyay A, Fontes FL, North EJ, Wang Y, Crans DC, et al. Novel insights into the mechanism of inhibition of MmpL3, a target of multiple pharmacophores in *Mycobacterium tuberculosis*. *Antimicrob Agents Chemother.* 2014;58(11):6413-23. doi: 10.1128/AAC.03229-14. PubMed PMID: 25136022; PubMed Central PMCID: PMC4249373.
362. Rao SP, Alonso S, Rand L, Dick T, Pethe K. The protonmotive force is required for maintaining ATP homeostasis and viability of hypoxic, nonreplicating *Mycobacterium tuberculosis*. *Proc Natl Acad Sci U S A.* 2008;105(33):11945-50. doi: 10.1073/pnas.0711697105. PubMed PMID: 18697942; PubMed Central PMCID: PMC2575262.
363. Shi L, Sohaskey CD, Kana BD, Dawes S, North RJ, Mizrahi V, et al. Changes in energy metabolism of *Mycobacterium tuberculosis* in mouse lung and under in vitro conditions affecting aerobic respiration. *Proc Natl Acad Sci U S A.* 2005;102(43):15629-34. doi: 10.1073/pnas.0507850102. PubMed PMID: 16227431; PubMed Central PMCID: PMC1255738.
364. Sohaskey CD. Nitrate enhances the survival of *Mycobacterium tuberculosis* during inhibition of respiration. *J Bacteriol.* 2008;190(8):2981-6. doi: 10.1128/JB.01857-07. PubMed PMID: 18296525; PubMed Central PMCID: PMC2293237.
365. Cook GM, Hards K, Vilcheze C, Hartman T, Berney M. Energetics of Respiration and Oxidative Phosphorylation in *Mycobacteria*. *Microbiol Spectr.* 2014;2(3). doi: 10.1128/microbiolspec.MGM2-0015-2013. PubMed PMID: 25346874; PubMed Central PMCID: PMC4205543.
366. Cook GM, Berney M, Gebhard S, Heinemann M, Cox RA, Danilchanka O, et al. Physiology of mycobacteria. *Adv Microb Physiol.* 2009;55:81-182, 318-9. doi: 10.1016/S0065-2911(09)05502-7. PubMed PMID: 19573696; PubMed Central PMCID: PMC3728839.

367. Kerscher S, Droese S, Zickermann V, Brandt U. The three families of respiratory NADH dehydrogenases. *Results Probl Cell Differ.* 2008;45:185-222. doi: 10.1007/400\_2007\_028. PubMed PMID: 17514372.
368. Weinstein EA, Yano T, Li LS, Avarbock D, Avarbock A, Helm D, et al. Inhibitors of type II NADH:menaquinone oxidoreductase represent a class of antitubercular drugs. *Proc Natl Acad Sci U S A.* 2005;102(12):4548-53. doi: 10.1073/pnas.0500469102. PubMed PMID: 15767566; PubMed Central PMCID: PMC555520.
369. Melo AM, Bandejas TM, Teixeira M. New insights into type II NAD(P)H:quinone oxidoreductases. *Microbiol Mol Biol Rev.* 2004;68(4):603-16. doi: 10.1128/MMBR.68.4.603-616.2004. PubMed PMID: 15590775; PubMed Central PMCID: PMC539002.
370. Yano T, Li LS, Weinstein E, Teh JS, Rubin H. Steady-state kinetics and inhibitory action of antitubercular phenothiazines on mycobacterium tuberculosis type-II NADH-menaquinone oxidoreductase (NDH-2). *J Biol Chem.* 2006;281(17):11456-63. doi: 10.1074/jbc.M508844200. PubMed PMID: 16469750.
371. Miesel L, Weisbrod TR, Marcinkeviciene JA, Bittman R, Jacobs WR, Jr. NADH dehydrogenase defects confer isoniazid resistance and conditional lethality in *Mycobacterium smegmatis*. *J Bacteriol.* 1998;180(9):2459-67. PubMed PMID: 9573199; PubMed Central PMCID: PMC107189.
372. Bald D, Koul A. Respiratory ATP synthesis: the new generation of mycobacterial drug targets? *FEMS Microbiol Lett.* 2010;308(1):1-7. doi: 10.1111/j.1574-6968.2010.01959.x. PubMed PMID: 20402785.
373. Youmans AS, Millman I, Youmans GP. The oxidation of compounds related to the tricarboxylic acid cycle by whole cells and enzyme preparations of *Mycobacterium tuberculosis* var. *hominis*. *J Bacteriol.* 1956;71(5):565-70. PubMed PMID: 13331869; PubMed Central PMCID: PMC357853.
374. Griffin JE, Gawronski JD, Dejesus MA, Ioerger TR, Akerley BJ, Sassetti CM. High-resolution phenotypic profiling defines genes essential for mycobacterial growth and cholesterol catabolism. *PLoS Pathog.* 2011;7(9):e1002251. doi: 10.1371/journal.ppat.1002251. PubMed PMID: 21980284; PubMed Central PMCID: PMC3182942.
375. Eoh H, Rhee KY. Multifunctional essentiality of succinate metabolism in adaptation to hypoxia in *Mycobacterium tuberculosis*. *Proc Natl Acad Sci U S A.* 2013;110(16):6554-9. doi: 10.1073/pnas.1219375110. PubMed PMID: 23576728; PubMed Central PMCID: PMC3631649.
376. Cecchini G, Schroder I, Gunsalus RP, Maklashina E. Succinate dehydrogenase and fumarate reductase from *Escherichia coli*. *Biochim Biophys Acta.* 2002;1553(1-2):140-57. PubMed PMID: 11803023.
377. Matsoso LG, Kana BD, Crellin PK, Lea-Smith DJ, Pelosi A, Powell D, et al. Function of the cytochrome bc<sub>1</sub>-aa<sub>3</sub> branch of the respiratory network in mycobacteria and network adaptation occurring in response to its disruption. *J Bacteriol.* 2005;187(18):6300-8. doi: 10.1128/JB.187.18.6300-6308.2005. PubMed PMID: 16159762; PubMed Central PMCID: PMC1236647.

378. Tran SL, Cook GM. The F1Fo-ATP synthase of *Mycobacterium smegmatis* is essential for growth. *J Bacteriol.* 2005;187(14):5023-8. doi: 10.1128/JB.187.14.5023-5028.2005. PubMed PMID: 15995221; PubMed Central PMCID: PMC1169501.
379. Lu P, Lill H, Bald D. ATP synthase in mycobacteria: special features and implications for a function as drug target. *Biochim Biophys Acta.* 2014;1837(7):1208-18. doi: 10.1016/j.bbabi.2014.01.022. PubMed PMID: 24513197.
380. Haagsma AC, Driessen NN, Hahn MM, Lill H, Bald D. ATP synthase in slow- and fast-growing mycobacteria is active in ATP synthesis and blocked in ATP hydrolysis direction. *FEMS Microbiol Lett.* 2010;313(1):68-74. doi: 10.1111/j.1574-6968.2010.02123.x. PubMed PMID: 21039782.
381. Sohaskey CD. Regulation of nitrate reductase activity in *Mycobacterium tuberculosis* by oxygen and nitric oxide. *Microbiology.* 2005;151(Pt 11):3803-10. doi: 10.1099/mic.0.28263-0. PubMed PMID: 16272401.
382. Sohaskey CD, Wayne LG. Role of *narK2X* and *narGHJI* in hypoxic upregulation of nitrate reduction by *Mycobacterium tuberculosis*. *J Bacteriol.* 2003;185(24):7247-56. PubMed PMID: 14645286; PubMed Central PMCID: PMC1169501.
383. Tran SL, Rao M, Simmers C, Gebhard S, Olsson K, Cook GM. Mutants of *Mycobacterium smegmatis* unable to grow at acidic pH in the presence of the protonophore carbonyl cyanide *m*-chlorophenylhydrazone. *Microbiology.* 2005;151(Pt 3):665-72. doi: 10.1099/mic.0.27624-0. PubMed PMID: 15758213.
384. de Jonge MR, Koymans LH, Guillemont JE, Koul A, Andries K. A computational model of the inhibition of *Mycobacterium tuberculosis* ATPase by a new drug candidate R207910. *Proteins.* 2007;67(4):971-80. doi: 10.1002/prot.21376. PubMed PMID: 17387738.
385. Shirude PS, Paul B, Roy Choudhury N, Kedari C, Bandodkar B, Ugarkar BG. Quinolinylnyl Pyrimidines: Potent Inhibitors of NDH-2 as a Novel Class of Anti-TB Agents. *ACS Med Chem Lett.* 2012;3(9):736-40. doi: 10.1021/ml300134b. PubMed PMID: 24900541; PubMed Central PMCID: PMC1169501.
386. Amaral L, Kristiansen JE, Abebe LS, Millett W. Inhibition of the respiration of multi-drug resistant clinical isolates of *Mycobacterium tuberculosis* by thioridazine: potential use for initial therapy of freshly diagnosed tuberculosis. *J Antimicrob Chemother.* 1996;38(6):1049-53. PubMed PMID: 9023652.
387. de Keijzer J, Mulder A, de Haas PE, de Ru AH, Heerkens EM, Amaral L, et al. Thioridazine Alters the Cell-Envelope Permeability of *Mycobacterium tuberculosis*. *J Proteome Res.* 2016;15(6):1776-86. doi: 10.1021/acs.jproteome.5b01037. PubMed PMID: 27068340.
388. Mogi T, Matsushita K, Murase Y, Kawahara K, Miyoshi H, Ui H, et al. Identification of new inhibitors for alternative NADH dehydrogenase (NDH-II). *FEMS Microbiol Lett.* 2009;291(2):157-61. doi: 10.1111/j.1574-6968.2008.01451.x. PubMed PMID: 19076229.
389. Pethe K, Bifani P, Jang J, Kang S, Park S, Ahn S, et al. Discovery of Q203, a potent clinical candidate for the treatment of tuberculosis. *Nat Med.* 2013;19(9):1157-60. doi: 10.1038/nm.3262. PubMed PMID: 23913123.

390. Stowe SD, Thompson RJ, Peng L, Su Z, Blackledge MS, Draughn GL, et al. Membrane-permeabilizing activity of reverse-amide 2-aminoimidazole antibiofilm agents against *Acinetobacter baumannii*. *Curr Drug Deliv.* 2015;12(2):223-30. PubMed PMID: 25348099; PubMed Central PMCID: PMC4640187.

391. Harris TL, Worthington RJ, Hittle LE, Zurawski DV, Ernst RK, Melander C. Small molecule downregulation of PmrAB reverses lipid A modification and breaks colistin resistance. *ACS Chem Biol.* 2014;9(1):122-7. doi: 10.1021/cb400490k. PubMed PMID: 24131198.

## CHAPTER TWO

### 2-AI compounds potentiate $\beta$ -lactam activity against *M. tuberculosis*

This chapter will cover the serendipitous, but critical observation of 2-AI compounds treated *M. tuberculosis* not being able to grow in the presence of carbenicillin. Given the possible significant impact of repurposing  $\beta$ -lactam antibiotics in TB therapeutics, this observation was further investigated to test if 2-AI compounds potentiate this class of antibiotics against *M. tuberculosis*. Herein, we report that 2-AI compounds effectively reversed *M. tuberculosis* intrinsic resistance to multiple classes of  $\beta$ -lactam antibiotics and the transcriptional analyses support possible potentiation through effects on *M. tuberculosis* cell envelope.

#### 1.1. Introduction

The ongoing, global spread of TB, is due in part to the lack of new and more effective antimicrobial drugs to treat drug-sensitive and MDR strains of *M. tuberculosis* [1]. In 2015 alone, an estimated 10.4 million people developed TB resulting in 1.4 million deaths. Moreover, the incidence of new MDR-TB cases continues to increase and was estimated at 480,000 [2]. Treating drug-sensitive TB is challenging and requires a minimum six month course of combination antimicrobial drug therapy consisting of the first-line drugs isoniazid, rifampicin, ethambutol, and pyrazinamide that result in undesirable side-effects in some patients [3]. Moreover, treatment of MDR-TB is considerably more difficult and expensive requiring stronger and potentially more toxic drug combination therapy lasting approximately 2 years [2]. In short, the difficulty in controlling TB partially stems from the prolonged treatment using classical chemotherapy and the low treatment success rate especially in patients infected with MDR strains of *M. tuberculosis*. Unfortunately, the current pipeline of new anti-TB drugs for the treatment of resistant infections have unproven efficacy with undesirable side effects [4, 5].

The 2-AI class of small molecules is derived from the marine sponge metabolites oroidin and bromoageliferin [6, 7]. Importantly, treatment with 2-AI reversed isoniazid tolerance of attached *M.*

*tuberculosis* communities and significantly reduced numbers of viable bacilli when combined with isoniazid in an *in vitro* model of non-replicating persistence [8, 9]. These observations suggested that combining 2-AI compounds and conventional antibiotics can be a viable option to overcome *M. tuberculosis* drug-tolerance or resistance as shown for other clinically important Gram-positive and Gram-negative bacteria [6, 10, 11]. For example, 2-AI derivatives were shown to revert oxacillin resistance in MRSA [12], and suppress PmrAB mediated colistin resistance of drug-resistant *Acinetobacter baumannii* [13-15]. Altogether, these reports suggest that 2-AI compounds have promising potential as an adjunctive therapy when combined with antibiotics to treat drug-tolerant or –resistant bacteria.

Since their introduction,  $\beta$ -lactam antibiotics, have proven to be safe and effective at controlling a variety of bacterial infections [16, 17]. However,  $\beta$ -lactams are not currently used to treat TB, due to the intrinsic resistance exhibited by *M. tuberculosis*. Since  $\beta$ -lactams are currently only considered in the treatment of drug-resistant TB, any strategy that circumvents *M. tuberculosis*  $\beta$ -lactam resistance may provide new opportunities to utilize this class of drugs to treat both drug susceptible and drug-resistant strains of *M. tuberculosis* [18, 19]. Indeed, there is renewed interest in repurposing  $\beta$ -lactams to treat TB in combination with  $\beta$ -lactamase inhibitors [20-22], which are supported by recent human clinical trials [23].

This study investigated the potential use of 2-AI compounds to potentiate  $\beta$ -lactams against *M. tuberculosis*. It was hypothesized that 2-AI compounds would restore  $\beta$ -lactam susceptibility in *M. tuberculosis*. Herein it is reported that 2-AI compounds lower MIC values and improve the bactericidal activity of  $\beta$ -lactams against *M. tuberculosis*. Taken together, results indicate that 2-AI compounds represent a novel class of small molecule compounds that can potentiate  $\beta$ -lactam antibiotics and may be of significant value in anti-TB therapies in combination with  $\beta$ -lactams.

## 2.2. Materials and Methods

### 2.2.1. Bacterial strains, media and culture conditions

Stock cultures of *M. tuberculosis* H37Rv ATCC 27294 and *M. smegmatis* mc<sup>2</sup>155 were stored frozen at -80°C in Proskauer-Beck media (50% v/v glycerol) and glycerol stock media (50% v/v glycerol, 7H9, ADC, Tween 80), respectively. For propagation of initial culture, frozen stocks were thawed and sub-cultured in Middlebrook 7H9 media with OADC (0.005% oleic acid, 0.5% bovine serum albumin fraction V, 0.2% dextrose, 0.0003% catalase), 0.2% glycerol, and 0.05% Tween 80 until reaching a desirable optical density (OD) for each experiment. 7H9 and OADC were purchased from BD (Franklin Lakes, NJ, USA). Glycerol and Tween 80 were purchased from Sigma-Aldrich (St. Louis, MO, USA). All experiments using virulent *M. tuberculosis* H37Rv were done in a BSL3 laboratory located at Colorado State University.

### 2.2.2. 2-AI compounds

Structures and synthesis of 2B8 [8] and RA11 [24] were previously disclosed (Figure 1.2). Compounds were dissolved at 100 mM as their HCl salts in molecular biology grade DMSO (Sigma-Aldrich, USA) and stored at -80°C until use.

### 2.2.3. Growth assays

The effect of 2-AI compounds in *M. tuberculosis* growth *in vitro* was evaluated by monitoring OD<sub>600</sub> and colony forming units (CFUs). *M. tuberculosis* H37Rv was grown in 7H9 media with OADC supplement at 37°C, shaking for 20 days in the presence of 2B8 (0 to 125 µM). At day 1, 5, 8, 12, 15, and 20, OD<sub>600</sub> was measured and CFUs were determined by plating on 7H11 agar (BD, USA). Similar growth assay was performed with modifications. After 24 h of treatment, cultures were centrifuged at 1,700×g and media was removed. Bacilli were washed with sterile PBS and resuspended in fresh 2-AI compound-free 7H9 media to an OD<sub>600</sub> of 0.1. OD<sub>600</sub> was measured continuously thereafter.

#### 2.2.4. Determination of minimum inhibitory concentration of $\beta$ -lactams against mycobacteria with or without 2-AI compounds

Determination of  $\beta$ -lactam MICs against mycobacteria was carried out by using a broth microdilution method with alamarBlue<sup>®</sup> (Invitrogen, Carlsbad, CA, USA) as previously described [25]. Briefly, in 96-well flat-bottomed cell culture plates (Thermo-Fisher, Waltham, MA, USA),  $\beta$ -lactams were serially two-fold diluted in 7H9 media starting from the following concentrations: 1024 mg/L (ampicillin, oxacillin, carbenicillin, penicillin V and amoxicillin), 512 mg/L (cefotaxime and ceftazidime), 256 mg/L (cefoxitin), and 16 mg/L (meropenem). *M. smegmatis* and *M. tuberculosis* H37Rv grown in 7H9 media to an OD<sub>600</sub> of 0.4 to 0.6 were further diluted 1:20 and inoculated to wells containing  $\beta$ -lactams. Final volume of each well was 200  $\mu$ L. Plates were incubated under stationary conditions at 37<sup>o</sup>C. After 48 h (for *M. smegmatis*) or 5 days (for *M. tuberculosis*), 20  $\mu$ L alamarBlue<sup>®</sup> was added to each well and incubated for an additional 6 h (for *M. smegmatis*) or 24 to 48 h (for *M. tuberculosis*). MIC was determined as the lowest drug concentration that prevented color change from blue to purple or pink. This was confirmed as MIC<sub>95</sub> when measured by fluorescence [26]. Briefly, fluorescence was recorded at 560<sub>ex</sub>/590<sub>em</sub> and % inhibition of reduction was calculated as follows:  $MIC = 1 - 100 \times (\text{Sample fluorescence intensity} - \text{Negative control fluorescence intensity}) / (\text{Positive control fluorescence intensity} - \text{Negative control fluorescence intensity})$ , where the positive control is *M. tuberculosis* without drugs and the negative control is media. All  $\beta$ -lactams were purchased from Sigma-Aldrich except for carbenicillin and meropenem (Gold Biotechnology, St. Louis, MO, USA).

For MIC determination when  $\beta$ -lactams are combined with 2-AI compounds, broth microdilution MIC assay was performed in the presence of two-fold diluted RA11 or 2B8 ranging between 7.8125 and 250  $\mu$ M. One column of the plate contained only 2-AI compounds without any  $\beta$ -lactams to determine the MIC of 2-AI compounds against mycobacteria. MICs were determined as above and MIC of  $\beta$ -lactams alone was divided by MIC of  $\beta$ -lactams combined with 2-AI compounds to calculate fold-reduction of MIC resulting from 2-AI treatment.

### **2.2.5. Evaluation of bactericidal activity of $\beta$ -lactams against *M. tuberculosis***

*M. tuberculosis* H37Rv was incubated at 37<sup>0</sup>C for five days in 96-well flat-bottomed cell culture plates containing different concentrations of  $\beta$ -lactams alone, or with 2B8 or potassium clavulanate (Sigma-Aldrich, USA). 2B8 was added at 31.25, 62.5, and 125  $\mu$ M and clavulanate was added at 8 mg/L. Tested concentrations for each  $\beta$ -lactam were as follows: carbenicillin (2 and 32 mg/L), amoxicillin (2 and 32 mg/L), ceftazidime (1 and 16 mg/L), and meropenem (0.03125 and 0.5 mg/L). After 5 days of incubation, cultures were serially diluted in sterile PBS and plated on Middlebrook 7H11 agar (BD, USA) with glycerol, OADC and 8 mg/L cyclohexamide (Gold biotechnology, USA). The number of CFUs was determined by counting visible colonies after three or four weeks of incubation at 37<sup>0</sup>C. Bactericidal activity (%) was calculated as follows:  $100 - 100 \times (\text{Treatment group CFUs}/\text{Control CFUs})$ . For this calculation, control CFUs were obtained from non-treated (for  $\beta$ -lactams only group), 2B8 only (for 2B8/ $\beta$ -lactams combination group), and clavulanate only (for clavulanate/ $\beta$ -lactams combination group) treated samples.

### **2.2.6. RNA isolation and next generation sequencing**

For RNA isolation, *M. tuberculosis* H37Rv was cultured in 7H9 media to an OD<sub>600</sub> of 0.4 then treated with 125  $\mu$ M 2B8 for 2 and 24 h. After treatment, mycobacterial RNA was extracted using trizol/chloroform (Sigma-Aldrich, USA) as previously described with minor modifications [27]. Briefly, cells were resuspended in trizol and disrupted using Zirconia beads (Biospec, Bartlesville, OK, USA) by beating six times for 30 sec and cooling on ice for one min in between. Beads were removed and chloroform was added to trizol (0.2:1, v/v). Samples were vortexed and centrifuged to extract solubilized RNA in the aqueous phase. To precipitate RNA, molecular grade 100% ethanol (Sigma-Aldrich Aldrich, USA) was added to the aqueous phase and incubated at -80<sup>0</sup>C overnight. The RNA was pelleted by centrifugation ( $\times 17,000g$ ) at 4<sup>0</sup>C, for 15 min followed by washing with 75% ethanol. DNA contamination was removed by treating with 10  $\mu$ L DNase1 (New England Biomed, Ipswich, MA, USA) at 37<sup>0</sup>C for 30

min. Then 100  $\mu$ L of acid phenol (Sigma-Aldrich, USA) was added to the samples and vortexed. After centrifugation ( $\times 17,000g$ ) for one min, the aqueous phase was collected and transferred to clean RNase-free tubes, followed by the addition of 33  $\mu$ L sodium acetate (Sigma-Aldrich, USA) and 250  $\mu$ L of 100% ethanol. Samples were gently mixed by inverting and placed at  $-80^{\circ}C$  overnight. Samples were centrifuged ( $\times 17,000g$ ) for 15 min at  $4^{\circ}C$  to collect RNA pellets. Pellets were further washed with 80% ethanol. After ethanol removal, pellets were air-dried at room temperature for five min and reconstituted in 15  $\mu$ L of RNase-free water (Corning, USA). Isolated total RNA samples were prepared for next generation sequencing (NGS) using the Illumina Stranded Total RNA Library Prep Kit (Illumina, San Diego, CA, USA) with the Epicentre Ribo-Zero Gram positive bacteria ribosomal RNA depletion (Illumina, USA). After validation and quantitation, the libraries were pooled for multiplexed sequencing. The pool was loaded on one lane of a HiSeq Rapid Run flow cell (v1) and sequenced in a  $1\times 50$  bp single end (SE50) format using Rapid SBS reagents. Base calling was performed by Illumina Real Time Analysis (RTA, Illumina, USA) v1.18.61 and output of RTA was de-multiplexed and converted to FastQ format with Illumina Bcl2fastq v1.8.4 (Illumina, USA). To compensate for the low number of reads obtained for one sample, MiSeq (SE50) sequencing was performed with this one library. Reads from both the HiSeq and MiSeq runs were combined for that particular sample. Sequencing data were analyzed following methods similar to those previously described [28]. Briefly, raw reads were subjected to trimming of low-quality bases and removal of adapter sequences using Trimmomatic (v0.32) [29] with a 4 bp sliding window, cutting when the read quality was below 15 (using the Phred33 quality scoring system) or read length was less than 36 bp. Trimmed reads were then aligned to the *M. tuberculosis* H37Rv genome (assembly 19595v2) using Bowtie (v1.0.0) [30] with the  $-S$  option to produce SAM files as output. Alignment quality control was performed using the HTSeq-qa function within the HTSeq software package (v.0.6.1) [31]. Further graphical quality control analyses were performed using the Qualimap software suite (v2.0) [32]. Sequencing depth was calculated using SAMtools (v1.2) [33]. Aligned reads were then counted per gene feature in the *M. tuberculosis* H37Rv genome using the HTSeq software suite (v0.6.1). Differential gene expression was calculated by normalizing the data utilizing the

trimmed mean of M-values normalization method [34] and filtering out genes that had <23 counts per million (CPM) within the edgeR package (v3.0.8) in R (v2.15.3) [35]. The transcriptional profiling data have been submitted to the NCBI GEO database (accession no. GSE95773).

### **2.2.7. Statistical analysis**

Statistical analyses were carried out using one-way ANOVA with Tukey's post hoc test using GraphPad Prism 5 (GraphPad Software, La Jolla, CA, USA). P values less than 0.05 were considered significant. For RNA transcriptome data, statistical analysis was performed in R Studio (ver. 0.98.1091) by the exact test with a negative binomial distribution for each set of conditions and testing for differential gene expression [36] using edgeR (v3.0.8). Differentially expressed genes were determined to be statistically significant based on a  $q < 0.05$  and >1.5-fold differentially regulated. Magnitude amplitude (MA) plots were generated by modifying a function within the edgeR package (v3.0.8).

## **2.3. Results**

### **2.3.1. Normal growth of *M. tuberculosis* is affected by the presence of 2B8**

When 2B8 was present at 125  $\mu\text{M}$  in the culture media, *M. tuberculosis* growth was thwarted significantly from day 1 to day 20 measured by  $\text{OD}_{600}$  (Figure 2.1A). 2B8 62.5  $\mu\text{M}$  significantly inhibited normal growth of *M. tuberculosis* at day 5, but resumed normal growth at day 8. There was no significant difference in growth between control (DMSO treated) and 2B8 31.25  $\mu\text{M}$  treated *M. tuberculosis*. Similar trend was observed with corresponding CFUs with 2B8 125  $\mu\text{M}$  as it significantly lowered CFUs of the culture from day 8 (Figure 2.1B). To see if the inhibition of growth can be removed by washing bacilli, *M. tuberculosis* culture was washed with sterile PBS after 24 h of treatment. Washed culture still grew slower than the control, but resumed to normal growth at day 7 (Figure 2.2).

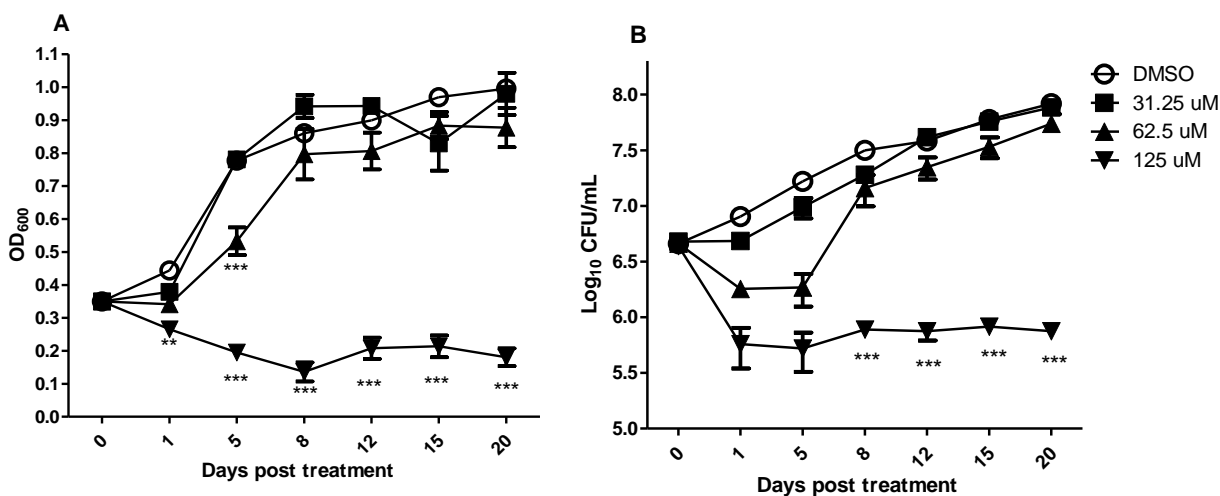


**Figure 2.1. 2B8 inhibits growth of *M. tuberculosis*.** The growth of *M. tuberculosis* in 7H9 media with or without 2B8 was evaluated by measuring OD<sub>600</sub> (A) and CFUs (B). 2B8 125 μM significantly affected growth while 31.25 and 62.5 μM resulted in minimal effect on growth. Experiments were done three separate times and representative data are shown. \*\* p<0.01, \*\*\* p<0.001 by ANOVA.

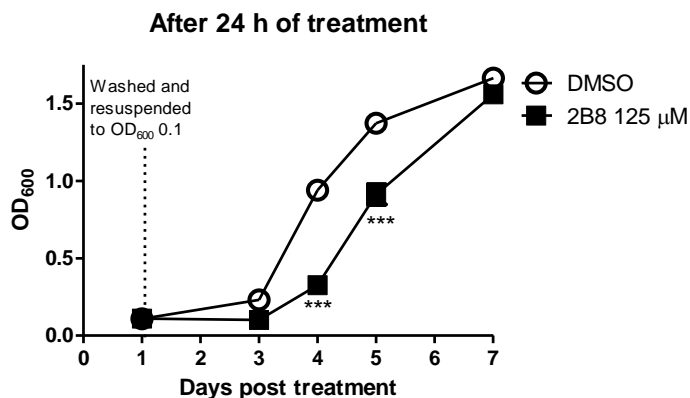


**Figure 2.2. Inhibition of *M. tuberculosis* growth by 2B8 is removed by washing the culture.** After 24 h of treatment with 2B8 125 μM, cultures were washed and resuspended in fresh 7H9 media without any 2B8 to OD<sub>600</sub> of 0.1. Washed culture returned to the OD<sub>600</sub> comparable to DMSO-control at day 7. Experiments were done two separate times and representative data are shown. \*\*\* p<0.001 by ANOVA.

### 2.3.2. 2B8 treated *M. tuberculosis* fails to grow in the presence of carbenicillin

When culturing *M. tuberculosis* in solid agar, a selective agar containing carbenicillin (50 mg/L) may be used to eliminate contaminating bacteria that grow faster than *M. tuberculosis*. Due to intrinsic

resistance against  $\beta$ -lactam antibiotics, growth of *M. tuberculosis* would not be affected by the presence of carbenicillin as shown in Figure 4A and 4B. In contrast, when *M. tuberculosis* was treated with 125  $\mu$ M 2B8, the lead 2-AI compound, the presence of carbenicillin abrogated growth (Figure 2.3D) whereas growth of 2-AI treated cultures was observed when carbenicillin was excluded from the media (Figure 2.3C).

### 2.3.3. 2-AI treatment reduces MIC of $\beta$ -lactams against mycobacteria

Based on the observation that 2B8 treated *M. tuberculosis* failed to grow in the presence of carbenicillin, it was hypothesized that 2-AI compounds could potentiate  $\beta$ -lactams against mycobacteria. Therefore, the MICs of multiple  $\beta$ -lactams against *M. tuberculosis* H37Rv and *M. smegmatis* were evaluated in the presence or absence of 2-AI compounds. Compared to the use of  $\beta$ -lactams alone, combination with 2B8 significantly reduced MIC values against both *M. smegmatis* and *M. tuberculosis* (Table 2.1).

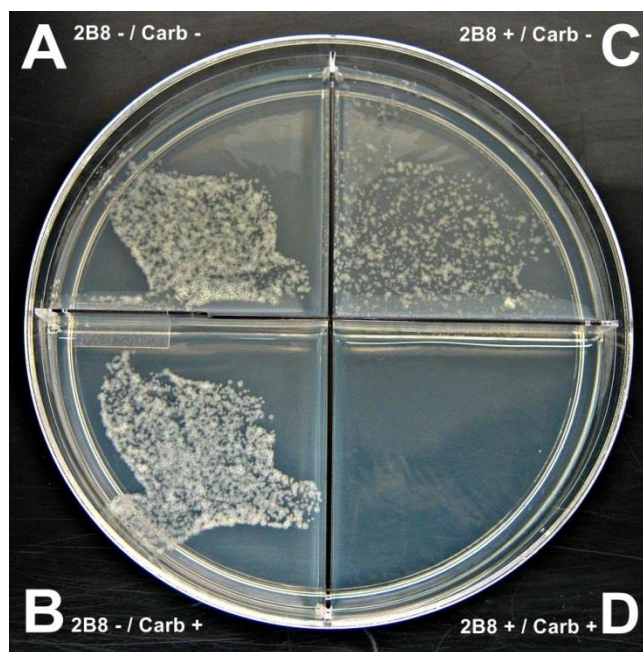


**Figure 2.3. 2B8 treated *M. tuberculosis* failed to thrive in the presence of carbenicillin.** A and B) Untreated *M. tuberculosis* H37Rv showing normal growth regardless of the presence of 100 mg/L carbenicillin. C) Growth of *M. tuberculosis* H37Rv treated with 125  $\mu$ M 2B8 was observed in the absence

of carbenicillin, albeit to a lesser extent than untreated (A). D) No visible colonies were observed for 2B8 treated *M. tuberculosis* H37Rv in carbenicillin-containing agar. The experiment was repeated three separate times in duplicate and a representative photo is shown.

For *M. smegmatis*, 2B8 reduced the MICs of the four  $\beta$ -lactams (carbenicillin, amoxicillin, ceftazidime, and meropenem) tested at 25% of the 2B8 MIC (10  $\mu$ M). MIC reduction was highest when 2B8 was used at 50% of its MIC (20  $\mu$ M), was 128-fold for cefotaxime and 32-fold for the other tested drugs. For *M. tuberculosis*, reduction in  $\beta$ -lactam MICs became evident at a 2B8 concentration of 12.5% of its MIC (31.25  $\mu$ M). When used at 50% of its MIC (125  $\mu$ M), 2B8 reduced the MICs of the five tested  $\beta$ -lactams at least 32-fold, with the highest fold-reductions of 128-fold observed for carbenicillin and meropenem. RA11, a 2B8 derivative differing only in its alkyl side chains [8], was also tested against *M. tuberculosis*. The addition of RA11 also resulted in a reduction in  $\beta$ -lactam MICs, but to a lesser degree than that for 2B8. For example, the amoxicillin MIC was reduced 64-fold by 2B8 while RA11 only reduced the MIC by 16-fold.

**Table 2.1. MIC of  $\beta$ -lactams against mycobacteria in combination with 2-AI compounds.**

<i>M. smegmatis</i>	MIC	MIC with 5 $\mu$ M 2B8	Fold	MIC with 10 $\mu$ M 2B8	Fold	MIC with 20 $\mu$ M 2B8	Fold
		(12.5% MIC*)	reduction	(25% MIC)	reduction	(50% MIC)	reduction
Ampicillin	256	256	1	128	2	8	32
Oxacillin	256	256	1	128	2	8	32
Cefotaxime	128	128	1	32	4	1	128
Cefoxitin	16	16	1	8	2	0.5	32
<i>M. tuberculosis</i>		MIC with 31.25 $\mu$ M		MIC with 62.5 $\mu$ M		MIC with 125 $\mu$ M 2B8	
H37Rv		2B8 (12.5% MIC*)		2B8 (25% MIC)		(50% MIC)	

Carbenicillin	512	32	16	8	64	4	128
Amoxicillin	512	64	8	16	32	8	64
Ceftazidime	256	128	2	32	8	8	32
Cefotaxime	256	128	2	32	8	4	64
Meropenem	8	2	4	0.25	32	0.0625	128
Penicillin V	512	64	8	16	32	8	64
<i>M. tuberculosis</i>	MIC with 31.25 $\mu$ M		MIC with 62.5 $\mu$ M		MIC with 125 $\mu$ M		
H37Rv	RA11 (12.5% MIC*)		RA11 (25% MIC)		RA11 (50% MIC)		
Carbenicillin	512	256	2	128	4	16	32
Amoxicillin	512	512	2	256	8	32	16
Ceftazidime	256	256	1	128	2	64	8
Cefotaxime	256	256	1	128	2	32	8
Meropenem	8	8	1	8	4	1	32
Penicillin V	512	256	1	128	4	32	8

All MIC values are represented as mg/L.

\*MIC of 2B8 against *M. smegmatis* and *M. tuberculosis* were 40  $\mu$ M and 250  $\mu$ M, respectively.

\*\*MIC of RA11 against *M. tuberculosis* was 250  $\mu$ M.

Experiments were carried out at least three independent times and representative data are shown.

### 2.3.4. 2-AI improves bactericidal effect of $\beta$ -lactams

Since 2-AI compounds reduced the MICs of  $\beta$ -lactams against *M. tuberculosis*, it was hypothesized that these compounds may augment bactericidal effects. This set of experiments focused on 2B8 because it showed a superior effect over RA11 in the MIC assays. It should be noted that at high concentrations (125  $\mu$ M), 2B8 treated *M. tuberculosis* had impaired growth compared to non-treated culture (Fig S2). Thus, the bactericidal activity was calculated from non-treated (for  $\beta$ -lactams only group), 2B8 only treated (2B8/ $\beta$ -lactams combination group), and clavulanate only treated (clavulanate/ $\beta$ -lactams combination group) cultures.

For the four  $\beta$ -lactams tested, co-treatment for five days with 2B8 led to a significant increase in bactericidal activity compared to  $\beta$ -lactams alone. For carbenicillin (2 mg/L), amoxicillin (2 mg/L), and ceftazidime (1 mg/L), a dose-dependent effect was observed with increasing concentrations of 2B8 (Figure 2). The combination of  $\beta$ -lactams with clavulanate, a widely used  $\beta$ -lactamase inhibitor, was also evaluated. As expected, improved bactericidal activity was observed when clavulanate was combined with all tested  $\beta$ -lactams as depicted in Fig 2.

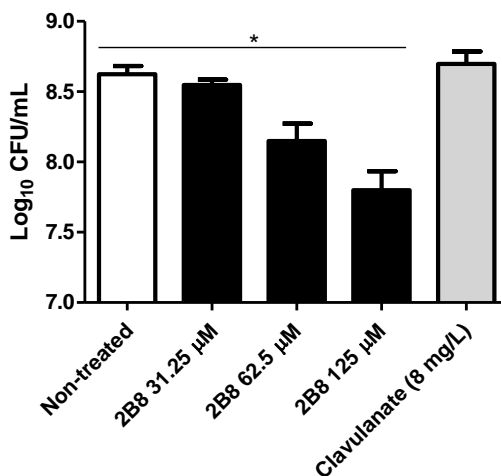


**Figure 2.4. 2B8 affects normal growth of *M. tuberculosis* H37Rv.** *M. tuberculosis* H37Rv was plated on 7H11 agar after five days of culture with or without clavulanate or increasing concentrations of 2B8, and CFUs were enumerated three weeks after. Compared to control, CFUs from cultures containing 2B8

were significantly lower, suggesting that 2B8 affects normal growth of *M. tuberculosis* by itself. In contrast, clavulanate did not affect bacterial growth. \* $p < 0.05$  by ANOVA.

For the four  $\beta$ -lactams tested, co-treatment for five days with 2B8 led to a significant decrease in bacterial viability compared to  $\beta$ -lactams alone. At 2 mg/L, carbenicillin co-treatment with 2B8 (62.5 and 125  $\mu$ M) resulted in significant decreases in survival (Figure 2.5A). However, when carbenicillin was increased to 32 mg/L, co-treatment with 2B8 resulted in a significant survival decrease even at 31.25  $\mu$ M 2B8. The same trend was observed for amoxicillin (Figure 2.5B). For ceftazidime, the effect of 2B8 was less significant than that for carbenicillin and amoxicillin (Figure 2.5C). However, when combined with 2B8, reduced survival was observed with ceftazidime at 16 mg/L, only 1/16 of the MIC when dosed alone (256 mg/L). Of the tested  $\beta$ -lactams, meropenem exhibited the lowest MIC against mycobacteria when evaluated in the absence of 2B8 (Table 2.1). When 2B8 was combined with meropenem at 0.03125 mg/L, percent survival decrease was significant with 62.5 and 125  $\mu$ M 2B8 (Figure 2.5D). At 0.5 mg/L meropenem, only 125  $\mu$ M 2B8 co-treatment resulted in a significant decrease in percent survival. The combination of  $\beta$ -lactams with clavulanate, a widely used  $\beta$ -lactamase inhibitor, was also evaluated. As expected, improved bacterial killing was observed when clavulanate was included with all tested  $\beta$ -lactams as depicted in Figure 2.5.

### **2.3.5. *M. tuberculosis* transcriptional responses to 2B8**

To further characterize the impact of 2-AI compounds on *M. tuberculosis* physiology, transcriptional profiling of *M. tuberculosis* exposed to 2B8 for 2 and 24 hours was performed. *M. tuberculosis* H37Rv was treated with 125  $\mu$ M 2B8 and following 2 or 24 h of treatment, RNA was isolated and transcriptional profiles were determined by RNA-sequencing (RNA-seq). At 2 h and 24 h post-treatment, genes were identified that were upregulated or downregulated  $>1.5$ -fold with a  $q < 0.05$ . To identify genes with both early and sustained differential gene expression, the gene lists at 2 and 24 h were compared for common differentially regulated genes (Figure 2.6A). At both time points, 124 genes

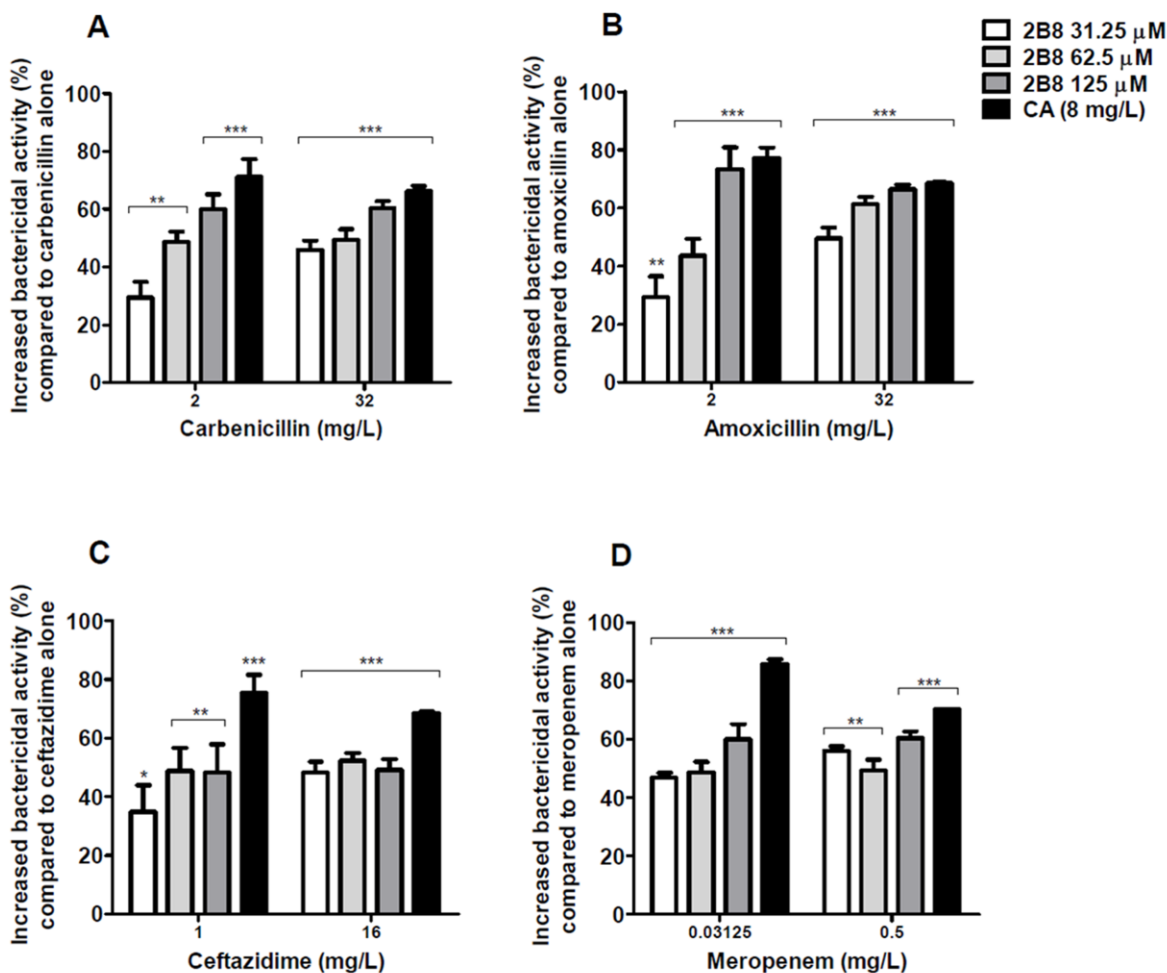
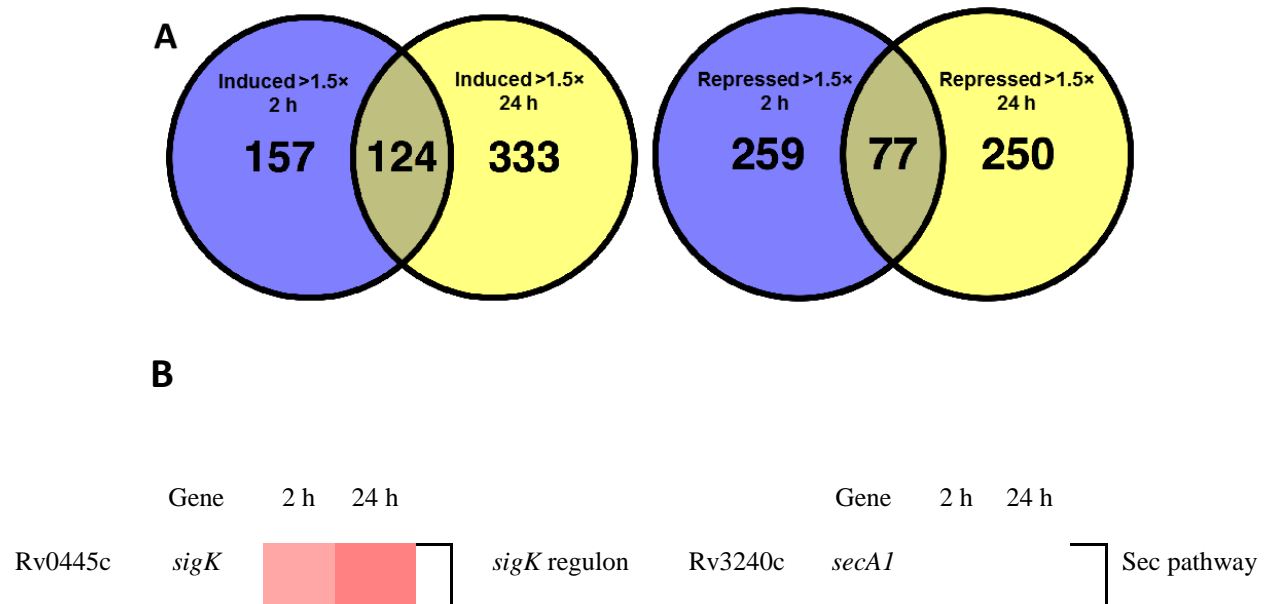


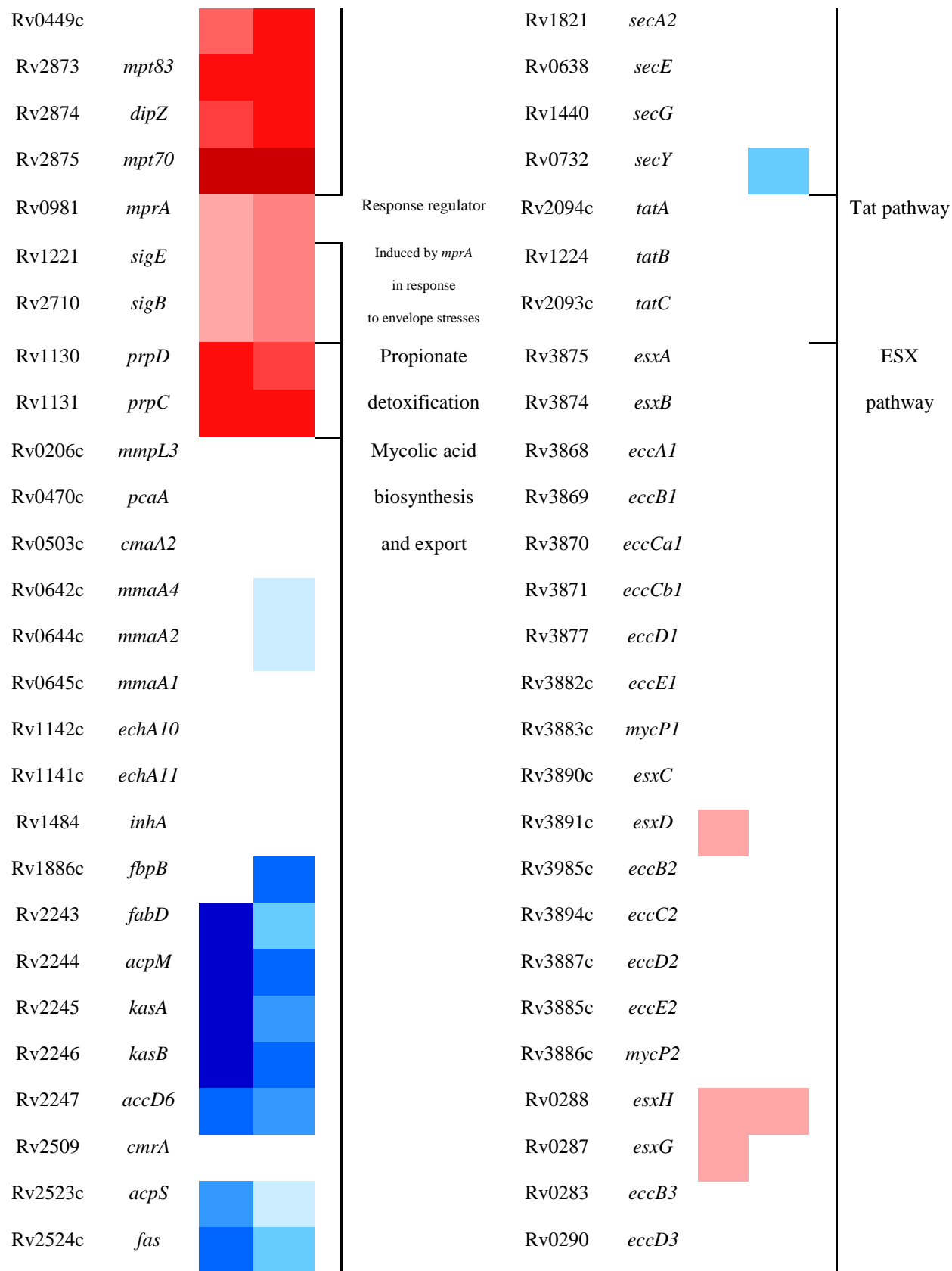
**Figure 2.5. 2B8 potentiates mycobactericidal activity of β-lactams.** Bactericidal activity of β-lactams against *M. tuberculosis* H37Rv was significantly increased after 5 days of treatment in combination with 2B8 or clavulanate compared to when β-lactams were used alone. Statistical significance was determined comparing each group with β-lactams only group. \* $p < 0.05$ , \*\* $p < 0.01$ , \*\*\* $p < 0.001$  by ANOVA. Experiments were carried out three separate times in duplicate and all results were pooled together for statistical analysis.

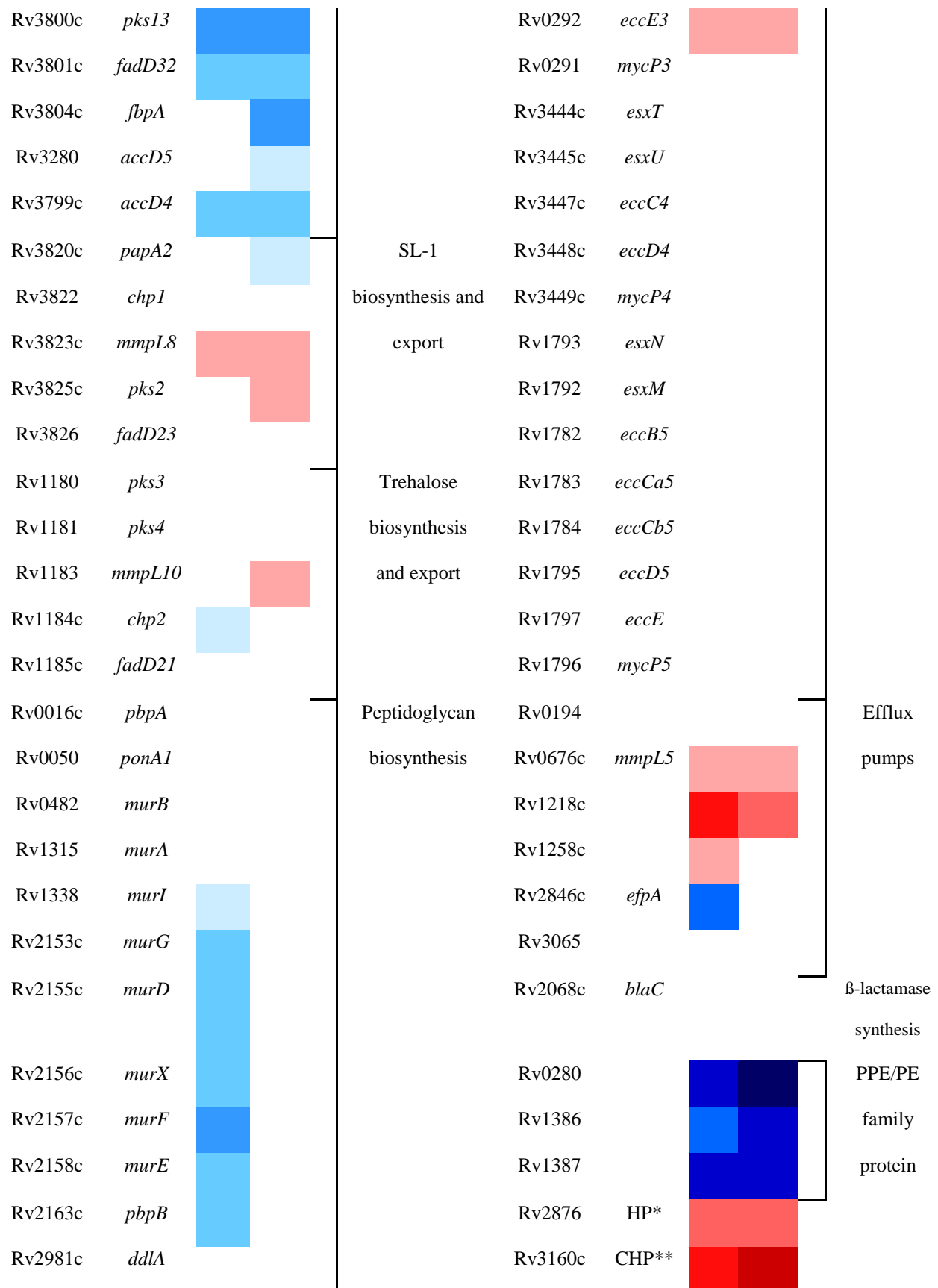
were induced and 77 genes were repressed ( $>1.5$ -fold,  $q < 0.05$ ). Genes encoding for several transcriptional regulators including the alternative sigma factors *sigB*, *sigE* and *sigK* and the response regulator *mprA*

were induced (1.5 to 1.8-fold for 2 h, 2 to 3.7-fold for 24 h) (Figure 2.6B). 2B8 treatment enhanced expression of SigK regulated genes including *mpt83*, *dipZ*, *mpt70*, and *rv0449c* [37], supporting that the SigK regulon was induced in a sustained manner by 2B8 (Fig 2.7B). Other genes of interest that were strongly induced at both time-points include: *prpCD* which is proposed to play a role in propionate detoxification [38], *rv3160c* and *rv3161c*, a putative dioxygenase and its regulator, previously shown to be strongly regulated by triclosan and suggested to be involved in degradation of arenes [39]. Finally, it was noted that *mmpL8* (2 and 24 h) and *mmpL10* (24 h) involved in SL-1 and acyl-trehalose export, respectively [40, 41], were induced by 2B8 treatment (Figure 2.6B).

The downregulated genes at both time-points show a strong signature for inhibition of genes associated with mycolic acid biosynthesis (Figure 2.6B) including *fas*, *fabD*, *acpM*, *kasAB*, *pks13* and *fadD32*. Multiple genes involved in peptidoglycan biosynthesis (*mur* family) were repressed, but genes involved in protein secretion were not generally modulated by 2B8, and *blaC* encoding for  $\beta$ -lactamase was also unaffected (Figure 2.6B). Finally, one of the most significantly downregulated genes was *rv0280*, which encodes for a member of the PE/PPE family with no known function to date, but previously reported to be downregulated in a *phoP* mutant strain [42].







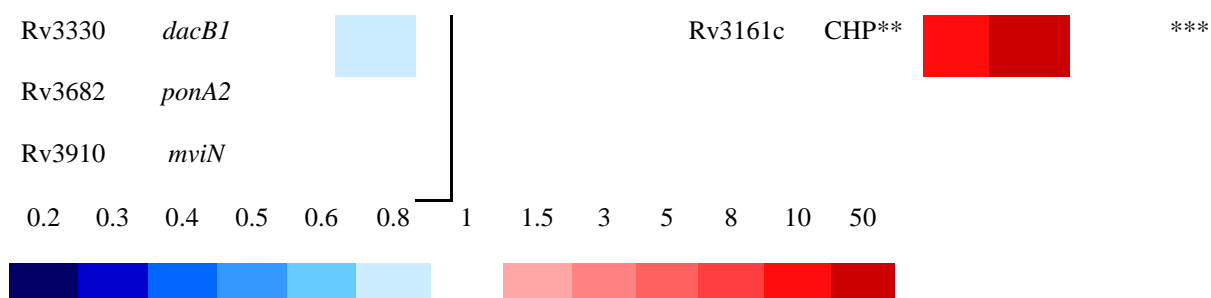


**Figure 2.7. Transcriptional responses of *M. tuberculosis* to 2B8.** RNA-seq analysis was performed on *M. tuberculosis* H37Rv treated with DMSO (untreated control) or with 125  $\mu$ M 2B8 for 2 and 24 h. Induced and repressed genes were defined as >1.5-fold change in expression compared to the untreated control,  $q < 0.05$ . A) Venn diagram showing number of genes induced or repressed after 2 and 24 h. B) Heat map showing differential transcriptional regulation of selected relevant genes. Genes that did not make the 1.5-fold cut-off and statistical significance ( $q < 0.05$ ) were considered no change (1 in fold-change scale, white color). \*Hypothetical protein, \*\*Conserved hypothetical protein, \*\*\*Upregulated in response to triclosan.

## 2.4. Discussion

Recently, we disclosed that a 2-aminoimidazole-based anti-biofilm agent was able to inhibit and disperse *M. tuberculosis* biofilms and in the process re-sensitize bacteria to the effects of isoniazid [8]. During these studies, we noted that treatment with this 2-AI derivative also potently sensitized planktonic *M. tuberculosis* to  $\beta$ -lactams. Specifically, 2-AI treated *M. tuberculosis* did not grow in agar plates containing carbenicillin. Based upon this observation, the goals of this study were to determine if the combination of 2-AI compounds and  $\beta$ -lactams circumvents *M. tuberculosis* intrinsic resistance to  $\beta$ -lactams. It is reported herein that selected 2-AI compounds were effective in reducing  $\beta$ -lactam MICs against *M. tuberculosis* while also improving their bactericidal activity. It is noteworthy that the effect of 2-AI was not limited to a specific class of  $\beta$ -lactams. Indeed, 2-AI's effect was observed (albeit to a different degree) across all  $\beta$ -lactams tested including carboxypenicillin (carbenicillin), aminopenicillin (amoxicillin), third generation cephalosporin (ceftazidime), and carbapenem (meropenem). In essence, 2-AI compounds effectively nullified *M. tuberculosis* intrinsic  $\beta$ -lactam resistance.

The concept of having an adjunctive element with  $\beta$ -lactam antibiotics has been already proven to be effective with successful example like clavamox which is a combination of amoxicillin and  $\beta$ -

lactamase inhibitor clavulanate. This signifies the importance of  $\beta$ -lactamase enzyme activity in conferring  $\beta$ -lactam resistance to bacteria. To date, three  $\beta$ -lactamase inhibitors were developed into clinical medicine: clavulanate, sulbactam, and tazobactam. These molecules are structurally similar with  $\beta$ -lactam antibiotics that enable them to binding with  $\beta$ -lactamase enzymes thus abrogating its effect. In general, these inhibitors are mostly active against class A  $\beta$ -lactamases and less active against class B, C, and D  $\beta$ -lactamases [43]. In TB, meropenem was surveyed as a potentially usable  $\beta$ -lactam as it has been shown to be resistant to *M. tuberculosis* produced  $\beta$ -lactamase enzyme and combination of meropenem with clavulanate has been shown to be effective both *in vitro* and *in vivo* [21, 44]. Additionally, a recently conducted clinical trial in human suggests that meropenem-clavamox combination was effective in reducing *M. tuberculosis* bacilli load in sputum samples [23]. In our studies, 2-AI compounds potentiated  $\beta$ -lactam drugs in a dose-dependent manner comparable to  $\beta$ -lactam-clavulanate combination. It is noteworthy that clavulante had minimal effect on bacterial growth by itself while 2-AI compounds alone also exhibited bacteriostatic effect on *M. tuberculosis* culture. This indicates that the pattern of  $\beta$ -lactam resistance reversal by 2-AI compounds in *M. tuberculosis* may be distinct from that by clavulanate. While clavulanate directly targets  $\beta$ -lactamase enzyme to inhibit its activity, one can assume 2-AI compounds are exerting its effect on bacilli itself and not directly on  $\beta$ -lactamase enzyme. Additionally, we observed similar level of potentiation of meropenem and other  $\beta$ -lactam antibiotics tested. As mentioned earlier, meropenem is less susceptible to degradation by *M. tuberculosis*  $\beta$ -lactamase and the fact that meropenem was potentiated comparable to other  $\beta$ -lactams can be indicative of other possible potentiation mechanism involved besides  $\beta$ -lactamase inhibition. Several hypotheses can be made at this point including the possible effect of 2-AI compounds might have on mycobacterial cell envelope. In *Acinetobacter baumannii* and *K. pneumoniae*, analogs of 2-AI compounds have been shown to modulate cell wall structural component while also having permeabilizing effect on the cell membrane [14]. Since mycobacterial cell envelope is a major diffusion barrier for hydrophilic molecules such as  $\beta$ -lactam antibiotics, the permeabilization of cell envelope by 2-AI compounds would definitely increase *M. tuberculosis* susceptibility to  $\beta$ -lactams [45].

Transcriptional analyses performed in *M. tuberculosis* treated with one of our 2-AI compounds, 2B8, provide further insights to the potentiation mechanism. The signature transcriptional response to 2B8 treatment was upregulation of extracellular sigma factor SigK (*Rv0447c*, *Rv0449c*, *Rv0446c*) and its regulon (*Rv2873* to *Rv2876*) that are dramatically induced after 2 h of treatment. Also, noticeable induction of *mprA* and both *sigB* and *sigE* was observed (Figure 2.6). The sigma factor regulatory network involving SigB and SigE has been shown to be responsible for the transcriptional changes in response to cell envelope associated damage or stress [46]. The upregulation of another gene further supports the possible impact of 2-AI on cell envelope. The *Rv0516c* encoding one of the PknD substrate was significantly induced which has been previously shown to be induced by osmotic pressure on cell wall. Also, the mutant of *Rv0516c* showed decrease in peptidoglycan thickness and increase of resistance to peptidoglycan biosynthesis targeting antibiotics [47]. Another interesting finding was that multiple genes that have been shown to be induced by triclosan treatment were also significantly induced with 2B8 such as *Rv3159c*, *Rv3160c*, and *Rv3161c* [39]. Triclosan has an impact on mycolic acid biosynthesis by inhibiting enoyl acyl carrier protein reductase InhA [48], and also has a broad cell envelope disruption effect if used at high concentration [49]. This overlap between triclosan induced genes and 2B8 induced genes leads to question whether 2B8 has an effect on mycolic acid biosynthesis. Indeed, the notable downregulated genes included *kasB* operon (*Rv2243* to *Rv2248*) which is required for elongation of acyl subunits of mycolic acids, fatty acids and polyketides [50]. Recently, diarylcoumarins have been shown to target FadD32 encoded by *Rv3801c* which was also downregulated with 2B8 treatment [51]. While 2B8 share no structural similarity with triclosan or diarylcoumarins, this suggests the possibility that 2B8 targets cell envelope integrity like those drugs.

It is also noteworthy that *Rv3161c* has been shown to be also induced by bioenergetics affecting drugs such as CCCP and TRZ [46, 52] since some genes encoding components of ETC including NDH-I (*nuo* family), cytochrome subunits, and ATP synthase subunits were found to be downregulated by 2B8 treatment. Therefore, it is logical to suspect that 2B8 could be affecting both ends of *M. tuberculosis* cell envelope, outer membrane and inner membrane which contains core complexes for the ETC.

The *blaC* gene encoding  $\beta$ -lactamase did not show difference with 2B8 treatment which shows that 2B8 is not directly reducing  $\beta$ -lactamase expression at transcriptional level. The fact that genes involved in Tat protein secretory pathways also did not change suggests 2B8 is not affecting  $\beta$ -lactamase secretion specifically. Other genes involved in protein secretion machinery including Sec and ESX pathways also had minimal changes. There was no noticeable suppression of efflux pumps encoding genes which could possibly lead to potentiation of antimicrobial agents.

Taken together, 2-AI compounds significantly potentiated  $\beta$ -lactam antibiotics against *M. tuberculosis* comparable to clavulanate. With the possibility of potentiation mechanism being different from that of clavulanate, the adjunctive therapeutic approach using 2-AI compounds in combination with  $\beta$ -lactams can be an innovative, yet effective alternative to conventional anti-TB chemotherapy. The approach will benefit from the proven efficacy and safety of  $\beta$ -lactams for use in human clinical medicine and may even help us to explore novel options for treatment of MDR-TB. The transcriptional response from 2B8 treatment suggests a significant impact on *M. tuberculosis* cell envelope which may be the primary mechanism of  $\beta$ -lactam potentiation. The suppression of mycolic acid biosynthesis is a feature that is similar to other InhA targeting drugs, but more like triclosan than isoniazid. It is also indicated that 2B8 may be having an effect on membrane bioenergetics of *M. tuberculosis*. Elucidation of how 2-AI compounds potentiate  $\beta$ -lactam antibiotics will lead to better understanding of unknown weaknesses of *M. tuberculosis* which we can exploit to combat drug resistance issues in TB.

## REFERENCES

1. Glickman MS, Jacobs WR, Jr. Microbial pathogenesis of *Mycobacterium tuberculosis*: dawn of a discipline. *Cell*. 2001;104(4):477-85. PubMed PMID: 11239406.
2. WHO. *Global Tuberculosis Report 2016*. 2016.
3. Awofeso N. Anti-tuberculosis medication side-effects constitute major factor for poor adherence to tuberculosis treatment. *Bull World Health Organ*. 2008;86(3):B-D. PubMed PMID: 18368191; PubMed Central PMCID: PMCPMC2647396.
4. Nachega JB, Chaisson RE. Tuberculosis drug resistance: a global threat. *Clin Infect Dis*. 2003;36(Suppl 1):S24-30. doi: 10.1086/344657. PubMed PMID: 12516027.
5. Zumla A, Chakaya J, Centis R, D'Ambrosio L, Mwaba P, Bates M, et al. Tuberculosis treatment and management--an update on treatment regimens, trials, new drugs, and adjunct therapies. *Lancet Respir Med*. 2015;3(3):220-34. doi: 10.1016/S2213-2600(15)00063-6. PubMed PMID: 25773212.
6. Stowe SD, Richards JJ, Tucker AT, Thompson R, Melander C, Cavanagh J. Anti-biofilm compounds derived from marine sponges. *Mar Drugs*. 2011;9(10):2010-35. doi: 10.3390/md9102010. PubMed PMID: 22073007; PubMed Central PMCID: PMCPMC3210616.
7. Fusetani N. Antifouling marine natural products. *Nat Prod Rep*. 2011;28(2):400-10. doi: 10.1039/c0np00034e. PubMed PMID: 21082120.
8. Ackart DF, Lindsey EA, Podell BK, Melander RJ, Basaraba RJ, Melander C. Reversal of *Mycobacterium tuberculosis* phenotypic drug resistance by 2-aminoimidazole-based small molecules. *Pathog Dis*. 2014;70(3):370-8. doi: 10.1111/2049-632X.12143. PubMed PMID: 24478046; PubMed Central PMCID: PMCPMC4367863.
9. Ackart DF, Hascall-Dove L, Caceres SM, Kirk NM, Podell BK, Melander C, et al. Expression of antimicrobial drug tolerance by attached communities of *Mycobacterium tuberculosis*. *Pathog Dis*. 2014;70(3):359-69. doi: 10.1111/2049-632X.12144. PubMed PMID: 24478060; PubMed Central PMCID: PMCPMC4361083.
10. Worthington RJ, Melander C. Overcoming resistance to beta-lactam antibiotics. *J Org Chem*. 2013;78(9):4207-13. doi: 10.1021/jo400236f. PubMed PMID: 23530949; PubMed Central PMCID: PMCPMC3644377.
11. Stephens MD, Hubble VB, Ernst RK, van Hoek ML, Melander RJ, Cavanagh J, et al. Potentiation of Resistance to Conventional Antibiotics through Small Molecule Adjuvants. *Medchemcomm*. 2016;7(1):128-31. doi: 10.1039/C5MD00353A. PubMed PMID: 26877862; PubMed Central PMCID: PMCPMC4749165.
12. Harris TL, Worthington RJ, Melander C. Potent small-molecule suppression of oxacillin resistance in methicillin-resistant *Staphylococcus aureus*. *Angew Chem Int Ed Engl*. 2012;51(45):11254-7. doi: 10.1002/anie.201206911. PubMed PMID: 23047322; PubMed Central PMCID: PMCPMC3829614.

13. Stowe SD, Thompson RJ, Peng L, Su Z, Blackledge MS, Draughn GL, et al. Membrane-permeabilizing activity of reverse-amide 2-aminoimidazole antibiofilm agents against *Acinetobacter baumannii*. *Curr Drug Deliv*. 2015;12(2):223-30. PubMed PMID: 25348099; PubMed Central PMCID: PMC4640187.
14. Harris TL, Worthington RJ, Hittle LE, Zurawski DV, Ernst RK, Melander C. Small molecule downregulation of PmrAB reverses lipid A modification and breaks colistin resistance. *ACS Chem Biol*. 2014;9(1):122-7. doi: 10.1021/cb400490k. PubMed PMID: 24131198.
15. Worthington RJ, Melander C. Combination approaches to combat multidrug-resistant bacteria. *Trends Biotechnol*. 2013;31(3):177-84. doi: 10.1016/j.tibtech.2012.12.006. PubMed PMID: 23333434; PubMed Central PMCID: PMC3594660.
16. Lewis K. Platforms for antibiotic discovery. *Nat Rev Drug Discov*. 2013;12(5):371-87. doi: 10.1038/nrd3975. PubMed PMID: 23629505.
17. Wivagg CN, Bhattacharyya RP, Hung DT. Mechanisms of beta-lactam killing and resistance in the context of *Mycobacterium tuberculosis*. *J Antibiот (Tokyo)*. 2014;67(9):645-54. doi: 10.1038/ja.2014.94. PubMed PMID: 25052484.
18. Wallis RS, Maeurer M, Mwaba P, Chakaya J, Rustomjee R, Migliori GB, et al. Tuberculosis--advances in development of new drugs, treatment regimens, host-directed therapies, and biomarkers. *Lancet Infect Dis*. 2016;16(4):e34-46. doi: 10.1016/S1473-3099(16)00070-0. PubMed PMID: 27036358.
19. Dooley KE, Obuku EA, Durakovic N, Belitsky V, Mitnick C, Nuermberger EL, et al. World Health Organization group 5 drugs for the treatment of drug-resistant tuberculosis: unclear efficacy or untapped potential? *J Infect Dis*. 2013;207(9):1352-8. doi: 10.1093/infdis/jis460. PubMed PMID: 22807518; PubMed Central PMCID: PMC3693592.
20. Almeida Da Silva PE, Palomino JC. Molecular basis and mechanisms of drug resistance in *Mycobacterium tuberculosis*: classical and new drugs. *J Antimicrob Chemother*. 2011;66(7):1417-30. doi: 10.1093/jac/dkr173. PubMed PMID: 21558086.
21. Hugonnet JE, Tremblay LW, Boshoff HI, Barry CE, 3rd, Blanchard JS. Meropenem-clavulanate is effective against extensively drug-resistant *Mycobacterium tuberculosis*. *Science*. 2009;323(5918):1215-8. doi: 10.1126/science.1167498. PubMed PMID: 19251630; PubMed Central PMCID: PMC2679150.
22. England K, Boshoff HI, Arora K, Weiner D, Dayao E, Schimel D, et al. Meropenem-clavulanic acid shows activity against *Mycobacterium tuberculosis* in vivo. *Antimicrob Agents Chemother*. 2012;56(6):3384-7. doi: 10.1128/AAC.05690-11. PubMed PMID: 22450968; PubMed Central PMCID: PMC3370771.
23. Diacon AH, van der Merwe L, Barnard M, von Groote-Bidingmaier F, Lange C, Garcia-Basteiro AL, et al. beta-Lactams against Tuberculosis--New Trick for an Old Dog? *N Engl J Med*. 2016;375(4):393-4. doi: 10.1056/NEJMc1513236. PubMed PMID: 27433841.
24. Rogers SA, Melander C. Construction and screening of a 2-aminoimidazole library identifies a small molecule capable of inhibiting and dispersing bacterial biofilms across order, class, and phylum. *Angew Chem Int Ed Engl*. 2008;47(28):5229-31. doi: 10.1002/anie.200800862. PubMed PMID: 18528836.

25. Franzblau SG, Witzig RS, McLaughlin JC, Torres P, Madico G, Hernandez A, et al. Rapid, low-technology MIC determination with clinical *Mycobacterium tuberculosis* isolates by using the microplate Alamar Blue assay. *J Clin Microbiol.* 1998;36(2):362-6. PubMed PMID: 9466742; PubMed Central PMCID: PMCPMC104543.
26. Page B, Page M, Noel C. A new fluorometric assay for cytotoxicity measurements in-vitro. *Int J Oncol.* 1993;3(3):473-6. PubMed PMID: 21573387.
27. Rustad TR, Roberts DM, Liao RP, Sherman DR. Isolation of mycobacterial RNA. *Methods Mol Biol.* 2009;465:13-21. doi: 10.1007/978-1-59745-207-6\_2. PubMed PMID: 20560069.
28. Johnson BK, Scholz MB, Teal TK, Abramovitch RB. SPARTA: Simple Program for Automated reference-based bacterial RNA-seq Transcriptome Analysis. *BMC Bioinformatics.* 2016;17:66. doi: 10.1186/s12859-016-0923-y. PubMed PMID: 26847232; PubMed Central PMCID: PMCPMC4743240.
29. Bolger AM, Lohse M, Usadel B. Trimmomatic: a flexible trimmer for Illumina sequence data. *Bioinformatics.* 2014;30(15):2114-20. doi: 10.1093/bioinformatics/btu170. PubMed PMID: 24695404; PubMed Central PMCID: PMCPMC4103590.
30. Langmead B, Trapnell C, Pop M, Salzberg SL. Ultrafast and memory-efficient alignment of short DNA sequences to the human genome. *Genome Biol.* 2009;10(3):R25. doi: 10.1186/gb-2009-10-3-r25. PubMed PMID: 19261174; PubMed Central PMCID: PMCPMC2690996.
31. Anders S, Pyl PT, Huber W. HTSeq--a Python framework to work with high-throughput sequencing data. *Bioinformatics.* 2015;31(2):166-9. doi: 10.1093/bioinformatics/btu638. PubMed PMID: 25260700; PubMed Central PMCID: PMCPMC4287950.
32. Garcia-Alcalde F, Okonechnikov K, Carbonell J, Cruz LM, Gotz S, Tarazona S, et al. Qualimap: evaluating next-generation sequencing alignment data. *Bioinformatics.* 2012;28(20):2678-9. doi: 10.1093/bioinformatics/bts503. PubMed PMID: 22914218.
33. Li H, Handsaker B, Wysoker A, Fennell T, Ruan J, Homer N, et al. The Sequence Alignment/Map format and SAMtools. *Bioinformatics.* 2009;25(16):2078-9. doi: 10.1093/bioinformatics/btp352. PubMed PMID: 19505943; PubMed Central PMCID: PMCPMC2723002.
34. Robinson MD, Oshlack A. A scaling normalization method for differential expression analysis of RNA-seq data. *Genome Biol.* 2010;11(3):R25. doi: 10.1186/gb-2010-11-3-r25. PubMed PMID: 20196867; PubMed Central PMCID: PMCPMC2864565.
35. Robinson MD, McCarthy DJ, Smyth GK. edgeR: a Bioconductor package for differential expression analysis of digital gene expression data. *Bioinformatics.* 2010;26(1):139-40. doi: 10.1093/bioinformatics/btp616. PubMed PMID: 19910308; PubMed Central PMCID: PMCPMC2796818.
36. Robinson MD, Smyth GK. Small-sample estimation of negative binomial dispersion, with applications to SAGE data. *Biostatistics.* 2008;9(2):321-32. doi: 10.1093/biostatistics/kxm030. PubMed PMID: 17728317.

37. Veyrier F, Said-Salim B, Behr MA. Evolution of the mycobacterial SigK regulon. *J Bacteriol.* 2008;190(6):1891-9. doi: 10.1128/JB.01452-07. PubMed PMID: 18203833; PubMed Central PMCID: PMCPMC2258859.
38. Griffin JE, Pandey AK, Gilmore SA, Mizrahi V, McKinney JD, Bertozzi CR, et al. Cholesterol catabolism by *Mycobacterium tuberculosis* requires transcriptional and metabolic adaptations. *Chem Biol.* 2012;19(2):218-27. doi: 10.1016/j.chembiol.2011.12.016. PubMed PMID: 22365605; PubMed Central PMCID: PMCPMC3292763.
39. Betts JC, McLaren A, Lennon MG, Kelly FM, Lukey PT, Blakemore SJ, et al. Signature gene expression profiles discriminate between isoniazid-, thiolactomycin-, and triclosan-treated *Mycobacterium tuberculosis*. *Antimicrob Agents Chemother.* 2003;47(9):2903-13. PubMed PMID: 12936993; PubMed Central PMCID: PMCPMC182614.
40. Converse SE, Mougous JD, Leavell MD, Leary JA, Bertozzi CR, Cox JS. MmpL8 is required for sulfolipid-1 biosynthesis and *Mycobacterium tuberculosis* virulence. *Proc Natl Acad Sci U S A.* 2003;100(10):6121-6. doi: 10.1073/pnas.1030024100. PubMed PMID: 12724526; PubMed Central PMCID: PMCPMC156336.
41. Belardinelli JM, Larrouy-Maumus G, Jones V, Sorio de Carvalho LP, McNeil MR, Jackson M. Biosynthesis and translocation of unsulfated acyltrehaloses in *Mycobacterium tuberculosis*. *J Biol Chem.* 2014;289(40):27952-65. doi: 10.1074/jbc.M114.581199. PubMed PMID: 25124040; PubMed Central PMCID: PMCPMC4183827.
42. Walters SB, Dubnau E, Kolesnikova I, Laval F, Daffe M, Smith I. The *Mycobacterium tuberculosis* PhoPR two-component system regulates genes essential for virulence and complex lipid biosynthesis. *Mol Microbiol.* 2006;60(2):312-30. doi: 10.1111/j.1365-2958.2006.05102.x. PubMed PMID: 16573683.
43. Drawz SM, Bonomo RA. Three decades of beta-lactamase inhibitors. *Clin Microbiol Rev.* 2010;23(1):160-201. doi: 10.1128/CMR.00037-09. PubMed PMID: 20065329; PubMed Central PMCID: PMCPMC2806661.
44. Payen MC, De Wit S, Martin C, Sergysels R, Muylle I, Van Laethem Y, et al. Clinical use of the meropenem-clavulanate combination for extensively drug-resistant tuberculosis. *Int J Tuberc Lung Dis.* 2012;16(4):558-60. doi: 10.5588/ijtld.11.0414. PubMed PMID: 22325421.
45. Brennan PJ. Structure, function, and biogenesis of the cell wall of *Mycobacterium tuberculosis*. *Tuberculosis (Edinb).* 2003;83(1-3):91-7. PubMed PMID: 12758196.
46. Dutta NK, Mehra S, Kaushal D. A *Mycobacterium tuberculosis* sigma factor network responds to cell-envelope damage by the promising anti-mycobacterial thioridazine. *PLoS One.* 2010;5(4):e10069. doi: 10.1371/journal.pone.0010069. PubMed PMID: 20386700; PubMed Central PMCID: PMCPMC2851646.
47. Hatzios SK, Baer CE, Rustad TR, Siegrist MS, Pang JM, Ortega C, et al. Osmosensory signaling in *Mycobacterium tuberculosis* mediated by a eukaryotic-like Ser/Thr protein kinase. *Proc Natl Acad Sci U S A.* 2013;110(52):E5069-77. doi: 10.1073/pnas.1321205110. PubMed PMID: 24309377; PubMed Central PMCID: PMCPMC3876250.

48. McMurry LM, Oethinger M, Levy SB. Triclosan targets lipid synthesis. *Nature*. 1998;394(6693):531-2. doi: 10.1038/28970. PubMed PMID: 9707111.
49. Gomez A, Andreu N, Ferrer-Navarro M, Yero D, Gibert I. Triclosan-induced genes Rv1686c-Rv1687c and Rv3161c are not involved in triclosan resistance in *Mycobacterium tuberculosis*. *Sci Rep*. 2016;6:26221. doi: 10.1038/srep26221. PubMed PMID: 27193696; PubMed Central PMCID: PMC4872132.
50. Takayama K, Wang C, Besra GS. Pathway to synthesis and processing of mycolic acids in *Mycobacterium tuberculosis*. *Clin Microbiol Rev*. 2005;18(1):81-101. doi: 10.1128/CMR.18.1.81-101.2005. PubMed PMID: 15653820; PubMed Central PMCID: PMC4872132.
51. Stanley SA, Kawate T, Iwase N, Shimizu M, Clatworthy AE, Kazyanskaya E, et al. Diarylcoumarins inhibit mycolic acid biosynthesis and kill *Mycobacterium tuberculosis* by targeting FadD32. *Proc Natl Acad Sci U S A*. 2013;110(28):11565-70. doi: 10.1073/pnas.1302114110. PubMed PMID: 23798446; PubMed Central PMCID: PMC3710825.
52. Boshoff HI, Myers TG, Copp BR, McNeil MR, Wilson MA, Barry CE, 3rd. The transcriptional responses of *Mycobacterium tuberculosis* to inhibitors of metabolism: novel insights into drug mechanisms of action. *J Biol Chem*. 2004;279(38):40174-84. doi: 10.1074/jbc.M406796200. PubMed PMID: 15247240.

## CHAPTER THREE

### **2-AI compounds reduce $\beta$ -lactamase secretion and increase cell envelope permeability of *M. tuberculosis***

In this chapter, we reveal the putative mechanism by which 2-AI compounds potentiate  $\beta$ -lactam antibiotics. Previously, it was shown by Dr. Melander's group that structurally similar 2-aminobenzimidazoles (2-AB) compounds sensitized mycobacteria to  $\beta$ -lactams, but had no effect on  $\beta$ -lactamase enzyme [1]. Thus, we evaluated if that observation holds true with 2-AI compounds against *M. tuberculosis* and report that 2-AI compounds suppress  $\beta$ -lactamase activity by reducing general protein secretion, and not by directly inhibiting  $\beta$ -lactamase enzyme. Furthermore, 2-AI compounds have been shown to alter the bacterial cell envelope and increase the permeability of the *M. tuberculosis* cell envelope to  $\beta$ -lactams is one of the major factors conferring *M. tuberculosis* intrinsic resistance to  $\beta$ -lactams [2-4]. The overall cell envelope permeability and the binding of antibiotics to the *M. tuberculosis* cell wall were evaluated. We obtained multiple lines of evidences of increased cell envelope permeability and thereby increased binding of  $\beta$ -lactam antibiotic and other cell wall targeting drug.

#### **3.1. Introduction**

It has long been known that *M. tuberculosis* is intrinsically resistant to  $\beta$ -lactam antibiotics [5]. The inherent resistance of *M. tuberculosis* to  $\beta$ -lactams is mainly attributed to two mechanisms: a) inactivation of the antibiotics by *blaC* encoded  $\beta$ -lactamase and b) low permeability of the mycobacteria cell envelope limiting the diffusion of antibiotics such as  $\beta$ -lactams [4, 6-10]. First, the contribution of a class A  $\beta$ -lactamase produced by *M. tuberculosis* to  $\beta$ -lactam resistance has been demonstrated through both deletion of *blaC* gene which led to significantly increased susceptibility [9] and combination with  $\beta$ -lactamase inhibitor [11].

As occurs in Gram-negative bacteria, mycobacteria have an outer cell membrane [12-14], a major permeability barrier against  $\beta$ -lactams targeting PBPs that reside in the periplasmic compartment [15].

The inner leaflet of the mycobacterial outer membrane is composed of mycolic acids, long fatty acids approximately 90 carbons in length, that are covalently bound to arabinogalactan and tightly packed together effectively blocking the diffusion of hydrophilic molecules. The outer leaflet of the *M. tuberculosis* outer membrane is enriched with non-covalently bound lipids such as TDM and PDIMs [12, 16]. Together, this outer membrane serves as a low fluidity and low permeability barrier to antibiotics.

This study investigated the mechanisms by which 2-AI compounds work to potentiate  $\beta$ -lactams. It was hypothesized that 2-AI compounds would interfere with several mechanisms conferring *M. tuberculosis* intrinsic  $\beta$ -lactam resistance. Herein it is reported that 2-AI compounds reduce *M. tuberculosis*  $\beta$ -lactamase activity by altering secretion of the enzyme rather than by directly inhibiting the enzymatic activity as in the case of classic  $\beta$ -lactamase inhibitors such as clavulanic acid. Mechanistic studies revealed that 2-AI treatment alters *M. tuberculosis* cell envelope composition, leading to increased permeability and accessibility of external agents and drugs targeting the cell wall biosynthesis. Taken together, results indicate that 2-AI compounds abolish at least two of the major defense mechanism of *M. tuberculosis* against  $\beta$ -lactams and suggest a possible unifying mechanism of altered bioenergetics.

## **3.2. Materials and Methods**

### **3.2.1. Bacterial strains, media and culture conditions**

For experiments using the BSL2 strain, *M. tuberculosis* H37Rv mc<sup>2</sup> 6206, bacteria was grown in 7H9 media supplemented with OADC, 0.2% casamino acid (BD, USA), 0.05% tyloxapol, 0.005% L-leucine, 0.0048% D-pantothenic acid, and 0.0025% kanamycin (Sigma-Aldrich, USA). *M. tuberculosis* H37Rv mc<sup>2</sup> 6206 was a kind gift from Dr. William R. Jacobs Jr. at Albert Einstein College of Medicine [17].

### **3.2.2. Collection of *M. tuberculosis* culture filtrate proteins (CFP)**

To obtain *M. tuberculosis* H37Rv CFP, it was grown to an OD<sub>600</sub> of 0.4 to 0.6 in glycerol-alanine-salts (GAS) media containing 0.03% Bacto Casitone (Difco, Franklin Lakes, NJ, USA), 0.005% ferric

ammonium citrate (Sigma-Aldrich, USA), 0.4% dibasic potassium phosphate, 0.2% citric acid, 0.1% L-alanine, 0.12% magnesium chloride hexahydrate, 0.06% potassium sulfate, 0.2% ammonium chloride, 0.18% sodium hydroxide, and 1% glycerol (all purchased from Sigma-Aldrich, USA). Subsequently, cultures were centrifuged ( $\times 1,700g$ ) for 10 min and supernatants were harvested. Collected supernatant was filtered through a 0.45  $\mu$ m syringe filter (Millipore, USA) to obtain CFP. Total protein concentration present in CFP was determined using the BCA assay (Pierce, Waltham, MA, USA) following the manufacturer's instruction. CFP was also obtained from 2-AI compounds treated *M. tuberculosis*. Briefly, after the initial culture in GAS media, cells were washed twice with sterile PBS and reconstituted in GAS media to an OD<sub>600</sub> of 0.4. Cultures were treated with 2-AI compounds (RA11 or 2B8) or clavulanate (8 mg/L) and incubated at 37<sup>0</sup>C for 24 h and CFP was harvested as described above.

### **3.2.3. $\beta$ -lactamase activity assay**

$\beta$ -lactamase activity was evaluated with the colorimetric kit from Biovision (Milpitas, CA, USA). Briefly, a total of 50  $\mu$ L samples were transferred to a 96-well cell flat-bottomed culture plate and nitrocefin included in the kit was added to a final concentration of 20  $\mu$ M. Immediately following the addition of nitrocefin to samples, absorbance at 490 nm was monitored every five min for 2 h at 37<sup>0</sup>C using a Synergy 2 multi-mode plate reader (BioTek, Winooski, VT, USA) to obtain a nitrocefin hydrolysis curve. A standard curve was derived from known amounts of hydrolyzed nitrocefin provided in the assay kit. Total nitrocefin hydrolyzed (nM) per min was calculated from a standard curve. Data were normalized to CFUs or nM nitrocefin hydrolyzed/min/mg of protein.

### **3.2.4. Preparation and analysis of *M. tuberculosis* cell envelope lipids**

*M. tuberculosis* H37Rv mc<sup>2</sup> 6206 BSL2 strain was grown to an OD<sub>600</sub> of 0.4. Cultures were treated with 2-AI compounds (RA11 or 2B8) at 2.5, 12.5 and 62.5  $\mu$ M for 24 h in the presence of 0.5  $\mu$ Ci of [1,2-<sup>14</sup>C] acetic acid (113 Ci/mol) and [1-<sup>14</sup>C] propionate (56.7 Ci/mol, MP Biomedicals, Santa Ana, CA, USA). Extractions and preparation of total lipids and cell-bound mycolic acids followed earlier

procedures [18]. In brief, cultures were centrifuged ( $\times 1,700g$ ) for 10 min, washed twice in sterile PBS. Cell pellets were subjected to chloroform:methanol (1:2, v/v, Sigma-Aldrich, USA) extraction in a tube spinner for 24 h at room temperature. Tubes were then centrifuged ( $\times 1,700g$ ) for 10 min to spin down cell pellets and supernatants were decanted into new tubes and dried under nitrogen gas. Remaining cell pellets were further extracted two more times with chloroform:methanol (1:1 then 2:1). All extractions were pooled and dried under nitrogen and reconstituted in chloroform:methanol (1:1). For recover of cell wall associated fatty acyl-, mycolic acyl-methylesters, bacterial pellets remaining after organic extractions were saponified in 15% tetrabutylammonium hydroxide (Sigma-Aldrich, USA) at  $100^{\circ}C$  overnight. Thereafter, water/dichloromethane/iodomethane (2:3:0.3, v/v/v, Sigma-Aldrich, USA) was added and incubated at room temperature for 4 h. After centrifugation ( $\times 1,700g$ ), the aqueous phase was discarded while the organic phase was dried under nitrogen. The dried material was resuspended in 4 mL of diethyl ether (Sigma-Aldrich, USA) and sonicated for five min. After drying with nitrogen, extracted methylesters were reconstituted in dichloromethane. Total radioactivity counts were measured for all samples before being analyzed by thin layer chromatography (TLC) on a silica gel 60-precoated plate F254 (Merck, Kenilworth, NJ, USA) in various solvent systems. For visualization of radiolabeled lipids, silica gel plates were scanned with Typhoon Trio Imager (GE Healthcare, Little Chalfont, UK) for autoradiogram. Densitometry analysis was performed using ImageQuant TL 8.1 (GE Healthcare, UK).

### **3.2.5. SDS sensitivity assay**

*M. tuberculosis* H37Rv was grown to an  $OD_{600}$  of 0.4 to 0.6 in 7H9 media with OADC supplement and 0.05% Tween 80, then treated with  $125 \mu M$  2B8 for 24 h. After treatment, bacterial pellets were washed twice with sterile PBS and reconstituted with PBS to an  $OD_{600}$  of 0.1. Sodium dodecyl sulfate (SDS, Cayman Chemical, Ann Arbor, MI, USA) was added to the cultures to achieve a final concentration of 0.005 and 0.05%. Cultures were plated on 7H11 agar plates at 0, 1, 2, 3 and 4 h post addition of SDS. After three or four weeks of incubation at  $37^{\circ}C$ , CFUs were enumerated and percent survival through 4 h was calculated for each sample and compared to starting CFUs at 0 h time-point.

### 3.2.6. Dye accumulation assays

*M. tuberculosis* H37Rv was grown to an OD<sub>600</sub> of 0.4 to 0.6 in 7H9 media supplemented with OADC and 0.05% Tween 80 and used for an ethidium bromide (EtBr) or Sytox Orange uptake assay as previously described [19, 20]. Briefly, cultures were dispensed in opaque-walled 96-well flat-bottomed cell culture plates (Corning, Corning, NY, USA) and pre-energized with 0.4% glucose (Sigma-Aldrich, USA) for five min. Thereafter, 2-AI compounds (RA11 or 2B8, 125 μM), reserpine (100 mg/L) or TRZ (80 μM) (Sigma-Aldrich, USA) were added, followed by EtBr (Sigma-Aldrich, USA) and Sytox Orange (Invitrogen, USA) to a final concentration of 10 μM and 100 nM, respectively. For both fluorescent dyes, relative fluorescence units (RFUs) were monitored every two minutes by 530<sub>ex</sub> nm/590<sub>em</sub> nm filter using Synergy 2 multi-mode plate reader for 90 min.

### 3.2.7. Evaluation of cell envelope permeability and cell membrane integrity using BOCILLIN<sup>®</sup>, BODIPY<sup>®</sup> FL vancomycin and propidium iodide

*M. tuberculosis* H37Rv was grown to an OD<sub>600</sub> of 0.4 to 0.6 in 7H9 media supplemented with OADC and 0.05% Tween 80, then diluted to OD<sub>600</sub> of 0.1 in the same media prior to use. Diluted cultures were treated with 62.5 and 125 μM 2-AI compounds (RA11 or 2B8), SDS 0.05% or 20 μM meropenem with 100 μM clavulanate (MCA) [21]. After treating for 30 min, 120 min, or 24 h at 37<sup>0</sup>C while shaking, cultures were aliquoted into 5 mL polystyrene tubes and stained with 1 mg/L BODIPY<sup>®</sup> FL vancomycin, 10 mg/L BODIPY<sup>®</sup>-tagged penicillin V (BOCILLIN<sup>®</sup>) or 15 μM propidium iodide (PI) (Life Technologies, Carlsbad, CA, USA), for 30 min at 37<sup>0</sup>C in the dark. Cells were pelleted by centrifuging (×1,700g) for 5 min to remove remaining free dye and washed with sterile PBS two times (PI stained samples were not washed, but directly fixed as described below after removing the supernatant). After these washes, PBS was removed and cell pellets were fixed with 4% paraformaldehyde (VWR, Radnor, PA, USA) in PBS for 15 min. After fixation, bacterial cells were analyzed by flow cytometry using an LSRII flow cytometer (BD, USA). The cytometer was adjusted as follows: Forward scatter (FSC) and

side scatter (SSC) were set to logarithmic scale, threshold was set at 2000 FSC and SSC, acquisition was set to low (< 1000 events/sec) and 10,000 to 50,000 events were collected for each sample. Fluorescence of BODIPY<sup>®</sup>-labeled antibiotics and PI was excited with the 488 nm blue laser and emission detected with the 530/30 nm and 610LP filters, respectively. Data were analyzed using Kaluza 1.3 software (Beckman Coulter, Brea, CA, USA). For competitive inhibition of BODIPY<sup>®</sup> FL vancomycin binding to *M. tuberculosis*, unlabeled vancomycin (Gold Biotechnology, USA) at 50×, 100×, and 500× the amount of BODIPY<sup>®</sup> FL vancomycin (1 mg/L), was added to 2B8 treated samples prior to the addition of BODIPY<sup>®</sup> FL vancomycin. Fixed BODIPY<sup>®</sup> FL vancomycin stained bacteria were also analyzed under a microscope equipped with X-cite 120 fluorescence illuminator (Excelitas Technologies, Waltham, MA, USA).

### **3.2.8. Statistical analysis**

Statistical analyses were done as described in Chapter 2.

## **3.3. Results**

### **3.3.1. 2-AI treated *M. tuberculosis* cultures have reduced $\beta$ -lactamase activity**

An important factor contributing to *M. tuberculosis* intrinsic  $\beta$ -lactam resistance is the synthesis and secretion of  $\beta$ -lactamase [9, 22, 23]. Indeed, the combination of a  $\beta$ -lactamase inhibitor such as clavulanate with meropenem has been demonstrated to be effective against MDR strains of *M. tuberculosis* [21, 24]. Thus, the possibility that 2-AI compounds potentiate  $\beta$ -lactams by reducing  $\beta$ -lactamase activity was investigated. To evaluate whether the compounds have a direct effect on the enzyme's activity, 2-AI compounds were added to either purified *Bacillus cereus*  $\beta$ -lactamase or *M. tuberculosis* CFP, a rich source of mycobacterial specific  $\beta$ -lactamase [25], and the enzymatic activity was evaluated using the nitrocefin hydrolysis assay. Under these experimental conditions, 2-AI compounds did not directly inhibit  $\beta$ -lactamase activity (Figure 3.1A and 3.1B). As expected, however, clavulanate efficiently inhibited  $\beta$ -lactamase activity from *M. tuberculosis* CFP (Figure 3.1B).

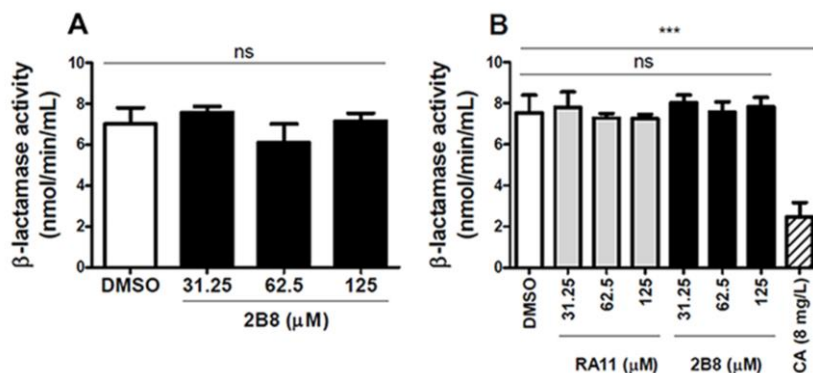


**Figure 3.1.  $\beta$ -lactamase is not directly inhibited by 2-AI compounds.** A) Purified  $\beta$ -lactamase enzyme from *B. cereus* was monitored for nitrocefin hydrolysis activity in the presence of 2B8. Presence of 2B8 did not have any effect in  $\beta$ -lactamase activity. B) Isolated CFP from *M. tuberculosis* H37Rv was monitored for nitrocefin hydrolysis activity in the presence of 2-AI compounds and clavulanate (CA, 8 mg/L). Clavulanate decreased  $\beta$ -lactamase activity significantly, but 2-AI compounds had no effect on  $\beta$ -lactamase activity in CFP. Experiments were carried out two separate times in duplicate and representative data are shown. Control: DMSO treated cells. \*\*\* $p < 0.001$  by ANOVA.

Alternatively,  $\beta$ -lactamase activity was measured in CFP obtained from 2-AI treated *M. tuberculosis* cultures. *M. tuberculosis* cultures treated with RA11 or 2B8 resulted in a dose-dependent decrease in  $\beta$ -lactamase activity after normalization of the data to the number of viable CFUs (Figure 3.2A). Consistent with results obtained from the assays described above, 2B8 more effectively reduced  $\beta$ -lactamase activity than RA11. Reduced  $\beta$ -lactamase activity in 2-AI treated cultures correlated with a lower protein concentration present in the CFP of these cultures (Figure 3.2B). In fact, no differences were observed between control and 2-AI treated cultures when  $\beta$ -lactamase activity was normalized to protein concentration (Figure 3.2C). Clavulanate treatment also effectively decreased  $\beta$ -lactamase activity when data were normalized to viable CFUs (Figure 3.2A), but did not have any effect in overall protein concentration in the CFP (Figure 3.2B). Therefore, clavulanate treatment still decreased  $\beta$ -lactamase activity in the sample even when the data were normalized by total protein concentration (Figure 3.2C).

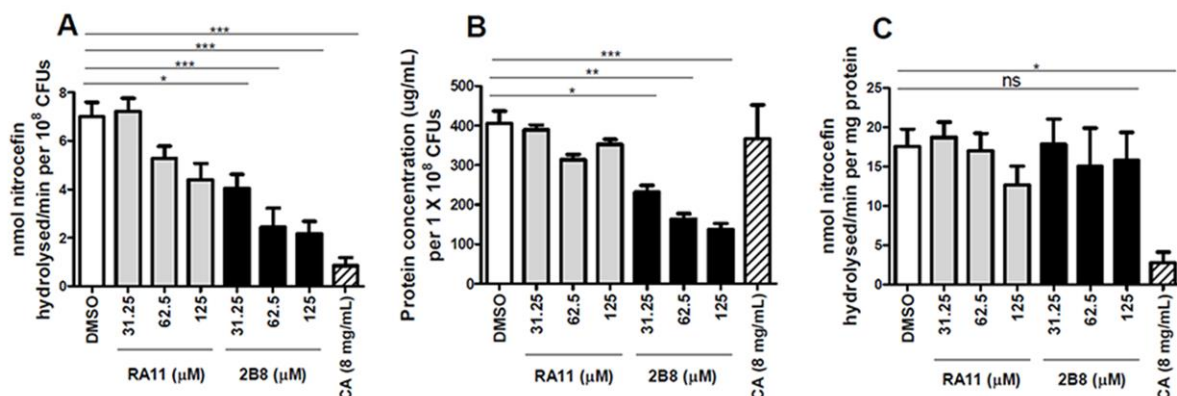
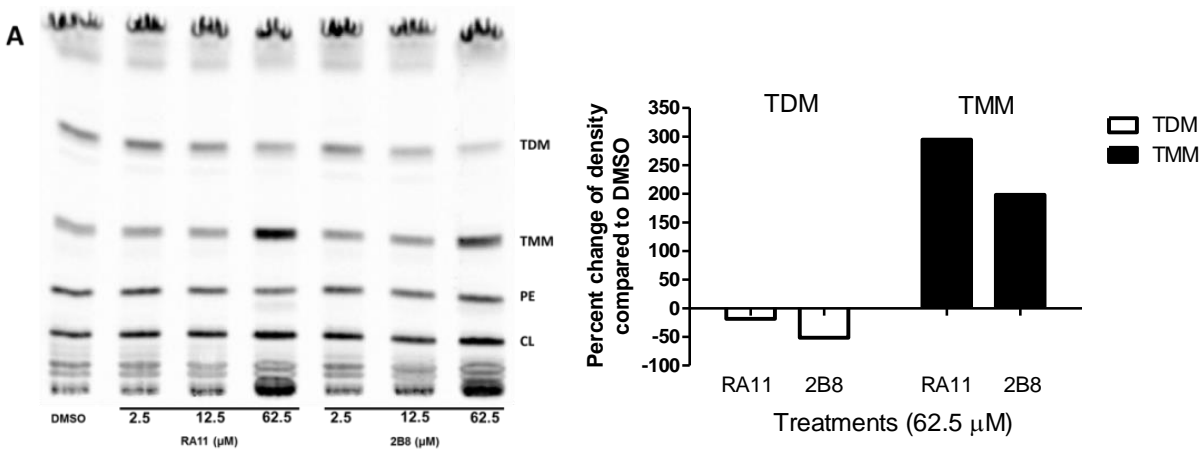


**Figure 3.2. Reduced  $\beta$ -lactamase activity in 2-AI treated *M. tuberculosis* CFP resulting from lower protein secretion.** A)  $\beta$ -lactamase activity in the CFP of *M. tuberculosis* H37Rv cultures after 24 h treatment with 2-AI compounds. Total nitrocefin hydrolysis activity was normalized to viable bacteria at the time of the assay. Compared to DMSO control, 2B8 (31.25 to 125  $\mu$ M) treated samples showed significantly decreased  $\beta$ -lactamase activity. In contrast, RA11 did not significantly decrease  $\beta$ -lactamase activity at any of the tested concentrations. B) Total protein concentration in CFP tested for  $\beta$ -lactamase activity (panel A), normalized to viable bacterial number. Significantly less protein concentration was observed in samples treated with 2B8 (31.25 to 125  $\mu$ M). Protein concentration in the CFP was not affected by clavulanate (CA, 8 mg/L) treatment. C)  $\beta$ -lactamase activity normalized to total protein concentration in the CFP. Except for clavulanate, treatment with 2B8 or RA11 did not reduce  $\beta$ -lactamase activity in the CFP when normalized to protein concentration. This suggests the reduced  $\beta$ -lactamase activity observed in panel A, was attributed to lower protein concentration in the CFP. \* $p < 0.05$ , \*\* $p < 0.01$ , \*\*\* $p < 0.001$  by ANOVA. Experiments were carried out three separate times in triplicate and representative data are shown.

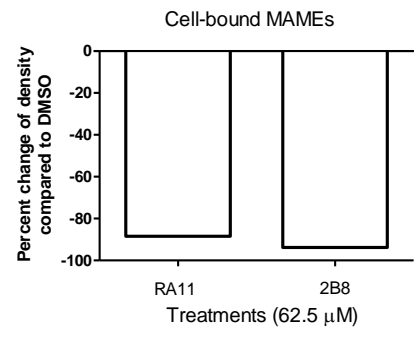
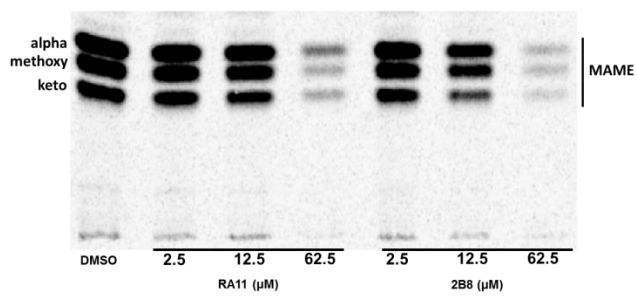
### 3.3.2. 2-AI treatment alters *M. tuberculosis* cell envelope lipid composition

Intrinsic resistance of mycobacteria to  $\beta$ -lactams has also been attributed to several unique features including the low permeability of the lipid rich cell envelope [26]. It was posited that 2-AI treatment could increase the susceptibility to  $\beta$ -lactams by altering the mycobacterial cell envelope composition and increasing permeability to this class of antibiotics. To investigate if 2-AI compounds impair mycobacterial cell envelope lipid synthesis or composition, metabolic labeling of mycobacterial lipids was performed with radiolabeled acetate or propionate and relative lipid abundance analyzed by TLC and autoradiogram.

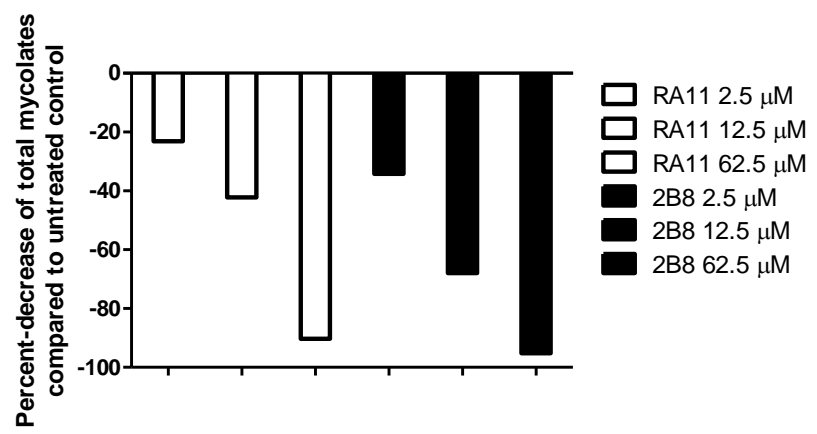
After 24 h of 2-AI treatment, total radioactive counts from treated samples showed a dose-dependent decrease, implying reduced biosynthesis of cell envelope extractable lipids (data not shown). Thus, TLC loading was normalized to total radioactive count so that every sample would have equal amounts of labeled total lipids. From TLC analysis of  $^{14}\text{C}$  acetate labelled extractable lipids (Figure 3.3A and 3.4), it was observed that 2-AI treatment led to decreased TDM biosynthesis while accumulating its precursor TMM. Also, significantly less mycolic acid methyl esters (MAMEs) were extracted from 2-AI treated samples (Figure 3.3B and 3.4). Consistent with the MIC assay results, 2B8 treatment exhibited superior potentiation than RA11 treatment. Importantly, the biosynthesis of total mycolic acids (determined as the sum of MAMEs from cell-bound and extractable lipids) was reduced in 2-AI treated bacilli (Figure 3.3C) as well as free mycolic acids (Figure 3.5). In the TLC analysis of  $^{14}\text{C}$  propionate labelled extractable lipids, a significant decrease in SL-1 and PAT biosynthesis in 2B8 treated cultures was observed (Figure 3.3D). However, DAT, a precursor of PAT, accumulated with 2B8 treatment. Again, 2B8 treatment more pronouncedly affected  $^{14}\text{C}$  propionate labelled lipids than RA11.



**B**



**C**



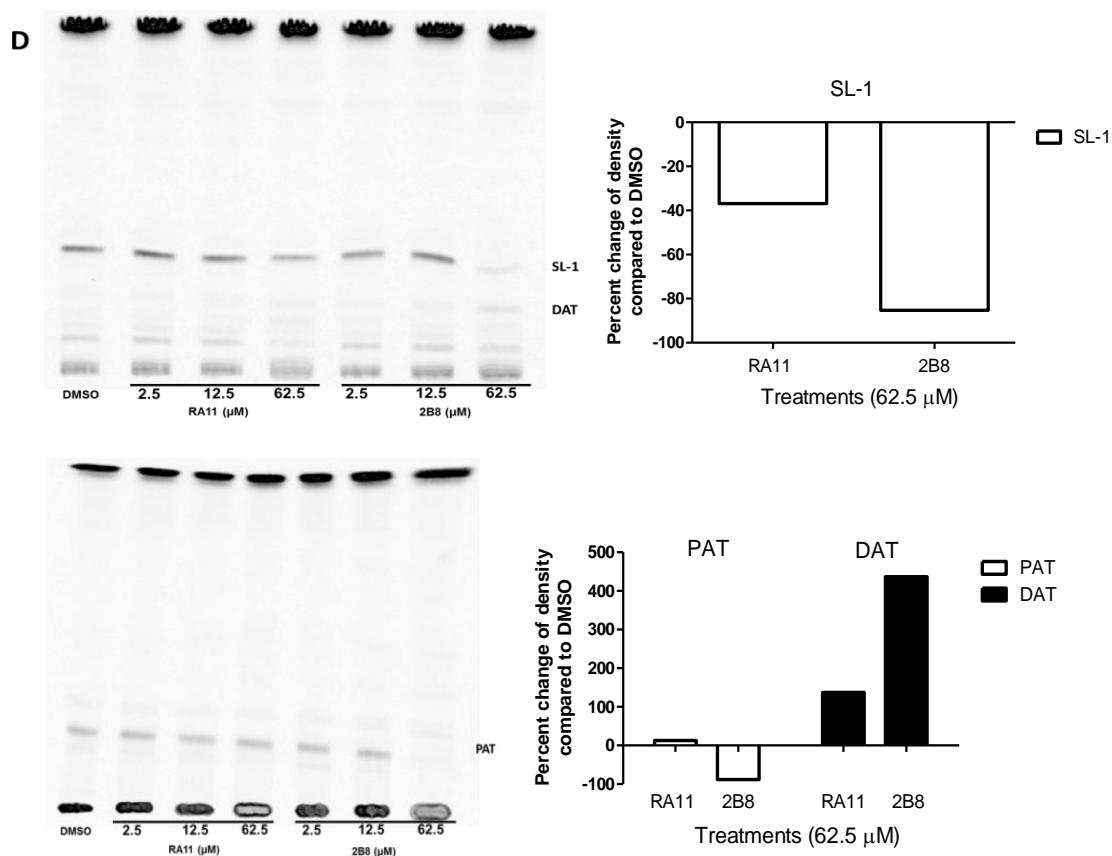


**Figure 3.3. 2-AI treatment alters cell envelope lipid composition of *M. tuberculosis*.** Radioactive metabolic labeling was performed on *M. tuberculosis* treated with increasing concentrations of 2-AI compounds (2.5, 12.5, and 62.5 μM) for 24 h. TLCs (left) of a representative experiment are shown with quantified comparison between specific bands as measured by densitometry (right). A) TLC of extractable lipids derived from [ $1\text{-}^{14}\text{C}$ ] acetate-labeled *M. tuberculosis* H37Rv mc<sup>2</sup> 6020 strain is shown. For visualization of TDM, TMM, PE and CL (A), a total of 10,000 cpm was loaded per lane and TLCs were developed in chloroform/methanol/water (20:4:0.5, v/v/v). Treatment with 2-AI compounds resulted in reduced levels of TDM, but increased TMM, as confirmed by densitometry analysis (right). B) TLC of cell wall associated mycolates is shown (Left panel). For visualization of MAMEs in cell-bound lipids, hexane/ethyl acetate (95:5, v/v, three developments) solvent system was used and samples were loaded volume to volume. Densitometry analysis confirmed significant reduction of MAMEs in 2-AI treated samples (Right panel). C) Samples treated with 2-AI showed reduced levels of total mycolate biosynthesis (sum of MAMEs from cell-bound, B, and extractable lipids, Figure S3). D) TLCs of extractable cell envelope lipids derived from [ $1\text{-}^{14}\text{C}$ ] propionate-labeled cultures are shown. TLCs were developed in chloroform/methanol/water (90:10:1, v/v/v) for visualization of SL-1 and DAT, and petroleum ether/acetone (92:8, v/v) for visualization of PAT. Treatment with 2-AI compounds reduced the amount of SL-1 and PAT, but increased DAT. Experiments were carried out three separate times and representative data are shown. PE: phosphatidylethanolamine, CL: cardiolipin.

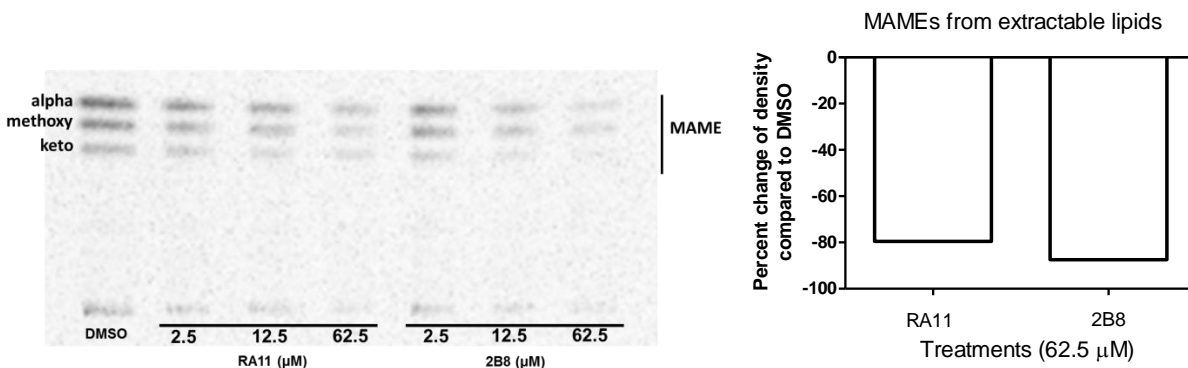


**Figure 3.4. 2-AI treatment reduces MAMEs from extractable lipids in *M. tuberculosis*.** Radioactive metabolic labeling was performed on *M. tuberculosis* treated with increasing concentrations of 2-AI compounds (2.5, 12.5, and 62.5 μM) for 24 h. MAMEs were derived from extractable lipids of [<sup>14</sup>C] acetate-labeled *M. tuberculosis* H37Rv mc<sup>2</sup> 6206 strain and analyzed by TLC as described in Figure 5B. Treatment with 2-AI compounds resulted in reduced MAMEs from extractable lipids. Experiments were carried out three separate times and representative data are shown.

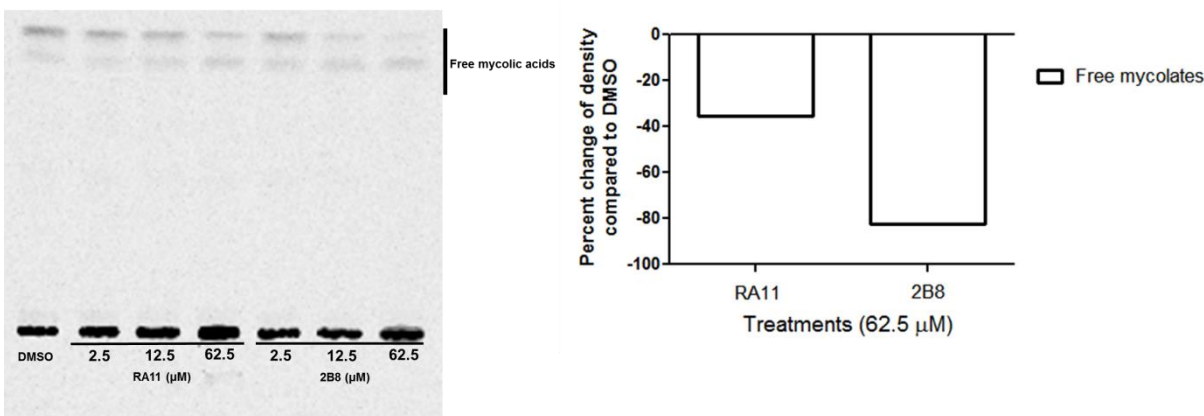


**Figure 3.5. 2-AI treatment reduces free mycolic acids in *M. tuberculosis*.** Radioactive metabolic labeling was performed on *M. tuberculosis* treated with increasing concentrations of 2-AI compounds (2.5, 12.5, and 62.5 μM) for 24 h. Using hexane/ethyl acetate (95:5, v/v, three developments) solvent system, extractable lipids of [<sup>14</sup>C] acetate-labeled *M. tuberculosis* H37Rv mc<sup>2</sup> 6206 strain were loaded count to count. Experiments were carried out three separate times and representative data are shown.

### 3.3.3. 2-AI treated *M. tuberculosis* becomes hypersensitive to SDS

The lipid rich cell envelope of *M. tuberculosis* is known to serve as an impermeable barrier to various chemicals and antibiotics [10]. Based on the alteration in cell envelope lipid composition after 2-

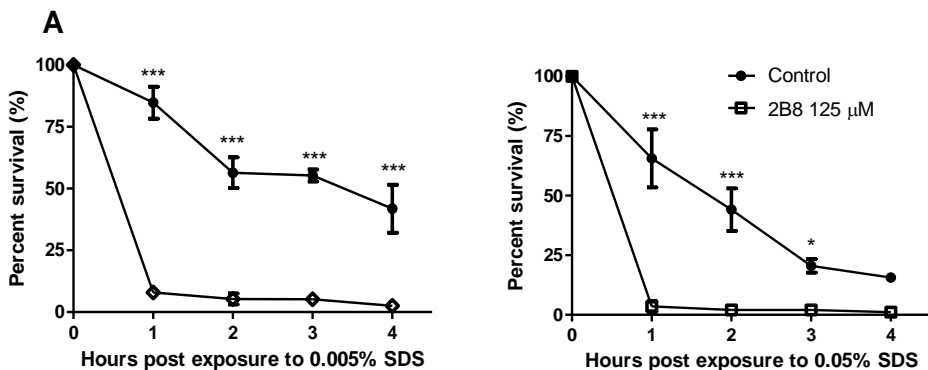
AI treatment, it was hypothesized that 2-AI treated *M. tuberculosis* would become hypersensitive to membrane-targeting agents such as detergents like SDS. After 24 h treatment with 125  $\mu$ M 2B8, *M. tuberculosis* cultures were exposed to 0.005% or 0.05% SDS. Following SDS exposure, CFUs were enumerated every hour for 4 h. As shown in Figure 6A, significant survival differences were observed between non-treated and 2B8-treated cultures exposed to 0.005% SDS (left panel). The viability of 2B8 treated cultures exposed to SDS dropped much more rapidly and to a greater extent than non-treated cultures. As expected, when exposed to SDS at 0.05%, the viability of all the samples declined throughout the course of exposure. However, the decline was more rapid and pronounced in 2B8 treated *M. tuberculosis* cultures (Figure 3.6A, right panel).

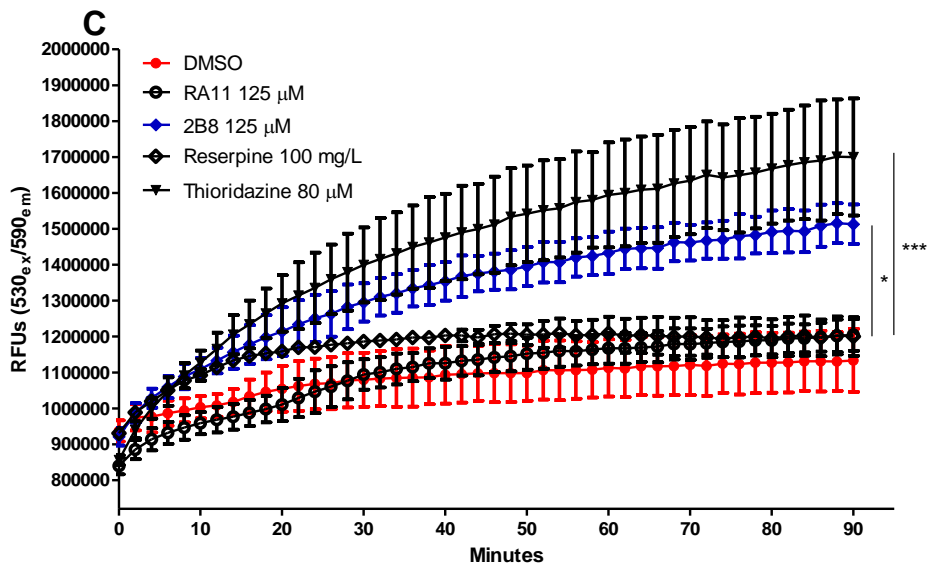
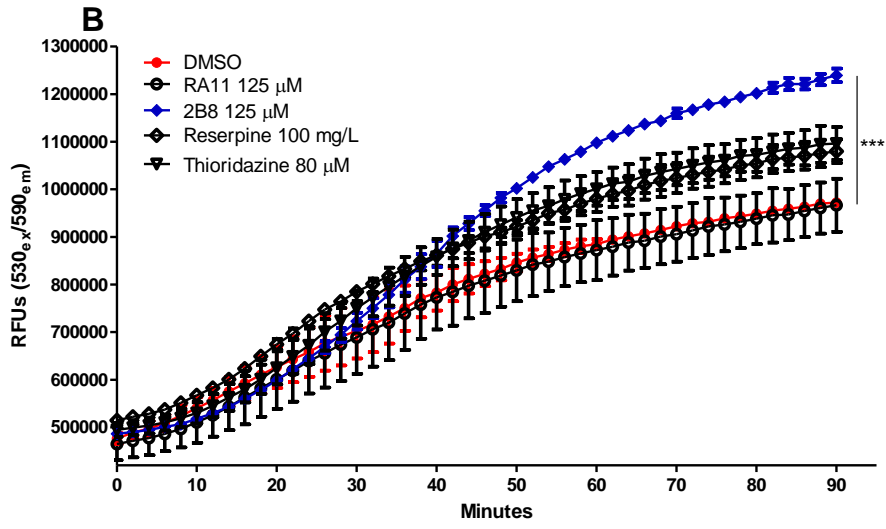
#### **3.3.4. 2-AI treatment increased *M. tuberculosis* permeability to nucleic acid staining dyes**

Accumulation of nucleic acid staining dyes such as EtBr and Sytox Orange have been used to evaluate the *M. tuberculosis* cell envelope permeability to external agents [19, 20, 27]. Based on the altered cell envelope lipid composition and increased sensitivity to SDS, it was hypothesized that 2-AI treatment would increase *M. tuberculosis* permeability to these dyes as well. EtBr or Sytox Orange was applied simultaneously with 2-AI compounds, and the kinetics of fluorescence signal due to dye accumulation was monitored over time.

*M. tuberculosis* treatment with 125  $\mu$ M 2B8 resulted in a time-dependent increase in EtBr fluorescent signal that was significantly higher than untreated control (Figure 3.6B). This increase was not seen in RA11 treated cultures. Net dye accumulation determined upon completion of the assay was also significantly higher in 2B8 treated cultures (Figure 3.7A). Reserpine, an inhibitor of the EtBr efflux pump [28], also increased EtBr accumulation within *M. tuberculosis*, however it was not statistically significant (Figure 3.6B). The same trend was observed using Sytox Orange, as both the time-dependent increase and net dye accumulation were significantly elevated in 2B8, but not in RA11 treated cultures (Figure 3.6C and Figure 3.7B). In agreement with a recent report [20], TRZ (an additional positive control) also increased Sytox Orange accumulation (Figure 3.6C).

Flow cytometry was performed to further evaluate the permeability of 2-AI treated *M. tuberculosis* to a third nucleic acid staining dye, PI. Despite sharing a similar chemical structure, PI is a better indicator of plasma membrane integrity than EtBr, due to its additional positive group [29]. In contrast to the above results with EtBr (Figure 3.6B) and Sytox Orange (Figure 3.6C), *M. tuberculosis* treatment with 2-AI compounds did not acutely increase permeability to PI when evaluated at 30 min and 120 min post-exposure (Figure 3.6D and 3.9D). However, approximately 30% of *M. tuberculosis* became permeable to PI, a classical marker of cell death, upon prolonged exposure to 2B8 for 24 h. Again, *M. tuberculosis* membrane disruption was greater for 2B8 than RA11 (Figure 3.6D). Finally, the two positive controls, SDS and MCA, showed potent *M. tuberculosis* cell membrane disrupting capacity, albeit with different kinetics. As expected, a detergent like SDS acutely lysed bacteria within 30 min (Figure 3.6D), while the effect of MCA only became significant after 24 h.





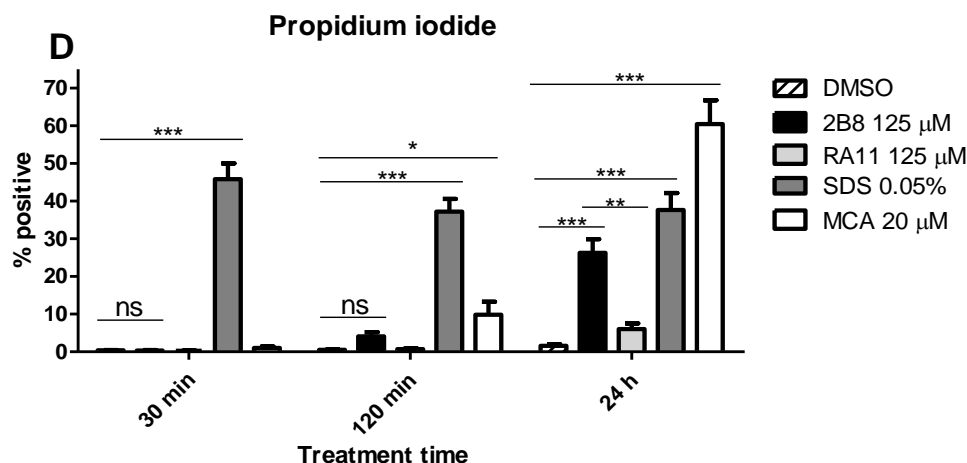


**Figure 3.6. 2-AI treatment increased *M. tuberculosis* sensitivity to SDS and permeability to nucleic acid staining dyes.** A) *M. tuberculosis* was treated or not with 125  $\mu$ M 2B8 for 24 h, exposed to 0.005% (left panel) or 0.05% (right panel) SDS and bacterial viability was monitored by plating on 7H11 agar hourly thereafter. 2B8 treated *M. tuberculosis* H37Rv was significantly more sensitive to killing by SDS at both tested concentrations (0.005% and 0.05%). B and C) *M. tuberculosis* H37Rv was treated with 2B8 while being exposed to EtBr or Sytox Orange, and the change in fluorescent signal was monitored for 90 min at 2 min intervals. Compared to DMSO treated culture, 2B8 treated culture showed significantly higher accumulation of EtBr and Sytox Orange after 90 min. 100 mg/L reserpine increased accumulation of EtBr albeit not statistically significant (panel B), while 80  $\mu$ M TRZ significantly increased accumulation of Sytox Orange. D) *M. tuberculosis* H37Rv was treated with 2B8 for 30, 120 min and 24 h. After treatment, cultures were stained with PI and analyzed by flow cytometry. As indicated by increased positive staining with PI, SDS acutely (30 min) permeabilized *M. tuberculosis* cell membrane, whereas 2B8 and RA11 treatment only compromised the membrane integrity past 2 h. Disruption of cell membrane by 2-AI compounds was more pronounced with 2B8 than RA11 (24 h). MCA treatment also resulted in increased staining with PI after 2 and 24 h of treatment. \* $p < 0.05$ , \*\* $p < 0.01$ , \*\*\* $p < 0.001$  by ANOVA, (For EtBr and Sytox Orange accumulation assay, statistical significance marked for 90 min time-point). Experiments were carried out three separate times and representative data are shown.

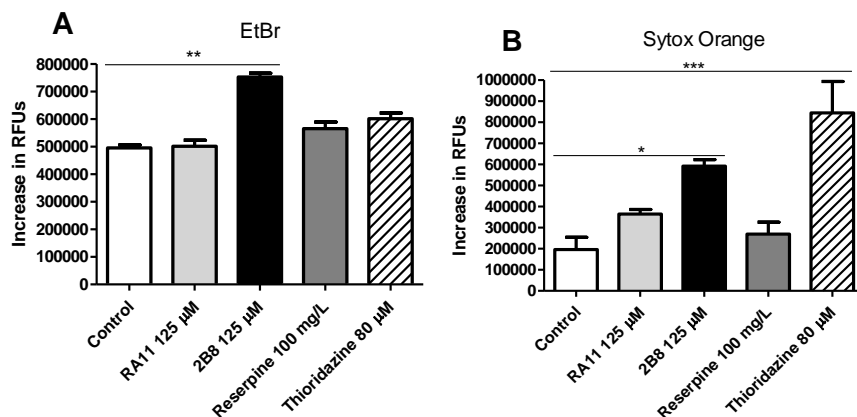


**Figure 3.7. 2B8 treatment increased *M. tuberculosis* net accumulation of nucleic acid staining dyes.** 2B8 treated *M. tuberculosis* accumulated both EtBr (A) and Sytox Orange (B) significantly more than untreated. Reserpine and TRZ increased net accumulation of EtBr, but it was not statistically significant (A). TRZ significantly increased accumulation of Sytox Orange (B). \* $p < 0.05$ , \*\* $p < 0.01$  by ANOVA.

### 3.3.5. 2-AI treatment acutely increases binding of penicillin V and vancomycin

Using fluorescent BODIPY<sup>®</sup>-labeled antibiotics, it was possible to directly measure if 2-AI compounds potentiate  $\beta$ -lactams by increasing mycobacterial cell envelope permeability and antibiotic accessibility to their respective cell wall targets. To accomplish this, *M. tuberculosis* was treated with 2-AI compounds for increasing amount of time (30 min, 120 min and 24 h), stained for 30 min with fluorescent-labeled BODIPY<sup>®</sup> FL vancomycin or BOCILLIN<sup>®</sup>, and analyzed by flow cytometry. Similar to what was observed with the tested  $\beta$ -lactams (Table 2.1), the MIC of vancomycin (Table 3.1) and penicillin V against *M. tuberculosis* was also lower after exposure to 2-AI compounds.

There was significantly increase in binding of both fluorescent penicillin V (Figure 3.8C, 3.9A and 3.10) and vancomycin (Figure 3.8B, 3.9B and 3.10) to *M. tuberculosis* compared to controls after an acute 30 min treatment with 2B8. For both fluorescent antibiotics, binding to treated *M. tuberculosis* increased proportionally to treatment duration. Treatment with RA11 also increased antibiotic binding to *M. tuberculosis* but the extent was much lower than that induced by 2B8. The binding of fluorescent vancomycin to *M. tuberculosis* increased when treated with MCA (Figure 3.9B), as expected considering

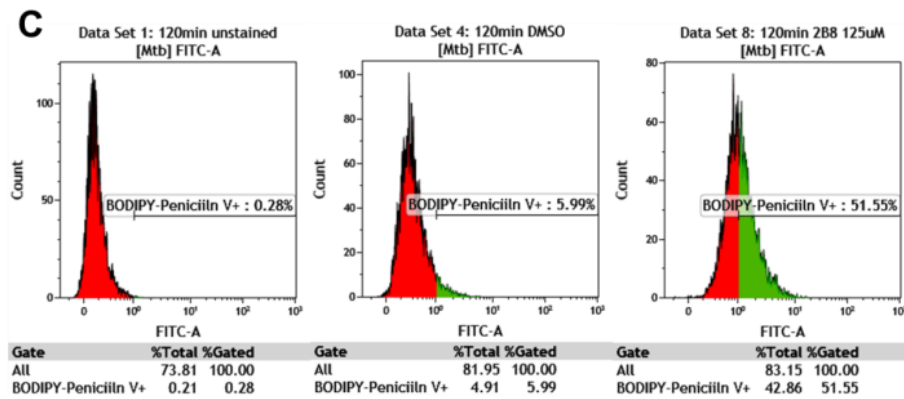
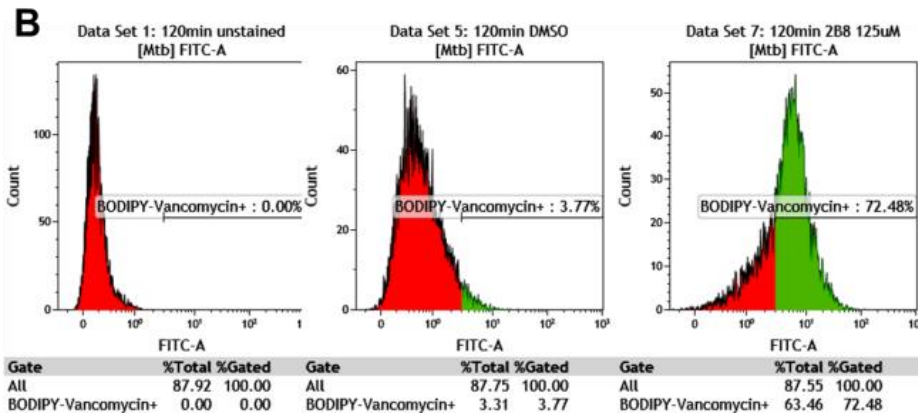
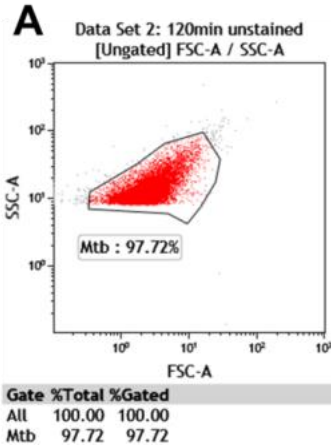
**Table 3.1. MIC of vancomycin against 2B8 treated *M. tuberculosis* H37Rv.**

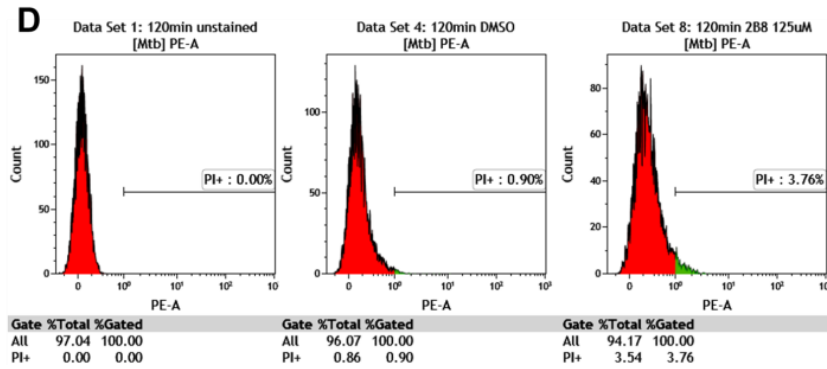
Organism and antibiotics	MIC	MIC with 2B8 (12.5% MIC)	Fold reduction	MIC with 2B8 (25% MIC)	Fold reduction	MIC with 2B8 (50% MIC)	Fold reduction
<i>M. tuberculosis</i> H37Rv							
Vancomycin	5	2.5	2	1.25	4	0.625	8

All MIC values are represented as mg/L.

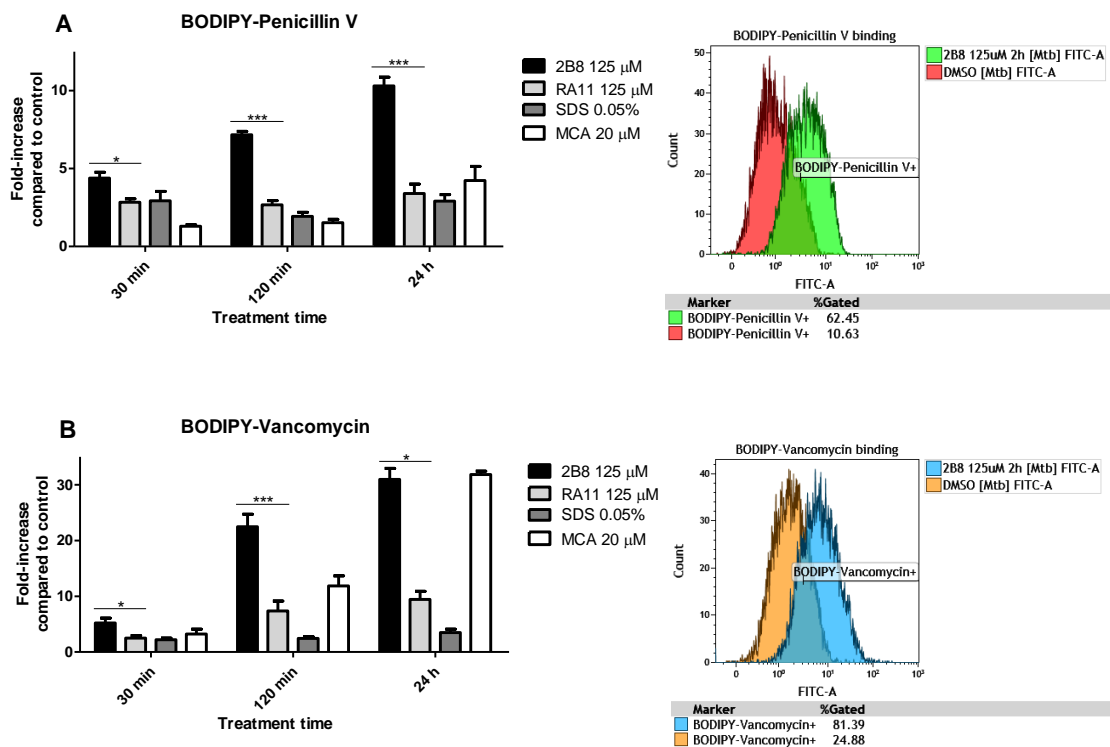
Experiments were carried out two independent times in duplicate and representative data are shown.

meropenem's inhibition of the mycobacterial D-carboxypeptidase that cleaves vancomycin's target, the D-ala-D-ala peptide motif [21]. However, this effect was delayed and only became evident after 24 h treatment. Moreover, despite being very potent at disrupting the cell membrane (Figure 3.9A and 3.9B), SDS only minimally increased binding of either BODIPY<sup>®</sup> FL vancomycin or BOCILLIN<sup>®</sup> to *M. tuberculosis*, suggesting that direct membrane disruption does not underpin activity. The specificity of BODIPY<sup>®</sup> FL vancomycin's staining was confirmed by a competitive inhibition assay and fluorescent microscopy. Increasing amounts of unlabeled vancomycin competitively inhibited binding of BODIPY<sup>®</sup> FL vancomycin to 2B8 treated *M. tuberculosis* (Figure 3.10). This demonstrates that the fluorescent drug is binding specifically to its cognate target, rather than non-specifically through the BODIPY<sup>®</sup> moiety. Furthermore, in accordance with previous publications [30, 31], a punctate staining predominantly at the mycobacterial poles, was observed when staining *M. tuberculosis* with BODIPY<sup>®</sup> FL vancomycin (Figure 3.9C). Consistent with the flow cytometry results, 2B8 treatment increased the number of stained bacteria and fluorescence intensity versus DMSO-treated control (Figure 3.9C). BOCILLIN<sup>®</sup>'s fluorescence was not bright enough for microscopy (data not shown).





**Figure 3.8. 2B8 acutely increases binding of BODIPY<sup>®</sup> FL vancomycin and BOCILLIN<sup>®</sup> to *M. tuberculosis* while having no effect on cell membrane integrity.** A) Representative scatter plot of gated population for *M. tuberculosis*. B and C) Representative histogram overlays of unstained, DMSO and 125  $\mu$ M 2B8 treated *M. tuberculosis* after staining with BODIPY<sup>®</sup> FL vancomycin (B) or BOCILLIN<sup>®</sup> (C). Treatment with 125  $\mu$ M 2B8 for 2 h resulted in significantly increased binding of both fluorescent vancomycin and penicillin V to *M. tuberculosis*. D) In contrast, this treatment did not significantly increase *M. tuberculosis* permeability to PI.



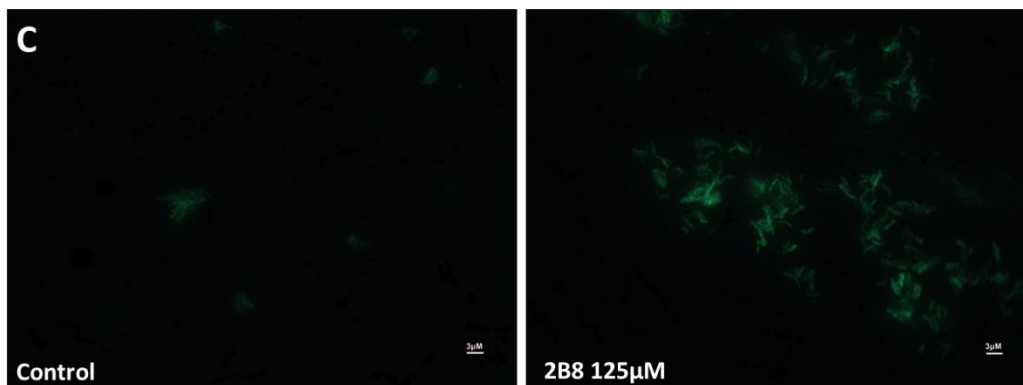


**Figure 3.9. 2-AI increased penicillin V and vancomycin binding to *M. tuberculosis*.** *M. tuberculosis* H37Rv was treated with 125  $\mu$ M 2-AI compounds (2B8 and RA11), 0.05% SDS, and 20  $\mu$ M MCA for 30, 120 min, and 24 h. After treatment, cultures were stained with BOCILLIN<sup>®</sup> (A) or BODIPY<sup>®</sup> FL vancomycin (B) for 30 min. Unbound fluorescent antibiotics were washed with PBS and single cells were analyzed for fluorescence intensity by flow cytometry. A and B) Representative histogram overlays (right panels) of BOCILLIN<sup>®</sup> or BODIPY<sup>®</sup> FL vancomycin stained *M. tuberculosis* after treatment with 125  $\mu$ M 2B8 or DMSO control. Fold-change staining (left panels) was determined by dividing percent of positively-stained treated bacteria by percent of positively-stained DMSO control bacteria. For BOCILLIN<sup>®</sup>, a time-dependent increase in staining was observed with 2B8, but not with RA11, SDS or MCA treatment. 2B8 treatment also increased staining with BODIPY<sup>®</sup> FL vancomycin in a time-dependent manner to a significantly higher extent than that of RA11 or SDS treatment. MCA treatment resulted in a time-dependent increase of BODIPY<sup>®</sup> FL vancomycin staining as expected. C) Fluorescent images ( $\times 1000$ , bar = 3  $\mu$ M) of *M. tuberculosis* stained with BODIPY<sup>®</sup> FL vancomycin after treatment or not with 125  $\mu$ M 2B8 for 120 min. Treatment with 2B8 (right panel) resulted in increased number of bacteria with higher fluorescence intensity than DMSO control. \* $p < 0.05$ , \*\* $p < 0.01$ , \*\*\* $p < 0.001$  by ANOVA. Experiments were repeated three separate times in triplicates and results were pooled together for statistical analysis. For clarity, significance is only shown for control and 2-AI compound treatment.

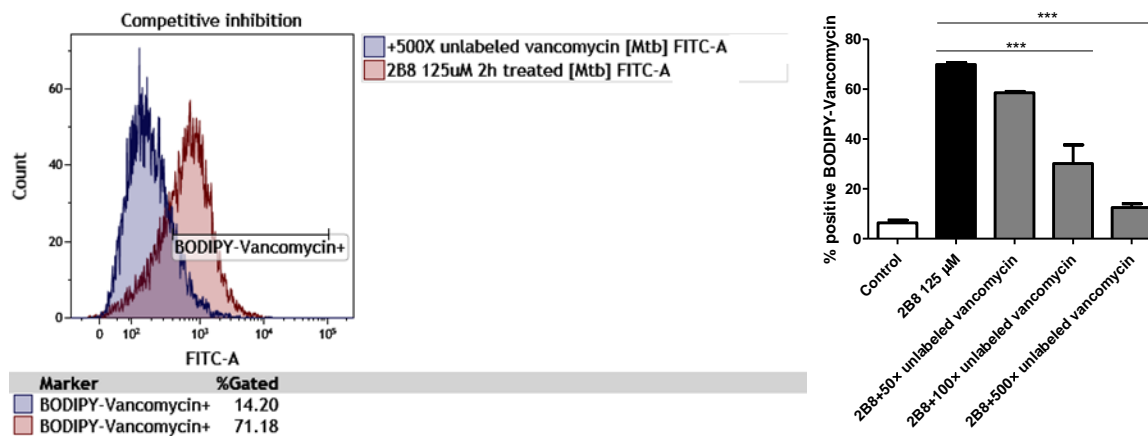


**Figure 3.10. Unlabeled vancomycin competitively inhibits binding of BODIPY<sup>®</sup> FL vancomycin to *M. tuberculosis*.** Prior to staining with BODIPY<sup>®</sup> FL vancomycin, unlabeled vancomycin at three different concentrations (50 $\times$ , 100 $\times$ , and 500 $\times$  the amount of BODIPY<sup>®</sup> FL vancomycin) was added to *M. tuberculosis* treated for 2 h with 2B8. Representative histogram overlay of 2B8 treated *M. tuberculosis* with or without addition of 500 $\times$  unlabeled vancomycin is shown (left panel). When 100 $\times$  or 500 $\times$  unlabeled vancomycin was added to 2B8 treated samples, binding of BODIPY<sup>®</sup> FL vancomycin was significantly inhibited (right panel). \*\*\* $p$  < 0.001 by ANOVA. Experiments were done three separate times and all individual samples were pooled together for statistical analysis.

### 3.4. Discussion

The goals of this study were to elucidate the  $\beta$ -lactam potentiation mechanism of 2-AI compounds in *M. tuberculosis*. Mechanistic studies have revealed that 2-AI compounds achieve this effect by at least two distinct mechanisms: a) reducing *M. tuberculosis*  $\beta$ -lactamase secretion and b) increasing *M. tuberculosis* cell envelope permeability and accessibility of cell wall targeting drugs.

Several lines of evidence indicate that a major mechanism contributing to  $\beta$ -lactam potentiation by 2-AI compounds is the alteration of the mycobacterial cell envelope and an increase in the accessibility of  $\beta$ -lactams to their target [2-4, 10, 26, 27]. Indeed, as early as 30 min post-treatment with 2-AI compounds, increased *M. tuberculosis* permeability to a fluorescent  $\beta$ -lactam or glycopeptide antibiotic, such as penicillin V and vancomycin, respectively was observed. In order to reach their targets located within the periplasmic space delimited between the outer and inner cell membrane, these antibiotics first have to diffuse through the outer cell membrane [8, 12, 32, 33]. It is well documented in both mycobacteria and Gram-negative bacteria that the presence of an outer cell membrane acts as a

permeability barrier to limit the diffusion of hydrophilic molecules [27, 34-37]. Specifically, in mycobacteria, the outer cell membrane impermeability is further enforced by the presence of mycolic acids and complex lipids such as TDM and PDIM in the inner and outer leaflets [12]. 2B8 treatment decreased TDM, MAMEs, SL-1 and PAT content while precursors TMM and DAT from 2-AI treated samples. Consistent with the MIC results (Table 2.1), 2B8 treatment resulted in a more dramatic effect than RA11 treatment. The fact that 2B8-treated *M. tuberculosis* was readily stained with a bulky antibiotic (such as BODIPY<sup>®</sup> FL vancomycin) in 30 min, in contrast to multiple hours usually required to stain mycobacteria [30, 38], strongly suggests that 2B8 could be increasing the mycobacterial outer cell membrane permeability. This hypothesis was further supported by the acutely (90 min) increased permeability of 2B8-treated *M. tuberculosis* to nucleic acid staining dyes such as EtBr and Sytox Orange, routinely used as markers of mycobacterial cell envelope integrity [26, 27]. The ability to increase the outer membrane permeability could potentially be attributed to 2-AI compound's alkyl chain(s) and could explain the different structure-function relationship of several related 2-AI compounds sharing the same 2-aminoimidazole polar head group but distinguished with distinct apolar, alkyl chains. As suggested by the results with fluorescent antibiotics and nucleic acid staining dyes, 2B8's branched, albeit short alkyl chain induces a superior effect on the mycobacterial outer cell membrane permeability than RA11's straight alkyl chain containing 11 carbons. Derivatization of the 2-aminoimidazole group with a straight 13-carbon alkyl chain (such as in another 2B8 derivative, RA13), completely abrogated the compound's activity in the mycobacterial biofilm dispersion assay [39]. This dependence on a critical chain length and structure of the hydrophobic tail could explain why SDS, with a straight 12-carbon acyl chain, failed to dramatically potentiate  $\beta$ -lactams (Table 3.2) or increase binding of fluorescent antibiotics to *M. tuberculosis* despite being a potent inner cell membrane disruptor (as determined by PI staining). Meanwhile, mycobacterial inner cell membrane disruption with 2B8 was only observed for a small fraction of bacilli after 24 h. In contrast, Stowe et al. previously reported acute and dramatic *Acinetobacter baumannii* lysis in the presence of reverse-amide 2-AIs [2]. Beyond the role played by their different hydrophobic tails, opposing outcomes induced by 2-AI compounds or SDS could also be

determined or modulated by their respective polar head group and charge, and this remains to be investigated. Collectively, these results indicate  $\beta$ -lactam potentiation by 2-AI compounds is probably uncoupled from direct inner cell membrane disruption.

**Table 3.2. MIC of  $\beta$ -lactams against SDS treated *M. tuberculosis* H37Rv.**

Organism and antibiotics	MIC	MIC with SDS (12.5% MIC*)	Fold reduction	MIC with SDS (25% MIC)	Fold reduction	MIC with SDS (50% MIC)	Fold reduction
<i>M. tuberculosis</i> H37Rv							
Carbenicillin	512	512	1	256	2	64	8
Amoxicillin	512	512	1	256	2	64	8
Ceftazidime	256	256	1	128	2	32	8
Meropenem	8	8	1	4	2	2	4
Penicillin V	512	512	1	256	2	128	4

All MIC values are represented as mg/L.

\*SDS MIC against *M. tuberculosis* H37Rv was 0.025%.

Experiments were carried out at least two independent times in duplicate and representative data are shown.

Further evidence that 2-AI compounds affect the mycobacterial cell envelope was obtained from metabolic labeling experiments evaluating *M. tuberculosis* cell envelope lipid composition, as well as from transcriptional responses to 2B8 (Figure 2.8). 2-AI treated *M. tuberculosis* had a dramatic decrease in mycolic acids covalently esterified to the cell wall (MAMEs), probably resulting from a combination of: a) reduced biosynthesis, b) defect in TMM export, and c) decreased crosslinking to arabinose residues in the mycolyl-arabinogalactan-peptidoglycan (mAGP) complex. Genes encoding for FAS-I (synthesizes mycolic acid's  $\alpha$ -alkyl chain), FAS-II (synthesizes mycolic acid's meromycolate chain) and pks13 (condenses both chains to form mycolic acids) [40, 41], were amongst the most significantly down-regulated genes at 2 h post-treatment. Furthermore, mycolic acid export was also compromised by 2B8 treatment as suggested by the inverse relationship between high TMM (precursor) and low TDM (end product) levels. However, this defect was not a consequence of reduced *mmpL3* transcription, recently

identified to encode for a TMM transporter [42]. Finally, by down-regulating expression of two members of the mycolyl-transferase complex (*fbpA* and *fbpB*), which catalyze mycolic acid-arabinose linkage [43], 2B8 could further compound the deficit of mycolic acid-dependent fortification of the mycobacterial cell wall core. Trehalose-based lipids such as SL-1 and PAT were also less abundant in 2-AI treated bacilli, while PAT's precursor, DAT, accumulated. Again, this deficit was not due to decreased transcription of their cognate transporters. In fact, transcription of *mmpL8* and *mmpL10*, encoding for SL-1 [44] and DAT transporter [45], respectively, was actually up-regulated. The fact that 2-AI treatment leads to mycobacterial accumulation of unexported lipid precursors without decreased transporter transcription, suggest that the defect is elsewhere, perhaps at the level of PMF generation required for MmpL-catalyzed transport of related lipids [46, 47]. Finally, it was recently shown that methyl-branched lipid biosynthesis acts as a propionate sink to limit its toxicity [48-50]. Interestingly, both *prpC* and *prpD* of the methyl-citrate cycle that plays a role in detoxifying propionate were strongly induced 17- and 34-fold, respectively, following 2 h of 2B8 treatment (Figure 2.8). This strong induction suggests that 2B8 may induce propionate toxicity, possibly as part of changes to the cell envelope. Altogether, beyond the acute increased outer cell membrane permeability discussed above, alterations in the biosynthesis and/or export of *M. tuberculosis* cell envelope lipids probably further contribute to  $\beta$ -lactam potentiation and enhanced SDS sensitivity induced by 2-AI compounds.

Bacteria respond to cell envelope stress by modulating their transcriptome through the activation of transcription regulators. Consistent with this, at 2 h after treatment, 2B8 induced several transcriptional regulators including the alternative sigma factors *sigB*, *sigE*, and *sigK* and the response regulator *mprA* (Figure 8B). Notably, the two component regulatory system MprAB regulates *sigB* and *sigE* [51] in response to envelope stresses, such as SDS or Triton X-100 treatment, which is consistent with 2-AI promoting envelope stress and stimulating the MprAB regulatory network. Both SigE and SigK belong to the family of ECF sigma factors, kept inactive/transcriptionally silent by remaining tethered to a transmembrane protein, an anti-sigma factor [52-54]. In the presence of extracellular stress, proteolytic cleavage of the anti-sigma factor releases the cognate sigma factor to become transcriptionally active and

regulate the expression of multiple genes. Particularly interesting was the upregulation of *sigK* and SigK regulated genes such as *mpt70*, *mpt83*, *dipZ*, and *rv0449c* [55], supporting that the SigK regulon is induced in a sustained manner by 2B8 (Figure 2.8). Unfortunately, not much is known about the biological role of the SigK regulon, besides the fact the *mpt70/83* are highly immunogenic proteins and their expression levels significantly differ between members of the *M. tuberculosis* complex [55, 56]. Two redox-sensitive cysteine residues were recently suggested to regulate the transcriptional activity of SigK by altering the interaction with RskA, the cognate anti-sigma factor [57]. This is a recurring mechanism regulating other ECF such as SigF and SigL [58, 59], however the upregulation of these sigma factors or their regulons in response to 2B8 was not observed. Thus, the mechanism leading to the specific upregulation of the SigK regulon by 2B8 is still unclear.

The *M. tuberculosis blaC* gene encodes for a highly active class A  $\beta$ -lactamase, which significantly contributes to *M. tuberculosis* intrinsic  $\beta$ -lactam resistance [9, 22]. Therefore, studies have attempted to circumvent this resistance by combining  $\beta$ -lactams with a  $\beta$ -lactamase inhibitor such as clavulanate. This combination has indeed proven to be promising against *M. tuberculosis* [11, 24, 60]. Thus, it was important to determine if 2-AI compounds potentiate  $\beta$ -lactams by interfering with any aspect of *M. tuberculosis*  $\beta$ -lactamase function. 2-AI compounds did not directly inhibit  $\beta$ -lactamase activity like a classical inhibitor such as clavulanate, supporting our recently published results obtained with additional compounds derived from the 2-AI scaffold [1]. This result was expected considering 2-AI compounds similarly potentiated  $\beta$ -lactams regardless of their respective susceptibility to  $\beta$ -lactamase degradation, suggesting  $\beta$ -lactamase inhibition was not the mechanism driving potentiation. Comparable MIC fold-reduction was observed for carbenicillin/amoxicillin/penicillin V (early generation of  $\beta$ -lactams highly susceptible to  $\beta$ -lactamase) and meropenem (a carbapenem with superior resistance to  $\beta$ -lactamase). Furthermore,  $\beta$ -lactam potentiation by 2B8 was not due to down-regulation of *blaC* expression *per se* or those encoding for the twin-arginine protein translocating system (*tat*), responsible for  $\beta$ -lactamase secretion [61-63]. However, reduced  $\beta$ -lactamase activity in the CFP of 2B8 treated *M. tuberculosis*, correlated with reduced protein concentration in this fraction. As 2B8 did not alter the transcription of

genes encoding for other major *M. tuberculosis* protein secretion systems (namely SecA, SecA2 or type VII, Figure 2.8), it is logical to explore if these compounds affect other parameters such as mycobacterial bioenergetics required for protein secretion and lipid export, as described above. Thus, it is concluded that reduced  $\beta$ -lactamase secretion could contribute in part to  $\beta$ -lactam potentiation by 2-AI compounds.

Other aspects of *M. tuberculosis* intrinsic resistance to  $\beta$ -lactams that could be affected by 2-AI treatment but were not directly evaluated, include the role of efflux pumps, peptidoglycan structure and PBPs or L,D-transpeptidases involved in peptidoglycan crosslinking [4]. However, through transcriptional profiling it was possible to rule out decreased gene expression of efflux pumps, PBPs or L,D-transpeptidases as a mechanism explaining  $\beta$ -lactam potentiation by 2-AI compounds. In fact, 2B8 induced *rv1218c* and *rv1258c*, previously shown to be specifically involved in  $\beta$ -lactam resistance [28, 64], as well as other efflux pumps associated with resistance to bedaquiline and clofazimine (*mmpL5*) [65]. Nevertheless, it cannot be excluded that 2-AI compounds have an indirect effect on  $\beta$ -lactam efflux pumps, via alteration of mycobacterial bioenergetics as discussed above. Finally, as suggested by lower expression levels for *mur* genes, 2B8 could potentially be reducing the amount of uncrosslinked peptidoglycan precursors, the substrates for PBPs and L,D-transpeptidases. Ultimately, in the face of dwindling amounts of peptidoglycan precursors, PBPs and L,D-transpeptidase inhibition by  $\beta$ -lactams would have additive catastrophic effects.

Taken together, the data suggests that 2-AI compounds potentiate  $\beta$ -lactams by affecting *M. tuberculosis* cell envelope integrity and  $\beta$ -lactamase secretion. This former effect serves to permeabilize the normally impenetrable cell wall, allowing increased antibiotic access. This effect, however, is distinct from non-specific membrane disruption that occurs by treatment by detergents like SDS that operate via rapid physical disruption of the membrane. Evidently, a limitation in this study was the high concentration of 2-AI compounds required for most of the assays. As the concentrations required to achieve activity preclude evaluating activity *in vivo*, we are currently augmenting compound activity to be active against *M. tuberculosis* at lower concentrations through medicinal chemistry. Identified compounds

with higher efficacy will be used in experiments to directly identify the target of these compounds as well as studies to validate activity against *M. tuberculosis*.

## REFERENCES

1. Nguyen TV, Blackledge MS, Lindsey EA, Minrovic BM, Ackart DF, Jeon AB, et al. The Discovery of 2-Aminobenzimidazoles That Sensitize *Mycobacterium smegmatis* and *M. tuberculosis* to beta-Lactam Antibiotics in a Pattern Distinct from beta-Lactamase Inhibitors. *Angew Chem Int Ed Engl.* 2017;56(14):3940-4. doi: 10.1002/anie.201612006. PubMed PMID: 28247991.
2. Stowe SD, Thompson RJ, Peng L, Su Z, Blackledge MS, Draughn GL, et al. Membrane-permeabilizing activity of reverse-amide 2-aminoimidazole antibiofilm agents against *Acinetobacter baumannii*. *Curr Drug Deliv.* 2015;12(2):223-30. PubMed PMID: 25348099; PubMed Central PMCID: PMC4640187.
3. Harris TL, Worthington RJ, Hittle LE, Zurawski DV, Ernst RK, Melander C. Small molecule downregulation of PmrAB reverses lipid A modification and breaks colistin resistance. *ACS Chem Biol.* 2014;9(1):122-7. doi: 10.1021/cb400490k. PubMed PMID: 24131198.
4. Wivagg CN, Bhattacharyya RP, Hung DT. Mechanisms of beta-lactam killing and resistance in the context of *Mycobacterium tuberculosis*. *J Antibiot (Tokyo).* 2014;67(9):645-54. doi: 10.1038/ja.2014.94. PubMed PMID: 25052484.
5. Iland CN. The effect of penicillin on the tubercle bacillus. *J Pathol Bacteriol.* 1946;58(3):495-500. PubMed PMID: 20283086.
6. Kwon HH, Tomioka H, Saito H. Distribution and characterization of beta-lactamases of mycobacteria and related organisms. *Tuber Lung Dis.* 1995;76(2):141-8. PubMed PMID: 7780097.
7. Kasik JE, Peacham L. Properties of beta-lactamases produced by three species of mycobacteria. *Biochem J.* 1968;107(5):675-82. PubMed PMID: 16742589; PubMed Central PMCID: PMC1198720.
8. Chambers HF, Moreau D, Yajko D, Miick C, Wagner C, Hackbarth C, et al. Can penicillins and other beta-lactam antibiotics be used to treat tuberculosis? *Antimicrob Agents Chemother.* 1995;39(12):2620-4. PubMed PMID: 8592990; PubMed Central PMCID: PMC163000.
9. Flores AR, Parsons LM, Pavelka MS, Jr. Genetic analysis of the beta-lactamases of *Mycobacterium tuberculosis* and *Mycobacterium smegmatis* and susceptibility to beta-lactam antibiotics. *Microbiology.* 2005;151(Pt 2):521-32. doi: 10.1099/mic.0.27629-0. PubMed PMID: 15699201.
10. Jarlier V, Nikaido H. Mycobacterial cell wall: structure and role in natural resistance to antibiotics. *FEMS Microbiol Lett.* 1994;123(1-2):11-8. PubMed PMID: 7988876.
11. Hugonnet JE, Blanchard JS. Irreversible inhibition of the *Mycobacterium tuberculosis* beta-lactamase by clavulanate. *Biochemistry.* 2007;46(43):11998-2004. doi: 10.1021/bi701506h. PubMed PMID: 17915954; PubMed Central PMCID: PMC163000.
12. Bansal-Mutalik R, Nikaido H. Mycobacterial outer membrane is a lipid bilayer and the inner membrane is unusually rich in diacyl phosphatidylinositol dimannosides. *Proc Natl Acad Sci U S A.*

2014;111(13):4958-63. doi: 10.1073/pnas.1403078111. PubMed PMID: 24639491; PubMed Central PMCID: PMC3977252.

13. Hoffmann C, Leis A, Niederweis M, Plitzko JM, Engelhardt H. Disclosure of the mycobacterial outer membrane: cryo-electron tomography and vitreous sections reveal the lipid bilayer structure. *Proc Natl Acad Sci U S A*. 2008;105(10):3963-7. doi: 10.1073/pnas.0709530105. PubMed PMID: 18316738; PubMed Central PMCID: PMC2268800.

14. Zuber B, Chami M, Houssin C, Dubochet J, Griffiths G, Daffe M. Direct visualization of the outer membrane of mycobacteria and corynebacteria in their native state. *J Bacteriol*. 2008;190(16):5672-80. doi: 10.1128/JB.01919-07. PubMed PMID: 18567661; PubMed Central PMCID: PMC2519390.

15. Wivagg CN, Wellington S, Gomez JE, Hung DT. Loss of a Class A Penicillin-Binding Protein Alters beta-Lactam Susceptibilities in *Mycobacterium tuberculosis*. *ACS Infect Dis*. 2016;2(2):104-10. doi: 10.1021/acsinfecdis.5b00119. PubMed PMID: 27624961.

16. Brennan PJ. Structure, function, and biogenesis of the cell wall of *Mycobacterium tuberculosis*. *Tuberculosis (Edinb)*. 2003;83(1-3):91-7. PubMed PMID: 12758196.

17. Jain P, Hsu T, Arai M, Biermann K, Thaler DS, Nguyen A, et al. Specialized transduction designed for precise high-throughput unmarked deletions in *Mycobacterium tuberculosis*. *MBio*. 2014;5(3):e01245-14. doi: 10.1128/mBio.01245-14. PubMed PMID: 24895308; PubMed Central PMCID: PMC4049104.

18. Rousseau C, Neyrolles O, Bordat Y, Giroux S, Sirakova TD, Prevost MC, et al. Deficiency in mycolipenate- and mycosanoate-derived acyltrehaloses enhances early interactions of *Mycobacterium tuberculosis* with host cells. *Cell Microbiol*. 2003;5(6):405-15. PubMed PMID: 12780778.

19. Purdy GE, Niederweis M, Russell DG. Decreased outer membrane permeability protects mycobacteria from killing by ubiquitin-derived peptides. *Mol Microbiol*. 2009;73(5):844-57. doi: 10.1111/j.1365-2958.2009.06801.x. PubMed PMID: 19682257; PubMed Central PMCID: PMC2747030.

20. de Keijzer J, Mulder A, de Haas PE, de Ru AH, Heerkens EM, Amaral L, et al. Thioridazine Alters the Cell-Envelope Permeability of *Mycobacterium tuberculosis*. *J Proteome Res*. 2016. doi: 10.1021/acs.jproteome.5b01037. PubMed PMID: 27068340.

21. Kumar P, Arora K, Lloyd JR, Lee IY, Nair V, Fischer E, et al. Meropenem inhibits D,D-carboxypeptidase activity in *Mycobacterium tuberculosis*. *Mol Microbiol*. 2012;86(2):367-81. doi: 10.1111/j.1365-2958.2012.08199.x. PubMed PMID: 22906310; PubMed Central PMCID: PMC3468717.

22. Wang F, Cassidy C, Sacchettini JC. Crystal structure and activity studies of the *Mycobacterium tuberculosis* beta-lactamase reveal its critical role in resistance to beta-lactam antibiotics. *Antimicrob Agents Chemother*. 2006;50(8):2762-71. doi: 10.1128/AAC.00320-06. PubMed PMID: 16870770; PubMed Central PMCID: PMC1538687.

23. Segura C, Salvado M, Collado I, Chaves J, Coira A. Contribution of beta-lactamases to beta-lactam susceptibilities of susceptible and multidrug-resistant *Mycobacterium tuberculosis* clinical isolates. *Antimicrob Agents Chemother*. 1998;42(6):1524-6. PubMed PMID: 9624510; PubMed Central PMCID: PMC105638.

24. England K, Boshoff HI, Arora K, Weiner D, Dayao E, Schimel D, et al. Meropenem-clavulanic acid shows activity against *Mycobacterium tuberculosis* in vivo. *Antimicrob Agents Chemother.* 2012;56(6):3384-7. doi: 10.1128/AAC.05690-11. PubMed PMID: 22450968; PubMed Central PMCID: PMC3370771.
25. Kong Y, Yao H, Ren H, Subbian S, Cirillo SL, Sacchettini JC, et al. Imaging tuberculosis with endogenous beta-lactamase reporter enzyme fluorescence in live mice. *Proc Natl Acad Sci U S A.* 2010;107(27):12239-44. doi: 10.1073/pnas.1000643107. PubMed PMID: 20566877; PubMed Central PMCID: PMC2901431.
26. Mukhopadhyay S, Chakrabarti P. Altered permeability and beta-lactam resistance in a mutant of *Mycobacterium smegmatis*. *Antimicrob Agents Chemother.* 1997;41(8):1721-4. PubMed PMID: 9257748; PubMed Central PMCID: PMC163992.
27. Rodrigues L, Ramos J, Couto I, Amaral L, Viveiros M. Ethidium bromide transport across *Mycobacterium smegmatis* cell-wall: correlation with antibiotic resistance. *BMC Microbiol.* 2011;11:35. doi: 10.1186/1471-2180-11-35. PubMed PMID: 21332993; PubMed Central PMCID: PMC3051877.
28. Danilchanka O, Mailaender C, Niederweis M. Identification of a novel multidrug efflux pump of *Mycobacterium tuberculosis*. *Antimicrob Agents Chemother.* 2008;52(7):2503-11. doi: 10.1128/AAC.00298-08. PubMed PMID: 18458127; PubMed Central PMCID: PMC2443884.
29. Banerjee A, Majumder P, Sanyal S, Singh J, Jana K, Das C, et al. The DNA intercalators ethidium bromide and propidium iodide also bind to core histones. *FEBS Open Bio.* 2014;4:251-9. doi: 10.1016/j.fob.2014.02.006. PubMed PMID: 24649406; PubMed Central PMCID: PMC3958746.
30. Joyce G, Williams KJ, Robb M, Noens E, Tizzano B, Shahrezaei V, et al. Cell division site placement and asymmetric growth in mycobacteria. *PLoS One.* 2012;7(9):e44582. doi: 10.1371/journal.pone.0044582. PubMed PMID: 22970255; PubMed Central PMCID: PMC3438161.
31. Dhiman RK, Dinadayala P, Ryan GJ, Lenaerts AJ, Schenkel AR, Crick DC. Lipoarabinomannan localization and abundance during growth of *Mycobacterium smegmatis*. *J Bacteriol.* 2011;193(20):5802-9. doi: 10.1128/JB.05299-11. PubMed PMID: 21840972; PubMed Central PMCID: PMC3187192.
32. Wise EM, Jr., Park JT. Penicillin: its basic site of action as an inhibitor of a peptide cross-linking reaction in cell wall mucopeptide synthesis. *Proc Natl Acad Sci U S A.* 1965;54(1):75-81. PubMed PMID: 5216369; PubMed Central PMCID: PMC285799.
33. Perkins HR. Specificity of combination between mucopeptide precursors and vancomycin or ristocetin. *Biochem J.* 1969;111(2):195-205. PubMed PMID: 5763787; PubMed Central PMCID: PMC1187807.
34. Danilchanka O, Pires D, Anes E, Niederweis M. The *Mycobacterium tuberculosis* outer membrane channel protein CpnT confers susceptibility to toxic molecules. *Antimicrob Agents Chemother.* 2015;59(4):2328-36. doi: 10.1128/AAC.04222-14. PubMed PMID: 25645841; PubMed Central PMCID: PMC4356772.

35. Niederweis M, Danilchanka O, Huff J, Hoffmann C, Engelhardt H. Mycobacterial outer membranes: in search of proteins. *Trends Microbiol.* 2010;18(3):109-16. doi: 10.1016/j.tim.2009.12.005. PubMed PMID: WOS:000276135500002.
36. Wiener MC, Horanyi PS. How hydrophobic molecules traverse the outer membranes of gram-negative bacteria. *Proc Natl Acad Sci U S A.* 2011;108(27):10929-30. doi: 10.1073/pnas.1106927108. PubMed PMID: 21693645; PubMed Central PMCID: PMC3131365.
37. Delcour AH. Outer membrane permeability and antibiotic resistance. *Biochim Biophys Acta.* 2009;1794(5):808-16. doi: 10.1016/j.bbapap.2008.11.005. PubMed PMID: 19100346; PubMed Central PMCID: PMC2696358.
38. Vijay S, Mukkayyan N, Ajitkumar P. Highly Deviated Asymmetric Division in Very Low Proportion of Mycobacterial Mid-log Phase Cells. *Open Microbiol J.* 2014;8:40-50. doi: 10.2174/1874285801408010040. PubMed PMID: 24949109; PubMed Central PMCID: PMC4062944.
39. Ackart DF, Lindsey EA, Podell BK, Melander RJ, Basaraba RJ, Melander C. Reversal of Mycobacterium tuberculosis phenotypic drug resistance by 2-aminoimidazole-based small molecules. *Pathog Dis.* 2014;70(3):370-8. doi: 10.1111/2049-632X.12143. PubMed PMID: 24478046; PubMed Central PMCID: PMC4367863.
40. Bhatt A, Molle V, Besra GS, Jacobs WR, Jr., Kremer L. The Mycobacterium tuberculosis FAS-II condensing enzymes: their role in mycolic acid biosynthesis, acid-fastness, pathogenesis and in future drug development. *Mol Microbiol.* 2007;64(6):1442-54. doi: 10.1111/j.1365-2958.2007.05761.x. PubMed PMID: 17555433.
41. Takayama K, Wang C, Besra GS. Pathway to synthesis and processing of mycolic acids in Mycobacterium tuberculosis. *Clin Microbiol Rev.* 2005;18(1):81-101. doi: 10.1128/CMR.18.1.81-101.2005. PubMed PMID: 15653820; PubMed Central PMCID: PMC544180.
42. Grzegorzewicz AE, Pham H, Gundi VA, Scherman MS, North EJ, Hess T, et al. Inhibition of mycolic acid transport across the Mycobacterium tuberculosis plasma membrane. *Nat Chem Biol.* 2012;8(4):334-41. doi: 10.1038/nchembio.794. PubMed PMID: 22344175; PubMed Central PMCID: PMC3307863.
43. Kremer L, Maughan WN, Wilson RA, Dover LG, Besra GS. The M. tuberculosis antigen 85 complex and mycolyltransferase activity. *Lett Appl Microbiol.* 2002;34(4):233-7. PubMed PMID: 11940150.
44. Converse SE, Mougous JD, Leavell MD, Leary JA, Bertozzi CR, Cox JS. MmpL8 is required for sulfolipid-1 biosynthesis and Mycobacterium tuberculosis virulence. *Proc Natl Acad Sci U S A.* 2003;100(10):6121-6. doi: 10.1073/pnas.1030024100. PubMed PMID: 12724526; PubMed Central PMCID: PMC156336.
45. Belardinelli JM, Larrouy-Maumus G, Jones V, Sorio de Carvalho LP, McNeil MR, Jackson M. Biosynthesis and translocation of unsulfated acyltrehaloses in Mycobacterium tuberculosis. *J Biol Chem.* 2014;289(40):27952-65. doi: 10.1074/jbc.M114.581199. PubMed PMID: 25124040; PubMed Central PMCID: PMC4183827.

46. Domenech P, Reed MB, Barry CE, 3rd. Contribution of the *Mycobacterium tuberculosis* MmpL protein family to virulence and drug resistance. *Infect Immun*. 2005;73(6):3492-501. doi: 10.1128/IAI.73.6.3492-3501.2005. PubMed PMID: 15908378; PubMed Central PMCID: PMC1111821.
47. Szekely R, Cole ST. Mechanistic insight into mycobacterial MmpL protein function. *Mol Microbiol*. 2016;99(5):831-4. doi: 10.1111/mmi.13306. PubMed PMID: 26710752.
48. Yang X, Nesbitt NM, Dubnau E, Smith I, Sampson NS. Cholesterol metabolism increases the metabolic pool of propionate in *Mycobacterium tuberculosis*. *Biochemistry*. 2009;48(18):3819-21. doi: 10.1021/bi9005418. PubMed PMID: 19364125; PubMed Central PMCID: PMC2771735.
49. Upton AM, McKinney JD. Role of the methylcitrate cycle in propionate metabolism and detoxification in *Mycobacterium smegmatis*. *Microbiology*. 2007;153(Pt 12):3973-82. doi: 10.1099/mic.0.2007/011726-0. PubMed PMID: 18048912.
50. Griffin JE, Pandey AK, Gilmore SA, Mizrahi V, McKinney JD, Bertozzi CR, et al. Cholesterol catabolism by *Mycobacterium tuberculosis* requires transcriptional and metabolic adaptations. *Chem Biol*. 2012;19(2):218-27. doi: 10.1016/j.chembiol.2011.12.016. PubMed PMID: 22365605; PubMed Central PMCID: PMC3292763.
51. He H, Hovey R, Kane J, Singh V, Zahrt TC. MprAB is a stress-responsive two-component system that directly regulates expression of sigma factors SigB and SigE in *Mycobacterium tuberculosis*. *J Bacteriol*. 2006;188(6):2134-43. doi: 10.1128/JB.188.6.2134-2143.2006. PubMed PMID: 16513743; PubMed Central PMCID: PMC1428128.
52. Brooks BE, Buchanan SK. Signaling mechanisms for activation of extracytoplasmic function (ECF) sigma factors. *Biochim Biophys Acta*. 2008;1778(9):1930-45. doi: 10.1016/j.bbamem.2007.06.005. PubMed PMID: 17673165; PubMed Central PMCID: PMC2562455.
53. Manganelli R, Provvedi R, Rodrigue S, Beaucher J, Gaudreau L, Smith I. Sigma factors and global gene regulation in *Mycobacterium tuberculosis*. *J Bacteriol*. 2004;186(4):895-902. PubMed PMID: 14761983; PubMed Central PMCID: PMC344228.
54. Manganelli R. Sigma Factors: Key Molecules in *Mycobacterium tuberculosis* Physiology and Virulence. *Microbiol Spectr*. 2014;2(1):MGM2-0007-2013. doi: 10.1128/microbiolspec.MGM2-0007-2013. PubMed PMID: 26082107.
55. Veyrier F, Said-Salim B, Behr MA. Evolution of the mycobacterial SigK regulon. *J Bacteriol*. 2008;190(6):1891-9. doi: 10.1128/JB.01452-07. PubMed PMID: 18203833; PubMed Central PMCID: PMC2258859.
56. Kao FF, Mahmuda S, Pinto R, Triccas JA, West NP, Britton WJ. The secreted lipoprotein, MPT83, of *Mycobacterium tuberculosis* is recognized during human tuberculosis and stimulates protective immunity in mice. *PLoS One*. 2012;7(5):e34991. doi: 10.1371/journal.pone.0034991. PubMed PMID: 22567094; PubMed Central PMCID: PMC3342273.
57. Shukla J, Gupta R, Thakur KG, Gokhale R, Gopal B. Structural basis for the redox sensitivity of the *Mycobacterium tuberculosis* SigK-RskA sigma-anti-sigma complex. *Acta Crystallogr D Biol Crystallogr*. 2014;70(Pt 4):1026-36. doi: 10.1107/S1399004714000121. PubMed PMID: 24699647.

58. Lee JH, Karakousis PC, Bishai WR. Roles of SigB and SigF in the *Mycobacterium tuberculosis* sigma factor network. *J Bacteriol.* 2008;190(2):699-707. doi: 10.1128/JB.01273-07. PubMed PMID: 17993538; PubMed Central PMCID: PMCPMC2223694.
59. Dainese E, Rodrigue S, Delogu G, Proveddi R, Laflamme L, Brzezinski R, et al. Posttranslational regulation of *Mycobacterium tuberculosis* extracytoplasmic-function sigma factor sigma L and roles in virulence and in global regulation of gene expression. *Infect Immun.* 2006;74(4):2457-61. doi: 10.1128/IAI.74.4.2457-2461.2006. PubMed PMID: 16552079; PubMed Central PMCID: PMCPMC1418919.
60. Hugonnet JE, Tremblay LW, Boshoff HI, Barry CE, 3rd, Blanchard JS. Meropenem-clavulanate is effective against extensively drug-resistant *Mycobacterium tuberculosis*. *Science.* 2009;323(5918):1215-8. doi: 10.1126/science.1167498. PubMed PMID: 19251630; PubMed Central PMCID: PMCPMC2679150.
61. Saint-Joanis B, Demangel C, Jackson M, Brodin P, Marsollier L, Boshoff H, et al. Inactivation of Rv2525c, a substrate of the twin arginine translocation (Tat) system of *Mycobacterium tuberculosis*, increases beta-lactam susceptibility and virulence. *J Bacteriol.* 2006;188(18):6669-79. doi: 10.1128/JB.00631-06. PubMed PMID: 16952959; PubMed Central PMCID: PMCPMC1595485.
62. Posey JE, Shinnick TM, Quinn FD. Characterization of the twin-arginine translocase secretion system of *Mycobacterium smegmatis*. *J Bacteriol.* 2006;188(4):1332-40. doi: 10.1128/JB.188.4.1332-1340.2006. PubMed PMID: 16452415; PubMed Central PMCID: PMCPMC1367255.
63. McDonough JA, Hacker KE, Flores AR, Pavelka MS, Jr., Braunstein M. The twin-arginine translocation pathway of *Mycobacterium smegmatis* is functional and required for the export of mycobacterial beta-lactamases. *J Bacteriol.* 2005;187(22):7667-79. doi: 10.1128/JB.187.22.7667-7679.2005. PubMed PMID: 16267291; PubMed Central PMCID: PMCPMC1280313.
64. Dinesh N, Sharma S, Balganes M. Involvement of efflux pumps in the resistance to peptidoglycan synthesis inhibitors in *Mycobacterium tuberculosis*. *Antimicrob Agents Chemother.* 2013;57(4):1941-3. doi: 10.1128/AAC.01957-12. PubMed PMID: 23335736; PubMed Central PMCID: PMCPMC3623302.
65. Hartkoorn RC, Uplekar S, Cole ST. Cross-resistance between clofazimine and bedaquiline through upregulation of MmpL5 in *Mycobacterium tuberculosis*. *Antimicrob Agents Chemother.* 2014;58(5):2979-81. doi: 10.1128/AAC.00037-14. PubMed PMID: 24590481; PubMed Central PMCID: PMCPMC3993252.

## CHAPTER FOUR

### Collapse of PMF and ETC blockage in mycobacteria by 2-aminoimidazoles

This chapter covers the investigation into the unifying mechanism that could potentially explain defects in both cell envelope lipid export and protein secretion of *M. tuberculosis* with 2-AI compounds treatment. We focused on the fact that both processes require proton motive force generated through membrane bioenergetics culminating in ATP synthesis. Thus, we evaluated if 2-AI compounds affect proton motive force and other relevant parameters related to membrane bioenergetics. Herein, it is reported that 2B8 effectively collapsed both components of proton motive force,  $\Delta\psi$  and  $\Delta\text{pH}$ . In addition, we showed that 2B8 blocks mycobacterial ETC, resulting in perturbation of bioenergetics homeostasis. Not only do these findings support the mechanism of  $\beta$ -lactam potentiation, but also provide the foundation to further develop 2-AI compounds targeting bacterial bioenergetics, a highly pursued area of research for new antimicrobial drug discovery.

#### 4.1. Introduction

During the rapid phase of antibiotics discovery and development between 1950s and 1980s, numerous drugs were developed to specifically target biosynthesis of bacterial DNA, RNA, proteins, and cell wall [1]. One caveat of these early-developed drugs was that these antibiotics are not effective in eliminating bacteria with low metabolic rates but rather were designed to target processes that dominate in organisms involved in active division. Many of the clinically important bacterial infections include microbial populations that are metabolically quiescent such as non-replicating *M. tuberculosis*, which contributes to the pathogenesis of persistent TB infections [2]. Therefore, interest in developing antimicrobial drugs that specifically target quiescent bacteria is growing. Targeting bacterial cell membrane and associated bioenergetics can be an effective approach to achieve such goals [3]. Indeed, recently approved antibiotics such as daptomycin and telavancin for *Staphylococcus aureus* treatment

demonstrate the effectiveness of disrupting functions of membrane-bound proteins involved in ETC within cell membrane even in bacterial populations that are not rapidly dividing [4-6].

Targeting mycobacterial bioenergetics therapeutically is a highly promising yet recently emerging field of research in terms of novel drug target discovery. The most recently developed anti-TB drug approved by FDA is BDQ, targets the subunit c of mycobacterial ATP synthase, which is essential for both rapidly dividing and non-replicating bacilli [7]. Additionally, there are multiple drug candidates that target bioenergetics specifically such as clofazimine, nitroimidazoles, and aminoalkoxydiphenylmethane, IPA derivatives (Q203) intended for TB therapy, which are in the discovery phase or in clinical trials [8-11]. Clofazimine induces membrane depolarization and reactive oxygen species release and nitroimidazoles exert anti-TB effects through a complex mode of action involving nitric oxide release and intracellular ATP depletion [12, 13]. Ro 48-8071, an aminoalkoxydiphenylmethane derivative, inhibits menaquinone biosynthesis resulting in ETC blockage [10]. The value of such antimicrobial agents targeting membrane bioenergetics stems from the essentiality of proper membrane function in both metabolically active and inactive bacteria needed to generate proton motive force required for numerous biological processes like protein secretion and macromolecules transport across the membrane.

From previous studies described in chapter 3, we observed two key findings linking mycobacterial bioenergetics as a possible mechanism of action of 2-AI compounds. Treatment with 2-AI compounds resulted in: 1) TMM accumulation with a concomitant decrease of TDM as determined by metabolic labeling experiments and 2) generalized decrease of protein secretion into the *M. tuberculosis* CFP. TMM biosynthesis takes place at the cytoplasmic side of the cell membrane and translocated across the cell membrane by Mmp13 [14, 15]. Being a RND family protein, Mmp13 requires sustained proton gradient to properly function [14, 16, 17]. On a similar note, protein secretion across the cell membrane also requires ATP generated through proton motive force [18]. Thus, we posited that 2-AI compounds may be affecting mycobacterial membrane bioenergetics, leading to a collapse of the proton motive force, thus compromising lipid and protein exports across the cell membrane.

In this study, we evaluated multiple parameters of mycobacterial bioenergetics in the presence of 2-AI compounds with the idea that this approach could provide us with a unifying mechanism underlying  $\beta$ -lactam potentiation and further elucidation of 2-AI compounds' target in *M. tuberculosis*.

## 4.2. Materials and methods

### 4.2.1. Bacterial strains, media, and culture conditions

Stock cultures of BSL1 strain *M. smegmatis* mc<sup>2</sup>155 and BSL2 strain *M. tuberculosis* H37Rv mc<sup>2</sup> 6206 were frozen in glycerol stock media (50% v/v glycerol, 7H9, ADC, Tween 80) at -80°C prior to use. For propagation of initial culture for *M. smegmatis*, frozen stocks were thawed and sub-cultured in Middlebrook 7H9 media with OADC (0.005% oleic acid, 0.5% bovine serum albumin fraction V, 0.2% dextrose, 0.0003% catalase), 0.2% glycerol, and 0.05% Tween 80. For assays, cultures in logarithmic phase were centrifuged ( $\times 1,700g$ ) and resuspended in 7H9 media supplemented with 0.2% dextrose and glycerol. 7H9 and OADC were purchased from BD. Glycerol, dextrose and Tween 80 were purchased from Sigma-Aldrich. For experiments using the *M. tuberculosis* H37Rv mc<sup>2</sup> 6206, bacteria was grown as previously described in Chapter 3.

### 4.2.2. Kinetic measurement of alamarBlue® reduction

*M. smegmatis* and *M. tuberculosis* were cultured to an OD<sub>600</sub> of 0.5 in 7H9 media supplemented with 0.2% dextrose (for *M. tuberculosis*, 0.005% L-leucine, 0.2% casamino acid, 0.0048% D-panthothenic acid, and 0.0025% kanamycin were added as described in chapter 3). After being adjusted to specific ODs (0.4 for *M. smegmatis*, 1.0 for *M. tuberculosis*), a total of 100  $\mu$ L for each culture was distributed to clear-bottomed black-walled 96-well cell culture plate (Corning, USA). Cultures were treated with DMSO, 2B8, RA13 (7.825 to 250  $\mu$ M), 15  $\mu$ M CCCP (Sigma-Aldrich, USA), 18  $\mu$ M BDQ (BOC Sciences, Shirley, NY, USA), or 80  $\mu$ M TRZ (Sigma-Aldrich). Immediately after treatment, 10  $\mu$ L of alamarBlue® reagent was added to all wells. Using Biotek Synergy 2 multi-mode plate reader (Biotek, Winooski, VT, USA), fluorescence was measured with 530<sub>ex</sub>/590<sub>em</sub> filter. For *M. smegmatis*, signal was

measured for 40 min every 20 min and for *M. tuberculosis*, signal was measured for 150 min every 10 min.

#### **4.2.3. Determination of $\Delta\psi$ by DiSC<sub>3</sub>(5)**

Determination of *M. smegmatis*  $\Delta\psi$  with 2-AI treatment was done using a membrane potential sensitive fluorescent probe 3,3'-dipropylthiodicarbocyanine (DiSC<sub>3</sub>(5), Life Technologies, Carlsbad, CA, USA) as previously described with some modifications [16, 19]. *M. smegmatis* was cultured to an OD<sub>600</sub> of 0.5 in 7H9 media with 0.2% dextrose and glycerol. On the day of the experiment, culture was diluted to OD<sub>600</sub> of 0.3. Prior to the assay, 10 mM dextrose and 1  $\mu$ M nigericin (Sigma-Aldrich, USA) were additionally added to the culture. Total of 100  $\mu$ L culture was distributed to clear-bottomed, black-walled 96-well cell culture plate (Corning, USA). After addition of 5  $\mu$ M DiSC<sub>3</sub>(5), fluorescence quenching due to bacterial uptake was monitored by fluorescence at 600<sub>ex</sub>/680<sub>em</sub>, 30<sup>0</sup>C in a Biotek Synergy HT multi-mode plate reader (Biotek). Once fluorescence was quenched, DMSO or different concentrations of 2-AI compounds (2B8 and RA13, 31.25 to 125  $\mu$ M), 15  $\mu$ M CCCP, 18  $\mu$ M BDQ, and 80  $\mu$ M TRZ were added. Depolarization of the membrane potential was determined by continuously monitoring fluorescence reversal due to bacterial release of the dye.

#### **4.2.4. Generation of inverted membrane vesicles**

Preparation of inverted membrane vesicles (IMVs) from *M. smegmatis* cells was done following the method previously described with some modifications [20]. In brief, net weight of 5 g of *M. smegmatis* cells were resuspended in 50 mM MOPS buffer (pH 7.5) with 2 mM MgCl<sub>2</sub> (Sigma-Aldrich, USA) and protease inhibitor cocktail (Roche, Basel, Switzerland). Suspension was stirred for 1 h at room temperature with 1.2 mg/mL lysozyme (Sigma-Aldrich, USA). Subsequently, 0.2 mg/mL DNase I (Sigma-Aldrich, USA) was added and MgCl<sub>2</sub> was further added to achieve final concentration of 15 mM. Cells were subjected to lysis by passing through a pre-chilled FrenchPress at 20,000 psi (Thermo Electron, Waltham, MA, USA) for six times on ice. Lysate was initially centrifuged at 3,000 $\times$ g for 30 min to

remove unbroken cells, then the supernatant was further centrifuged at 27,000×g for 30 min to remove cell wall. Again, the supernatant was collected and centrifuged at 100,000×g using an ultracentrifuge (Beckman Coulter, Brea, CA, USA) for 1 h to finally harvest membrane vesicles. IMVs were resuspended in 50 mM MOPS buffer (pH 7.5, 2 mM MgCl<sub>2</sub>) and protein concentration was measured by Pierce BCA protein assay (Thermo Scientific, Waltham, MA, USA). Glycerol was added up to a final concentration of 10% and aliquots of IMVs were stored in -80°C until further use.

#### **4.2.5. Determination of ΔpH with IMVs**

Translocation of protons into *M. smegmatis* IMVs was determined as previously described, but using the pH-sensitive fluorescent dye 9-amino-6-chloro-2-methoxyacridine (ACMA, Life Technologies, USA) instead of acridine orange [21]. The assay buffer contained 10 mM HEPES (pH 7.5), 100 mM KCl, 5 mM MgCl<sub>2</sub> (Sigma-Aldrich, USA). In a clear-bottomed, black-walled 96-well cell culture plate, (Corning, USA), a total of 0.1125 mg/mL IMVs were pre-incubated with 2 μM ACMA at 37°C for 30 minutes and baseline 410<sub>ex</sub>/480<sub>em</sub> fluorescence was measured using a Biotek Synergy HT multi-mode plate reader (Biotek, USA). Quenching of ACMA fluorescence was initiated by adding 5 mM NADH. When ACMA fluorescence quenching was saturated, IMVs were treated with DMSO or different concentrations of 2-AI compounds (2B8 and RA13, 31.25 to 125 μM), 15 μM CCCP, 18 μM BDQ, 80 μM TRZ, and 10 μM nigericin. Reversal of fluorescence was measured for an additional 4 minutes.

#### **4.2.6. Real-time measurement of oxygen consumption rate by high-resolution respirometry**

Oxygen consumption of *M. smegmatis* in the presence of 2-AI compounds and other drugs were monitored in real-time using Oroboros Oxygraph-2k (<http://www.orooboros.at>, Oroboros Instruments, Innsbruck, Austria). Oxygen consumption rates (OCR) were directly obtained through Datlab4 software (Oroboros Instruments). Mid-log phase *M. smegmatis* or *M. tuberculosis* cultures were adjusted to an OD<sub>600</sub> of 0.5 as described above in 7H9 media with 0.2% dextrose and glycerol. Either media with BSA or without BSA were used. For experiments using media with BSA, media was supplemented further with

0.5% fatty acid-free BSA (Sigma-Aldrich). The chambers of Oroboros Oxygraph-2k, were filled with 2.5 mL of media and interior oxygen level (nmol/mL) and OCR (pmol/s×mL) were measured and calibrated without any bacteria. Using a Hamilton Microliter Syringes (Hamilton Company, Reno, NV, USA), 100  $\mu$ L (*M. smegmatis*) or 400  $\mu$ L (*M. tuberculosis*) culture was injected into the chambers. The initial baseline OCR level with non-treated bacteria was recorded and equilibrated. Subsequently, 2-AI compounds, CCCP, BDQ, or TRZ were injected as indicated in each experiment while OCR was continuously measured in real-time and normalized to approximate CFUs.

#### **4.2.7. Determination of 2-AI compounds MICs against mycobacteria with or without BSA**

*M. smegmatis* and *M. tuberculosis* H37Rv mc<sup>2</sup> 6206 were cultured to an OD<sub>600</sub> of 0.5 7H9 media with OADC supplement as described above. Cultures were washed with sterile PBS and diluted 1:20 the original OD in 7H9 media supplemented with 0.2% dextrose and glycerol with or without 0.5% fatty acid free-BSA. Total of 200  $\mu$ L cultures was distributed in 96-well cell culture plate per wells (Corning). Different concentrations of 2-AI compounds (2B8 and RA13, 3.91  $\mu$ M to 1 mM) were added to cultures and incubated at 37<sup>0</sup>C stationary for 48 h (*M. smegmatis*) or 5 days (*M. tuberculosis*). Total of 20  $\mu$ L alamarBlue<sup>®</sup> (Life Technologies) was added to each well and incubated for additional 6 h (*M. smegmatis*) or two days (*M. tuberculosis*). Color reduction of alamarBlue<sup>®</sup> reagent to violet or purple was recorded as growth. MIC was determined as the lowest concentration of 2-AI compounds that prevented color reduction of alamarBlue<sup>®</sup>.

#### **4.2.8. Quantification of intracellular ATP**

*M. tuberculosis* was cultured to an OD<sub>600</sub> of 0.5 and treated with DMSO, three concentrations of 2B8 and RA13 (31.25, 62.5, and 125  $\mu$ M), 15  $\mu$ M CCCP, 18  $\mu$ M BDQ, 80  $\mu$ M TRZ. Treated cultures were incubated at 37<sup>0</sup>C, for 2 or 24 h under agitation. Thereafter, cultures were centrifuged ( $\times$  1,700g), washed one time with sterile PBS, and reconstituted in 500  $\mu$ L PBS. Reconstituted bacterial cells were transferred to screw-cap 2 mL microtubes (Fisher Scientific, Waltham, MA, USA) with 100  $\mu$ m Zirconia

beads (Biospec, Bartlesville, OK, USA). Cells were lysed by bead-beating six times for 30 sec and cooling on ice for one min in between. Samples were briefly centrifuged and a total of 100  $\mu$ L of supernatant was transferred to clear-bottomed white-walled 96-well cell culture plate (Corning, USA). ATP concentration was quantified using BacTiter-Glo™ Microbial Cell Viability Assay (Promega, Madison, WI, USA) as previously described following the manufacturer's instruction with some modifications [22]. Briefly, equal volume of sample and BacTiter-Glo™ reagent were mixed. After shaking the plate at RT for 5 min, luminescence at 550 nm was recorded using Biotek Synergy 2 multi-mode plate reader. Before bead-beating, a portion of cultures were also plated on 7H11 agar (BD, USA) for CFU enumeration. Data were represented as relative luminescence units (RLUs)/viable CFUs.

#### **4.2.9. ETC activity assay with IMVs**

The ETC activity was measured as previously described with minor modifications [23]. Briefly, 5  $\mu$ L of 0.1125 mg/mL *M. smegmatis* IMVs were distributed to a clear-bottomed, transparent 96-well cell culture plate (Corning, USA) and a total of 20  $\mu$ L 10 mM HEPES (pH 7.5) buffer were added. Subsequently, 25  $\mu$ L of 4 mM 2-(*p*-idophenyl)-3-(*p*-nitrophenyl)-5-phenyl tetrazolium chloride (INT, Sigma-Aldrich) were added to each well. Drug treatments were made by adding DMSO, four concentrations of 2B8 (62.5  $\mu$ M to 125  $\mu$ M), 125  $\mu$ M RA13, 15  $\mu$ M CCCP, 18  $\mu$ M BDQ, 80  $\mu$ M TRZ, and 5 mM potassium cyanide (KCN, Signa-Aldrich). A total of 75  $\mu$ L PBS substrate solution containing 0.2 % Triton X-100 (Sigma-Aldrich, USA) with 1 mM NADH or 130 mM sodium succinate (Sigma-Aldrich, USA) or both was added to wells and the 490 nm absorbance was immediately monitored at 37°C for 10 minutes using SpectraMax M series multi-mode plate reader (Molecular Devices, Sunnyvale, CA, USA).

#### **4.2.10. Determination of NADH/NAD<sup>+</sup> ratio**

NADH/NAD<sup>+</sup> ratio after 2-AI compounds treatment was determined as previously described with minor modifications [24]. *M. tuberculosis* H37Rv mc<sup>2</sup> 6206 was cultured to an OD<sub>600</sub> of 0.5. For 1 mL of

culture, three different concentrations of 2B8 or RA13 (31.25, 62.5, 125  $\mu\text{M}$ ), 15  $\mu\text{M}$  CCCP, 18  $\mu\text{M}$  BDQ, 80  $\mu\text{M}$  TRZ were added. After treatment for 2 or 24 h at 37 $^{\circ}\text{C}$ , cultures were split into two 500  $\mu\text{L}$  aliquots (for separate extraction of NADH and NAD $^{+}$ ). Aliquots were centrifuged ( $\times$  1,700g) and media were removed. A total of 300  $\mu\text{L}$  of 0.2 M HCl (for NAD $^{+}$  extraction) or 0.2 M NaOH (for NADH extraction) was added and placed in 55 $^{\circ}\text{C}$  water bath for 10 min, followed by immediate cooling on ice. After cooling, sample pH was neutralized with 300  $\mu\text{L}$  0.1 M NaOH (for NAD $^{+}$  extraction) or 0.1 M HCl (for NADH extraction), respectively. After a brief centrifugation step to remove precipitates, 50  $\mu\text{L}$  of supernatant was transferred to a clear-bottomed 96-well cell culture plate (Corning, USA). NADH or NAD $^{+}$  was quantified using the NADH/ NAD $^{+}$  quantification kit from Sigma-Aldrich per the manufacturer's instructions. Briefly, NAD $^{+}$  cycling enzyme mix (100  $\mu\text{L}$  total volume) was added to 50  $\mu\text{L}$  samples and incubated for 5 min at RT, under constant shaking to convert NAD $^{+}$  to NADH. Then 10  $\mu\text{L}$  of NADH developer was added to each well and incubated at RT for 1 to 2 h until color development. End point absorbance (450 nm) was measured using a Biotek Synergy multi-mode plate reader (Biotek, USA) and the NADH/NAD $^{+}$  ratio was calculated.

#### **4.2.11. Determination of NADH oxidation by IMVs**

NADH oxidation was measured using fluorescence at 480 nm when excited at 340 nm as previously described [25]. *M. smegmatis* IMVs at 0.1125 mg/mL were resuspended in 10 mM HEPES (pH 7.5), 100 mM KCl, 5 mM MgCl $_2$  (Sigma-Aldrich, USA) and 10 mM NADH. A total of 100  $\mu\text{L}$  aliquots were distributed in a clear-bottomed, black-walled 96-well cell culture plate (Corning, USA) containing DMSO, four concentrations of 2B8 (62.5  $\mu\text{M}$  to 125  $\mu\text{M}$ ), 125  $\mu\text{M}$  RA13, 15  $\mu\text{M}$  CCCP, 18  $\mu\text{M}$  BDQ, 80  $\mu\text{M}$  TRZ, or 5 mM KCN. Thereafter, the fluorescence (340 $_{\text{ex}}$ /480 $_{\text{em}}$ ) was monitored using a Biotek Synergy HT multi-mode plate reader (Biotek, USA) at 37 $^{\circ}\text{C}$  for 9 minutes.

#### 4.2.12. Rescue of NADH oxidation block with clofazimine

NADH oxidation assay were set up as described above. *M. smegmatis* IMVs were incubated with 10 mM NADH in the presence of 125  $\mu$ M 2B8, 80  $\mu$ M TRZ or 5 mM KCN and NADH oxidation was monitored for 2 min. Thereafter, to determine if clofazimine (CFZ, Sigma-Aldrich, USA) could rescue the block of NADH oxidation by acting as an alternative electron acceptor for NDH-2 [26], 42  $\mu$ M CFZ or DMSO was added and NADH oxidation was monitored for additional 10 minutes. CFZ or DMSO addition followed by monitoring its effect on NADH oxidation was repeated one more time.

#### 4.2.13. $\beta$ -lactam potentiation assay with bioenergetics-affecting drugs

MICs of CCCP, BDQ, TRZ, valinomycin, and nigericin against *M. tuberculosis* H37Rv mc<sup>2</sup> 6206 was determined by a broth microdilution method as previously described in Chapter 2. Determination of carbenicillin and meropenem MICs against mycobacteria with or without bioenergetics-affecting drugs at their 50% MIC was carried out by using a broth microdilution method with alamarBlue<sup>®</sup> (Invitrogen, Carlsbad, CA, USA). Briefly, carbenicillin and meropenem were serially two-fold diluted in 7H9 media starting from the following concentrations: 1024 mg/L carbenicillin and 16 mg/L meropenem. *M. tuberculosis* H37Rv mc<sup>2</sup> 6206 was grown in 7H9 media to an OD<sub>600</sub> of 0.4 to 0.6 and further diluted 1:20 to be inoculated to wells containing  $\beta$ -lactams. CCCP 10  $\mu$ M, BDQ 0.063  $\mu$ M, TRZ 31.25  $\mu$ M, valinomycin 7.83  $\mu$ M (Sigma-Aldrich), and nigericin 7.83  $\mu$ M (Sigma-Aldrich) were added and plates were incubated under stationary conditions at 37<sup>o</sup>C. After 5 days, 20  $\mu$ L alamarBlue<sup>®</sup> was added to each well and incubated for an additional 48 h. Bacterial growth in each well was recorded where blue color was scored as no growth and purple to pink color was scored as growth. Finally, the lowest drug concentration that prevented color change from blue to purple or pink was determined as the MICs and MICs of  $\beta$ -lactams alone was divided by MICs of  $\beta$ -lactams combined with drugs to calculate fold-reduction of MIC resulting from drug treatment.

#### 4.2.14. Statistical analysis

Statistical analyses were carried out using one way ANOVA with Tukey's post hoc test using Graphpad Prism 5 (GraphPad Software, La Jolla, CA, USA). P values less than 0.05 were considered significant.

### 4.3. Results

#### 4.3.1. 2B8 alters mycobacterial redox potential

We initially evaluated reduction of alamarBlue<sup>®</sup> in the presence of 2-AI compound to evaluate mycobacterial redox potential [27]. Fluorescence was monitored to detect an increase of the reduced form of this reagent. In *M. smegmatis*, while 2B8 31.25  $\mu$ M and RA13 125  $\mu$ M treatment did not produce any difference in alamarBlue<sup>®</sup> reduction, 2B8 62.5 and 125  $\mu$ M resulted in significant inhibition of alamarBlue<sup>®</sup> reduction. Among additionally tested drugs, CCCP 15  $\mu$ M and TRZ 80  $\mu$ M also inhibited alamarBlue<sup>®</sup> reduction (Figure 4.1A). TRZ 80  $\mu$ M treatment was the most potent drug in inhibiting alamarBlue<sup>®</sup> reduction in both *M. smegmatis* and *M. tuberculosis*. A similar trend was observed in *M. tuberculosis*, but interestingly, 2B8 62.5  $\mu$ M did not inhibit alamarBlue<sup>®</sup> reduction significantly in *M. tuberculosis* in contrast to the result in *M. smegmatis*. The rest of treatments yielded similar observations (Figure 4.1B). Taken together, these results suggest that 2B8 alters redox potential of mycobacteria.

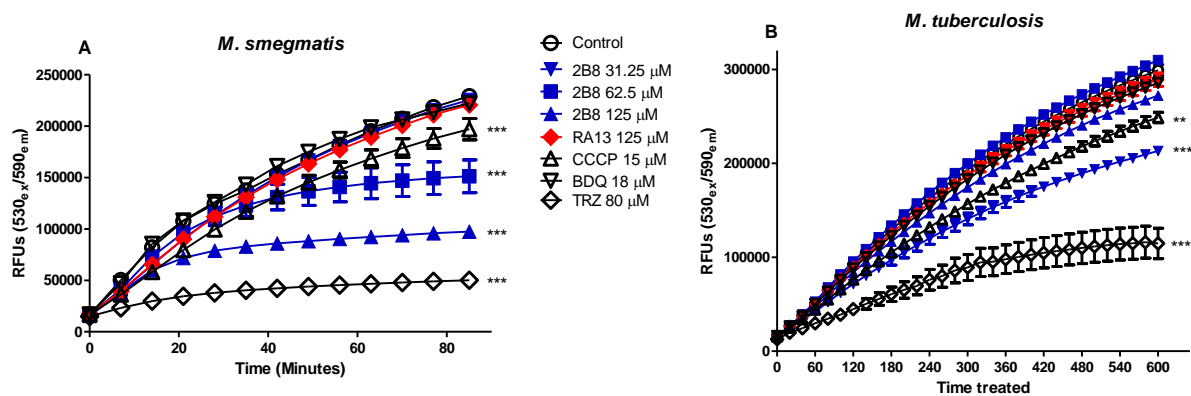


**Figure 4.1. 2B8 inhibits alamarblue® reduction by mycobacteria.** *M. smegmatis* and *M. tuberculosis* cultures were treated with 2-AI compounds or known drugs that affect mycobacterial bioenergetics, while being monitored for alamarblue® reduction immediately following treatment. A) After 80 min, 62.5 and 125  $\mu\text{M}$  2B8, 15  $\mu\text{M}$  CCCP, and 80  $\mu\text{M}$  TRZ inhibited alamarblue® reduction by *M. smegmatis*. However, 125  $\mu\text{M}$  RA13 and 10 mg/L BDQ did not. B) For *M. tuberculosis*, 125  $\mu\text{M}$  2B8, 15  $\mu\text{M}$  CCCP and 80  $\mu\text{M}$  TRZ inhibited alamarblue® reduction. Unlike the case with *M. smegmatis*, 62.5  $\mu\text{M}$  2B8 did not inhibit alamarblue® reduction significantly. Consistent with data in *M. smegmatis*, 125  $\mu\text{M}$  RA13 and 18  $\mu\text{M}$  BDQ, did not inhibit alamarblue® reduction by *M. tuberculosis*. Experiments were repeated three separate times and representative data are shown. \*  $p < 0.05$ , \*\*  $p < 0.01$ , \*\*\*  $p < 0.001$  by ANOVA.

#### 4.3.2. 2B8 depolarizes mycobacterial membrane potential

Based on our previous findings of 2B8 inhibiting *M. tuberculosis* cell wall lipid export and protein secretion described in Chapter 3, we reasoned that 2B8 collapses proton motive force required for such cellular processes. Proton motive force is collectively established by two parameters;  $\Delta\psi$  and  $\Delta\text{pH}$  [28]. We first evaluated membrane potential of intact *M. smegmatis* with 2-AI compound treatment using a membrane potential-sensitive dye, DiSC<sub>3</sub>(5). All three concentration tested for 2B8 (31.25 to 125  $\mu\text{M}$ ) resulted in immediate depolarization of the membrane upon treatment (Figure 4.2A). Treatment with 5  $\mu\text{M}$  valinomycin and 15  $\mu\text{M}$  CCCP also resulted in abrupt membrane depolarization similar with 2B8 treatments, whereas 80  $\mu\text{M}$  TRZ treatment resulted in gradual and intermediate reversal of fluorescence (Figure 4.2B). However, 125  $\mu\text{M}$  RA13 (Figure 4.2A) and 18  $\mu\text{M}$  BDQ (Figure 4.2B) did not depolarize membranes. Taken together, this result suggests that 2B8 acutely depolarizes mycobacterial membrane potential.

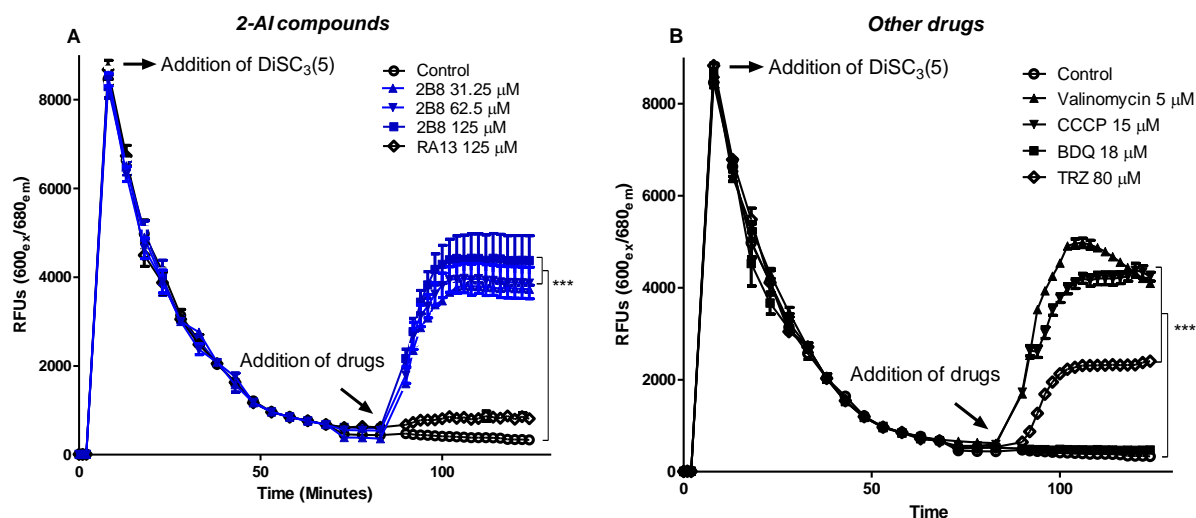


**Figure 4.2. 2B8 depolarizes *M. smegmatis* membrane potential.** Depolarization of *M. smegmatis* cell membrane potential by 2-AI compounds was evaluated using the fluorescent dye DiSC<sub>3</sub>(5). After DiSC<sub>3</sub>(5) was quenched within *M. smegmatis* due to dye uptake, bacteria were treated with different compounds and monitored for fluorescence reversal. Treatment with 31.25, 62.5 and 125 μM 2B8 (A), 5 μM valinomycin, and 15 μM CCCP (B) abruptly reversed the quenching of fluorescence by *M. smegmatis*. In contrast, fluorescence reversal was gradual when *M. smegmatis* was treated with 80 μM TRZ (B) and non-significant with 125 μM RA13 treatment (A) or 18 μM BDQ (B). Experiments were repeated three separate times and representative data are shown. \*\*\* p<0.001.

#### 4.3.4. 2B8 collapses ΔpH of *M. smegmatis* IMVs

Next we evaluated the remaining component of proton motive force, ΔpH, using a pH gradient sensitive dye ACMA with *M. smegmatis* IMVs. All three concentrations of 2B8 tested (31.25 to 125 μM) and 125 μM RA13 resulted in significant fluorescence reversal indicating the collapse of ΔpH, while lower concentrations of RA13 failed to induce dramatic reversal (Figure 4.3A). All other drugs tested including 15 μM CCCP, 18 μM BDQ, 80 μM TRZ, and 10 μM nigericin demonstrated ΔpH collapse indicated by the fluorescence reversal. Collectively with dissipation of Δψ, this result shows that 2B8 collapses proton motive force in mycobacteria.

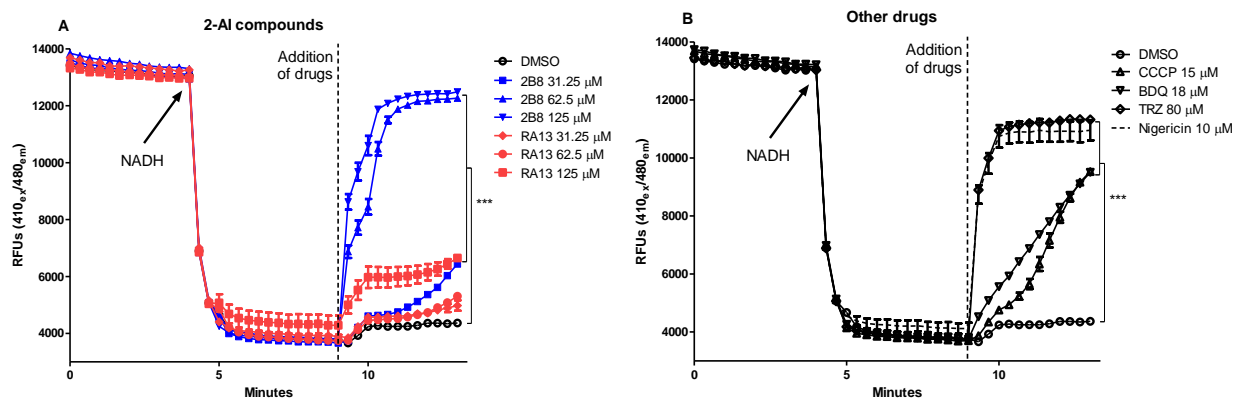


**Figure 4.3. 2B8 collapses  $\Delta$ pH in mycobacterial IMVs.** Collapse of  $\Delta$ pH in *M. smegmatis* IMVs was evaluated using the fluorescent dye ACMA. ACMA fluorescence was quenched by IMVs after addition of NADH (arrow), followed by fluorescence reversal upon addition of different compounds (dotted line). Fluorescence reversals with 62.5 and 125  $\mu$ M 2B8 (A), 10  $\mu$ M nigericin, and 80  $\mu$ M TRZ (B) were more dramatic and immediate compared to the gradual and less prominent reversals observed with 31.25  $\mu$ M 2B8, all tested concentrations of RA13 (A), and 15  $\mu$ M CCCP (B). Experiments were repeated three separate times and representative data are shown. \*\*\*  $p < 0.001$ .

#### 4.3.5. 2B8 uncouples mycobacterial oxidative phosphorylation

In normoxic energized bacterial membranes, the electrons passing through the ETC react with the final electron acceptor  $O_2$  to generate water. In this process, a proton gradient is formed and this drives ATP synthesis from ADP, hence the term oxidative phosphorylation. In essence, oxygen consumption is coupled with ATP synthesis. Increase in oxygen consumption that does not lead to ATP synthesis is therefore referred to as uncoupling effect [29]. Drug such as CCCP is a classical uncoupler because it collapses proton motive force by shuttling protons from outside to inside of the cell membrane[30]. As a result, the ETC is driven without being able to generate ATP and leads to a dramatic increase of oxygen consumption. Knowing 2B8 collapsed proton motive force of mycobacterial membrane, we hypothesized that 2B8 may act similarly with CCCP as an uncoupler. Thus, we evaluated changes in mycobacterial OCR as it was being treated with increasing concentrations of 2B8.

Typically, 7H9 medium used for growing *M. tuberculosis* is supplemented by OADC which has 0.5% bovine serum albumin (BSA). Previously, BSA was reported to strongly bind small molecules such

as CCCP, aspirin, and ibuprofen thus reduce their biological activities [31-33]. When we determined the changes in OCR in *M. smegmatis* in response to 2B8 treatment, a striking difference was observed between the presence and the absence of BSA in the media (Figure 4.4). The presence of BSA affected the outcome of mycobacterial respiration in response to both 2B8 and CCCP. While 70  $\mu\text{M}$  2B8 and 15  $\mu\text{M}$  CCCP continued to increase OCR in the presence of BSA, the increase of OCR was observed at much lower concentrations and 70  $\mu\text{M}$  2B8 and 15  $\mu\text{M}$  CCCP resulted in subsequent decrease in OCR. Additionally, we observed higher MICs for 2B8 against *M. smegmatis* and *M. tuberculosis* when BSA was present in the media (Table 4.1). This result suggested that BSA might be also binding to 2-AI compounds thereby sequestering them from being available to act against the bacteria. Due to this observation, OADC was omitted from the media for subsequent OCR assays and only supplemented with 0.2% dextrose and glycerol.

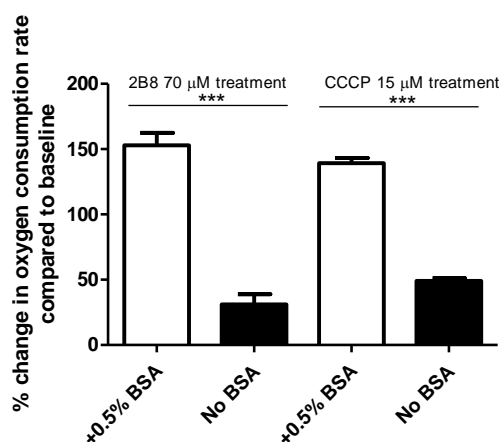


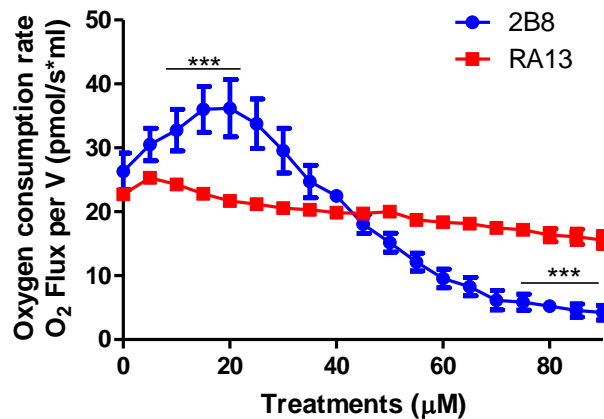
**Figure 4.4. Presence of BSA determines the outcome of 2B8 and CCCP-mediated changes in *M. smegmatis* respiration.** Changes in *M. smegmatis* OCR were determined after adding 2B8 or CCCP in the presence or absence of BSA. In the presence of BSA, 70  $\mu\text{M}$  2B8 or 15  $\mu\text{M}$  CCCP had an uncoupling effect as evidenced by increased *M. smegmatis* OCR. In contrast, *M. smegmatis* OCR was significantly inhibited when these compounds were tested in the absence of BSA. Experiments were repeated three separate times and all data were pooled together for analysis. \*\*\*  $p < 0.001$  by ANOVA.

**Table 4.1. MICs of 2-AI compounds against *M. smegmatis* and *M. tuberculosis* in the presence or the absence of BSA.**

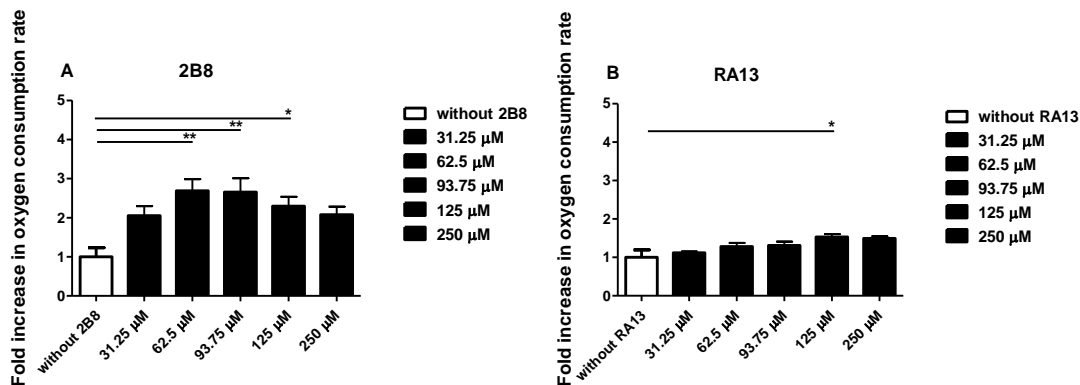
	<i>M. tuberculosis</i> H37Rv mc <sup>2</sup> 6020		<i>M. smegmatis</i>	
	+0.5% BSA	No BSA	+0.5% BSA	No BSA
2B8	250-500	250	125-250	62.5
RA13	> 1000	> 1000	> 1000	> 1000

All MIC values are presented as  $\mu\text{M}$ .

After addressing the problem with BSA, we continued to assess if 2B8 increases oxygen consumption in mycobacteria. In *M. smegmatis*, 2B8 increased OCR in a dose-dependent manner until 20  $\mu\text{M}$ . Additional 2B8 treatment resulted in gradual decrease of oxygen consumption and even reached below the starting baseline level prior to any 2B8 treatment (Figure 4.5). In contrast, RA13 did not exhibit any noticeable increase or decrease of OCR compared to 2B8. A similar trend was observed in *M. tuberculosis*, albeit requiring more than 62.5  $\mu\text{M}$  2B8 to reach the maximum uncoupling effect before the decrease of oxygen consumption begins (Figure 4.6A). Again, RA13 induced minimal changes in OCR in *M. tuberculosis* (Figure 4.6B). Both CCCP and BDQ also showed similar pattern with 2B8 as they increase oxygen consumption at lower concentrations and started to decrease oxygen consumption at higher concentrations (Figure 4.6C and 4.6D). TRZ also increased oxygen consumption, but did not decrease oxygen consumption as other drugs did (Figure 4.6E). In sum, 2B8 increases oxygen consumption at lower concentrations until 62.5  $\mu\text{M}$  where it reaches maximum level of uncoupling, then decreases oxygen consumption. This result suggested that at higher concentrations, 2B8 could also be affecting the ETC.



**Figure 4.5. 2B8 increases *M. smegmatis* respiration at low concentration.** *M. smegmatis* OCR was monitored using high-resolution respirometry. 2B8 or RA13 were added to *M. smegmatis* at 5 µM increments up to 90 µM. Addition of 2B8 (blue dots) significantly increased OCR and the effect reached its maximum level at 20 µM. Thereafter, further addition of 2B8 drastically inhibited *M. smegmatis* respiration, becoming almost undetectable at 90 µM. In contrast, RA13 did not significantly increase or decrease *M. smegmatis* respiration. Experiments were repeated three separate times and replicates were pooled together for analysis. Statistical significance is shown comparing 2B8 and RA13 at the same concentrations. Experiments were repeated twice and representative data are shown. \*\*\* p<0.001.



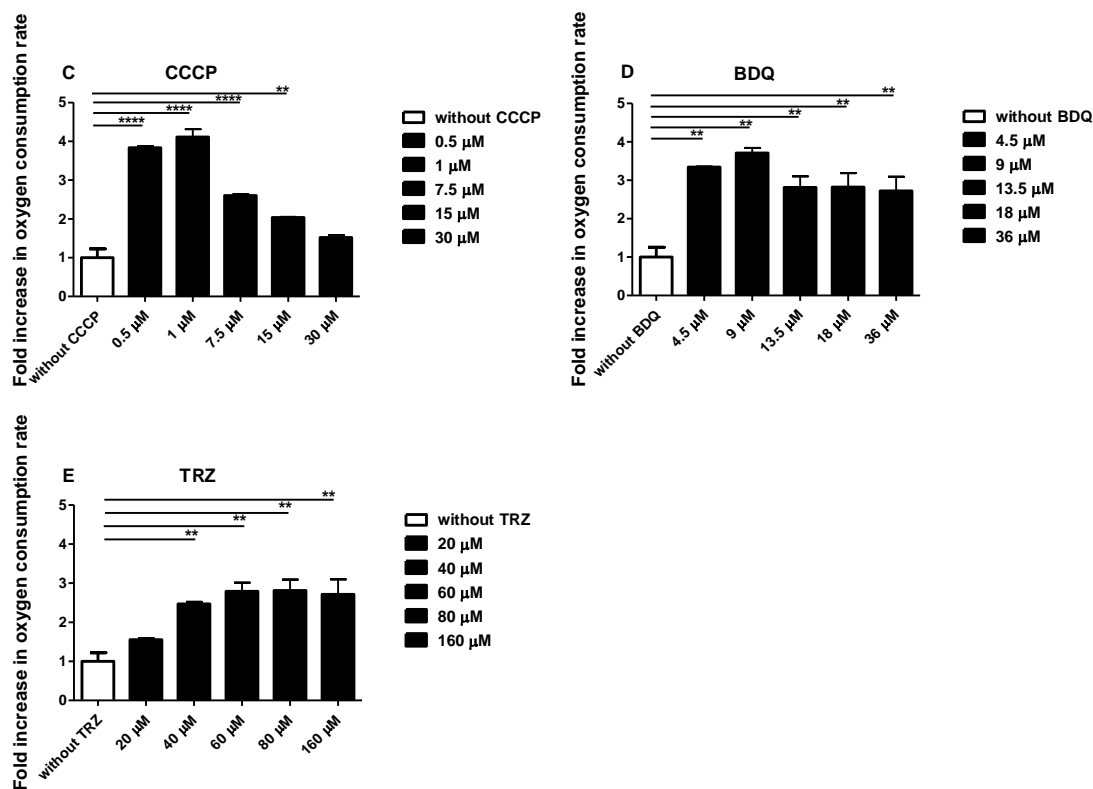


**Figure 4.6. 2B8 increases *M. tuberculosis* respiration at low concentrations.** Oxygen consumption of *M. tuberculosis* mc<sup>2</sup> 6206 strain was monitored in real-time using high-resolution respirometry. The OCR at steady state without any treatments was measured and calibrated, then changes after treatments were shown as fold-increase compared to the steady state without any treatment. A) 2B8 steadily increased OCR until the total concentration reached 93.75 μM. Further addition of 2B8 decreased OCR thereafter. B) RA13 induced minimal changes in OCR, showing only small increase at 125 μM total concentration compared to that of 2B8. C) CCCP dramatically increased OCR at 0.5 and 1 μM then rapidly decreased OCR with higher doses. D) BDQ also dramatically increased OCR until 90 μM and decreased thereafter but maintained elevated OCR unlike CCCP which reverted back to its steady state. E) TRZ also increased OCR until 60 μM and maintained the maximum increased oxygen consumption level upon further addition. Experiments were repeated three different times and all biological replicates were analyzed together. \* p<0.05, \*\* p<0.01, \*\*\* p<0.001 by ANOVA.

#### 4.3.6. 2B8 prevents CCCP from further increase of oxygen consumption

To evaluate if 2B8 could be also affecting the ETC, we performed an experiment in which bacilli were initially treated with 2B8 at low concentration to induce sub-maximal or maximal OCR increase. Thereafter, CCCP was added at small increments to induce further stimulation of bacterial respiration, unless the ETC activity was being blocked by 2B8. *M. tuberculosis* was treated with 39.06 μM and 46.88

$\mu\text{M}$ , concentrations that induce sub-maximal level of oxygen consumption increase, and with  $54.69 \mu\text{M}$  which was approximately the concentration inducing maximal level of OCR. With sub-maximal 2B8 pre-treatment ( $39.06$  and  $46.88 \mu\text{M}$ ),  $0.5 \mu\text{M}$  CCCP was able to additionally increase oxygen consumption. However, pre-treatment with  $54.69 \mu\text{M}$  2B8 prevented CCCP from stimulating additional oxygen consumption increase (Figure 4.7). Since the increase of oxygen consumption requires constant flow of electrons through ETC, this result suggests that 2B8 may be blocking the ETC.

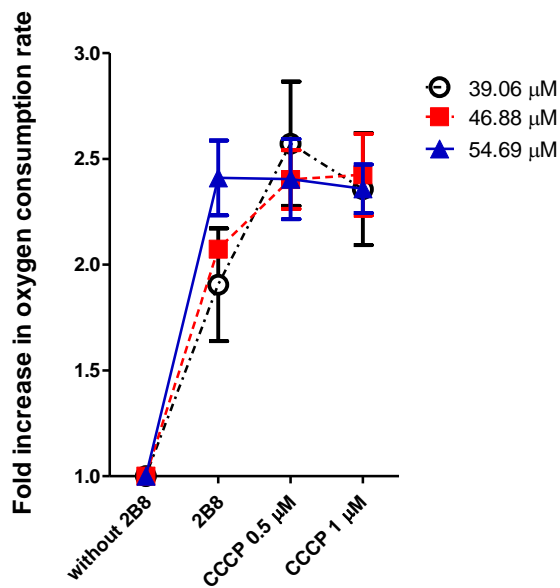


**Figure 4.7. 2B8 prevents CCCP from increasing OCR further.** *M. tuberculosis* was treated with three concentrations of 2B8 ( $39.0625$ ,  $46.8750$ , and  $54.6875 \mu\text{M}$ ) prior to addition of CCCP. At all three concentrations, 2B8 increased oxygen consumption. However, pre-treatment with  $39.0625 \mu\text{M}$  and  $46.8750 \mu\text{M}$  2B8 resulted in a significant increase of OCR with  $0.5 \mu\text{M}$  CCCP whereas pre-treatment of  $54.6875 \mu\text{M}$  did not allow CCCP to increase OCR any higher. Experiments were repeated three different times and all biological replicates were analyzed together.

#### 4.3.7. 2B8 depletes intracellular ATP levels in *M. tuberculosis*

Acting as an uncoupling agent is generally confirmed by fulfilment of three criteria: 1) collapse of proton motive force, 2) increase in oxygen consumption, and 3) decrease in ATP synthesis [29]. We

demonstrated that 2B8 collapsed proton motive force and also increase OCR. Thus, to conclude that 2B8 acts as an uncoupler at low concentrations, we evaluated intracellular ATP levels in 2B8 treated *M. tuberculosis*. After 2 h treatment, 2B8 did not affect *M. tuberculosis* intracellular ATP levels significantly (Figure 4.8A). However, ATP levels decreased after 24 h of 2B8 treatments in a dose dependent manner (Figure 4.8B). In contrast, RA13 did not change ATP levels at both time points. 18 BDQ and 80  $\mu\text{M}$  TRZ reduced ATP levels consistently through both time points. This result indicates that 2B8 depletes intracellular ATP levels in *M. tuberculosis* and confirms that 2B8 act as an uncoupler at low concentrations (31.25 to 62.5  $\mu\text{M}$ ).

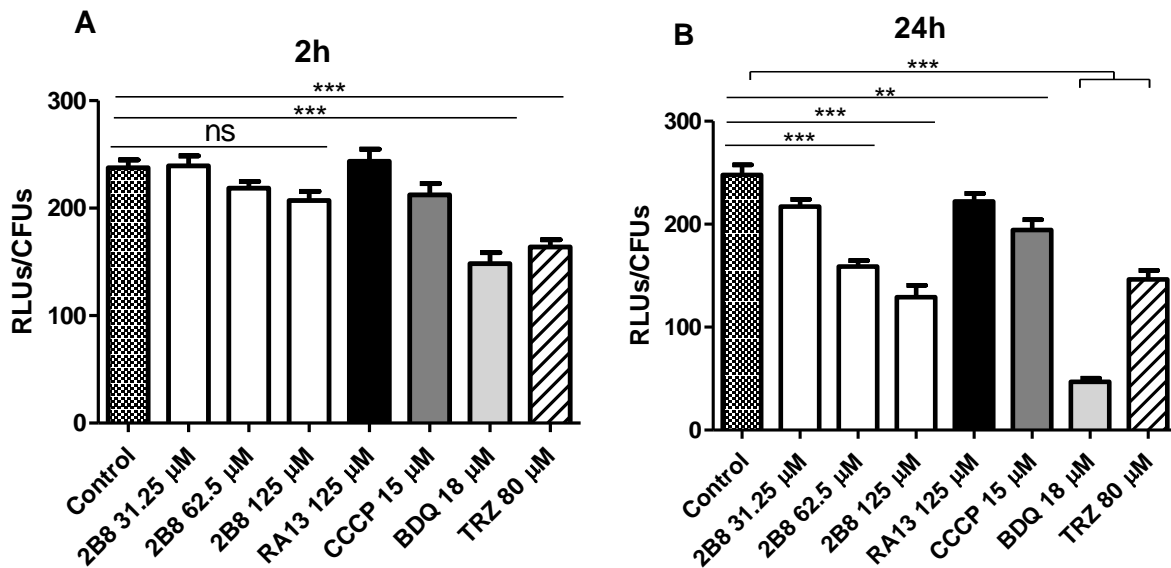
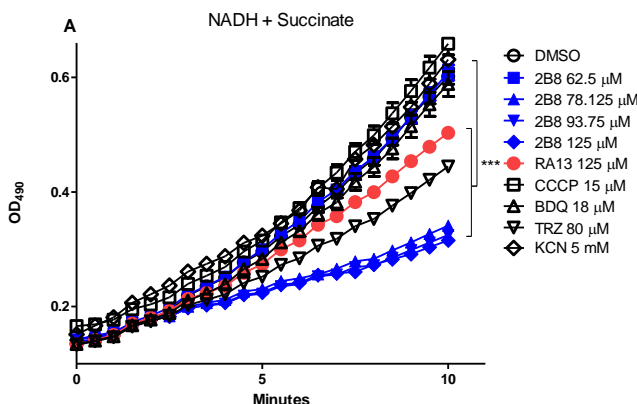


**Figure 4.8. 2B8 reduces *M. tuberculosis* intracellular ATP levels.** After treating *M. tuberculosis* with 2-AI compounds for 2 (A) and 24 (B) h, intracellular ATP was quantified by RLUs. Number of CFUs was also determined in parallel and data normalized to RLUs/CFUs. A) After 2 h treatment, only BDQ and TRZ significantly reduced *M. tuberculosis* intracellular ATP levels. B) After 24 h of treatment, 15  $\mu\text{M}$  CCCP, 62.5 and 125  $\mu\text{M}$  2B8 significantly reduced intracellular ATP, while RA13 had no effect. BDQ and TRZ continued to show significant reduction in ATP levels at 24 h. Experiments were repeated three separate times and all replicates were pooled together for analysis. \*\*  $p < 0.01$ , \*\*\*  $p < 0.001$  by ANOVA.

#### 4.3.8. 2B8 blocks ETC in *M. smegmatis* IMVs

Several results obtained in the above assays suggested that 2B8 might hinder proper electron transfer in the ETC. First of all, at concentrations higher than 62.5  $\mu\text{M}$ , 2B8 decreased OCR and prevented CCCP from further increasing it additionally. Second, 2B8 treatment led to decrease of ATP generation which is the end product of proton motive force established by ETC. Therefore, we directly evaluated ETC activity in *M. smegmatis* IMVs in the presence of 2B8.

The ETC was initiated by providing NADH, succinate or combination of both. When the ETC was initiated with a combination of NADH and succinate, 78.125 to 125  $\mu\text{M}$  2B8, 125  $\mu\text{M}$  RA13, and 80  $\mu\text{M}$  TRZ inhibited its activity (Figure 4.9A). Since INT is reduced prior to cytochrome *c* oxidase [34], treating with KCN did not result in the inhibit INT reduction. As expected, 80  $\mu\text{M}$  TRZ (a NDH-2 inhibitor) potently inhibited ETC activity that was initiated with NADH only (Figure 4.9B), but not when succinate was used (Figure 4.9C). In stark contrast, 78.125 to 125  $\mu\text{M}$  2B8 potently inhibited the ETC activity when initiated by NADH (Figure 4.9B) or succinate (Figure 4.9C), or both (Figure 4.9A). Of all the tested drugs, only 2B8 potently blocked ETC activity consistently in the presence of succinate only. In sum, 2B8 blocks ETC initiated by both NADH and succinate.



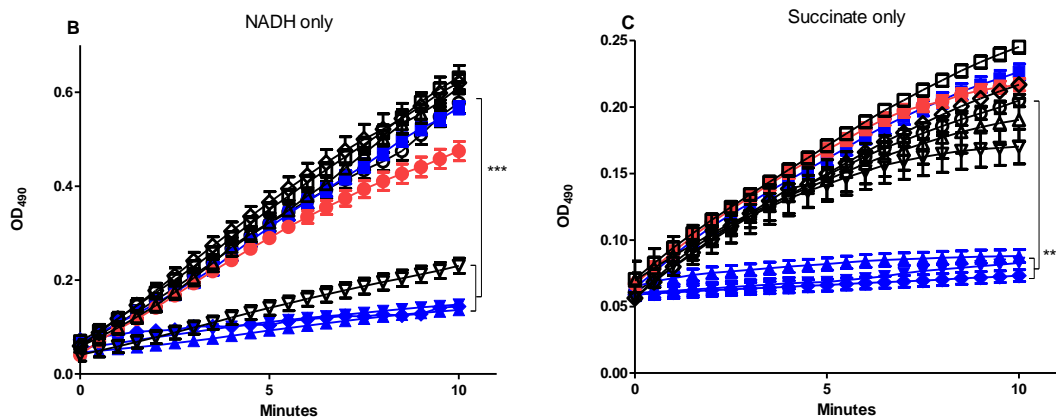


**Figure 4.9. 2B8 blocks ETC activity in mycobacterial IMVs.** The ETC of mycobacterial IMVs was initiated with NADH and succinate (A), NADH only (B) or succinate only (C), and was evaluated by 490 nm absorbance measuring reduction of INT, an artificial electron acceptor. A) When the ETC was activated by addition of both NADH and succinate, 78.125, 93.75, and 125  $\mu\text{M}$  2B8 significantly inhibited INT reduction as well as TRZ 80  $\mu\text{M}$  and RA13 125  $\mu\text{M}$  albeit to a lesser extent. B) 2B8 78.125, 93.75, and 125  $\mu\text{M}$  still significantly inhibited INT reduction when the ETC was activated by NADH only. TRZ 80  $\mu\text{M}$  and RA13 125  $\mu\text{M}$  inhibited INT reduction as well. C) When the ETC was activated by succinate only, TRZ 80  $\mu\text{M}$  and RA13 125  $\mu\text{M}$  did not inhibit INT reduction while 2B8 78.125, 93.75, and 125  $\mu\text{M}$  significantly inhibited the reduction. Experiments were repeated three separate times and representative data are shown. \*  $p < 0.05$ , \*\*  $p < 0.005$ , \*\*\*  $p < 0.001$ .

#### 4.3.9. 2B8 alters NADH/NAD<sup>+</sup> ratio in *M. tuberculosis*

NDH-2 in *M. tuberculosis* has been shown to be a crucial electron donor for the mycobacterial ETC. Moreover, proper function of NDH-2 and subsequent ETC was required to replenish the NAD<sup>+</sup> pool to maintain redox homeostasis [22]. With the blockage of ETC, we posited that this balance between NADH and NAD<sup>+</sup> may be disrupted by 2B8. Indeed, the intracellular NADH/NAD<sup>+</sup> ratio was significantly increased as early as 2 h after 31.25 to 125  $\mu\text{M}$  2B8 treatment (Figure 4.10A and 4.10B). 125  $\mu\text{M}$  RA13 did not alter NADH/NAD<sup>+</sup> ratio and 80  $\mu\text{M}$  TRZ increased this ratio significantly as expected. This result suggests that 2B8 disrupts the balance between NADH and NAD<sup>+</sup> by increasing the amount of NADH compared to NAD<sup>+</sup>.

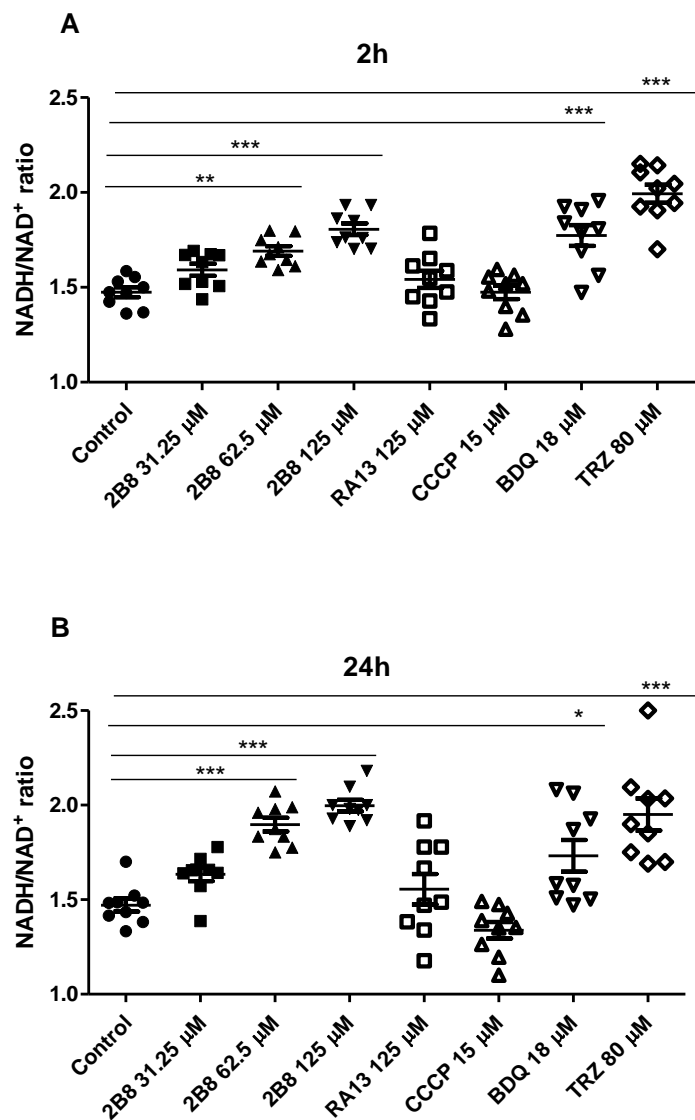


**Figure 4.10. 2B8 alters *M. tuberculosis* NADH/NAD<sup>+</sup> ratio.** After a 2 (A) or 24 (B) h treatment with 2-AI compounds, intracellular NADH and NAD<sup>+</sup> concentrations were determined and the NADH/NAD<sup>+</sup> ratio was calculated. A) Treatment with 62.5 and 125 μM 2B8 for 2 h resulted in a significant increase of the NADH/NAD<sup>+</sup> ratio. Treatment with BDQ and TRZ also increased the ratio significantly. In contrast, 125 μM RA13 did not significantly alter this ratio. B) After 24 h of treatment, 62.5 and 125 μM 2B8, BDQ, and TRZ persistently resulted in a significantly elevated NADH/NAD<sup>+</sup> ratio. However, RA13 and CCCP were ineffective at changing NADH/NAD<sup>+</sup> ratio. Experiments were repeated three separate times and all replicates were pooled for analysis. \* p<0.05, \*\* p<0.01, \*\*\* p<0.001 by ANOVA.

#### 4.3.10. 2B8 blocks NADH oxidation

To directly test whether 2B8 increased the NADH/NAD<sup>+</sup> ratio through inhibiting NADH oxidation catalyzed by NADH dehydrogenases, we measured NADH decay by *M. smegmatis* IMVs in the presence of 2B8. The monitoring of NADH oxidation is classically done by examining absorbance at 340 nm as NADH loses its absorbance at that wavelength when it is oxidized [25]. However, we observed significant peak of 340 nm absorbance coming from 2B8, thereby preventing the accurate read out of NADH oxidation. Therefore as an alternative, we measured NADH oxidation by monitoring fluorescence at 340<sub>ex</sub>/480<sub>em</sub> since NADH fluoresces at 340<sub>ex</sub>/480<sub>em</sub> and loses its fluorescence as it is oxidized and 2B8 did not emit any fluorescence at 340<sub>ex</sub>/480<sub>em</sub>. Consistent with the ETC activity assay results, 78.125 to 125 μM 2B8 significantly inhibited NADH oxidation (Figure 4.11). As expected, 80 μM TRZ and 5 mM KCN also inhibited NADH oxidation (Figure 4.11), by inhibition of NDH-2 and accumulation of reducing equivalents, respectively. Interestingly, 18 μM BDQ also delayed NADH oxidation compared to DMSO control, but 125 μM RA13 did not have any effect while 15 μM CCCP even accelerated the rate of NADH oxidation. This result demonstrates that 2B8 may be increasing NADH/NAD<sup>+</sup> ratio by inhibiting NADH oxidation through complex I in ETC.

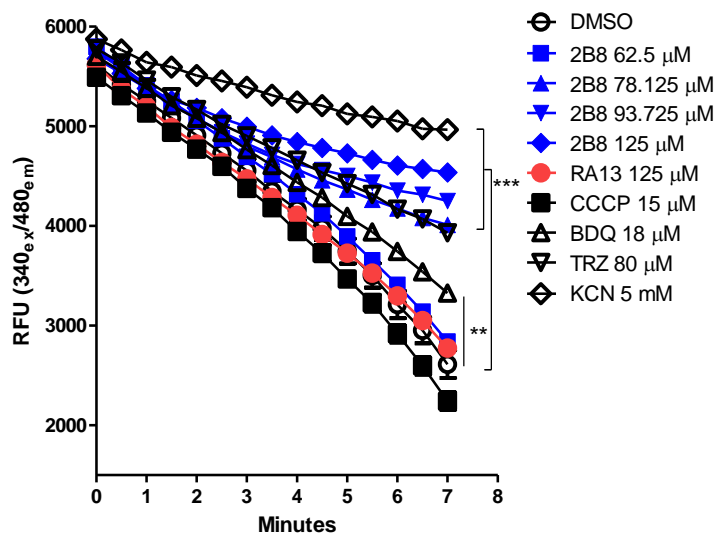
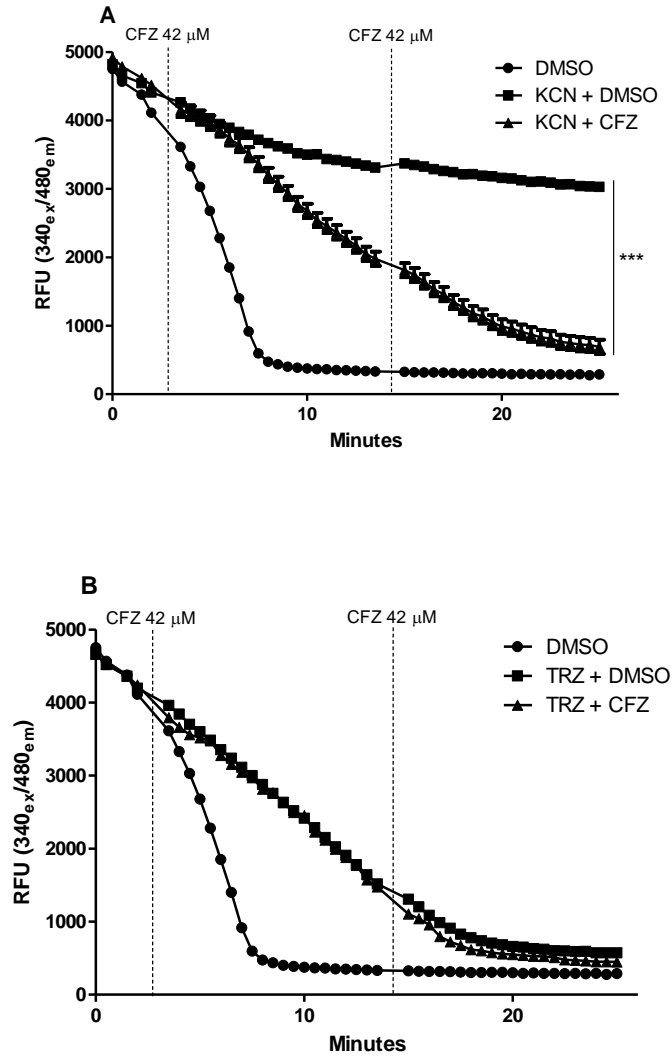


**Figure 4.11. 2B8 blocks NADH oxidation by mycobacterial IMVs.** NADH oxidation by *M. smegmatis* IMVs was evaluated by monitoring the rate of fluorescence decay at 340<sub>ex</sub>/480<sub>em</sub>. Treatment with 78.125, 93.725, and 125 μM 2B8, 5 mM KCN and 80 μM TRZ potently inhibited NADH oxidation. In contrast, NADH oxidation was minimally inhibited by 62.5 μM 2B8 and 125 μM RA13, whereas 18 μM BDQ had an intermediate inhibition. Also, 15 μM CCCP led to accelerated NADH oxidation compared to DMSO control. Experiments were repeated three separate times and representative data are shown. \* p<0.05, \*\* p<0.005, \*\*\* p<0.001.

#### 4.3.11. NADH oxidation block by 2B8 can be rescued by CFZ

From the above assays, we obtained that 2B8 inhibited the ETC activity initiated by NADH and also blocked NADH oxidation, suggesting it might be blocking NDH-2. However, 2B8 also blocked the ETC activity initiated by succinate. Unless 2B8 simultaneously inhibited both complex I and II, the most likely scenario is that 2B8's effect of NADH oxidation block is indirect, perhaps due to build-up of reducing equivalents as a consequence of inhibiting one of the downstream complex in the ETC. To discriminate between these two possibilities, we set up an experiment to determine if NADH oxidation could be rescued by CFZ. It was previously shown that in the presence of a reduced ETC (i.e. KCN treatment), CFZ can act as an alternative electron acceptor in a NDH-2 catalyzed reaction that rescues blocked NADH oxidation which was not the case with NADH oxidation block with a NDH-2 inhibitor, TRZ [26]. Consistent with this previous findings, CFZ addition rescued KCN-induced NADH oxidation

blockage (Figure 4.12A), but not in TRZ treated IMVs (Figure 4.12B). NADH oxidation inhibition by 2B8 was partially and transiently rescued compared to that of KCN (Figure 4.12C). This result indicates that NADH oxidation inhibition by 2B8 is probably not through direct inhibition of mycobacterial NDH-2.



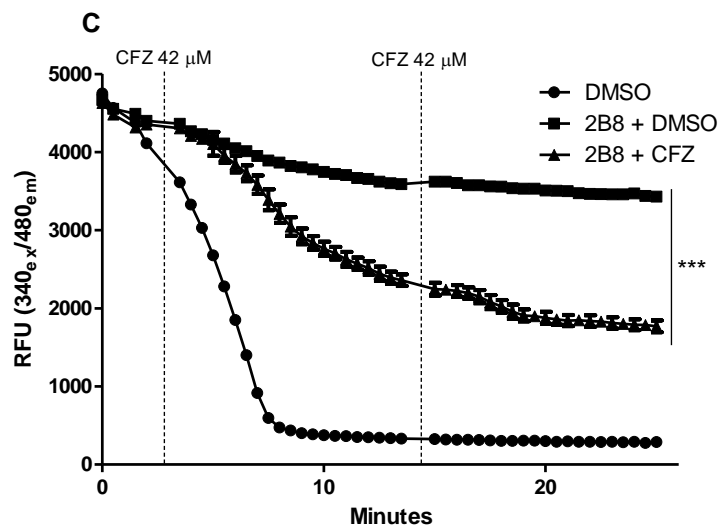


**Figure 4.12. CFZ partially rescues 2B8-induced blockage of NADH oxidation.** NADH oxidation rescue by reduction of CFZ was measured in *M. smegmatis* IMVs after they have been blocked with 5 mM KCN (A), 80  $\mu$ M TRZ (B), or 125  $\mu$ M 2B8 (C). Addition of 42  $\mu$ M CFZ (dotted lines) was able to rescue NADH oxidation by IMVs previously inhibited by KCN. CFZ did not affect TRZ-treated samples. Addition of CFZ also rescued NADH oxidation blockage in 2B8-treated IMVs, but partially compared to the rescue of KCN-treated samples. Experiments were done three separate times and representative data are shown. \*\*\*  $p < 0.001$  by ANOVA.

#### 4.3.12. Bioenergetics-affecting drugs potentiate $\beta$ -lactams, but to a lesser extent than 2B8

Lastly, we questioned if disrupting membrane bioenergetics is sufficient to reach the level of  $\beta$ -lactam potentiation achieved by 2B8. Multiple drugs with different mode of actions were used (at their respective 50% MIC against *M. tuberculosis*) in combination with carbenicillin and meropenem against *M. tuberculosis*. All tested drugs reduced  $\beta$ -lactams MIC to some extent (Table 4.2), but not as dramatic as 2B8 (Table 2.1). Among the bioenergetics-targeting drugs, TRZ was the most effective potentiator of  $\beta$ -lactam antibiotics, followed by CCCP.

**Table 4.2. Fold-reduction of  $\beta$ -lactam MICs against *M. tuberculosis* in combination with bioenergetics-targeting drugs.**

$\beta$ -lactams	MIC	+CCCP	Fold reduction	+BDQ	Fold reduction	+TRZ	Fold reduction	+ nigericin	Fold reduction	+ valinomycin	Fold reduction
Carbenicillin	1000	125	8	250	4	62.5	16	250	4	500	2
Meropenem	8	0.5	16	1	8	0.25	32	2	4	2	4

MICs of bioenergetics-targeting drugs against *M. tuberculosis*: CCCP (20  $\mu$ M), BDQ (0.125  $\mu$ M), TRZ (62.5  $\mu$ M), nigericin (15.625  $\mu$ M), valinomycin (15.625  $\mu$ M)

#### 4.4. Discussion

Maintenance of proton motive force and bioenergetics homeostasis are a crucial part of bacterial physiology because they are prerequisites for multiple anabolic and catabolic pathways [35]. It was hypothesized that 2B8 would collapse proton motive force in mycobacteria based on previous findings in Chapters 2 and 3. Notably, a protein secretion defect was observed with 2B8 treatment (Figure 3.2B). Additionally, there was an evident defect in transporting lipid precursors from the cytoplasmic space outside the cell membrane, as shown by the accumulation of TMM with decreased amount of TDM (Figure 3.3A). Through a series of mechanistic studies, it is shown herein that not only does 2B8 collapse the proton motive force, but also blocks ETC, collectively disturbing bioenergetics homeostasis. We observed that 2B8 induced changes in multiple parameters required for optimally energized membranes, including redox potential, both components of the proton motive force ( $\Delta\psi$  and  $\Delta\text{pH}$ ), oxygen consumption, ATP generation, ETC activity, NADH/NAD<sup>+</sup> ratio and NADH oxidation. Most of the 2B8-induced bioenergetics alterations occurred acutely, before any indication of cell membrane lysis (Figure 3.6D). Therefore, it is suggested that 2B8 acutely induces these perturbation of mycobacterial bioenergetics through a specific mechanism before any generalized membrane disruption takes place.

It is also important to note that treatment with low (62.5  $\mu$ M and below) or high concentrations of 2B8 (higher than 62.5  $\mu$ M) yielded different phenotypes in mycobacterial bioenergetics (Table 4.3). The difference is more evident in assays that were assessed acutely (less than 2 h after treatment) than in assays that were evaluated after more than 2 h treatment. Specifically, OCR is increased with low 2B8

concentrations whereas higher concentrations start to decrease oxygen consumption. It is proposed that 2B8 acts as an uncoupler of oxidative phosphorylation at low concentrations since it affected the three parameters (proton motive force collapse, increase of oxygen consumption, and depletion of ATP) altered by classic uncouplers like CCCP [36]. How 2B8 uncouples the oxidative phosphorylation in mycobacteria is not understood. At concentrations higher than 62.5  $\mu\text{M}$ , the most notable effect was on the ETC. Above this concentration, we observed a block in electron flow leading to decreased OCR, as well as inhibition of NADH oxidation inhibition. This evidence suggests that 2B8 also acts as an ETC blocker and the precise site of action remains to be determined.

**Table 4.3. Comparison of low and high concentrations of 2B8 in assays conducted in this study.**

	Low ( $\leq 62.5 \mu\text{M}$ )	High ( $> 62.5 \mu\text{M}$ )
Proposed action	Uncoupler	ETC blocker
<b>Acute (<math>\leq 2</math> h)</b>		
$\Delta\psi$	↓	↓
$\Delta\text{pH}$	↓	↓
$\text{O}_2$ consumption rate	↑	↓
ETC activity	No effect	↓
NADH oxidation	No effect	↓
<b>Delayed (<math>&gt; 2</math> h)</b>		
alamarblue reduction	No effect	↓
ATP generation	↓	↓
NADH/NAD <sup>+</sup> ratio	↑	↑

Drugs previously known to affect different mycobacterial bioenergetics parameters were included as controls in the assays. Altogether, it is clear that 2B8 induced a distinct effect than these drugs, indicating that the mechanism of action for 2B8 might be different (Table 4.4). Of the tested drugs, TRZ, a NDH-2 inhibitor, shared the most similar outcomes with 2B8. Thus, it was first suspected that 2B8 might be a NDH-2 blocker. Unlike other bacteria, mycobacteria rely more on NDH-2 than classical NDH-1 to initiate ETC and also replenish the NAD<sup>+</sup> pool, especially under low oxygen conditions [22, 29].

**Table 4.4. Summary of read-outs for all tested drugs.**

Read-out	<b>2B8</b>	<b>CCCP</b>	<b>BDQ</b>	<b>TRZ</b>	<b>KCN</b>
	Uncoupling/ ETC block at unknown site	Uncoupling/ Proton ionophore	ATP synthase inhibitor	NDH-2 inhibitor	ETC block at cytochrome <i>c</i> oxidase
alamarblue reduction	Strong ↓	Weak ↓	No effect	Strong ↓	Not tested
$\Delta\psi$	Strong ↓	Strong ↓	No effect	Intermediate ↓	Not tested
$\Delta\text{pH}$	Strong ↓	Intermediate ↓	Intermediate ↓	Strong ↓	Not tested
O <sub>2</sub> consumption rate	↑ then ↓	↑ then ↓	↑	↑	Not tested
ATP generation	Strong ↓	Intermediate ↓	Strong ↓	Strong ↓	Not tested
ETC activity	Strong ↓	Weak ↑	No effect	Strong ↓	N/A
NADH/NAD <sup>+</sup> ratio	Strong ↑	No effect	Intermediate ↑	Strong ↑	Not tested
NADH oxidation	Strong ↓	Weak ↑	Intermediate ↓	Strong ↓	Strong ↓
Rescue by CFZ	Partial	No effect	Not tested	No	Yes
$\beta$ -lactam potentiation	Strong ↑	Intermediate ↑	Weak ↑	Intermediate ↑	Not tested

N/A: Not applicable due to electron accepting sites of INT.

Therefore, we tested this hypothesis by conducting multiple assays to evaluate ETC activity, NADH/NAD<sup>+</sup> ratio, and NADH oxidation. From the ETC activity assay, we obtained compelling evidence that 2B8 did not specifically inhibit NDH-2, as 2B8 blocked ETC activity even when the chain was initiated only with succinate, but TRZ did not. We further validated this finding by confirming that CFZ could rescue the block of NADH oxidation induced by KCN and 2B8 (albeit to a lesser degree), but not TRZ. In the presence of KCN, inhibition of cytochrome *c* oxidation leads to menaquinone accumulation in its reduced state. In this scenario, NADH oxidation is blocked because NDH-2 is unable to transfer electrons to its usual substrate, oxidized menaquinone. CFZ can act as an alternative electron acceptor as it is directly reduced by a functional NDH-2 and in this process, rescues NADH oxidation blocked by KCN (or 2B8), but not by TRZ [26]. These results collectively suggest that 2B8 blocks the mycobacterial ETC downstream of NDH-2. It is also unlikely that 2B8 specifically blocks succinate dehydrogenase enzyme (complex II) as ETC activity was consistently inhibited when fueled with either NADH (fueling complex I) or succinate (fueling complex II). Additional results evaluating the ETC

activity, suggest that in contrast to KCN, 2B8 does not affect the cytochrome aa<sub>3</sub> subunit present in complex IV [37]. In the presence of KCN, INT (used as an artificial electron acceptor in our ETC activity assay) could be reduced at any point upstream of complex IV [34]. Interestingly, KCN did not affect INT reduction whereas 2B8 potently inhibited INT reduction. Taken together, we propose that at high concentrations, 2B8 is an ETC blocker at an unknown site downstream of complex I and II (menaquinone reduction) and upstream of complex IV (Figure 4.13). Thus, the current working model posits 2B8's effect on cytochrome *c* reductase (complex III). Additional experiments are being performed to determine 2B8's effect on menaquinone redox state and cytochrome *c* reductase activity. Interestingly, an IPA derivative Q203, having an imidazole ring was recently shown to target cytochrome bc<sub>1</sub> complex [38].

Lastly, known drugs that target bacterial bioenergetics were evaluated for β-lactams potentiation capacity. Not surprisingly, many of the drugs including CCCP and TRZ potentiated carbenicillin and meropenem. A common mechanism of action for these two drugs and 2B8 seems to be the collapse of proton motive force. TRZ was slightly better in potentiating β-lactams than CCCP, this could be due in part to TRZ's additional ability to permeabilize mycobacterial cell envelope [39]. While the proton motive force collapse will lead to less β-lactamase secretion and alterations in cell envelope lipids composition, the ability to acutely increase binding of antibiotics to its relevant target as shown for 2B8 (chapter 3) may be a critical factor in β-lactam potentiation, uniquely accomplished by 2B8.

In conclusion, we discovered that 2B8 collapses the mycobacterial proton motive force and ETC activity, providing a unifying mechanism underlying protein secretion and lipid export defects. Further investigation into the target of 2B8 in mycobacterial ETC may lead to elucidation of a novel drug target in *M. tuberculosis*.

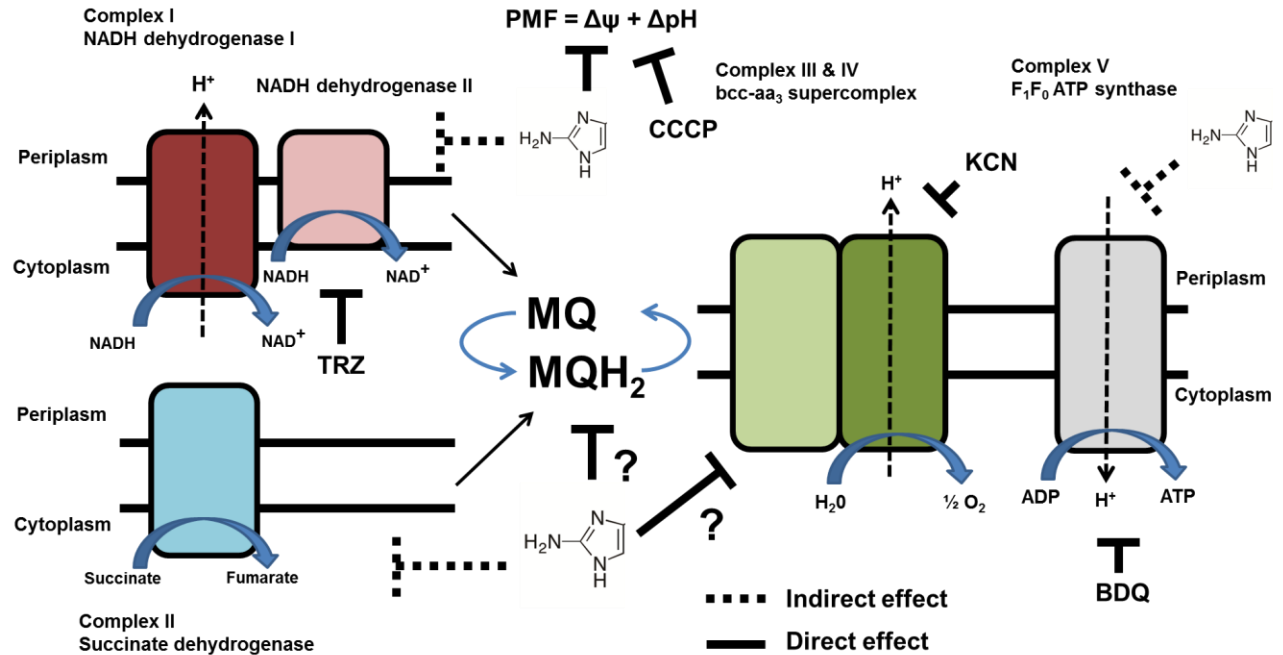


**Figure 4.13. Diagram of 2B8's effect on mycobacterial membrane bioenergetics.** Known bioenergetics-affecting drugs are noted as well. Dotted lines indicate 2B8 affects the complex indirectly and solid lines indicate 2B8 affects the complex directly. The question mark shows unevaluated areas where 2B8 possibly directly inhibit.

## REFERENCES

1. Chopra I, Hesse L, O'Neill AJ. Exploiting current understanding of antibiotic action for discovery of new drugs. *J Appl Microbiol.* 2002;92 Suppl:4S-15S. PubMed PMID: 12000608.
2. Stewart GR, Robertson BD, Young DB. Tuberculosis: a problem with persistence. *Nat Rev Microbiol.* 2003;1(2):97-105. doi: 10.1038/nrmicro749. PubMed PMID: 15035039.
3. Hurdle JG, O'Neill AJ, Chopra I, Lee RE. Targeting bacterial membrane function: an underexploited mechanism for treating persistent infections. *Nat Rev Microbiol.* 2011;9(1):62-75. doi: 10.1038/nrmicro2474. PubMed PMID: 21164535; PubMed Central PMCID: PMCPMC3496266.
4. Xiong YQ, Abdelhady W, Tang C, Bayer AS. Comparative efficacy of telavancin and daptomycin in experimental endocarditis due to multi-clonotype MRSA strains. *J Antimicrob Chemother.* 2016;71(10):2890-4. doi: 10.1093/jac/dkw249. PubMed PMID: 27353467.
5. Straus SK, Hancock RE. Mode of action of the new antibiotic for Gram-positive pathogens daptomycin: comparison with cationic antimicrobial peptides and lipopeptides. *Biochim Biophys Acta.* 2006;1758(9):1215-23. doi: 10.1016/j.bbamem.2006.02.009. PubMed PMID: 16615993.
6. Xiong YQ, Hady WA, Bayer AS, Chen L, Kreiswirth BN, Yang SJ. Telavancin in therapy of experimental aortic valve endocarditis in rabbits due to daptomycin-nonsusceptible methicillin-resistant *Staphylococcus aureus*. *Antimicrob Agents Chemother.* 2012;56(11):5528-33. doi: 10.1128/AAC.00922-12. PubMed PMID: 22890759; PubMed Central PMCID: PMCPMC3486568.
7. Koul A, Dendouga N, Vergauwen K, Molenberghs B, Vranckx L, Willebrords R, et al. Diarylquinolines target subunit c of mycobacterial ATP synthase. *Nat Chem Biol.* 2007;3(6):323-4. doi: 10.1038/nchembio884. PubMed PMID: 17496888.
8. Mukherjee T, Boshoff H. Nitroimidazoles for the treatment of TB: past, present and future. *Future Med Chem.* 2011;3(11):1427-54. doi: 10.4155/fmc.11.90. PubMed PMID: 21879846; PubMed Central PMCID: PMCPMC3225966.
9. Cholo MC, Steel HC, Fourie PB, Germishuizen WA, Anderson R. Clofazimine: current status and future prospects. *J Antimicrob Chemother.* 2012;67(2):290-8. doi: 10.1093/jac/dkr444. PubMed PMID: 22020137.
10. Dhiman RK, Mahapatra S, Slayden RA, Boyne ME, Lenaerts A, Hinshaw JC, et al. Menaquinone synthesis is critical for maintaining mycobacterial viability during exponential growth and recovery from non-replicating persistence. *Mol Microbiol.* 2009;72(1):85-97. doi: 10.1111/j.1365-2958.2009.06625.x. PubMed PMID: 19220750; PubMed Central PMCID: PMCPMC4747042.
11. Hoagland DT, Liu J, Lee RB, Lee RE. New agents for the treatment of drug-resistant *Mycobacterium tuberculosis*. *Adv Drug Deliv Rev.* 2016;102:55-72. doi: 10.1016/j.addr.2016.04.026. PubMed PMID: 27151308; PubMed Central PMCID: PMCPMC4903924.
12. Lechartier B, Cole ST. Mode of Action of Clofazimine and Combination Therapy with Benzothiazinones against *Mycobacterium tuberculosis*. *Antimicrob Agents Chemother.* 2015;59(8):4457-

63. doi: 10.1128/AAC.00395-15. PubMed PMID: 25987624; PubMed Central PMCID: PMC4505229.

13. Manjunatha U, Boshoff HI, Barry CE. The mechanism of action of PA-824: Novel insights from transcriptional profiling. *Commun Integr Biol.* 2009;2(3):215-8. PubMed PMID: 19641733; PubMed Central PMCID: PMC4505229.

14. Grzegorzewicz AE, Pham H, Gundi VA, Scherman MS, North EJ, Hess T, et al. Inhibition of mycolic acid transport across the *Mycobacterium tuberculosis* plasma membrane. *Nat Chem Biol.* 2012;8(4):334-41. doi: 10.1038/nchembio.794. PubMed PMID: 22344175; PubMed Central PMCID: PMC3307863.

15. Belisle JT, Vissa VD, Sievert T, Takayama K, Brennan PJ, Besra GS. Role of the major antigen of *Mycobacterium tuberculosis* in cell wall biogenesis. *Science.* 1997;276(5317):1420-2. PubMed PMID: 9162010.

16. Li W, Upadhyay A, Fontes FL, North EJ, Wang Y, Crans DC, et al. Novel insights into the mechanism of inhibition of MmpL3, a target of multiple pharmacophores in *Mycobacterium tuberculosis*. *Antimicrob Agents Chemother.* 2014;58(11):6413-23. doi: 10.1128/AAC.03229-14. PubMed PMID: 25136022; PubMed Central PMCID: PMC4249373.

17. Nikaido H, Takatsuka Y. Mechanisms of RND multidrug efflux pumps. *Biochim Biophys Acta.* 2009;1794(5):769-81. doi: 10.1016/j.bbapap.2008.10.004. PubMed PMID: 19026770; PubMed Central PMCID: PMC2696896.

18. Feltcher ME, Sullivan JT, Braunstein M. Protein export systems of *Mycobacterium tuberculosis*: novel targets for drug development? *Future Microbiol.* 2010;5(10):1581-97. doi: 10.2217/fmb.10.112. PubMed PMID: 21073315; PubMed Central PMCID: PMC3034451.

19. Li K, Schurig-Briccio LA, Feng X, Upadhyay A, Pujari V, Lechartier B, et al. Multitarget drug discovery for tuberculosis and other infectious diseases. *J Med Chem.* 2014;57(7):3126-39. doi: 10.1021/jm500131s. PubMed PMID: 24568559; PubMed Central PMCID: PMC4084622.

20. Koul A, Vranckx L, Dendouga N, Balemans W, Van den Wyngaert I, Vergauwen K, et al. Diarylquinolines are bactericidal for dormant mycobacteria as a result of disturbed ATP homeostasis. *J Biol Chem.* 2008;283(37):25273-80. doi: 10.1074/jbc.M803899200. PubMed PMID: 18625705.

21. Hards K, Robson JR, Berney M, Shaw L, Bald D, Koul A, et al. Bactericidal mode of action of bedaquiline. *J Antimicrob Chemother.* 2015;70(7):2028-37. doi: 10.1093/jac/dkv054. PubMed PMID: 25754998.

22. Rao SP, Alonso S, Rand L, Dick T, Pethe K. The protonmotive force is required for maintaining ATP homeostasis and viability of hypoxic, nonreplicating *Mycobacterium tuberculosis*. *Proc Natl Acad Sci U S A.* 2008;105(33):11945-50. doi: 10.1073/pnas.0711697105. PubMed PMID: 18697942; PubMed Central PMCID: PMC2575262.

23. Upadhyay A, Fontes FL, Gonzalez-Juarrero M, McNeil MR, Crans DC, Jackson M, et al. Partial Saturation of Menaquinone in *Mycobacterium tuberculosis*: Function and Essentiality of a Novel Reductase, MenJ. *ACS Cent Sci.* 2015;1(6):292-302. doi: 10.1021/acscentsci.5b00212. PubMed PMID: 26436137; PubMed Central PMCID: PMC4582327.

24. Vilcheze C, Weisbrod TR, Chen B, Kremer L, Hazbon MH, Wang F, et al. Altered NADH/NAD<sup>+</sup> ratio mediates coresistance to isoniazid and ethionamide in mycobacteria. *Antimicrob Agents Chemother.* 2005;49(2):708-20. doi: 10.1128/AAC.49.2.708-720.2005. PubMed PMID: 15673755; PubMed Central PMCID: PMCPMC547332.
25. Held P. *Determination of NADH Concentrations with the Synergy™ 2 Multi-Detection Microplate Reader using Fluorescence or Absorbance* Vermont, USA: Biotek Instruments; 2007.
26. Yano T, Kassovska-Bratinova S, Teh JS, Winkler J, Sullivan K, Isaacs A, et al. Reduction of clofazimine by mycobacterial type 2 NADH:quinone oxidoreductase: a pathway for the generation of bactericidal levels of reactive oxygen species. *J Biol Chem.* 2011;286(12):10276-87. doi: 10.1074/jbc.M110.200501. PubMed PMID: 21193400; PubMed Central PMCID: PMCPMC3060482.
27. Rampersad SN. Multiple applications of Alamar Blue as an indicator of metabolic function and cellular health in cell viability bioassays. *Sensors (Basel).* 2012;12(9):12347-60. doi: 10.3390/s120912347. PubMed PMID: 23112716; PubMed Central PMCID: PMCPMC3478843.
28. Maloney PC, Kashket ER, Wilson TH. A protonmotive force drives ATP synthesis in bacteria. *Proc Natl Acad Sci U S A.* 1974;71(10):3896-900. PubMed PMID: 4279406; PubMed Central PMCID: PMCPMC434292.
29. Cook GM, Hards K, Vilcheze C, Hartman T, Berney M. Energetics of Respiration and Oxidative Phosphorylation in Mycobacteria. *Microbiol Spectr.* 2014;2(3). doi: 10.1128/microbiolspec.MGM2-0015-2013. PubMed PMID: 25346874; PubMed Central PMCID: PMCPMC4205543.
30. Kasianowicz J, Benz R, McLaughlin S. The kinetic mechanism by which CCCP (carbonyl cyanide *m*-chlorophenylhydrazone) transports protons across membranes. *J Membr Biol.* 1984;82(2):179-90. PubMed PMID: 6096547.
31. Ni Y, Zhu R, Kokot S. Competitive binding of small molecules with biopolymers: a fluorescence spectroscopy and chemometrics study of the interaction of aspirin and ibuprofen with BSA. *Analyst.* 2011;136(22):4794-801. doi: 10.1039/c1an15550d. PubMed PMID: 21952617.
32. Dilley RA, Schreiber U. Correlation between membrane-localized protons and flash-driven ATP formation in chloroplast thylakoids. *J Bioenerg Biomembr.* 1984;16(3):173-93. PubMed PMID: 6100298.
33. Nishio JN, Whitmarsh J. Dissipation of the proton electrochemical potential in intact and lysed chloroplasts : I. The electrical potential. *Plant Physiol.* 1991;95(2):522-8. PubMed PMID: 16668015; PubMed Central PMCID: PMCPMC1077563.
34. Smith JJ, McFeters GA. Effects of substrates and phosphate on INT (2-(4-iodophenyl)-3-(4-nitrophenyl)-5-phenyl tetrazolium chloride) and CTC (5-cyano-2,3-ditolyl tetrazolium chloride) reduction in *Escherichia coli*. *J Appl Bacteriol.* 1996;80(2):209-15. PubMed PMID: 8642015.
35. Zhang Y, Wade MM, Scorpio A, Zhang H, Sun Z. Mode of action of pyrazinamide: disruption of *Mycobacterium tuberculosis* membrane transport and energetics by pyrazinoic acid. *J Antimicrob Chemother.* 2003;52(5):790-5. doi: 10.1093/jac/dkg446. PubMed PMID: 14563891.

36. Terada H. *Uncouplers of oxidative phosphorylation. Environ Health Perspect.* 1990;87:213-8. PubMed PMID: 2176586; PubMed Central PMCID: PMC1567840.
37. Kim MS, Jang J, Ab Rahman NB, Pethe K, Berry EA, Huang LS. *Isolation and Characterization of a Hybrid Respiratory Supercomplex Consisting of Mycobacterium tuberculosis Cytochrome bcc and Mycobacterium smegmatis Cytochrome aa3. J Biol Chem.* 2015;290(23):14350-60. doi: 10.1074/jbc.M114.624312. PubMed PMID: 25861988; PubMed Central PMCID: PMC4505504.
38. Pethe K, Bifani P, Jang J, Kang S, Park S, Ahn S, et al. *Discovery of Q203, a potent clinical candidate for the treatment of tuberculosis. Nat Med.* 2013;19(9):1157-60. doi: 10.1038/nm.3262. PubMed PMID: 23913123.
39. de Keijzer J, Mulder A, de Haas PE, de Ru AH, Heerkens EM, Amaral L, et al. *Thioridazine Alters the Cell-Envelope Permeability of Mycobacterium tuberculosis. J Proteome Res.* 2016;15(6):1776-86. doi: 10.1021/acs.jproteome.5b01037. PubMed PMID: 27068340.

## CHAPTER FIVE

### Concluding remarks and future directions

A battle to conquer TB is facing a major setback due in part to the problems associated with drug-resistance. Even for drug-sensitive cases, although the treatment success rate is high, the multidrug treatment regimen requires 6 to 9 months which contributes to poor patient compliances and undesirable side effects. These problems may also lead to development of drug-resistance from drug-sensitive cases [1]. A novel therapeutic approach that will circumvent the possible emergence of resistance against anti-TB drugs has the potential to greatly improve current strategies to control TB globally.  $\beta$ -lactam antibiotics are drugs with proven efficacy and safety and there are many that are currently FDA approved that can be readily used [2]. The problem is that *M. tuberculosis* is intrinsically resistant to  $\beta$ -lactams owing to their  $\beta$ -lactamase secretion and unusually impermeable lipid rich cell envelope [3]. Recently, attempts to repurpose this effective class of antibiotics for TB therapy have been tested both in the laboratory and clinical setting [4-8]. However, these approaches rely on the presence of classical  $\beta$ -lactamase inhibitor such as clavulanate and we have witnessed the emergence of resistance to  $\beta$ -lactam- $\beta$ -lactamase inhibitor combinations in other pathogenic bacteria [9-11]. In this regard, a different adjunctive approach that potentiates  $\beta$ -lactam antibiotics by other mechanisms may further support the feasibility of this therapeutic approach. Derivatives of 2-AI compounds have been shown to be effective in reversing both phenotypic drug-tolerance and intrinsic drug-resistance of diverse bacterial species [12-17]. This study investigated whether 2-AI compounds can be combined with  $\beta$ -lactam antibiotics to effectively eliminate *M. tuberculosis*. Additionally, the mechanism of action of 2-AI compounds in mycobacteria was also addressed by series of mechanistic studies.

Previously, our group showed that 2-AI compounds potently reverse phenotypic isoniazid tolerance expressed by *M. tuberculosis* grown *in vitro* [18]. The antimicrobial tolerance was significant when bacilli were able to grow in a biofilm-like communities embedded within host-derived macromolecules. The addition of 2-AI compounds to attached microbial communities resensitized bacilli

to isoniazid comparable to their planktonic counterparts, demonstrating that 2-AI compounds reverse phenotypic drug-tolerance in *M. tuberculosis* [12]. Another keen observation was made when 2-AI compounds potentiated carbenicillin against *M. tuberculosis* and was further confirmed when 2-AI compounds, especially 2B8, significantly reduced multiple  $\beta$ -lactam antibiotics MICs against mycobacteria while improving their bactericidal effect against *M. tuberculosis*. It was demonstrated that 2-AI compounds achieve this by two distinctive mechanisms: 1) reducing  $\beta$ -lactamase secretion, and 2) increasing cell envelope permeability. It is noteworthy that the effect on cell envelope permeability by 2-AI compounds was distinct with that of conventional detergent, SDS. While SDS acutely lysed inner cell membrane and poorly potentiated  $\beta$ -lactam antibiotics, 2-AI compounds did not affect inner cell membrane integrity, but significantly increase the binding of antibiotics to their targets in cell wall. The differences between effects of 2-AI compounds and SDS suggest that the increased binding of  $\beta$ -lactam antibiotics to their cognate targets is what primarily drives the  $\beta$ -lactam potentiation by 2-AI compounds in regards to the cell envelope permeability. It is hypothesized that this acute effect is achieved by physical interaction of 2-AI compounds with mycobacterial cell envelope structures allowing a better penetration of  $\beta$ -lactam antibiotics through the cell wall. Investigating the physical manifestation of the mycobacterial cell envelope structure after treatment with 2-AI compounds can further test this hypothesis.

However, beyond the acute physical alteration on the cell envelope, the underlying mode of action that also drives  $\beta$ -lactam potentiation was shown to be the disturbance of mycobacterial bioenergetics. Importantly, we noticed a limitation in transportation of molecules across the membrane such as proteins and cell wall lipids. The energy supporting these processes is the PMF generated by the energized membrane [19], which we chose to investigate further as a primary mechanism of action. Subsequent studies regarding mycobacterial bioenergetics gave us compelling results as we evaluated redox potential, PMF, oxygen consumption, ATP concentration, and multiple parameters of mycobacterial ETC. As hypothesized, 2B8 collapsed the PMF underpinning the idea of lipid export and protein secretion defect being consequences from perturbation of bioenergetics homeostasis. In addition

to collapsing the PMF, 2B8 also increased the OCR while inhibiting ATP generation in a dose-dependent manner. These data suggested that 2B8 uncouples oxidative phosphorylation in mycobacteria and an additive effect of ETC block was additionally identified with concentrations higher than 62.5  $\mu$ M. The block in ETC was observed in a manner independent of complex I, II, and IV providing a clue that 2B8 may be acting between of these complexes. Taken together, 2-AI compounds warrant further investigation as it may lead to identification of a unique target site within the mycobacterial ETC.

For studies conducted in Chapter 2 and 3, two different 2-AI compounds were used. 2B8 was chosen because of its superior effect in reversing phenotypic drug-tolerance in our *in vitro* *M. tuberculosis* biofilm model. The other compound RA11 was chosen because it had a known target of response regulator BfmR in *Acinetobacter baumannii* [20]. Using the two different compounds provided us with the opportunity to expose the structure-activity-relationship which has been shown to be crucial in our goal of designing additional compounds with improved potency and efficacy [21]. RA11 consistently exhibited intermediate effects compared to 2B8 throughout the assays. This made it difficult to pinpoint what structural difference is driving the discrepancy between the two compounds. Therefore, we decided to use another analog RA13, which has elongated alkyl chains by two additional carbons to RA11 for studies conducted in Chapter 4. It was logical to use RA13 over RA11 because RA13 also did not have any potent effect in reversing *M. tuberculosis* phenotypic drug-tolerance [12]. Fortunately, the difference of treatment phenotypes between 2B8 and RA13 was even greater than that of 2B8 and RA11. Therefore, this confirms the importance of the conformation and the length of alkyl chains in the tail group in the activity of these compounds. For some assays conducted in IMVs, RA13 showed significant effects albeit still less than 2B8. Using IMVs, we showed that compounds do not have to diffuse through lipophilic mycobacterial cell envelope and this may be beneficial to RA13 which virtually had no effect on assays conducted with intact cells. However, there was still major differences in the potency between 2B8 and RA13 indicating that 2B8's short, branched alkyl chain may be required for tight fitting of the compound onto its cognitive target in mycobacteria whereas RA13's long, single alkyl chain hinders such

interactions. Taken together, this study is informative going forward in the development of the next generation of compounds that are more effective at much lower concentrations.

At this point, several questions still remain unanswered. These include where specifically is the ETC block by 2B8 occurring and how findings in this study are related to responses seen in our original biofilm model. As far as the target of 2B8 is concerned, some of the direct approaches to reveal small molecule and protein interaction were unsuccessful. Protein purification using biotinylated 2B8 or novel assays such as the drug affinity responsive target stability assay were attempted but failed to identify a single functional protein interacting with 2B8. Our attempt to obtain resistant mutants was also unsuccessful, which further illustrates the potential value of this class of small molecules. Therefore in this study, we employed a deductive approach and narrowed down the blocking site by 2B8 in mycobacterial ETC to either electron carrier molecule menaquinone or complex III cytochromes. Future plans include a strategy to first assess oxidation and reduction states of mycobacterial cytochromes using spectroscopy. Each cytochrome subunit are identifiable due to differences in absorbance peaks at specific wavelengths when reduced [22-25]. This approach will allow us to examine whether cytochrome *bc<sub>1</sub>* complex remains oxidized when treated with 2B8 meaning it directly inhibits electron transfer from reduced menaquinone to cytochrome *aa<sub>3</sub>* oxidase through cytochrome *bc<sub>1</sub>* complex. We will also determine whether externally provided menaquinone rescues ETC block by 2B8 [26].

The export of cell wall lipids has been viewed as an attractive drug target, because of its essentiality in mycobacterial physiology [27]. The family of MmpI proteins governs a variety of translocation process for different lipid molecules [28-31]. Inhibition of this processes by specific chemical inhibitors resulted in a similar cell envelope lipid profiles induced by 2-AI compounds treatment. For example, inhibition of MmpI3 with SQ109 leads to accumulation of TMM, reduction of TDM, and reduced mycolic acids covalently bound to the cell wall core [32], similar to the alterations that followed 2-AI treatment. Moreover, deletion of *mmpI8* or *mmpI10* results in reduced SL-1 and reduced PAT [30, 31], respectively, which are also observed with 2-AI treatment. This creates a compelling case for 2-AI compounds as a broad-spectrum lipid transporter inhibitor, which may be more effective than a selective

MmpL protein inhibitor. Additionally, the defect in lipid export by 2-AI compounds may contribute to the dispersal of surface attached *M. tuberculosis* when cultured as a biofilm. It has been shown that the EPS of mycobacterial biofilms contains a large amount of free mycolic acids [33-35], and that 2B8 greatly reduced the accumulation of free mycolic acids as shown in this study. Also, other macromolecules such as cellulose and proteins are essential components of mycobacterial biofilm EPS and their export and secretion are also dependent on the energized membrane [36]. Further investigation into how free mycolic acids or other secreted macromolecules contribute to the expression of drug-by surface-attached *M. tuberculosis* therefore revealing the link between effects on mycobacterial bioenergetics and biofilm inhibition/dispersal by 2-AI compounds.

In conclusion, this study illustrates a novel mechanism by which small molecule compounds potentiate  $\beta$ -lactam antibiotics against *M. tuberculosis*, which was previously only thought possible through direct deactivation of the  $\beta$ -lactamase enzyme by clavulanate. Importantly, 2-AI compounds targeting mycobacterial ETC led to *M. tuberculosis* phenotypes with altered cell envelope and reduced  $\beta$ -lactamase secretion. This finding also confirms that 2-AI compounds represent a valuable tool for further investigating mycobacterial bioenergetics and its relevance to drug-resistance. Moreover, future studies will be aimed at determining the specific target of 2-AI compounds specifically within the ETC and thus aid in the identification of additional novel drug targets in *M. tuberculosis*.

## REFERENCES

1. Lienhardt C, Glaziou P, Uplekar M, Lonnroth K, Getahun H, Raviglione M. Global tuberculosis control: lessons learnt and future prospects. *Nat Rev Microbiol.* 2012;10(6):407-16. doi: 10.1038/nrmicro2797. PubMed PMID: 22580364.
2. Mohr KI. History of Antibiotics Research. *Curr Top Microbiol Immunol.* 2016;398:237-72. doi: 10.1007/82\_2016\_499. PubMed PMID: 27738915.
3. Wivagg CN, Bhattacharyya RP, Hung DT. Mechanisms of beta-lactam killing and resistance in the context of *Mycobacterium tuberculosis*. *J Antibiot (Tokyo).* 2014;67(9):645-54. doi: 10.1038/ja.2014.94. PubMed PMID: 25052484.
4. Diacon AH, van der Merwe L, Barnard M, von Groote-Bidlingmaier F, Lange C, Garcia-Basteiro AL, et al. beta-Lactams against Tuberculosis--New Trick for an Old Dog? *N Engl J Med.* 2016;375(4):393-4. doi: 10.1056/NEJMc1513236. PubMed PMID: 27433841.
5. Nguyen TV, Blackledge MS, Lindsey EA, Minrovic BM, Ackart DF, Jeon AB, et al. The Discovery of 2-Aminobenzimidazoles That Sensitize *Mycobacterium smegmatis* and *M. tuberculosis* to beta-Lactam Antibiotics in a Pattern Distinct from beta-Lactamase Inhibitors. *Angew Chem Int Ed Engl.* 2017;56(14):3940-4. doi: 10.1002/anie.201612006. PubMed PMID: 28247991.
6. Kumar P, Arora K, Lloyd JR, Lee IY, Nair V, Fischer E, et al. Meropenem inhibits D,D-carboxypeptidase activity in *Mycobacterium tuberculosis*. *Mol Microbiol.* 2012;86(2):367-81. doi: 10.1111/j.1365-2958.2012.08199.x. PubMed PMID: 22906310; PubMed Central PMCID: PMC3468717.
7. Hugonnet JE, Tremblay LW, Boshoff HI, Barry CE, 3rd, Blanchard JS. Meropenem-clavulanate is effective against extensively drug-resistant *Mycobacterium tuberculosis*. *Science.* 2009;323(5918):1215-8. doi: 10.1126/science.1167498. PubMed PMID: 19251630; PubMed Central PMCID: PMC2679150.
8. Nadler JP, Berger J, Nord JA, Cofsky R, Saxena M. Amoxicillin-clavulanic acid for treating drug-resistant *Mycobacterium tuberculosis*. *Chest.* 1991;99(4):1025-6. PubMed PMID: 1901260.
9. Duytschaever G, Huys G, Boulanger L, De Boeck K, Vandamme P. Amoxicillin-clavulanic acid resistance in fecal Enterobacteriaceae from patients with cystic fibrosis and healthy siblings. *J Cyst Fibros.* 2013;12(6):780-3. doi: 10.1016/j.jcf.2013.06.006. PubMed PMID: 23867070.
10. Stapleton P, Wu PJ, King A, Shannon K, French G, Phillips I. Incidence and mechanisms of resistance to the combination of amoxicillin and clavulanic acid in *Escherichia coli*. *Antimicrob Agents Chemother.* 1995;39(11):2478-83. PubMed PMID: 8585729; PubMed Central PMCID: PMC162968.
11. Oteo J, Campos J, Lazaro E, Cuevas O, Garcia-Cobos S, Perez-Vazquez M, et al. Increased amoxicillin-clavulanic acid resistance in *Escherichia coli* blood isolates, Spain. *Emerg Infect Dis.* 2008;14(8):1259-62. doi: 10.3201/eid1408.071059. PubMed PMID: 18680650; PubMed Central PMCID: PMC2600377.

12. Ackart DF, Lindsey EA, Podell BK, Melander RJ, Basaraba RJ, Melander C. Reversal of *Mycobacterium tuberculosis* phenotypic drug resistance by 2-aminoimidazole-based small molecules. *Pathog Dis.* 2014;70(3):370-8. doi: 10.1111/2049-632X.12143. PubMed PMID: 24478046; PubMed Central PMCID: PMC4367863.
13. Worthington RJ, Melander C. Combination approaches to combat multidrug-resistant bacteria. *Trends Biotechnol.* 2013;31(3):177-84. doi: 10.1016/j.tibtech.2012.12.006. PubMed PMID: 23333434; PubMed Central PMCID: PMC3594660.
14. Worthington RJ, Bunders CA, Reed CS, Melander C. Small molecule suppression of carbapenem resistance in NDM-1 producing *Klebsiella pneumoniae*. *ACS Med Chem Lett.* 2012;3(5):357-61. doi: 10.1021/ml200290p. PubMed PMID: 22844552; PubMed Central PMCID: PMC3405495.
15. Harris TL, Worthington RJ, Melander C. Potent small-molecule suppression of oxacillin resistance in methicillin-resistant *Staphylococcus aureus*. *Angew Chem Int Ed Engl.* 2012;51(45):11254-7. doi: 10.1002/anie.201206911. PubMed PMID: 23047322; PubMed Central PMCID: PMC3829614.
16. Rogers SA, Huigens RW, 3rd, Cavanagh J, Melander C. Synergistic effects between conventional antibiotics and 2-aminoimidazole-derived antibiofilm agents. *Antimicrob Agents Chemother.* 2010;54(5):2112-8. doi: 10.1128/AAC.01418-09. PubMed PMID: 20211901; PubMed Central PMCID: PMC2863642.
17. Stowe SD, Richards JJ, Tucker AT, Thompson R, Melander C, Cavanagh J. Anti-biofilm compounds derived from marine sponges. *Mar Drugs.* 2011;9(10):2010-35. doi: 10.3390/md9102010. PubMed PMID: 22073007; PubMed Central PMCID: PMC3210616.
18. Ackart DF, Hascall-Dove L, Caceres SM, Kirk NM, Podell BK, Melander C, et al. Expression of antimicrobial drug tolerance by attached communities of *Mycobacterium tuberculosis*. *Pathog Dis.* 2014;70(3):359-69. doi: 10.1111/2049-632X.12144. PubMed PMID: 24478060; PubMed Central PMCID: PMC4361083.
19. Rao SP, Alonso S, Rand L, Dick T, Pethe K. The protonmotive force is required for maintaining ATP homeostasis and viability of hypoxic, nonreplicating *Mycobacterium tuberculosis*. *Proc Natl Acad Sci U S A.* 2008;105(33):11945-50. doi: 10.1073/pnas.0711697105. PubMed PMID: 18697942; PubMed Central PMCID: PMC2575262.
20. Thompson RJ, Bobay BG, Stowe SD, Olson AL, Peng L, Su Z, et al. Identification of BfmR, a response regulator involved in biofilm development, as a target for a 2-Aminoimidazole-based antibiofilm agent. *Biochemistry.* 2012;51(49):9776-8. doi: 10.1021/bi3015289. PubMed PMID: 23186243; PubMed Central PMCID: PMC3567222.
21. Richards JJ, Melander C. Controlling bacterial biofilms. *Chembiochem.* 2009;10(14):2287-94. doi: 10.1002/cbic.200900317. PubMed PMID: 19681090.
22. Kim MS, Jang J, Ab Rahman NB, Pethe K, Berry EA, Huang LS. Isolation and Characterization of a Hybrid Respiratory Supercomplex Consisting of *Mycobacterium tuberculosis* Cytochrome bcc and *Mycobacterium smegmatis* Cytochrome aa3. *J Biol Chem.* 2015;290(23):14350-60. doi: 10.1074/jbc.M114.624312. PubMed PMID: 25861988; PubMed Central PMCID: PMC4505504.

23. Kana BD, Weinstein EA, Avarbock D, Dawes SS, Rubin H, Mizrahi V. Characterization of the *cydAB*-encoded cytochrome *bd* oxidase from *Mycobacterium smegmatis*. *J Bacteriol.* 2001;183(24):7076-86. doi: 10.1128/JB.183.24.7076-7086.2001. PubMed PMID: 11717265; PubMed Central PMCID: PMCPMC95555.
24. Matsoso LG, Kana BD, Crellin PK, Lea-Smith DJ, Pelosi A, Powell D, et al. Function of the cytochrome *bc1-aa3* branch of the respiratory network in mycobacteria and network adaptation occurring in response to its disruption. *J Bacteriol.* 2005;187(18):6300-8. doi: 10.1128/JB.187.18.6300-6308.2005. PubMed PMID: 16159762; PubMed Central PMCID: PMCPMC1236647.
25. Yano T, Kassovska-Bratinova S, Teh JS, Winkler J, Sullivan K, Isaacs A, et al. Reduction of clofazimine by mycobacterial type 2 NADH:quinone oxidoreductase: a pathway for the generation of bactericidal levels of reactive oxygen species. *J Biol Chem.* 2011;286(12):10276-87. doi: 10.1074/jbc.M110.200501. PubMed PMID: 21193400; PubMed Central PMCID: PMCPMC3060482.
26. Li K, Schurig-Briccio LA, Feng X, Upadhyay A, Pujari V, Lechartier B, et al. Multitarget drug discovery for tuberculosis and other infectious diseases. *J Med Chem.* 2014;57(7):3126-39. doi: 10.1021/jm500131s. PubMed PMID: 24568559; PubMed Central PMCID: PMCPMC4084622.
27. Degiacomi G, Benjak A, Madacki J, Boldrin F, Provvedi R, Palu G, et al. Essentiality of *mmpL3* and impact of its silencing on *Mycobacterium tuberculosis* gene expression. *Sci Rep.* 2017;7:43495. doi: 10.1038/srep43495. PubMed PMID: 28240248; PubMed Central PMCID: PMCPMC5327466.
28. Szekely R, Cole ST. Mechanistic insight into mycobacterial *MmpL* protein function. *Mol Microbiol.* 2016;99(5):831-4. doi: 10.1111/mmi.13306. PubMed PMID: 26710752.
29. Varela C, Rittmann D, Singh A, Krumbach K, Bhatt K, Eggeling L, et al. *MmpL* genes are associated with mycolic acid metabolism in mycobacteria and corynebacteria. *Chem Biol.* 2012;19(4):498-506. doi: 10.1016/j.chembiol.2012.03.006. PubMed PMID: 22520756; PubMed Central PMCID: PMCPMC3370651.
30. Belardinelli JM, Larrouy-Maumus G, Jones V, Sorio de Carvalho LP, McNeil MR, Jackson M. Biosynthesis and translocation of unsulfated acyltrehaloses in *Mycobacterium tuberculosis*. *J Biol Chem.* 2014;289(40):27952-65. doi: 10.1074/jbc.M114.581199. PubMed PMID: 25124040; PubMed Central PMCID: PMCPMC4183827.
31. Converse SE, Mougous JD, Leavell MD, Leary JA, Bertozzi CR, Cox JS. *MmpL8* is required for sulfolipid-1 biosynthesis and *Mycobacterium tuberculosis* virulence. *Proc Natl Acad Sci U S A.* 2003;100(10):6121-6. doi: 10.1073/pnas.1030024100. PubMed PMID: 12724526; PubMed Central PMCID: PMCPMC156336.
32. Tahlan K, Wilson R, Kastrinsky DB, Arora K, Nair V, Fischer E, et al. *SQ109* targets *MmpL3*, a membrane transporter of trehalose monomycolate involved in mycolic acid donation to the cell wall core of *Mycobacterium tuberculosis*. *Antimicrob Agents Chemother.* 2012;56(4):1797-809. doi: 10.1128/AAC.05708-11. PubMed PMID: 22252828; PubMed Central PMCID: PMCPMC3318387.
33. Ojha A, Anand M, Bhatt A, Kremer L, Jacobs WR, Jr., Hatfull GF. *GroEL1*: a dedicated chaperone involved in mycolic acid biosynthesis during biofilm formation in mycobacteria. *Cell.* 2005;123(5):861-73. doi: 10.1016/j.cell.2005.09.012. PubMed PMID: 16325580.

34. Ojha AK, Baughn AD, Sambandan D, Hsu T, Trivelli X, Guerardel Y, et al. Growth of *Mycobacterium tuberculosis* biofilms containing free mycolic acids and harbouring drug-tolerant bacteria. *Mol Microbiol.* 2008;69(1):164-74. doi: 10.1111/j.1365-2958.2008.06274.x. PubMed PMID: 18466296; PubMed Central PMCID: PMCPMC2615189.

35. Sambandan D, Dao DN, Weinrick BC, Vilcheze C, Gurcha SS, Ojha A, et al. Keto-mycolic acid-dependent pellicle formation confers tolerance to drug-sensitive *Mycobacterium tuberculosis*. *MBio.* 2013;4(3):e00222-13. doi: 10.1128/mBio.00222-13. PubMed PMID: 23653446; PubMed Central PMCID: PMCPMC3663190.

36. Trivedi A, Mavi PS, Bhatt D, Kumar A. Thiol reductive stress induces cellulose-anchored biofilm formation in *Mycobacterium tuberculosis*. *Nat Commun.* 2016;7:11392. doi: 10.1038/ncomms11392. PubMed PMID: 27109928; PubMed Central PMCID: PMCPMC4848537.

## LIST OF ABBREVIATIONS

2-AB.....	2-aminobenzimidazole
2-AI.....	2-aminoimidazole
ABC.....	ATP binding cassette
ACMA.....	9-amino-6-chloro-2-methoxyacridine
ACP.....	Acyl carrier protein
ADC.....	Albumin, dextrose, and catalase
ADP.....	Adenosine diphosphate
ANOVA.....	Analysis of variance
ATP.....	Adenosine triphosphate
BCG.....	Bacillus Calmette–Guérin
BDQ.....	Bedaquiline
BSA.....	Bovine serum albumin
BSL.....	Biosafety level
CCCP.....	Carbonyl cyanide m-chlorophenyl hydrazine
CFP.....	Culture filtrate protein
CFU.....	Colony forming unit
CFZ.....	Clofazimine
CPM.....	Counts per million
DAT.....	Diacyltrehalose
$\Delta\psi$ .....	Delta psi (membrane potential)
$\Delta\text{pH}$ .....	Delta pH (pH gradient)
DiSC(3)5.....	3,3'-Dipropylthiadicarbocyanine iodide
DMSO.....	Dimethyl sulfoxide
DNA.....	Deoxyribonucleic acid
ECF.....	Extra-cytoplasmic function
eDNA.....	Extracellular deoxyribonucleic acid
em.....	Emission
EPS.....	Extracellular polymeric substances
ESAT.....	Early secretory antigenic target
EtBr.....	Ethidium bromide
ETC.....	Electron transport chain
ex.....	Excitation
FADH.....	Flavin adenine dinucleotide
FAS.....	Fatty acid synthase
FDA.....	Food and Drug Administration
GAS.....	Glycerol-alanine-salts
GMP.....	Guanylate monophosphate
h.....	Hours
HIV.....	Human immunodeficiency virus
IGRA.....	Interferon gamma release assay
INH.....	Isoniazid
INT.....	2-(4-Iodophenyl)-3-(4-nitrophenyl)-5-phenyl-2H-tetrazolium chloride
IMV.....	Inverted membrane vesicle
IPA.....	Imidazopyridine amide
KCN.....	Potassium cyanide
LM.....	Lipomannan

LAM.....	Lipoarabinomannan
LTBI.....	Latent tuberculosis infection
mAGP .....	Mycolyl-arabinogalactan-peptidoglycan
ManLAM .....	Mannose-capped lipoarabinomannan
MAME.....	Mycolic acid methyl ester
MCA .....	Meropenem-clavulanate
MDR .....	Multi-drug resistant
MIC.....	Minimum inhibitory concentration
min .....	Minutes
MOPS.....	3-(N-morpholino)propanesulfonic acid
MRSA .....	Methicillin resistant <i>Staphylococcus aureus</i>
NADH.....	Nicotinamide adenine dinucleotide
NAG.....	N-acetylglucosamine
NAM .....	N-acetylmuramic acid
NDH.....	Nicotinamide adenine dinucleotide dehydrogenase
NRP.....	Non-replicative persistence
OADC .....	Oleic acid, albumin, dextrose, and catalase
OCR.....	Oxygen consumption rate
OD.....	Optical density
PAT .....	Polyacetyltrehalose
PBP .....	Penicillin binding protein
PBS .....	Phosphate buffered saline
PDIM .....	Phthiocerol dimycocerosate
PGL.....	Phenolic glycolipid
PI.....	Propidium iodide
PIM .....	Phosphatidylinositol mannoside
PMF .....	Proton motive force
RFU.....	Relative fluorescence unit
RIF .....	Rifampicin
RLU .....	Relative luminescence unit
RNA.....	Ribonucleic acid
RNA-seq .....	Ribonucleic acid sequencing
RND.....	Resistance-nodulation-division
rRNA.....	Ribosomal ribonucleic acid
RPMI.....	Roswell Park Memorial Institute
RT .....	Room temperature
SDS .....	Sodium dodecyl sulfate
SL-1 .....	Sulfolipid-1
Tat.....	Twin arginine
TB .....	Tuberculosis
TCA .....	Tricarboxylic acid
TDM.....	Trehalose dimycolate
TDR .....	Totally drug resistant
TLC.....	Thin layer chromatography
TMM.....	Trehalose monomycolate
TRZ.....	Thioridazine
TST .....	Tuberculin skin test
WHO.....	World Health Organization
XDR.....	Extensively drug resistant